Cumulative Dissertation

Diversity effects on ecosystem functions of tritrophic food webs

Author:

Ruben Ceulemans

Submitted in fulfillment of the requirements for the degree of Dr. rer. nat. in Ecology

Ecology and Ecosystem Modelling Group
Institute of Biochemistry and Biology
Faculty of Science
Universität Potsdam

Supervisor:
Prof. Dr. Ursula Gaedke
Mentor:
Dr. Michael Sieber

Evaluation:
Prof. Dr. Ursula Gaedke
Prof. Dr. Lutz Becks
Prof. Dr. Nicolas Loeuille

Potsdam, December 15, 2020

"Before moving along, I'd just like to remind us all that ecology is not a luxury science, and it's not about pleasant appearances: it's about survival.
About whether we're all going to make it."

Benjamin Horne, *Twin Peaks*

Detail from *The Garden of Earthly Delights*, Hieronymus Bosch

Abstract

There is a general consensus that diverse ecological communities are better equipped to adapt to changes in their environment, but our understanding of the mechanisms by which they do so remains incomplete. Accurately predicting how the global biodiversity crisis affects the functioning of ecosystems, and the services they provide, requires extensive knowledge about these mechanisms.

Mathematical models of food webs have been successful in uncovering many aspects of the link between diversity and ecosystem functioning in small food web modules, containing at most two adaptive trophic levels. Meaningful extrapolation of this understanding to the functioning of natural food webs remains difficult, due to the presence of complex interactions that are not always accurately captured by bitrophic descriptions of food webs. In this dissertation, we expand this approach to tritrophic food web models by including the third trophic level. Using a functional trait approach, coexistence of all species is ensured using fitness-balancing trade-offs. For example, the defense-growth trade-off implies that species may be defended against predation, but this defense comes at the cost of a lower maximal growth rate. In these food webs, the functional diversity on a given trophic level can be varied by modifying the trait differences between the species on that level.

In the first project, we find that functional diversity promotes high biomass on the top level, which, in turn, leads to a reduction in the temporal variability due to compensatory dynamical patterns governed by the top level. Next, these results are generalized by investigating the average behavior of tritrophic food webs, for wide intervals of all parameters describing species interactions in the food web. We find that the diversity on the top level is most important for determining the biomass and temporal variability of all other trophic levels, and show how biomass is only transferred efficiently to the top level when diversity is high everywhere in the food web. In the third project, we compare the response of a simple food chain against a nutrient pulse perturbation, to that of a food web with diversity on every trophic level. By joint consideration of the resistance, resilience, and elasticity, we uncover that the response is efficiently buffered when biomass on the top level is high, which is facilitated by functional diversity on every trophic level in the food web. Finally, in the fourth project, we show that even in a simple consumer-resource model without any diversity, top-down control on the intermediate level frequently causes the phase difference between the intermediate and basal level to deviate from the quarter-cycle lag rule. By adding a top predator, we show that these deviations become even more likely, and anti-phase cycles are often observed.

The combined results of these projects show how the properties of the top trophic level, including its functional diversity, have a decisive influence on the functioning of tritrophic food webs from a mechanistic perspective. Because top species are often among the most vulnerable to extinction, our results emphasize the importance of their conservation in ecosystem management and restoration strategies.

Zusammenfassung

Wissenschaftliche Erkenntnisse über die in natürlichen Ökoystemen beobachtete Artenvielfalt hat gezeigt, dass die Artenvielfalt fast überall auf der Erde rapide abnimmt. Dieser Rückgang ist hauptsächlich auf den zunehmenden menschlichen Einfluss auf die Umwelt zurückzuführen. Insbesondere die zunehmende Landnutzung z. B. für die Landwirtschaft, die Verschmutzung und die Überfischung wirken sich negativ auf die Biodiversität aus. Den Einfluss von Biodiversität auf die Funktion von natürlichen Ökosystemen ist ein sehr aktives Forschungsgebiet der Ökologie. Insbesondere hat sich herausgestellt, dass die Biodiversität einen entscheidenden Einfluss auf wichtige Eigenschaften von Ökosystemen hat, wie z.B. die Menge an Biomasse, die sich etablieren kann, wie groß die Schwankungen der Biomasse im Laufe der Zeit sind, wie effizient Energie durch das gesamte Ökosystem übertragen wird und wie es auf Umweltstörungen reagiert.

In dieser Dissertation wird der Zusammenhang zwischen Biodiversität und Ökosystemfunktionen mit Hilfe mathematischer Modelle von Nahrungsnetzen untersucht um mit Hilfe dieses Ansatz wichtige Eigenschaften und deren Relevanz zu ermitteln. Ein Nahrungsnetz beschreibt einen zentralen Teil dessen, wie Arten in einem Ökosystem miteinander interagieren, nämlich wer wen frisst. Unsere Modelle enthalten drei trophische Ebenen: eine basale Ebene (z.B. Pflanzen), die einer mittleren Ebene (Pflanzenfresser) als Nahrungsquelle dient, die wiederum von einer oberen Ebene (Fleischfresser) gefressen werden. Die Koexistenz mehrerer Arten auf einer trophischen Ebene ist über Trade-offs zwischen wichtigen Merkmalen der Arten sichergestellt. Ein Trade-off zwischen Fraßschutz und Wachstum bedeutet zum Beispiel, dass jeder Mechanismus, mit dem sich eine Art vor Fressfeinden schützen kann (z. B. die Bildung von Stacheln), mit einer geringeren Wachstumsrate erkauft wird (die Pflanze muss Energie für die Bildung der Stacheln aufgewendet werden). Auf diese Weise ist die Koexistenz mehrerer Arten möglich: kein Fraßschutz und eine hohe Wachstumsrate, gegenüber hohem Fraßschutz und einer niedrigen Wachstumsrate.

Wir zeigen, dass die Eigenschaften der obersten trophischen Ebene, wie z. B. ihr Biomasseanteil und ihre Diversität, einen sehr großen Einfluss auf die Eigenschaften aller anderen trophischen Ebenen im Nahrungsnetz ausüben. Insbesondere beobachten wir, dass eine hohe Biomasse und Diversität auf der obersten trophischen Ebene zu einem Nahrungsnetz führt, das zeitlich stabiler ist, die verfügbaren anorganischen Nährstoffe besser ausnutzt und die erhöhte Produktivität der basalen trophischen Ebene effizienter an die Spitze des Nahrungsnetzes weitergibt. Darüber hinaus stellen wir fest, dass die oberste trophische Ebene eine Schlüsselrolle bei der Abschwächung von Auswirkungen auf ein Nahrungsnetz durch externe Störungen spielt. Zudem verstärkt sich dieser Effekt der obersten trophischen Ebene, wenn die anderen trophischen Ebenen ebenfalls eine hohe Diversität aufzeigen.

Unsere Ergebnisse unterstreichen somit die Bedeutung von Diversität in allen Nahrungsnetzen, um einen Fortbestand von Ökosystemdienstleistungen zu gewährleisten, auf die wir angewiesen sind.

Acknowledgements

This dissertation would not have been possible without the help of everyone who supported me along the way.

First of all, I would like to thank my supervisor Ursula for giving me the opportunity to become an ecologist. Your efforts to make me feel welcome in your research group, in the field of ecology, and in Germany are deeply appreciated. Your indispensable guidance, advice, ideas, encouragement, and open door during the last four years are an essential part of this work.

Christian, without your signposts and footsteps to follow along the way through the maze between physics and ecology, I would certainly not have made it this far. Thank you for your immensely helpful guidance and illuminating insights.

I want to thank everyone at the Maulbeerallee for welcoming me into the group and creating an enjoyable and productive atmosphere. Elias and Michael, thank you for making our little corner office an atmosphere from which we could all benefit. Markus and Nadja, thank you for all the helpful comments and ideas throughout our weekly meetings. Toni, thank you for your energy and inspiring ideas, they have never failed to motivate me. Laurie, thank you for making quick progress on our joint project possible and satisfying. Many thanks also to Ellen, for always being helpful; to Stefan for making the lunchtime walks memorable and the coffee breaks possible; and to Apostolos and Xiaoxiao for the stimulating conversations.

Markus, thank you for your incredible help with proofreading this dissertation, suggesting improvements, and for translating the *Zusammenfassung* into German. I also thank Michael Sieber for agreeing to be my mentor, and for his helpful advice on some of my research projects.

I am grateful to the DFG and DynaTrait (GA 401/25-1) for making this research financially possible.

I would also like to thank the people who made Germany feel like home over the last few years. Elias, Janne, Julia, Markus and Sarah, Michael and Larissa, Moritz, thanks for the unforgettable moments during and after work. Momo and Daniel, thank you for the wonderful memories, and for being there when needed. Many thanks to our neighbors, Peter and Taylor, for your support, and for constantly being at our side (literally) during lockdown times; and to Suse, for your tireless efforts to create an environment in which everyone always felt welcome.

Arnaud, Alex, Bram, Jonas, ik ben jullie heel dankbaar voor onze vrienschap die tijd en ruimte moeiteloos overbrugt. Aan de familie Wouters, bedankt voor het advies doorheen de jaren, en om me altijd deel te laten voelen van jullie gezin. Kim, bedankt voor alle aanmoediging, inspiratie, en wijsheid.

Laurine en Rodric, bedankt voor jullie onvoorwaardelijke vriendschap, de onvergetelijke momenten, en om er altijd te zijn voor Charlotte en mij.

Mama, Papa, Maura, Oma, Opa, Hilde, jullie bedank ik om altijd in me te geloven, voor jullie onvoorwaardelijke liefde, jullie advies en steun, en voor een plek om altijd thuis te kunnen noemen.

Charlotte, wij begonnen samen aan dit avontuur, en komen samen aan het eindpunt. Bedankt om het de voorbije negen maanden aan één bureau met mij uit te houden. Bedankt voor alles.

Contents

Chapter 1

General introduction

Research on the diversity of species observed in natural systems has shown that biodiversity is rapidly declining almost everywhere on Earth (Worm et al., 2006; Pimm et al., 2014; Newbold et al., 2015). This decline is mainly due to increased anthropogenic influence on the environment: in particular, increased land usage for e.g. agriculture, pollution, and overfishing crucially affect biodiversity in a negative way (Brooks et al., 2002; Dudgeon et al., 2006; Butchart et al., 2010; Horváth et al., 2019). If we want to minimize the extent to which our activities are damaging to ecosystems and the services they provide, it is essential to understand the ways in which the drastic decline in biodiversity can affect the structure and behaviour of these ecosystems. This knowledge is crucial for developing effective ecosystem management and restoration strategies.

1.1   Biodiversity from a functional perspective

Biodiversity may refer to many different aspects of biological variety. Here, and in the chapters that follow, we will always approach biodiversity from a functional perspective. This means that individuals are grouped together into functional groups, according to the function they fulfill in the ecosystem. The morphological, physiological, or behavioral feature of an individual that is responsible for fulfilling this function is called a functional trait (Weithoff, 2003; McGill et al., 2006; Violle et al., 2007). This categorization of individuals into functional groups may be different from the taxonomic grouping into species, due to phenotypic plasticity, or other sources of natural variation in important traits, such as body size, between individuals of the same species.

   In this way, the functional diversity of species in an ecosystem can be seen as an important aspect of biodiversity. It becomes clear how biodiversity loss, through decreasing functional diversity, can severely disturb ecosystem functioning: the loss of a functional group of individuals from the system necessarily affects the corresponding ecosystem function. For example, it has been shown that removal of certain functional groups, such as all shrubs, from tiny lake islands severely affected several local ecosystem functions (Wardle and Zackrisson, 2005). By investigating these

interactions on several islands of different size, the authors highlight the context-dependency of this link: depending on the other species present in the ecosystem, removal of a functional group may have different effects.

By definition, functional traits affect the fitness of an individual in an ecosystem. Since most ecosystems contain a wide variety of coexisting species, certain functional traits must necessarily be negatively correlated with each other (Stearns, 1989; Ehrlich, 2019). Such trade-offs between functional traits are an essential part of a functional description of the mechanisms by which species interact with each-other. In general, trade-offs are expected to be multidimensional (Edwards, Klausmeier, and Litchman, 2011; Amado and Campos, 2019), but for practical reasons, most theoretical and experimental research into trade-offs has only considered the interaction of two functional traits. Nevertheless, many of these two-dimensional trade-offs are considered fundamental for explaining species coexistence (Chesson, 2000), such as a trade-off between the competitive ability for different nutrient types (Litchman et al., 2007), the defense-growth trade-off (Ehrlich, Kath, and Gaedke, 2020), or the gleaner-opportunist trade-off (Ryabov and Blasius, 2011).

Adopting such a trait-based functional perspective has thus proven highly informative in uncovering the mechanisms by which species interact with each other (Hillebrand and Matthiessen, 2009; Schmidtke, Gaedke, and Weithoff, 2010). Moreover, such mechanisms can be assumed to hold for many ecosystems in a general way, precisely because they are based on the interaction of functional groups and not precisely defined species.

Diversity-stability

The first quantitative mathematical research into the link between diversity and stability dates back to May (1973), whose approach showed how increasing diversity has a destabilizing effect on the dynamics of food webs. This result was directly opposite to the widespread belief at the time, and started the well-known diversity-stability debate in the following decades (McCann, 2000). Currently, at least some of the initial confusion around the attempts to reconcile these seemingly contradictory results has been cleared up by specifying exactly what is meant by the terms diversity and stability (Bodin and Wiman, 2004). In Chapters 2-4, diversity will always refer to functional diversity, which allows for investigation of changes in diversity without the confounding effect of changing species richness on food web dynamics (Duffy et al., 2007).

In an ecological context, stability often used to refer to the amount of variation experienced in time (McCann, 2000). This definition is, however, completely unrelated to how stability is used in a mathematical context, where it is often used to measure the "attractiveness" of a solution to a differential equation model (Strogatz, 1994). To make matters worse, stability has over time been used to denote a multitude of different vaguely related concepts (Pimm, 1984). For this reason, special care has been taken in Chapters 2-4 to make sure that terms related to stability are

always defined clearly, following the definitions suggested by Grimm and Wissel (1997).

1.2 Embracing dynamical complexity

There is an ever-growing amount of evidence from both theory and experiments that complex ecological systems frequently exhibit complex dynamical behavior. Yet, a large body of ecological theory only examines these systems in regions where linearization approximations hold. While this strategy has several practical advantages, such as the ability to calculate analytical solutions and fast calculation of numerical solutions, it ignores potentially crucial non-linear ecological mechanisms. This subsection contains an overview of some highly relevant phenomena that can only be seriously studied when the intrinsic non-linearity of ecological systems is not ignored. Even though it is generally impossible to calculate analytical solutions, and our intuitive expectation based on linear systems is often misleading, the ever-increasing availability of computing power makes going down this path exceedingly rewarding.

Cycles and chaos

An important debate in ecological theory concerns the authenticity of predator-prey cycles in real-word communities. Even the Lotka-Volterra predator-prey model (Lotka, 1925; Volterra, 1926), arguably the simplest one in structure, predicts that a predator-prey system can exhibit intrinsically driven cyclic behavior. This phenomenon has also routinely been observed in the field (e.g., the well-known Lynx-Snowshoe Hare cycle Elton and Nicholson, 1942) and in controlled lab environments (e.g., McCauley et al., 1999; Fussmann et al., 2000).

However, evidence that cycles do not result from external influences, such as spatial effects (Stenseth et al., 2004), and are persistent in time, remained inconclusive. Even though limit cycles can be attractive, in which case they constitute a non-linear stable dynamical state, they are often viewed as unstable from an ecological point of view. Naturally, when the amplitude of the limit cycle is such that part of the oscillation reaches unrealistically low biomasses, it cannot represent a physical solution of the system. However, the relevance of the underlying mechanisms in natural food webs is sometimes fundamentally contested. A simple heuristic argument is that, when populations are cycling, they may be particularly vulnerable to an external disturbance at the population minima. Thus, in the presence of quasi-constant stochastic disturbances, cycling populations are presumed not to exist perpetually in natural food webs (Rosenzweig, 1971; May, 1972). Recently, Blasius et al. (2020) showed that long-term persistence of predator-prey cycles is possible in a controlled microcosm environment, providing strong evidence for predator-prey cycles as a genuine ecological phenomenon and not simply a modeling artifact.

Extending simple predator-prey models to describe more complex communities causes the complexity of outcomes predicted by the model to increase correspondingly. In particular, as a result of the Poincaré-Bendixon theorem, the possible outcomes of a two-dimensional continuous dynamical system (such as a predator-prey system) are essentially restricted to either a fixed point, or a closed orbit (Strogatz, 1994). Dynamical systems in three or more dimensions can exhibit much more complex behavior, such as chaos. Chaotic behavior is indeed predicted by many simple ecological models (Hastings and Powell, 1991; Hastings et al., 1993; Rinaldi and De Feo, 1999; Vandermeer, 2004; Dakos et al., 2009), and has also been demonstrated in a controlled experimental microcosm (Becks et al., 2005).

In each of the four projects presented in this dissertation, cyclic behavior is prominently featured and plays a central role in uncovering important mechanisms regulating food web functioning.

Beyond bitrophic systems

Acquisition of the necessary resources for survival is a defining feature of any living organism. Predator-prey (or consumer-resource) interactions are therefore viewed as one of the most fundamental ways in which species interact with each other. This feeding interaction is so important that it alone lies at the basis of many fundamental concepts in ecology, such as food chains, food webs, and trophic levels.

Using a reductionist perspective, a vast amount of research has been performed into the interactions in a consumer-resource system in isolation, in order to describe the dynamics of complex food webs. Because of its relatively simple structure, detailed knowledge of such a system can accurately be obtained using mathematical models where analytical calculations are possible, such as the famous Lotka-Volterra predator-prey model (Lotka, 1925; Volterra, 1926), or the more intricate Rosenzweig-MacArthur model (Rosenzweig and MacArthur, 1963). Even when going beyond a simple consumer-resource system by allowing two diverse trophic levels to interact with each other, well-controlled experiments are possible and the models used to described them are still numerically tractable. This approach has been particularly successful in trying to understand how rapid evolution can affect the dynamics of an adaptive predator-prey system: microcosm lab experiments have been able to identify such eco-evolutionary processes resulting from the presence of multiple prey genotypes (Yoshida et al., 2003; Becks et al., 2010). In these experiments, it is observed how the more defended prey genotype is promoted when predation pressure is high, which affects the shape and phase relationships of predator-prey cycles (Hiltunen et al., 2014).

However, natural systems almost always consist of more than two trophic levels (Matsuno and Nobuaki, 1996). An accurate description of many important phenomena responsible for governing the dynamics of whole ecosystems, such as trophic

cascades, requires at least three trophic levels (Abdala-Roberts et al., 2019). Moreover, when studying a bitrophic system, the two trophic levels studied are necessarily the first and the second trophic level. But there is an enormous amount of evidence from field observations that interactions with higher trophic levels play a decisive role in determining the structure and functioning of the whole food web (Bruno and O'Connor, 2005; Pimm et al., 2014; Ehrlich and Gaedke, 2020).

Expanding our knowledge about bitrophic systems, and what happens when they become adaptive, to tritrophic systems is thus a very natural next step in gaining detailed understanding of the mechanisms that govern the dynamics and functioning of natural food webs. The increase in complexity that results from extending food web models to incorporate a third (potentially adaptive) trophic level manifests itself in a multitude of ways: not only are there more state variables and model parameters, but even in simple tritrophic models the dynamical possibilities are much more varied (Hastings and Powell, 1991; Rinaldi and De Feo, 1999). In the four chapters that follow, different approaches are taken in how to deal with the increased complexity of tritrophic models.

Alternative stable states

The presence of more than one stable state on which a system can be found is a well-known aspect of dynamical systems. Related phenomena, such as regime shifts and hysteresis are observed and presumed to exist in a wide variety of different ecosystems (Beisner, Haydon, and Cuddington, 2003; Scheffer and Carpenter, 2003; Schröder, Persson, and De Roos, 2005). Such transitions can rapidly alter the functioning of whole ecosystems, which may be problematic from an ecosystem services perspective. It is therefore of crucial importance that we understand the mechanisms which lead to the existence of alternative stable states. Doing so requires appropriate mathematical models that are sufficiently complex to be able to capture the relevant properties (Scheffer and Carpenter, 2003). Another large area of research concerns attempting to predict whether a regime shift is about to happen. By identifying indications in the system's dynamics that the tipping point is near, early warning signals may be applied to real-world data to estimate the likelihood of a regime shift in the near future (Kéfi et al., 2014; Dakos et al., 2019).

We will explicitly consider the dynamics and global implications of any alternative stable states present, by taking special care to investigate the complete phase space of the food webs studied in Chapters 2-4.

1.3 Adaptive food webs

In Chapters 2-4, different aspects of the functioning of tritrophic food webs are studied, depending on the amount of functional diversity contained within. The fundamental idea behind the modeling approach, outlined below, is the same.

The starting point for ensuring coexistence of multiple types per trophic level are the trade-offs between their functional traits. In Chapters 2 and 4, based on Tirok and Gaedke (2010), we assume that each prey type faces a trade-off between their maximum growth rate, and their defense against predation; and each consumer type faces a trade-off between their prey spectrum and their ability to exploit low prey densities. In Chapter 3 only the defense-growth trade-off is adopted for both prey and consumers to create a slightly simplified food web structure. In any case, out-competition of any one species by another is thus prevented by the existence of sufficient ecological niches. Inspiration for the structure of these food webs was drawn from interactions of complex plankton communities. Planktonic micro-organisms have developed several strategies to prevent consumption, such as shell or colony formation, or behavioral changes (Litchman and Klausmeier, 2008; Pančić and Kiørboe, 2018). The specific way in which an individual's growth rate is affected differs between each strategy, but a general negative relationship is observed (Litchman et al., 2007).

In Chapters 2 and 4, functional diversity within trophic levels is controlled by the trait difference parameter Δ which applies to all trophic levels simultaneously. In Chapter 3, the functional diversity can be set on each trophic level individually through the trait difference parameters Δ_B, Δ_I and Δ_T for the basal (B), intermediate (I), and top (T) levels, respectively. A schematic example for how the trait difference parameter sets the trait values on a trophic level is given for the basal trophic level in Fig. 1.1 (left panels). When $\Delta_B = 0$, both types' trait values are equal (cross in Fig. 1.1, bottom left). Increasing Δ_B moves the two types in opposite directions on the trade-off curve. The same principle applies for trade-offs between other traits, see Fig. 2.1, Chapter 2.

While these trait difference parameters can be changed to influence the food web structure, there are no internal mechanisms which can modify them. They are a parameter of the differential equations, and not a state variable. This approach differs from a quantitative trait approach, where the trait values are state variables themselves and thus directly impact the model dynamics (such as in e.g. Mougi and Iwasa, 2011; Klauschies, Vasseur, and Gaedke, 2016; Van Velzen and Gaedke, 2017; Raatz, Velzen, and Gaedke, 2019). Importantly, this does not imply that the models presented here are not adaptive. In our case, the trait response to internal or environmental changes lies in shifts of the mean trait value from a community perspective (Fig. 1.1, right side). In this example, the increased predation intensity due to the dominance of the undefended prey type B_u causes the fitness of the defended prey type to increase, ultimately shifting the mean defense of the basal level upwards. The range between which the mean trait value can shift is set by the corresponding trait difference parameter (Fig. 1.1, bottom right).

Trade-off structure on basal
trophic level

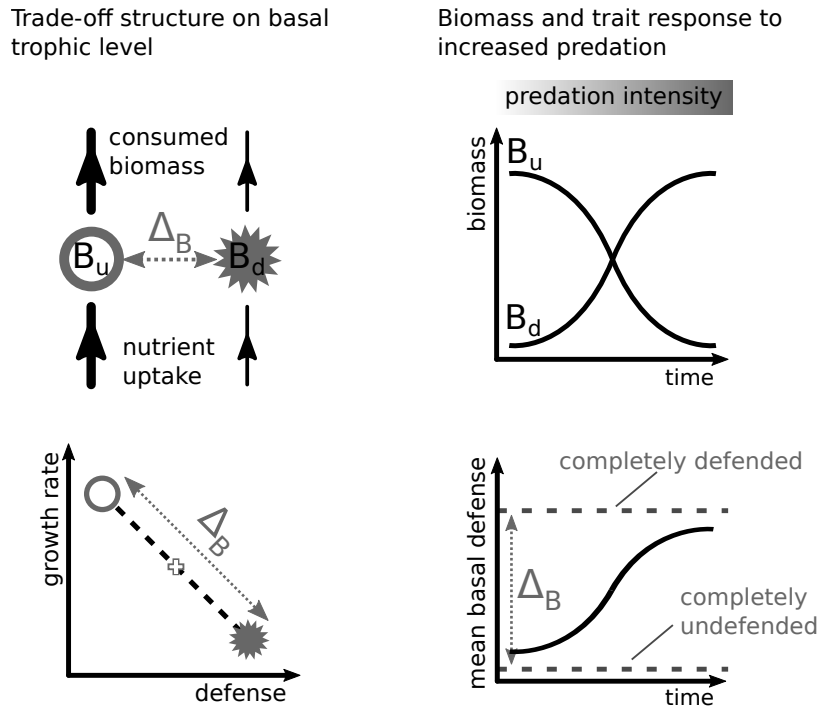Biomass and trait response to
increased predation

FIGURE 1.1: Schematic overview of the response of an adaptive basal trophic level to increased predation pressure. One way for two types of basal species to coexist is to assume a trade-off between their defense against predation and their growth rate. The undefended basal type (B_u) thus has a higher growth rate, but faces higher consumption rates than the defended basal type (B_d) (top left). The basal trait difference Δ_B controls the position of B_u and B_d on the defense-growth trade-off curve, such that when $\Delta_B = 0$ both types have the same intermediate trait values, marked by the cross (bottom left). This implies that, when predation pressure is low, B_u is dominant due to its higher competitiveness for nutrients. In a complex community, this abundance of easily consumable prey would lead to an increase in consumer biomass. The gradually increasing predation pressure on the basal level then increases the relative fitness of B_d, eventually making it the dominant type when predation pressure is very high (top right). In this way, he basal level can adapt to changing circumstances by a shift in its mean defense, which can change between the trait values of B_u (basal level is completely undefended) and B_d (basal level is completely defended) (bottom right).

1.4 Thesis overview

In the following four chapters of this dissertation, the mechanisms behind the functioning of tritrophic food webs will be investigated from different angles. We will start with a detailed investigation of the role of functional diversity in a food web that is adaptive at every trophic level in Chapter 2. In Chapter 3, we generalized these results to a collection of tritrophic food webs with different structure. In Chapter 4, we return to the model used in Chapter 2, and investigate its response to a nutrient pulse perturbation, and the role played by diversity, in more detail. Finally, in Chapter 5, inspired by the phase relationships between predator-prey pairs in the complex food web described in Chapter 2, we investigate these relationships in two very simple systems without any diversity. A more detailed overview of each chapter is found below.

Chapter 2

In this chapter we investigated how increasing trait variation on all trophic levels in a tritrophic food web influences its dynamics and important functions such as biomass production, temporal variation and the resilience of alternative stable states. Notably, it is the first study to provide a mechanistic understanding of how diversity affects these ecosystem functions in a food web with diversity on 3 trophic levels (B, I, and T). This study was published in Scientific Reports (Ceulemans et al., 2019).

We show that, independent on the amount of diversity in the food web, the system contains two alternative stable states. In the high-production (HP) state, the nutrients are efficiently exploited, the biomass on the top trophic level is high, and the temporal variation of the biomass dynamics is low. In contrast, in the low-production (LP) state the free nutrient concentration is much higher, the top trophic level biomass is lower, and the temporal variation is higher. Detailed examination of the phase relationships between the different populations in the food web reveals the difference in top-down control and the trait-separated compensatory dynamical patterns which lead to the differences between the states.

By comparing the sizes of the basin of attraction of the two states, we found that a highly diverse system is primarily in the HP state, whereas the LP state is preferred when diversity is low. Importantly, a reduction in diversity may cause an irreversible transition to occur from the HP to the LP state.

Chapter 3

To achieve results of high generality, the approach taken in Chapter 2 was modified to compare functioning of tritrophic food webs in which the diversity on each trophic level can be set independently of the diversity on the other levels. To overcome the additional dependence of any relationship between diversity and functioning on model parameters, and allow for the possibility of alternative stable states, $128,000$ randomly selected parameter combinations were investigated, each for 200 randomly selected initial conditions. Analysis of this data was aided by using a Random Forest machine learning model. This study is currently under review at Ecology (original decision: major revision), and is available on bioRxiv (Ceulemans, Guill, and Gaedke, 2020). Our method provides context-free information on the relationship between the biomasses, temporal variation, and biomass production efficiency of the different trophic levels, as a function of the diversity on each trophic level separately.

We find that, only when diversity is high everywhere in the food web, simultaneously operating bottom-up and top-down interactions synergize to provide efficient biomass transfer to the top trophic level. We also observe the generality of the complex relationship between diversity and temporal variation: initially, variation decreases with diversity, but as the system becomes more complex the temporal

variation increases again. The parameter importance estimates provided by the random forest also shows that the parameters affecting the top level, including the top functional diversity, are of the highest importance in determining the biomass and temporal variation of all trophic levels.

Chapter 4

In this chapter, we examined how eutrophication, in the form of a nutrient pulse perturbation, affects the resistance, resilience and elasticity of a tritrophic system, based on the food web model used in Chapter 2. By comparing a food chain to an adaptive food web, we examine the influence of functional diversity on these effects.

We find that these three quantities provide complementary information on the changes in dynamics and functioning of both the food chain and the food web, and show that the system's response is affected by the type and shape of the dynamical attractor at which the perturbation is applied. By studying the transient dynamics after the perturbation in detail, we are able to identify important differences between the response of an adaptive food web and a food chain, which ultimately affect the resistance, resilience and elasticity. We also show the importance of sufficient top-down control on the intermediate level, which is higher in the adaptive food web, in dampening the system's response.

Chapter 5

Using highly suggestive results from Chapter 2, we investigated whether the observed correlation between the interaction strength of a consumer-resource pair in a complex food web, and their relative phase relationship, holds for simpler and more tractable communities. It is often claimed that in a "purely ecological system" (i.e., no evolution is possible) where resource and consumer exhibit oscillatory behavior, the consumer always lags behind the resource by a quarter of a cycle. However, our results show that, even in simple purely ecological systems, deviations from this rule are common and depend on how strongly the resource and consumer are interacting with each other. We thus claim that a deviation from the quarter-cycle-lag "rule" does not necessarily mean that evolution has occurred in the system, and caution should be taken when carelessly attributing such a deviation to eco-evolutionary effects rather than purely ecological processes.

1.5 Declaration of contributions

Chapter 2: *"The effects of functional diversity on biomass production, variability, and resilience of ecosystem functions in a tritrophic system"*

Authors: Ruben Ceulemans, Ursula Gaedke, Toni Klauschies, & Christian Guill
Published in *Scientific Reports* (2019).

Theoretical work and numerical simulations were carried out by R.C., under joint supervision of C.G. and U.G. The initial project outline was developed by U.G., C.G., and T.K. The manuscript was written by R.C., in close cooperation with T.K., and with valuable feedback by C.G. and U.G.

Chapter 3: *"Top predators govern multitrophic diversity effects in tritrophic food webs"*

Authors: Ruben Ceulemans, Christian Guill, & Ursula Gaedke
Under review at *Ecology* (original decision: major revision).

Development of the project idea was performed by R.C., C.G., and U.G. Theoretical and numerical work and data analysis were performed by R.C., under joint supervision of C.G. and U.G. Writing of the manuscript was performed by R.C., in close cooperation with U.G., and with valuable feedback from C.G.

Chapter 4: *"Functional diversity alters the effects of a nutrient pulse on food web resistance, resilience, and elasticity"*

Authors: Ruben Ceulemans*, Laurie Anne Wojcik*, & Ursula Gaedke
*: Equally contributing authors
To be submitted.

Numerical simulations and analysis of the results were performed by R.C. and L.W., under supervision of U.G. The initial project outline was developed by R.C. and U.G. The manuscript was written by R.C. and L.W., with valuable feedback from U.G.

Chapter 5: *"Phase relationships in consumer-resource systems"*

To be submitted as part of a two-part study.
Authors: Ruben Ceulemans*, Christian Guill*, Michael Raatz, & Ellen van Velzen
*: Equally contributing authors

The following statement of author contributions refers only to the part of the study that is presented in this chapter, not to the entire (yet to be finalized) study.
The initial idea was conceived by all four authors. Theoretical work was performed by R.C. and C.G., literature research was performed by R.C. and M.R., and numerical simulations were performed by R.C., in close cooperation with M.R., and with valuable feedback from C.G. and E.V. The chapter was written by R.C., with valuable feedback from M.R. and C.G.

Potsdam, December 15th 2020

Ruben Ceulemans   Prof. Dr. Ursula Gaedke

References

Abdala-Roberts, L. et al. (2019). "Tri-trophic interactions: bridging species, communities and ecosystems". In: *Ecology Letters*. DOI: 10.1111/ele.13392.

Amado, A. and Campos, P. R. (2019). "Ecological specialization under multidimensional trade-offs". In: *Evolutionary Ecology* 33.6, pp. 769–789. DOI: 10.1007/s10682-019-10013-4.

Becks, L., Ellner, S. P., Jones, L. E., and Hairston Nelson G., J. G. (2010). "Reduction of adaptive genetic diversity radically alters eco-evolutionary community dynamics". In: *Ecology Letters* 13.8, pp. 989–997. DOI: 10.1111/j.1461-0248.2010.01490.x.

Becks, L., Hilker, F. M., Malchow, H., Jürgens, K., and Arndt, H. (2005). "Experimental demonstration of chaos in a microbial food web". In: *Nature* 435.7046, pp. 1226–1229. DOI: 10.1038/nature03627.

Beisner, B. E., Haydon, D. T., and Cuddington, K. (2003). "Alternative stable states in ecology". In: *Frontiers in Ecology and the Environment* 1.7, pp. 376–382. DOI: 10.1890/100071.

Blasius, B., Rudolf, L., Weithoff, G., Gaedke, U., and Fussmann, G. F. (2020). "Long-term cyclic persistence in an experimental predator–prey system". In: *Nature* 577.7789, pp. 226–230. DOI: 10.1038/s41586-019-1857-0.

Bodin, P. and Wiman, B. L. B. (2004). "Resilience and other stability concepts in ecology: notes on their origin , validity". In: *ESS Bulletin* 2.2, pp. 33–43.

Brooks, T. M. et al. (2002). "Habitat loss and extinction in the hotspots of biodiversity". In: *Conservation Biology* 16.4, pp. 909–923. DOI: 10.1046/j.1523-1739.2002.00530.x.

Bruno, J. F. and O'Connor, M. I. (2005). "Cascading effects of predator diversity and omnivory in a marine food web". In: *Ecology Letters* 8.10, pp. 1048–1056. DOI: 10.1111/j.1461-0248.2005.00808.x.

Butchart, S. H. et al. (2010). "Global biodiversity: Indicators of recent declines". In: *Science* 328.5982, pp. 1164–1168. DOI: 10.1126/science.1187512.

Ceulemans, R., Gaedke, U., Klauschies, T., and Guill, C. (2019). "The effects of functional diversity on biomass production, variability, and resilience of ecosystem functions in a tritrophic system". In: *Scientific Reports* 9.1. DOI: 10.1038/s41598-019-43974-1.

Ceulemans, R., Guill, C., and Gaedke, U. (2020). "Top predators govern multitrophic diversity effects in tritrophic food webs". In: *bioRxiv*, p. 2020.07.31.230375. DOI: 10.1101/2020.07.31.230375.

Chesson, P. (2000). "Mechanisms of maintenance of species diversity". In: *Annual Review of Ecology and Systematics* 31, pp. 343–366. DOI: 10.1146/annurev.ecolsys.31.1.343.

Dakos, V., Benincà, E., Van Nes, E. H., Philippart, C. J., Scheffer, M., and Huisman, J. (2009). "Interannual variability in species composition explained as seasonally entrained chaos". In: *Proceedings of the Royal Society B: Biological Sciences* 276.1669, pp. 2871–2880. DOI: 10.1098/rspb.2009.0584.

Dakos, V., Matthews, B., Hendry, A. P., Levine, J., Loeuille, N., Norberg, J., Nosil, P., Scheffer, M., and De Meester, L. (2019). "Ecosystem tipping points in an evolving world". In: *Nature Ecology and Evolution* 3.3, pp. 355–362. DOI: 10.1038/s41559-019-0797-2.

Dudgeon, D. et al. (2006). "Freshwater biodiversity: Importance, threats, status and conservation challenges". In: *Biological Reviews of the Cambridge Philosophical Society* 81.2, pp. 163–182. DOI: 10.1017/S1464793105006950.

Duffy, J. E., Cardinale, B. J., France, K. E., McIntyre, P. B., Thébault, E., and Loreau, M. (2007). "The functional role of biodiversity in ecosystems: Incorporating trophic complexity". In: *Ecology Letters* 10.6, pp. 522–538. DOI: 10.1111/j.1461-0248.2007.01037.x.

Edwards, K. F., Klausmeier, C. A., and Litchman, E. (2011). "Evidence for a three-way trade-off between nitrogen and phosphorus competitive abilities and cell size in phytoplankton". In: *Ecology* 92.11, pp. 2085–2095. DOI: 10.1890/11-0395.1.

Ehrlich, E. (2019). "On the Role of Trade-offs in Predator-Prey Interactions". PhD thesis. University of Potsdam. DOI: https://doi.org/10.25932/publishup-43063.

Ehrlich, E. and Gaedke, U. (2020). "Coupled changes in traits and biomasses cascading through a tritrophic plankton food web". In: *Limnology and Oceanography*, lno.11466. DOI: 10.1002/lno.11466.

Ehrlich, E., Kath, N. J., and Gaedke, U. (2020). "The shape of a defense-growth trade-off governs seasonal trait dynamics in natural phytoplankton". In: *ISME Journal*, pp. 1451–1462. DOI: 10.1038/s41396-020-0619-1.

Elton, C. and Nicholson, M. (1942). "The Ten-Year Cycle in Numbers of the Lynx in Canada". In: *The Journal of Animal Ecology* 11.2, p. 215. DOI: 10.2307/1358.

Fussmann, G. F., Ellner, S. P., Shertzer, K. W., and Hairston, J. (2000). "Crossing the hopf bifurcation in a live predator-prey system". In: *Science* 290.5495, pp. 1358–1360. DOI: 10.1126/science.290.5495.1358.

Grimm, V. and Wissel, C. (1997). "Babel, or the ecological stability discussions: An inventory and analysis of terminology and a guide for avoiding confusion". In: *Oecologia* 109.3, pp. 323–334. DOI: 10.1007/s004420050090.

Hastings, A., Hom, C. L., Ellner, S., Turchin, P., and Godfray, H. C. (1993). "Chaos in ecology: Is mother nature a strange attractor?" In: *Annual Review of Ecology and Systematics* 24, pp. 1–33. DOI: 10.1146/annurev.es.24.110193.000245.

Hastings, A. and Powell, T. (1991). "Chaos in a three-species food chain". In: *Ecology* 72.3, pp. 896–903. DOI: 10.2307/1940591.

Hillebrand, H. and Matthiessen, B. (2009). "Biodiversity in a complex world: Consolidation and progress in functional biodiversity research". In: *Ecology Letters* 12.12, pp. 1405–1419. DOI: 10.1111/j.1461-0248.2009.01388.x.

Hiltunen, T., Hairston, N. G., Hooker, G., Jones, L. E., and Ellner, S. P. (2014). "A newly discovered role of evolution in previously published consumer-resource dynamics". In: *Ecology Letters* 17.8, pp. 915–923. DOI: 10.1111/ele.12291.

Horváth, Z., Ptacnik, R., Vad, C. F., and Chase, J. M. (2019). "Habitat loss over six decades accelerates regional and local biodiversity loss via changing landscape connectance". In: *Ecology Letters* 22.6, pp. 1019–1027. DOI: 10.1111/ele.13260.

Kéfi, S., Guttal, V., Brock, W. A., Carpenter, S. R., Ellison, A. M., Livina, V. N., Seekell, D. A., Scheffer, M., Van Nes, E. H., and Dakos, V. (2014). "Early warning signals of ecological transitions: Methods for spatial patterns". In: *PLoS ONE* 9.3, e92097. DOI: 10.1371/journal.pone.0092097.

Klauschies, T., Vasseur, D. A., and Gaedke, U. (2016). "Trait adaptation promotes species coexistence in diverse predator and prey communities". In: *Ecology and Evolution* 6.12, pp. 4141–4159. DOI: 10.1002/ece3.2172.

Litchman, E. and Klausmeier, C. A. (2008). "Trait-Based Community Ecology of Phytoplankton". In: *Annual Review of Ecology, Evolution, and Systematics* 39.1, pp. 615–639. DOI: 10.1146/annurev.ecolsys.39.110707.173549.

Litchman, E., Klausmeier, C. A., Schofield, O. M., and Falkowski, P. G. (2007). "The role of functional traits and trade-offs in structuring phytoplankton communities: Scaling from cellular to ecosystem level". In: *Ecology Letters* 10.12, pp. 1170–1181. DOI: 10.1111/j.1461-0248.2007.01117.x.

Lotka, A. J. (1925). "Elements of Physical Biology". In:

Matsuno, K. and Nobuaki, O. (1996). "How many trophic levels are there?" In: *Journal of Theoretical Biology* 180.2, pp. 105–109. DOI: 10.1006/jtbi.1996.0085.

May, R. M. (1972). "Limit cycles in predator-prey communities". In: *Science* 177.4052, pp. 900–902. DOI: 10.1126/science.177.4052.900.

May, R. M. (1973). *Stability and complexity in model ecosystems*. Vol. 6. New Jersey: Princeton University Press. DOI: 10.2307/3743.

McCann, K. S. (2000). "The diversity–stability debate". In: *Nature* 405.6783, pp. 228–233. DOI: 10. 1038/35012234.

McCauley, E., Nisbet, R. M., Murdoch, W. W., De Roos, A. M., and Gurney, W. S. (1999). "Large-amplitude cycles of Daphnia and its algal prey in enriched environments". In: *Nature* 402.6762, pp. 653–656. DOI: 10.1038/45223.

McGill, B. J., Enquist, B. J., Weiher, E., and Westoby, M. (2006). "Rebuilding community ecology from functional traits". In: *Trends in Ecology and Evolution* 21.4, pp. 178–185. DOI: 10.1016/j.tree. 2006.02.002.

Mougi, A. and Iwasa, Y. (2011). "Unique coevolutionary dynamics in a predator-prey system". In: *Journal of Theoretical Biology* 277.1, pp. 83–89. DOI: 10.1016/j.jtbi.2011.02.015.

Newbold, T. et al. (2015). "Global effects of land use on local terrestrial biodiversity". In: *Nature* 520.7545, pp. 45–50. DOI: 10.1038/nature14324.

Pančić, M. and Kiørboe, T. (2018). "Phytoplankton defence mechanisms: traits and trade-offs". In: *Biological Reviews* 93.2, pp. 1269–1303. DOI: 10.1111/brv.12395.

Pimm, S. L., Jenkins, C. N., Abell, R., Brooks, T. M., Gittleman, J. L., Joppa, L. N., Raven, P. H., Roberts, C. M., and Sexton, J. O. (2014). "The biodiversity of species and their rates of extinction, distribution, and protection". In: *Science* 344.6187. DOI: 10.1126/science.1246752.

Pimm, S. L. (1984). "The complexity and stability of ecosystems". In: *Nature* 307, pp. 321–307.

Raatz, M., Velzen, E. van, and Gaedke, U. (2019). "Co-adaptation impacts the robustness of predator–prey dynamics against perturbations". In: *Ecology and Evolution* 9.7, pp. 3823–3836. DOI: 10. 1002/ece3.5006.

Rinaldi, S. and De Feo, O. (1999). "Top-predator abundance and chaos in tritrophic food chains". In: *Ecology Letters* 2.1, pp. 6–10. DOI: 10.1046/j.1461-0248.1999.21035.x.

Rosenzweig, M. L. and MacArthur, R. H. (1963). "Graphical Representation and Stability Conditions of Predator-Prey Interactions". In: *The American Naturalist* 97.895, pp. 209–223. DOI: 10.1086/ 282272.

Rosenzweig, M. L. (Jan. 1971). "Paradox of Enrichment: Destabilization of Exploitation Ecosystems in Ecological Time". In: *Science* 171.3969, pp. 385–387. DOI: 10.1126/science.171.3969.385.

Ryabov, A. B. and Blasius, B. (2011). "A graphical theory of competition on spatial resource gradients". In: *Ecology Letters* 14.3, pp. 220–228. DOI: 10.1111/j.1461-0248.2010.01574.x.

Scheffer, M. and Carpenter, S. R. (2003). "Catastrophic regime shifts in ecosystems: Linking theory to observation". In: *Trends in Ecology and Evolution* 18.12, pp. 648–656. DOI: 10.1016/j.tree.2003. 09.002.

Schmidtke, A., Gaedke, U., and Weithoff, G. (2010). "A mechanistic basis for underyielding in phytoplankton communities". In: *Ecology* 91.1, pp. 212–221. DOI: 10.1890/08-2370.1.

Schröder, A., Persson, L., and De Roos, A. M. (2005). "Direct experimental evidence for alternative stable states: A review". In: *Oikos* 110.1, pp. 3–19. DOI: 10.1111/j.0030-1299.2005.13962.x.

Stearns, S. C. (1989). "Trade-Offs in Life-History Evolution". In: *Functional Ecology* 3, pp. 259–268.

Stenseth, N. C., Ehrich, D., Rueness, E. K., Lingjærde, O. C., Chan, K. S., Boutin, S., O'Donoghuell, M., Robinson, D. A., Viljugrein, H., and Jakobsen, K. S. (2004). "The effect of climatic forcing on population synchrony and genetic structuring of the Canadian lynx". In: *Proceedings of the National Academy of Sciences of the United States of America* 101.16, pp. 6056–6061. DOI: 10.1073/ pnas.0307123101.

Strogatz, S. H. (1994). *Nonlinear Dynamics and Chaos: With Applications to Physics, Biology, Chemistry and Engineering*. Westview Press.

Tirok, K. and Gaedke, U. (2010). "Internally driven alternation of functional traits in a multispecies predator- prey system". In: *Ecology* 91.6, pp. 1748–1762. DOI: 10.1890/09-1052.1.

Van Velzen, E. and Gaedke, U. (2017). "Disentangling eco-evolutionary dynamics of predator-prey co-evolution: The case of antiphase cycles". In: *Scientific Reports* 7.1, p. 17125. DOI: 10.1038/s41598-017-17019-4.

Vandermeer, J. (2004). "Coupled Oscillations in Food Webs: Balancing Competition and Mutualism in Simple Ecological Models". In: *The American Naturalist* 163.6, pp. 857–867. DOI: 10.1086/420776.

Violle, C., Navas, M.-L., Vile, D., Kazakou, E., Fortunel, C., Hummel, I., and Garnier, E. (2007). "Let the concept of trait be functional!" In: *Oikos* 116.5, pp. 882–892. DOI: 10.1111/j.2007.0030-1299.15559.x.

Volterra, V. (1926). "Variazioni e fluttuazioni del numero d'individui in specie animali conviventi". In: *Mem. Acad. Lincei Roma.* 2, pp. 31–113.

Wardle, D. A. and Zackrisson, O. (2005). "Effects of species and functional group loss on island ecosystem properties". In: *Nature* 435.7043, pp. 806–810. DOI: 10.1038/nature03611.

Weithoff, G. (2003). "The concepts of 'plant functional types' and 'functional diversity' in lake phytoplankton – a new understanding of phytoplankton ecology?" In: *Freshwater Biology* 48.9, pp. 1669–1675.

Worm, B. et al. (2006). "Impacts of Biodiversity Loss on Ocean Ecosystem Services". In: *Science* 314.5800, pp. 787–790. DOI: 10.1126/science.1132294.

Yoshida, T., Jones, L. E., Ellner, S. P., Fussmann, G. F., and Hairston, N. G. (2003). "Rapid evolution drives ecological dynamics in a predator-prey system". In: *Nature* 424.6946, pp. 303–306. DOI: 10.1038/nature01767.

Chapter 2

The effects of functional diversity on biomass production, variability, and resilience of ecosystem functions in a tritrophic system

Ruben Ceulemans, Ursula Gaedke, Toni Klauschies, & Christian Guill
Published in Scientific Reports: 9, Article number: 7541 (2019)

Abstract

Diverse communities can adjust their trait composition to altered environmental conditions, which may strongly influence their dynamics. Previous studies of trait-based models mainly considered only one or two trophic levels, whereas most natural system are at least tritrophic. Therefore, we investigated how the addition of trait variation to each trophic level influences population and community dynamics in a tritrophic model. Examining the phase relationships between species of adjacent trophic levels informs about the strength of top-down or bottom-up control in non-steady-state situations. Phase relationships within a trophic level highlight compensatory dynamical patterns between functionally different species, which are responsible for dampening the community temporal variability. Furthermore, even without trait variation, our tritrophic model always exhibits regions with two alternative states with either weak or strong nutrient exploitation, and correspondingly low or high biomass production at the top level. However, adding trait variation increased the basin of attraction of the high-production state, and decreased the likelihood of a critical transition from the high- to the low-production state with no apparent early warning signals. Hence, our study shows that trait variation enhances resource use efficiency, production, stability, and resilience of entire food webs.

2.1 Introduction

Functional diversity has proven to be important for linking community structure to ecosystem functions such as biomass production and resource use efficiency (Hooper et al., 2005; Tilman, Reich, and Knops, 2006; Worm et al., 2006; Schneider et al., 2016). Our understanding of the multifaceted impact of functional diversity on ecosystem functioning, and on the dynamics of populations and communities, has been greatly advanced by adopting a trait-based point of view (Hillebrand and Matthiessen, 2009; Krause et al., 2014). In particular, functional traits link morphological, physiological or phenological features of a species to a certain community or ecosystem function (Violle et al., 2007). A prevalent example is simply body size, which is related to several functions such as growth (larger organisms tend to grow slower), prey preference (predators tend to be larger than their prey), or nutrient uptake (larger cells have higher nutrient demands) (Weithoff, 2003; Brown et al., 2004; Brose, Williams, and Martinez, 2006; Litchman et al., 2007). Trait-based models of simple food web modules have facilitated detailed mechanistic understanding of dynamics observed in the laboratory (Ellner and Becks, 2011) and in the field (Tirok and Gaedke, 2010). For example, observed anti-phase predator-prey cycles between zooplankton and algae have been attributed to the co-occurrence of fast-growing undefended and slow growing, well defended prey phenotypes(Yoshida et al., 2003; Becks et al., 2010).

However, such trait-based models have mainly been restricted to describing trait variation on one or two trophic levels (Abrams and Matsuda, 1996; Litchman and Klausmeier, 2008; Tirok and Gaedke, 2010; Erbach, Lutscher, and Seo, 2013). Likewise, only up until recently, empirical studies on functional diversity have been limited to considering trait variation in only autotrophs (plants or algae) (Duffy, 2002; Gamfeldt et al., 2015), or both autotrophs and herbivores (Steiner et al., 2005; Filip et al., 2014), with few exceptions (Rasher, Hoey, and Hay, 2013). This strongly contrasts with the fact that natural food webs are in general complex multitrophic networks (Digel et al., 2014). Focusing only on direct, bitrophic predator-prey interactions neglects the intricate effects of more complex, partly indirect interactions spanning multiple trophic levels, such as trophic cascades (Levine et al., 2017) . These multi-trophic effects may be very important factors affecting the relevant ecosystem functions (Peet, Deutsch, and Peacock-López, 2005; Nakazawa, 2011; Golubski et al., 2016). For instance, the total number of trophic levels may strongly influence the efficiency of nutrient exploitation (Wang and Brose, 2018). In addition, as predation is an important factor in many food webs, trait variation on the predator level is expected to have an important influence on ecosystem functioning (Tilman, Isbell, and Cowles, 2014; Gamfeldt et al., 2015; Schneider et al., 2016). Hence, including additional trophic levels with functional diversity is a very natural step towards improving the accuracy and descriptive power of trait-based models.

We developed a tritrophic model to study the effects of trait variation at all
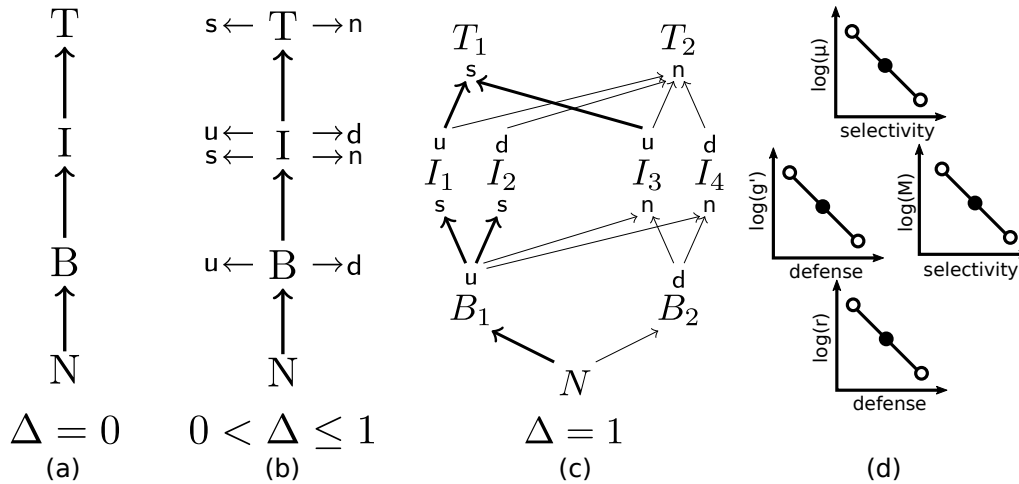
FIGURE 2.1: *(a) A simple linear tritrophic chain, where nutrients N are taken up by a basal species B, which is grazed by an intermediate species I, which in turn is consumed by a top species T. (b) Gradually introducing trait variation, where species can be undefended (u) or defended (d) against predators, and/or selective (s) or non-selective (n) consumers, starting from a linear chain. (c) Maximally trait-separated food web model. The basal and top species have only one trait, but the intermediate species have two. The thickness of the arrows indicates the intensity of the trophic interaction, reflecting that selective consumers can exploit their limited resources spectrum more efficiently. (d) Schematic shape of the trade-off curves for the top species (top row), intermediate species (middle row), and basal species (bottom row). The solid circles indicate that for $\Delta = 0$, all species on a given trophic level have the same trait values, whereas the open circles demonstrate how the trait values between the species differ as Δ is increased to one.*

trophic levels on food web dynamics. Particularly, the dynamics of a simple tritrophic linear food chain will be compared to a tritrophic food web where prey species are either defended or undefended, and predator species are either selective or non-selective feeders. Trade-offs between these traits are explicitly built in such that defended prey have a lower growth rate, and selective feeders have a lower half-saturation constant to allow for efficient feeding at low prey densities (Tirok and Gaedke, 2010; Coutinho, Klauschies, and Gaedke, 2016; Van Velzen and Gaedke, 2017). Our model structure allows for a gradual increase of the trait differences between the species at each trophic level, from a simple linear chain up to a fully separated food web with maximal trait differences (Fig. 2.1). As the trait differences increase, the species will fulfill increasingly different functions; in this way, we are able to link trait differences to functional diversity.

We use the tritrophic model to investigate how an increasing degree of trait variation affects:

- the production of the system,

- the efficiency of the energy transfer towards the higher trophic levels,

- the temporal biomass variability at the population and community level, and

- the dynamic properties and the resilience of alternative stable system states.

Our results provide theoretical evidence that trait variation has a significant impact on all of these properties. To the best of our knowledge, we present the first

systematic, multi-trophic study which mechanistically explains such patterns and explicitly discusses their relevance to ecosystem functions and stability.

2.2 Methods

We developed a tritrophic model where basal species are consumed by intermediate species, which in turn are consumed by top species. The species biomass densities are denoted by respectively B, I, and T. In addition, the uptake of a limiting nutrient with concentration N (in this case nitrogen) by the basal species is modeled explicitly. We assume a chemostat environment, which causes all nutrients and biomass of species to be washed out at an equal rate, δ, the dilution rate. The washed out volume is replaced by new medium rich in nutrients.

Model equations

As in (Tirok and Gaedke, 2010; Bauer et al., 2014), we include two relevant functional traits. The prey species B and I may be defended against predation: specifically, there will be defended (d) and undefended (u) species. Investing in a defense strategy requires sacrificing a certain amount of resources which could have otherwise been put into growth. Hence, the defended species have a lower growth rate than the undefended species, but are rewarded by being insusceptible to certain consumers. The consumer species I and T are able to specialize feeding on a certain prey species, leading to selective (s) and non-selective (n) species. Here, the non-selective consumer species consume all species on the trophic level below. In contrast, the selective species are only able to consume the undefended prey species, but they are able to exploit low food densities at a higher rate, reflected in a lower half-saturation constant.

Representing each possible trait combination on all trophic levels by one species leads to a food web with two basal species, four intermediate species and two top species (Fig. 2.1c). In order to write down the equations compactly, the following equivalence is explicitly stated:

$$B^{\mathsf{u}} \equiv B_1, \quad B^{\mathsf{d}} \equiv B_2, \quad I_{\mathsf{s}}^{\mathsf{u}} \equiv I_1, \quad I_{\mathsf{s}}^{\mathsf{d}} \equiv I_2 \tag{2.1}$$

$$I_{\mathsf{n}}^{\mathsf{u}} \equiv I_3, \quad I_{\mathsf{n}}^{\mathsf{d}} \equiv I_4, \quad T_{\mathsf{s}} \equiv T_1, \quad T_{\mathsf{n}} \equiv T_2. \tag{2.2}$$

In their most general form, the equations used have the following shape:

$$\begin{cases} \dot{N} & = \delta(N_0 - N) - \dfrac{c_N}{c_C} \sum_i r_i B_i \\[2mm] \dot{B}_i & = r_i B_i - \sum_j g_{ji} I_j - \delta B_i \\[2mm] \dot{I}_j & = e \sum_i g_{ji} I_j - \sum_i \gamma_{ij} T_i - \delta I_j \\[2mm] \dot{T}_i & = \epsilon \sum_j \gamma_{ij} T_i - \delta T_i \end{cases} \tag{2.3}$$

with $i \in \{1, 2\}$, $j \in \{1, 2, 3, 4\}$, where N_0 denotes the incoming nutrient concentration. Following typical experimental conditions, we assume nitrogen as the limiting nutrient (N). Hence, the nutrients are measured in nitrogen concentration, as compared to carbon for biomass, therefore, the nitrogen-to-carbon weight ratio (c_N/c_C) is required to scale the basal (B_i) growth terms. Moreover, the basal growth rate r_i is described by a Monod function (Monod, 1950; Tilman, S. S. Kilham, and P. Kilham, 1982), with maximum growth rate r_i' and a nutrient-uptake half-saturation constant h_N. The intermediate and top species have a generalized Holling-type-III functional response, with maximum growth rates g_j' and γ_i', half-saturation constants M and μ, and Hill coefficients h and η, respectively (Williams and Martinez, 2004; Kalinkat et al., 2013). This means:

$$r_i = r_i' \frac{N}{N + h_N} \tag{2.4}$$

$$g_{ji} = g_j' \frac{(p_{ji} B_i)^h}{\sum_{i'} (p_{ji'} B_{i'})^h + 1} \tag{2.5}$$

$$\gamma_{ij} = \gamma_i' \frac{(\phi_{ij} I_j)^\eta}{\sum_{j'} (\phi_{ij'} I_{j'})^\eta + 1}, \tag{2.6}$$

and,

$$p = \begin{pmatrix} \frac{1}{M_{u,s}} & \frac{1}{M_{d,s}} \\ \frac{1}{M_{u,s}} & \frac{1}{M_{d,s}} \\ \frac{1}{M_{u,n}} & \frac{1}{M_{d,n}} \\ \frac{1}{M_{u,n}} & \frac{1}{M_{d,n}} \end{pmatrix} \begin{matrix} I_s^u \\ I_s^d \\ I_n^u \\ I_n^d \end{matrix}, \qquad \phi = \begin{pmatrix} \frac{1}{\mu_{u,s}} & \frac{1}{\mu_{d,s}} & \frac{1}{\mu_{u,s}} & \frac{1}{\mu_{d,s}} \\ \frac{1}{\mu_{u,n}} & \frac{1}{\mu_{d,n}} & \frac{1}{\mu_{u,n}} & \frac{1}{\mu_{d,n}} \end{pmatrix} \begin{matrix} T_s \\ T_n \end{matrix} \tag{2.7}$$

such that e.g. $M_{u,s}$ indicates the half saturation constant of the undefended species being grazed by the selective species, etc.

Finally, our model includes a parameter, Δ, which explicitly controls the species' trait values. Abstract traits such as defense and selectivity are linked to concrete and

measurable parameters describing the species' interactions. For the basal species, their maximal growth rate r_i' is linked to their position on the defense axis (Fig. 2.1d). The intermediate species have two trait values: defense is again linked to their maximal growth rate g_j'/e, and the half saturation constant M_i is determined by their degree of selectivity; both of these traits affect the overall growth rate of the intermediate consumers. The top species have only one trait, selectivity, which is linked to their half saturation constant μ_i. As will be shown below, the equations are parametrized in a way such that for $\Delta = 0$ the linear chain system, where all species per trophic level are functionally identical, will be described (Fig. 2.1a). As Δ is increased, the system changes in a continuous way, where some prey species gradually become more and more defended (Fig. 2.1b), such that they can be preyed on less and less by the selective species. In addition, the selective species are gradually able to feed more efficiently on the undefended species. Finally, for $\Delta = 1$ the trait differences are maximal, as is the case in Fig. 2.1c: the selective species do not feed on the defended prey anymore.

The parameter values are set to vary logarithmically with Δ. This implies that parameter changes occur proportional to the starting value in both directions, since r_i' and g_i' appear as linear factors in the differential equations. For consistency, the elements of p and ϕ are also varied logarithmically. Concretely, this means that:

$$\log[\theta(\Delta)] = \log \theta_0 + \Delta \cdot (\log \theta_1 - \log \theta_0) \tag{2.8}$$

where θ is r_u', r_d', g_u', g_d' or any of p_{ij} or ϕ_{ji}. In this way, $\Delta = 0$ implies $\theta = \theta_0$ such that all the trait values are equal in the following manner:

$$r_u'(\Delta = 0) \;=\; r_0' \;=\; r_d'(\Delta = 0), \tag{2.9}$$

$$g_u'(\Delta = 0) \;=\; g_0' \;=\; g_d'(\Delta = 0), \tag{2.10}$$

$$\frac{1}{M_{u,s}}(\Delta = 0) \;=\; \frac{1}{M_0} \;=\; \frac{1}{M_{u,n}}(\Delta = 0), \tag{2.11}$$

and similarly for the other elements of p or ϕ. We define the parameter values θ_0 of the $\Delta = 0$ system as arithmetic averages of the extreme values θ_1 in the $\Delta = 1$ system, on a logarithmic scale, e.g.:

$$\log r_0' = \frac{\log[r_d'(\Delta = 1)] + \log[r_u'(\Delta = 1)]}{2}, \tag{2.12}$$

and similarly for the other parameters. These extreme values are shown in Table 2.1.

As the logarithm of 0 is undefined, this requires the elements of p and ϕ related to the defended-selective species' interactions for $\Delta = 1$ to be nonzero. In this case 10^{-4} was taken, which is low enough not to affect our results (see Fig. A.1, Appendix A). Note also that the set of 9 equations in Equation (2.3), when the species on each trophic level are exactly equal ($\Delta = 0$), is mathematically equivalent to a linear chain

Body mass ratio between adjacent trophic levels	$m_I/m_B = m_T/m_I = 10^3$
Allometric scaling exponent	$\lambda = -0.15$
Inflow nutrient concentration	$N_0 = 1120\,\mu g\,\mathrm{N}/l$
Dilution rate	$\delta = 0.055$
Nutrient half-saturation const. of B	$h_n = 10\,\mu g\,\mathrm{N}/l$
Nitrogen to carbon ratio of B	$c_N/c_C \approx 0.175$
B^u max. growth rate	$r_1' = 1/\mathrm{day}$
B^d max. growth rate	$r_2' = 0.66/\mathrm{day}$
I conversion efficiency	$e = 0.33$
I^u max. grazing rate	$g_{1,3}' \approx 1.08/\mathrm{day}$
I^d max. grazing rate	$g_{2,4}' \approx 0.70/\mathrm{day}$
I_s half-saturation const.	$M_{1,2} = 300\,\mu g\,C/l$
I_n half-saturation const.	$M_{3,4} = 600\,\mu g\,C/l$
T conversion efficiency	$\epsilon = 0.33$
T max. grazing rate	$\gamma_{1,2}' \approx 0.38/\mathrm{day}$
T_s half-saturation const.	$\mu_1 = M_{1,2} = 300\,\mu g\,C/l$
T_n half-saturation const.	$\mu_2 = M_{3,4} = 600\,\mu g\,C/l$

TABLE 2.1: *Standard parameter values used in this study when the trait differences are maximal, i.e., $\Delta = 1$.*

system with 4 equations, up to a slight parameter transformation. Specifically, the 9-equation food web system corresponds to a 4-equation food chain by setting $M \rightarrow 2^{(h-1)/h}M$ and $\mu \rightarrow 4^{(h-1)/h}\mu$. For details of the derivation, see Section A.2, Appendix A.

Model parametrization and analysis

In order to decrease the number of free parameters, and simultaneously increase the realism of the model, the species' growth rates were scaled allometrically to their body mass (Brose, Williams, and Martinez, 2006; De Castro and Gaedke, 2008):

$$\frac{\text{intermediate growth rate}}{\text{basal growth rate}} = \left[\frac{m_I}{m_B}\right]^\lambda, \tag{2.13}$$

with body masses m and the exponent λ given typical for planktonic systems (Moloney and Field, 1989) (Table 2.1). The same relationship holds true for the ratio between the maximum growth rates of the intermediate and the top species.

This model was developed as a chemostat model, with an eye towards potential experimental application. Chemostat experiments have been very successful in identifying and understanding ecological and evolutionary interactions of planktonic (Fussmann et al., 2005), and many other microbiological systems (Elena and Lenski, 2003). In such experiments, many factors influencing dynamics in question, such as nutrient supply, light supply, temperature, etc., are kept constant and/or closely monitored. This procedure greatly facilitates observation of the interactions of interest between species in the chemostat. For this reason, extra care was taken to have empirically motivated and realistic values of the remaining model parameter

values (Table 2.1). Specifically, the parameter values we use are representative for planktonic chemostats. However, this does not mean that our results apply only to planktonic systems. In fact, as we show in Section A.1, Appendix A, similar results are obtained when the model parametrization is more adapted towards terrestrial food webs, for example.

To get a better understanding of how much certain values of Δ sets the species on the three trophic levels apart, we here consider a few exemplary cases. At $\Delta = 0$, the varied parameters are identical (and so are the species), while at $\Delta = 0.2$, maximal growth and grazing rates of the undefended species are 9% higher than those of defended species, and half saturation constants of non-selective species are 15% higher than selective species. At $\Delta = 0.5$, the differences are 23% and 42%, respectively; at $\Delta = 1$ they are 50% and 100%.

For simplicity and to reduce the dimensionality of the system somewhat, in the rest of the text it will be assumed that

$$h = \eta, \quad \text{and} \quad M = \mu. \tag{2.14}$$

Hence, h will denote the Hill exponent, and M the half-saturation constant, of the functional response between both the first and the second, and between the second and the third trophic level. Additional narrowing of parameter ranges was achieved by requiring coexistence of the species in both the chain and the maximally separated food web. More information on the size of the range for which all species are able to coexist, as well as generalizations of our results for different model structures can be found in Section A.1, Appendix A.

To characterize the differences between the different attractors, the different phase relationships between predator-prey pairs were investigated. These phase relationships were obtained by calculating the Discrete Fourier Transform (DFT) of the simulated time series. Due to the non-sinusoid shape of the biomass oscillations, a signal with only a single frequency will generate an infinite amount of peaks in the frequency spectrum. These are necessarily multiples of the original frequency f, and the height of the peaks will scale as $1/f$ (Bracewell, 1999). This means they are easily identified in the frequency spectra when shown on a log-scale, by the linear decay in peak height.

The solutions of the differential equations presented were obtained numerically in C using the SUNDIALS CVODE solver (Hindmarsh et al., 2005), with relative and absolute tolerances of 10^{-10}. Output data were studied using Python and several Python packages; in particular NumPy, SciPy and Matplotlib (Van Der Walt, Colbert, and Varoquaux, 2011; Hunter, 2007).

2.3   Results

Firstly, we compare the biomass dynamics of the linear chain to the dynamics of the maximally trait-separated food web, where trait differences within each trophic level are maximal. Secondly, we study certain properties of the system, such as the temporal variability of population and community biomasses, and the relative abundances of species, while gradually increasing the amount of standing trait variation at each trophic level from a linear food chain to the maximally trait-separated food web.

The amount of trait variation is described by Δ ranging continuously from 0 to 1. When $\Delta = 0$ we describe the linear chain without trait variation, and when $\Delta = 1$ we describe the maximally trait-separated food web. This fully separated food web consists of defended and undefended prey species, which are being preyed upon by non-selective and/or selective predator species (Fig. 2.1c). The benefits and costs of the different offense-defense strategies are linked to each other through predefined trade-offs (see Methods). The defended species have a lower growth rate than the undefended species, but in turn, they are not preyed upon by the selective species of the next trophic level in the fully separated web. Similarly, the selective species, while unable to prey on the defended species, are able to graze the undefended species more efficiently at low prey concentrations than their non-selective counterparts.

Our results are first summarized schematically in Fig. 2.2, subsequent mechanistic details are presented in the sections and figures below. We observe two alternative stable states with low vs. high total production (State 1 and 2 in Fig. 2.2) in both the linear chain (low trait variation) and the maximally separated food web (high trait variation). In the low-production state, the high mean concentration of free nutrients corresponds to a low amount of total biomass and consequently, a low total production. In the high-production state, in contrast, the low mean nutrient concentration implies that most of the nutrients are stored in the biomass which implies a high total production. Note that at equilibrium, the total amount of nutrients in the system is always constant because the chemostat model's dilution rate δ is constant for all species.

In the food chain without trait variation (left part of the biomass pyramids in Fig. 2.2), the population-level biomass dynamics for the low-production state (Fig. 2.3a) exhibit pronounced predator-prey cycles, while the high-production state exhibits slower cycles with lower amplitudes (Fig. 2.3b) . The respective phase relationships of these oscillations (right part in Fig. 2.2, Fig. 2.3c-d) may inform about the ecological mechanism behind the two different states (for details, see section 2.3.1). In the low-production state, fast cycles with high amplitudes occur due to the strong coupling between adjacent trophic levels. Such a strong interaction between predators and their prey is indicated by the quarter-cycle phase lags (henceforth referred to as ¼-lag cycles) (Fig. 2.3c). In the high-production state the top and intermediate
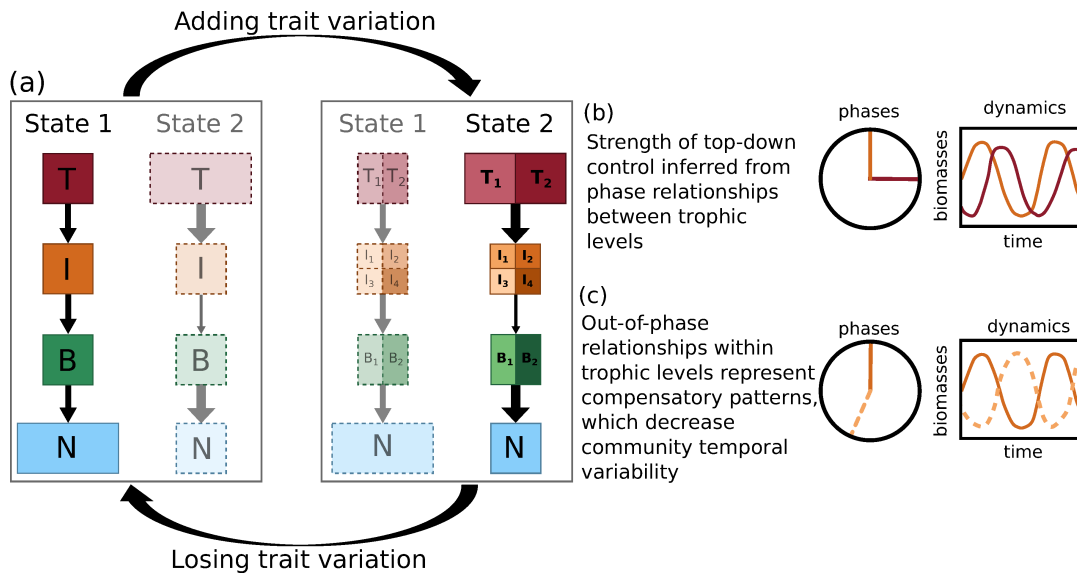
FIGURE 2.2: Schematic overview of our results. (a) The model system (with *B* basal species, *I* intermediate consumers and *T* top predators) always exhibits two alternative stable states, State 1 (low-production) and 2 (high-production), for both low and high amounts of trait variation. As trait variation is added, the system tends toward the high-production state with the top-heavy biomass pyramid (solidly drawn states have a larger basin of attraction than grayed out states). (b) The phase differences between predators and their prey inform about the intensity of top-down control in the system as indicated by arrow width in (a), i.e. ¼-lag cycles indicate strong coupling between predator and prey. (c) Within trophic level out-of-phase cycles indicate compensatory dynamical patterns, where the different species exploit different temporal niches, and hence, reduce the community temporal variability.

level still exhibit ¼-lag cycles, but the phase difference between the intermediate and basal level is significantly larger (Fig. 2.3d). This offset in the phase-relationship indicates that the top-down control over the intermediate level is so strong in the high-production state that the intermediate level's dynamics are less closely coupled to the basal level than in the low-production state. The basal level is then free to fully exploit the available nutrients.

The decoupling of the intermediate and basal level results in a lower temporal variability, especially at the basal level, and hence, reduces times of strong basal suppression during which the nutrients can almost reach their capacity as observed in the low-production state. In the high-production state, the overall higher primary production combined with the lower temporal variability between the basal and the intermediate level enhances the energy transfer through the food chain and results in a top-heavy biomass pyramid.

When the food chain becomes a food web by adding trait variation (right part of the biomass pyramids in Fig. 2.2), the biomass dynamics of the low-production (Fig. 2.4a) and high-production state (Fig. 2.4b) as well as their respective phase-relationships (Fig. 2.4c-f) become more complex because a slow and a fast timescale underlie the oscillations (see Section 2.3.1 for details). Information regarding intensity of top-down control is only deduced from the phase-relationships of the oscillatory mode that explains most of the observed variation, i.e. the fast timescale of the
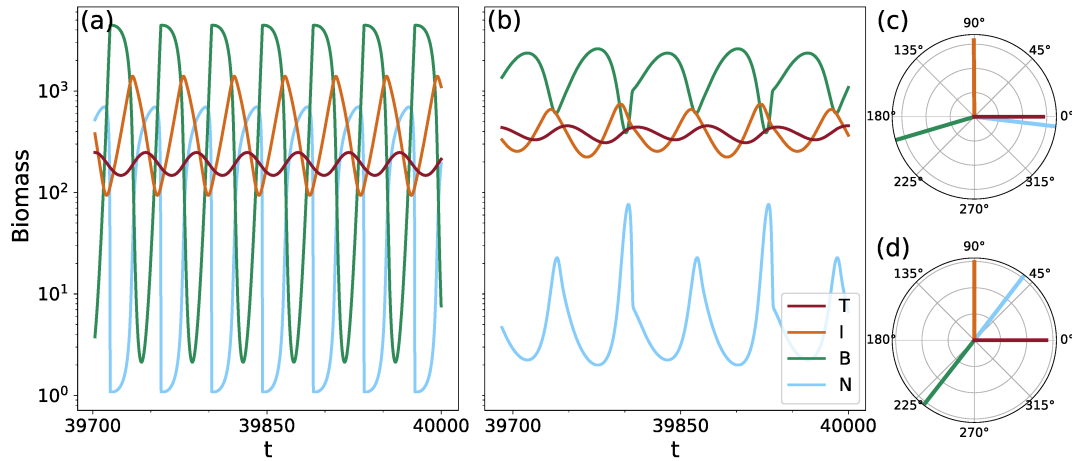
FIGURE 2.3: Biomass and nutrient dynamics on the two different states for the tritrophic chain for $h = 1.1 \, (= \eta)$, and their corresponding phase relationships. (N = nutrients, B = basal species, I = intermediate species and T = top species). The relative phases of the low-production state shown in (a) (mean nutrient level $\approx 250 \, \mu g \, N/l$) are plotted in panel (c). The phases of the high-production state shown in (b) (mean nutrient level $\approx 10 \, \mu g \, N/l$) are plotted in panel (d). In both cases the phases relative to the top species are shown.

low-production state (Fig. 2.4d) and the slow timescale of the high-production state (Fig. 2.4e). Similar to the food chain without trait variation, the strong top-down control by the top level and subsequently, the decoupling of the intermediate and basal level in the high production state again results in lower temporal variability, a temporally more balanced nutrient use, and a more efficient energy transfer towards the top level. Importantly, the high-production state becomes more likely than the low-production state with increasing trait variation, i.e., its basin of attraction increases, making it more resilient against external disturbances (for details, see Fig. 2.5 and Section 2.3.2).

As trait variation (Δ) increases, selective and non-selective consumers at the top level exploit different temporal niches and force the intermediate level to split up into two distinct groups comprising the defended and the undefended species, respectively. As both groups include both selective and non-selective consumers, this further weakens the interaction between the intermediate and basal levels, strengthening the aforementioned mechanisms that stabilize the high-production state. Notably, the mean population biomasses stay relatively constant as trait variation increases (cf. Fig. 2.6c & 2.6d), while the community temporal variability decreases (Fig. 2.6e & 2.6f, gray lines). This effect could also be predicted from the phase relationship diagrams, which show that with increasing trait variation, competing species within the same trophic level move out-of-phase with each other (Fig. 2.4c-f). Such out-of-phase cycles indicate compensatory dynamical patterns with potentially high amplitudes at the population level. However, because the different species are able to exploit different temporal niches, the community temporal variability is kept low.

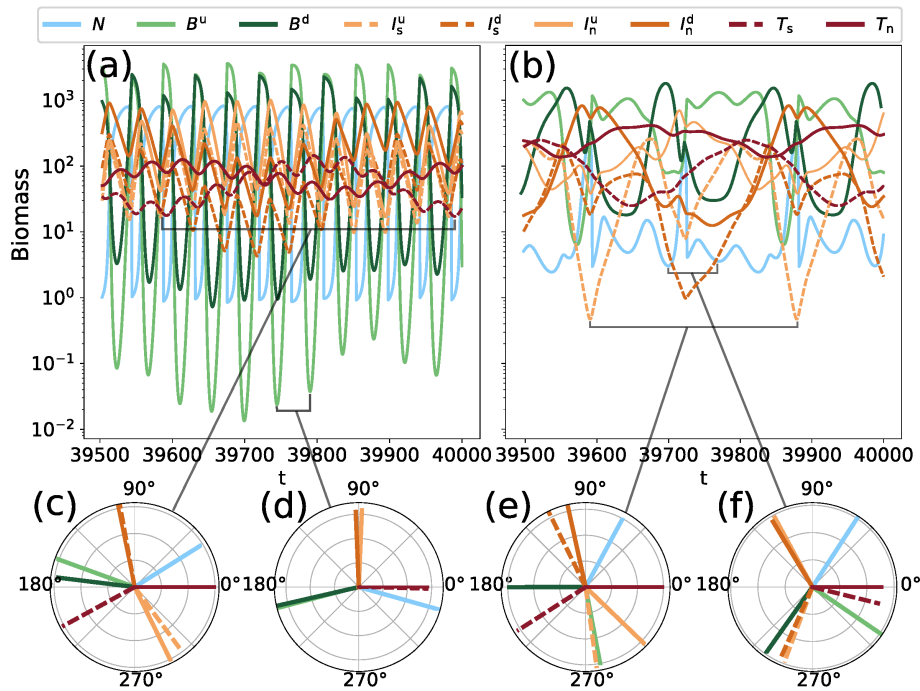In summary, adding trait variation safeguards the high-production state which

FIGURE 2.4: The dynamics of the maximally separated food web (see Fig. 2.1c for structure and species names), for $h = 1.05 (= \eta)$. Fig. (a) and (b) show the biomass time series on the low- and high-production state, respectively. The phase relationships (relative to T_n) of the two main temporal modes on the states are shown in panels (c), (e) (slow) and (d), (f) (fast). (See Fig. 2.5 and its explanation in the text for why the chosen value of $h = 1.05$ is different from the one used to compare the two states on the chain in Fig. 2.3.)

is characterized by a high top-level biomass resulting from an efficient transfer of energy towards the higher trophic levels, and low temporal variability due to weak coupling between the intermediate and basal levels and prominent compensatory dynamics within the lower trophic levels. Contrarily, losing trait variation increases the risk of an irreversible transition to the low-production state, which is characterized by a lower top-level biomass resulting from the less efficient transfer of energy towards the higher trophic levels, and higher temporal variability. With trait variation added, primary production increases from the low- to the high production state by a factor of 1.5 and the efficiency of the energy transfer towards the top level increases by a factor of 2 (See Table A.1, Appendix A). Hence, adding trait variation results in a more productive and energy-efficient food web.

More details about the above-mentioned results are presented in the respective sections below.

2.3.1 Phase relationships as a way to identify underlying mechanisms

In order to understand how to use the phase relationships between different populations of a complex food web, such as the maximally trait-separated web (Fig. 2.1c), to uncover the mechanisms driving their dynamics, let us first look at the simpler linear chain containing only three species (Fig. 2.1a). As mentioned above, the state
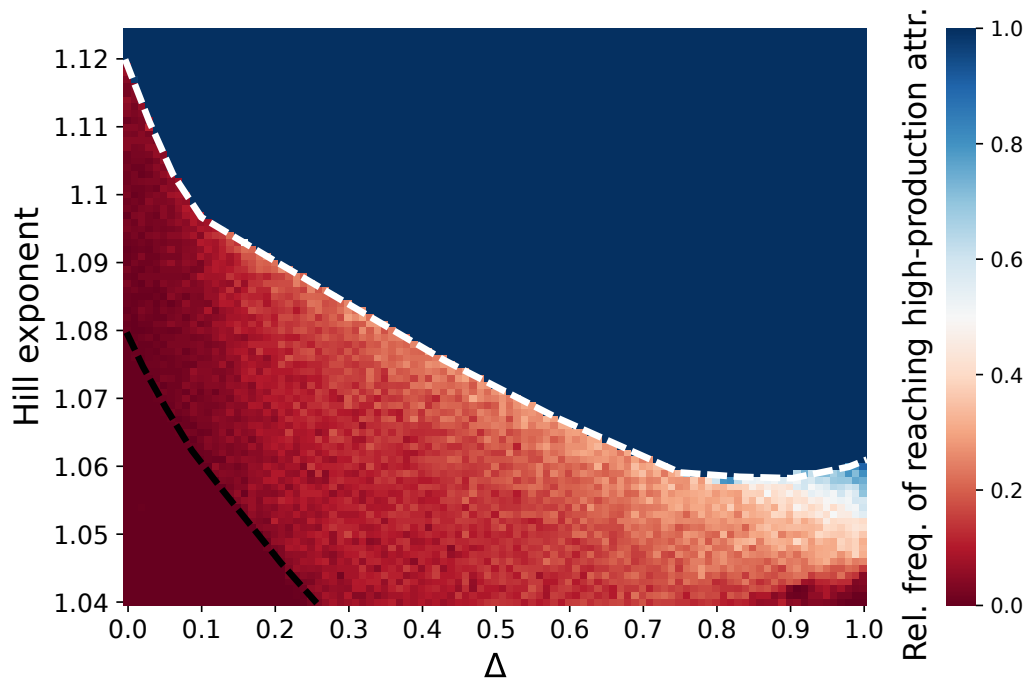
FIGURE 2.5: Relative frequency of reaching the high-production state, as a function of the trait difference Δ and the Hill-exponents $h = \eta$. Each of the points in the 101×85 grid shows the relative frequency of reaching the high-production state, sampling 200 random initial conditions. The black dashed line shows the approximate location of the boundary crisis of the high-production state. The low-production attractor also undergoes a boundary crisis, the approximate location of which is indicated by the white dashed line.

shown in Fig. 2.3a with a mean nutrient concentration of about $250 \, \mu g \, \text{N}/l$ will be called the low-production state, relative to the other state (Fig. 2.3b) which has a much lower mean nutrient concentration of around $10 \, \mu g \, \text{N}/l$ and therefore will be called the high-production state.

Closer inspection of the time series reveals the origin of the difference in mean free nutrient levels between the two states. In the low-production state (Fig. 2.3a) the intermediate level is able to grow to sufficiently high densities to graze the bottom level down significantly, despite the predation pressure imposed by the top species. Hence, the nutrient uptake is strongly reduced for a considerable amount of time leading to a relatively high mean nutrient level. Conversely, in the high-production state (Fig. 2.3b), the higher biomass at the top level implies a stronger grazing pressure on the intermediate level. The intermediate species are thus not able to grow to the density levels reached on the low-production state, and in turn, do not graze the basal level down to low densities. Hence, the mean nutrient level is much lower. Here, we define top-down effects simply as effects arising from the terms linking a species to the trophic level above it, and vice-versa for bottom-up effects. In this way, increased grazing pressure constitutes an increase in top-down control.

Using this definition, we could conclude that the overall control exerted by the top level is higher in the high-production state than on the low-production state.
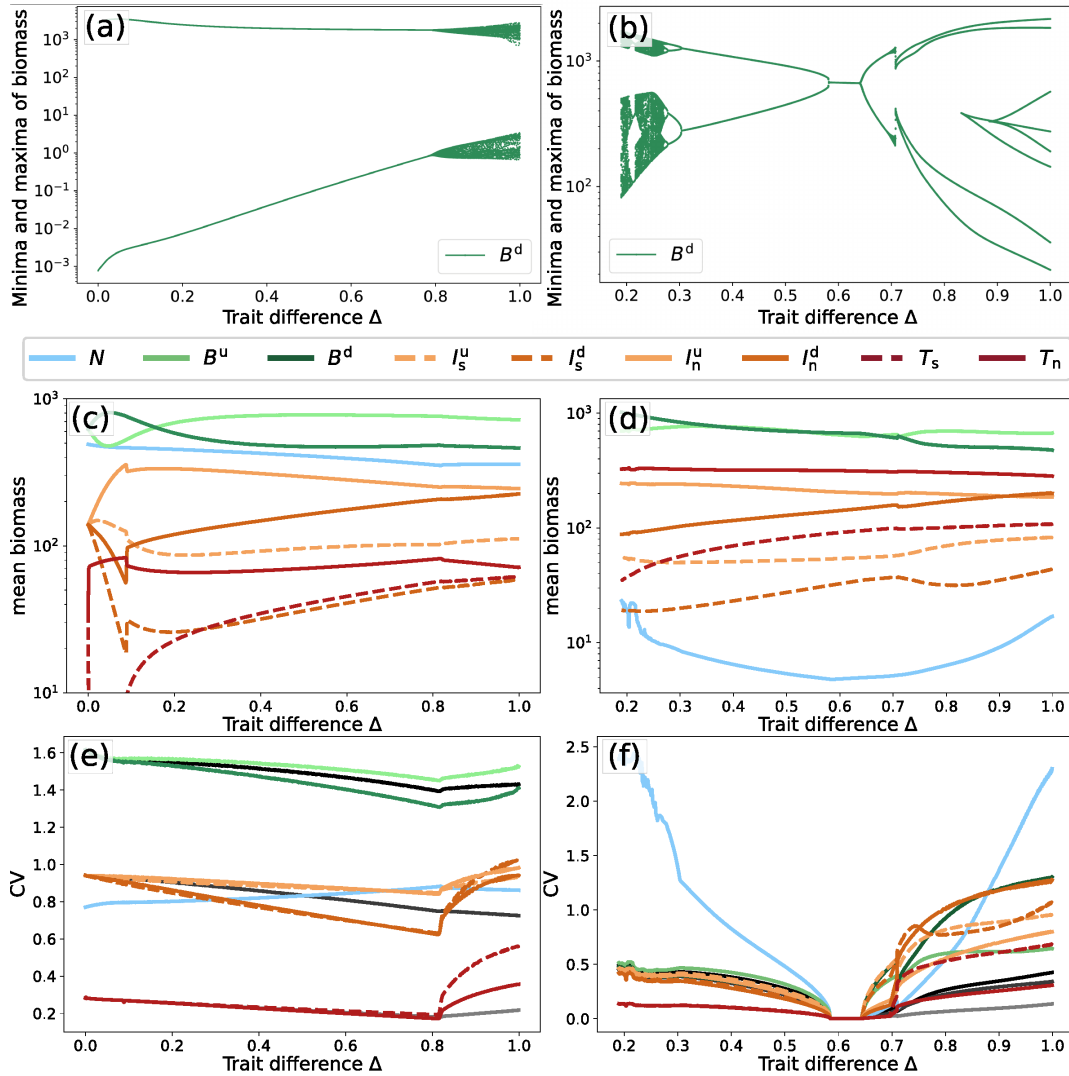
FIGURE 2.6: Bifurcation diagrams of the defended basal species, B^d ((a), (b)), mean biomasses ((c), (d)), and CV ((e), (f)) of all the species in the system, for the low-production (left) and the high-production (right) attractors, for $h = 1.05$. For the bifurcation diagrams of the other species see Section A.3, Appendix A. The CV of the selective top predator is not plotted for the region where it goes extinct ($0 \lessgtr \Delta \lessgtr 0.1$ in panel (e)). In panels (e) and (f), the black to gray lines respectively denote the CV of the first, second, and third trophic level as a whole. Note the different scales on the x- and y-axes.

Such an observation cannot be made as straightforwardly by inspecting only the mean biomass levels, as the temporal averages of the intermediate and basal biomasses are quite similar in both states and thus, they do not inform about potential changes in the production at each level. Therefore, examining the degree of top-down or bottom-up control in the case of non-static dynamics requires information about the oscillations themselves.

Interestingly, the phase differences between the different trophic levels contain sufficient information to reach the same conclusions regarding the strength of top-down control in the two states. In the low-production state, the phase differences between the top and intermediate level, and intermediate and bottom level, are about

a $1/4$-cycle Fig. 2.3c), reflecting the presence of clear predator-prey oscillations, i.e., cyclic change between top-down and bottom-up control, between both the top and intermediate level, and the intermediate and basal level. In contrast, in the high-production state, the phase lag between the intermediate and basal level is significantly more than a $1/4$-cycle (Fig. 2.3d), indicating rather weak interactions between these two different trophic levels.

With this in mind, we now investigate the fully trait-separated food web ($\Delta = 1$, Fig. 2.1c), whose dynamics are shown in Fig. 2.4a and 2.4b. Just as the linear chain, the system settles down to a stable limit cycle. While the dynamics are visually much more complex when compared to the linear chain, the basic properties and differences between the two states remain the same. However, in contrast to the chain, the discrete Fourier frequency spectra (cf. Fig. A.11, Appendix A) reveal two distinct frequencies at substantially different timescales. Despite this increase in complexity, our results clearly show that the phase relationships between distinct populations of adjacent trophic levels provide substantial information about the regulations of trophic interactions and changes therein. The absence of qualitatively different interaction types (e.g., omnivory) allows us to meaningfully compare the phase relationship between each individual predator-prey pair in our trait-separated food web to its expected value in isolation(Ellner and Becks, 2011).

The low-production state of the maximally separated food web (Fig. 2.4a) exhibits two important timescales governing the overall dynamics. First, the same high-frequency oscillations as were observed for the food chain are present, with the $1/4$-lag cycles indicative of predator-prey oscillations (Fig. 2.4d). Second, oscillations on a slower timescale are found. Their phase relationships show that they arise from the trait differences between species (Fig. 2.4c). Here, the top species are almost completely out of phase relative to each other. Consider first the selective predator T_s, which preys only on the undefended intermediate species I_s^u and I_n^u. The phase relationship diagram shows that these species precede T_s by the regular $1/4$-lag. The same is true for T_n, which is preceded by a quarter-cycle by the defended intermediate species I_s^d and I_n^d. Quarter-lag cycles are not observed between the basal and intermediate trophic level, which indicates that the trait differences within the top trophic level influence the intermediate level more strongly as those on the intermediate level influence the basal level. As the two alternating groups of defended and undefended intermediate species contain a selective and non-selective grazer on the basal species, they exert together approximately the same grazing pressure on both types of basal species. Consequently, no clear phase relationship between the intermediate and basal level is found. However, visual inspection combined with analysis of the Discrete Fourier Transform (DFT) spectrum (Fig. A.11, Appendix A) shows that the high-frequency component is the dominant one, explaining most of the observed variation in the biomass. Hence, the biomass dynamics reflect an overall balance between top-down and bottom-up interactions in the low-production state, similar to the simple linear chain.

In the high-production state of the maximally separated food web (Fig. 2.4b), the difference in dynamics as compared to the linear chain is even more pronounced. The basal species exhibit a clear compensatory dynamical pattern, with alternating biomass peaks of defended and undefended species. While the dynamics appear highly irregular, the frequency spectrum shows that they are also mainly driven by two frequencies. On the lower of these frequencies, which explains most of the variation observed in this state, the phase relationships resemble those of the low frequency in the low-production state (Fig. 2.4e vs. 2.4c), with the exception of the basal species, which now cycle out of phase. The selective and non-selective top species also move out of phase, which leads the groups of defended and undefended intermediate species to behave similarly, as they each precede their respective main predator. As in the low-production state, no further relationship can be identified between the intermediate and the basal level.

However, the high frequency roughly corresponding to that of the chain also has an influential component in the Fourier spectrum. On this frequency, the phase relationships show that the basal species also move out-of-phase. In contrast to the dominant lower frequency, the intermediate species are now split into two groups according to their main prey type. The non-selective intermediate species follow the defended basal species, and the selective intermediate species the undefended basal species, by a $1/4$-lag. As each of these two groups of intermediate species contains both a defended and undefended type, no further relationship can be drawn between the phases of the intermediate and the top level.

In summary, the strength of top-down control across trophic levels may be inferred from the phase relationships in both the linear chain and the maximally separated food web. The phase-relationships further reveal compensatory dynamics within trophic levels in the fully separated web.

2.3.2 Trait variation increases resilience of the high-production state

Recall that trait differences between the modeled species at each trophic level, determined by Δ (Eq. (2.8)), can be varied continuously. Varying Δ between $\Delta = 0$ (chain) and $\Delta = 1$ (maximally separated web) reveals the intermediate region between the two extremes considered so far.

In this intermediate region, the food web is not yet completely separated as is the case for Fig. 2.1c, although there are already trait differences between different species at each trophic level. That is, the selective predator species are not yet fully specialized: they are still able to prey on the defended species albeit with a lower efficiency than the undefended species. Accordingly, the undefended species are not fully defended against the selective predators. The difference in growth rates between defended and undefended species is thus gradually increased to its maximum value, which is obtained when $\Delta = 1$. In this way the trade-offs between defense and growth rate, and between selectivity and prey grazing efficiency, are explicitly built into the model.

To investigate the effect of trait variation on the likelihood of the system adopting either of the two alternative stable states, we determined the size of the basin of attraction of the high-production state. Fig. 2.5 shows the relative frequency of a random initial value falling in this basin of attraction, as Δ is varied. The random initial values were sampled from the set of all potentially accessible biomass configurations of the chemostat system, i.e., the total carbon content in the system does not exceed the maximum possible carbon content attainable by the incoming nutrient concentration N_0.

The region of intermediate frequency values confirms that the bistability is an important aspect of the system. The typical behavior when varying Δ from 0 to 1 is an increasing probability of reaching the high-production state. Furthermore, the graph shows an important dependency on the predator-prey functional responses' Hill coefficient h: increasing the exponent also increases the probability of reaching the high-production state. Investigating the effect of other model parameters on the presence of bistability reveals that it is quite common for this type of model structure, and that the trends presented here are not limited to this particular part of the parameter space. For details, see Section A.1, Appendix A.

Over the whole range of Δ, there is a very sharp transition between the region where only the high-production state exists (dark blue), and the region where both states exist, indicated by the white dashed line (Fig. 2.5). Notably, the border decreases steeply as the trait difference Δ is increased, indicating the much lower dependence on low-density grazing suppression for higher amounts of standing trait variation. The sharp border between the two regions is an indication that the low-production state undergoes a catastrophic bifurcation, where it suddenly disappears. Similar behavior is observed for the high-production state, indicated by the black dashed line. This transition is of particular ecological interest as it implicates the sudden disappearance of the high-production, low-temporally-variable state. The region for $h < 1.04$ was not considered, as the amount of extinctions was too high. However, the graph indicates that the probability of reaching the high-production state decreases further.

2.3.3 Dynamical properties of the alternative stable states under gradual changes in trait variation

Consider now $h = 1.05$ as a representative value catching the most complex region in Fig. 2.5, to study the possible effects of varying Δ on the system's dynamics. In this case, the low-production state exists over the whole range of Δ, its the bifurcation diagram for the defended basal species B^{d} is shown in Fig. 2.6a. The qualitative features of the diagram are representative for the other species in the network, whose bifurcation diagrams are shown in Fig. A.9 and A.10, Appendix A . For $\Delta = 0$, the oscillations are simple, in the sense that they are governed by a single timescale and have a constant amplitude, as the maxima and respectively minima each fall on the same position. As Δ increases, this situation remains unchanged, up until the

species become different enough for the second timescale to emerge, in which they exhibit a compensatory dynamical pattern. This explains the variation of the values of the extrema as the two timescales interact destructively and constructively.

The mean biomasses of the species (Fig. 2.6c) reveal that the selective top predator goes extinct for low values of Δ. In this case, the species are too similar to stably coexist due to a lack of niche differences, and the non-selective predator outcompetes the selective species. However, it quickly recovers as Δ is increased and the species become more different. While this event causes some disturbances in the mean biomasses of the other species, outside of this range the values are more or less constant.

Disregarding the initial region of Δ where the selective top predator goes extinct, all species' CV exhibit a gradual decrease as Δ is increased, up to the point where the second timescale enters the system (Fig. 2.6e). At this point, a sharp increase is observed as the complexity is enhanced by the interaction of the two timescales. The black to gray lines, depicting the CV of the biomasses at each trophic level as a whole, show that the sharp increase is not present on the trophic-level-scale. Hence, the increase in CV for each of the species can be solely attributed to the introduction of the second, slower timescale. As discussed above, species with different traits may move out of phase on this timescale, and thus the effects of the slower timescale on the temporal variability for the trophic level as a whole cancel out.

The bifurcation diagram for the high-production attractor (Fig. 2.6b) does not cover the full range of $0 \leq \Delta \leq 1$ for $h = 105$, as it only exists on the right side of the black dashed line in Fig. 2.5. Furthermore, the attractor exhibits a much richer structure as Δ is varied than the low-production attractor. Multiple bifurcations occur in which the dynamics are altered. In particular, lowering Δ sufficiently the system undergoes a series of period-doubling bifurcations which lead to chaotic dynamics. Eventually the attractor undergoes a boundary crisis, as indicated by both the sudden disappearance of the then chaotic attractor and the presence of a chaotic transient (Fig. A.12, Appendix A).

The species' mean biomass on the high-production state (Fig. 2.6d) reveal a similar monotonicity as those on the low-production state (Fig. 2.6c). A notable observation is the very low mean nutrient level along the whole range of Δ. The nutrients show a very high CV (Fig. 2.6f), which can be attributed to their low mean value. In addition, the CV for each of the species is higher on the right side of the Hopf-bifurcations (higher Δ), as compared to the left side for lower values of Δ. However, just as for the low-production state, these increases are buffered when looking at the temporal variability of the trophic levels as a whole (black to gray lines). This reflects the compensatory dynamical pattern of the high-production state, where some of the species move out of phase, which leads to a reduction in temporal variability on the entire trophic level.

2.4 Discussion

We developed a generic tritrophic model to investigate the effect of varying degrees of trait variation on the dynamics of multitrophic food webs and their associated ecosystem functions such as the mean resource use efficiency, biomass production, temporal variability and resilience. By increasing the trait difference parameter Δ from 0, the system increases in complexity while it changes gradually from a simple chain without trait variation to a complex web with selective and non-selective consumers, and correspondingly defended and undefended prey. The relevant parameters affecting these traits (growth rate, edibility, food preference, and half saturation constant) are closely linked to the functions of the individual species in the food web. Hence, increasing Δ also increases the functional differences between the species, and thus, the functional diversity of the system. For $\Delta > 0$ but low, the trait differences are small which means the species are very similar, hence, the functional diversity at each trophic level is low. Correspondingly, for Δ close to one, the functional diversity of the system is high, even though the number of species is kept constant. Therefore, varying Δ is a means to study the effects of changing functional diversity on all three trophic levels on the dynamics of the whole system without potentially confounding effects of changing the number of species. The different aspects of how trait variation impacts the food web dynamics are discussed in detail below.

Phase relationships help unravel complex trophic interactions

Traditionally, effects of multi-trophic interactions such as trophic cascades and the degree of bottom-up or top-down control were studied using a rigid linear chain in equilibrium (Carpenter, Kitchell, and Hodgson, 1985; Pace et al., 1999). However, natural systems are usually not simple chains, but highly complex webs with functionally diverse species at all trophic levels (Boit et al., 2012; Wollrab, Diehl, and De Roos, 2012). Moreover, their dynamics may not evolve towards an equilibrium fixed point, but rather to a limit cycle (May, 1972), or a strange attractor (Hastings et al., 1993) where they will perpetually exhibit oscillatory behavior. This phenomenon can be separated from stochastic noise and has been observed in natural communities (Kendall, 1998). Such oscillatory behavior gives rise to certain phase relationships between the biomass dynamics of the different species.

Additionally, in the maximally trait-separated food web (Fig. 2.1c), calculation of the Discrete Fourier Spectrum clearly exposes the two timescales at which major driving mechanisms take place. The emergence of a second timescale does not rely on the addition of a third trophic level as this feature has already been found in bitrophic models that considered multiple species or phenotypes at only one (Yamamichi, Yoshida, and Sasaki, 2011) or both trophic levels (Tirok and Gaedke, 2010). However, our treatment highlights how the phase relationships may shed

light on the mechanisms driving complex systems by disentangling the different timescales at which these mechanisms may act.

Strength of trophic interactions

We found that the main dynamical differences between the two alternative stable states present in our system can be explained by an increased top-down control of the top level on the intermediate level. When the intermediate level is strongly controlled, such as is the case on the high-production state, its species are unable to control the basal level. The basal level is in turn able to fully exploit the available nutrients, increasing the overall production in the system (see Table A.1, Appendix A).

This result holds independent of the amount of trait variation present, and is in line with previous studies showing that reduced top-down control may result in an increased phase difference between predator and prey (Yoshida et al., 2003; Becks et al., 2010). Importantly, the larger than ¼-cycle phase difference between the basal prey and intermediate predator observed in our system with only one species per trophic level (Fig. 2.1a) shows that the common conception of anti-phase cycles as a "smoking gun" for the presence of evolution, or other mechanisms causing trait changes (Ellner and Becks, 2011; Hiltunen et al., 2014) does not hold any longer when considering multitrophic systems in which the intermediate predator faces strong top-down control by the top predator.

Role of compensatory dynamics

When a community consists of functionally diverse populations, a decline in one functional group can be accompanied by an increase of another (Klug et al., 2000). In this way, even though the individual populations exhibit high temporal variability in their biomasses in our model, the variability of the community biomass per trophic level remains low (Fig. 2.6f). Such an effect has been observed before in studies investigating the effect of standing trait variation or phenotypic plasticity on population dynamics (Kovach-Orr and Fussmann, 2013; Bauer et al., 2014), and it is often made possible through compensatory dynamics between the species (Micheli et al., 1999; Vasseur and Gaedke, 2007; Gonzalez and Loreau, 2009). Hence, compensatory dynamics can be understood as a mechanism by which ecosystem functions such as biomass production can stay rather constant while individual populations may be highly variable (Hooper et al., 2005; Bauer et al., 2014). Compensatory dynamics are observed in both the high- and low-production state, for sufficiently high Δ (Fig. 2.4a & 2.4b). When present, they effectively decrease the biomass CV of the trophic level as whole, even though the CVs of the species' individual biomass may be relatively high (Fig. 2.6e & 2.6f). These compensatory dynamical patterns naturally keep species within a trophic level moving out-of-phase relative to each other, and thus, can also be inferred by analyzing phase relationship diagrams.

Notably, the compensatory dynamics on the low-production state are only present at the slower timescale related to the trait dynamics (Fig. 2.4c). For example, the dominant faster timescale does not exhibit compensatory dynamics (Fig. 2.4d), and thus, given substantial variation in the biomass of the individual populations, the CV at the community level remains relatively high (Fig. 2.6e). Even so, the sharp increase in temporal variation on the population level for high trait variation is buffered on the community scale, through the compensatory dynamics taking place on a different timescale than the dominant one. Our time-scale dependent phase-relationships between populations are in line with empirical observations showing that phytoplankton populations may exhibit compensatory dynamics on the sub-annual scale, likely associated with trophic interactions, combined with synchronous dynamics on the annual, externally driven timescale (Vasseur and Gaedke, 2007). Similarly, zooplankton dynamics may be governed by two distinct timescales: seasonal variation and experimentally varied environmental conditions (Keitt and Fischer, 2006). Hence, unraveling the different timescales governing the population dynamics may help to understand the major processes driving them.

Trait variation promotes high production at the top-level

In line with our results, bistability has been observed in other food chain models (Abrams and Roth, 1994; Letellier and Aziz-Alaoui, 2002; Van Voorn, Kooi, and Boer, 2010; Erbach, Lutscher, and Seo, 2013), ontogenetic growth models (Guill, 2009; Nakazawa, 2011), and in other, broader ecological contexts (Beisner, Haydon, and Cuddington, 2003). The presence of two alternative states in our system is an important feature as it may have far-reaching consequences regarding the stability and perseverance of food webs when confronted with external perturbations. A commonly made distinction when studying the effects of perturbations is whether they consist of a change to the state variables, or to the actual model parameters (Bender, Case, and Gilpin, 1984; Beisner, Haydon, and Cuddington, 2003). The first kind, for example a sudden decrease in one of the species' biomass, is often called a pulse perturbation because of its short duration. The second kind is called a press perturbation, because the change to the perturbed parameters is permanent, such as a decrease in the nutrient inflow concentration. In a multistable system, pulse perturbations, particularly when they are large, might push the system over the edge of one basin of attraction into another, where the dynamics are potentially completely different. Press perturbations may produce a similar outcome by causing large changes to an attractor's basin of attraction, or by crossing a bifurcation point where the dynamics change significantly. Therefore, the size of the basin of attraction may be used as a measure of resilience (Beisner, Haydon, and Cuddington, 2003). A highly resilient system will nearly always return to its original state, hence its basin of attraction must be very large. Conversely, a non-resilient or fragile system is easily pushed out of one basin of attraction into another one.

Recall that the two states in our system have very different dynamical properties: the low-production state with low top biomass production and high variability, compared to the high-production state with high top biomass production and low variability. From an ecosystem function perspective, low variability or high biomass in higher trophic levels are beneficial for e.g. fish yield. Therefore, it may be desirable to keep the system on the high-production state.

While biomass production of a community is known to be mostly positively correlated with its functional diversity (Tilman et al., 1997; Naeem, Duffy, and Zavaleta, 2012), we also found the high-production state in the food chain. This corresponds to, e.g., modern agricultural systems, which typically consist of monocultures with a low functional diversity, but a high biomass production available for higher trophic levels. However, even though such monocultures may produce more biomass than some functionally highly diverse mixtures, they are very fragile against external disturbances (Yachi and Loreau, 1999; Loreau et al., 2001). In this way, functional diversity is regarded as an insurance against external perturbations. We clearly observed such an effect in our system, for both pulse and press perturbations, as illustrated by Fig. 2.5. Since the basin of attraction of the high-production attractor increases in size with Δ, the system becomes less likely to be pushed out of the basin of attraction by a pulse perturbation. This trend is persistent when varying not only the Hill exponents, but also the dilution rate, and the nutrient inflow concentration (Fig. A.3, Appendix A), and is thus not limited to a particular part of the model's parameter space. In addition, the boundary crisis causing the sudden disappearance of the high-production attractor (Fig. 2.5, black dashed line) is only present for low values of Δ. Hence, functional diversity also protects the high-production state from suddenly disappearing under a press perturbation.

Typical for a boundary crisis, as the high-production state undergoes when decreasing Δ, are the long transients that are still present near the crisis point (Grebogi, Ott, and Yorke, 1982) (Fig. A.12, Appendix A). In an ecological context this could be problematic as such a long transient implies there is no way to know exactly when the crisis point has been passed and the basin of attraction no longer exists, until the system eventually accelerates towards the only remaining attractor. Such regime shifts were empirically observed and predicted by a variety of ecosystem models in different contexts (Scheffer and Carpenter, 2003), such as woodlands threatened by fires turning into grasslands (Dublin, Sinclair, and McGlade, 1990), and shallow lakes threatened by eutrophication turning from a macrophyte to a phytoplankton dominated state (Scheffer et al., 1993). The key idea is that a small perturbation near the bifurcation point may move the system to an alternative stable state, but once this has happened, a much larger perturbation is needed in order to return back to the original state. It has been argued that, under certain circumstances, one may be able to observe early-warning signals that a transition is imminent (Scheffer et al., 2009; Carpenter et al., 2011; Kéfi et al., 2014). For example, near some types of bifurcations a dampening of the speed-of-return after a pulse perturbations may

be observed, called critical slowing down (Wissel, 1984; Scheffer et al., 2009). In the case of a boundary crisis, showing the existence of any early-warning signals has proven to be difficult (Hastings and Wysham, 2010; Boettiger and Hastings, 2012). However, even if their existence could be shown mathematically, they will almost certainly be very difficult or impossible to detect in a real-life setting, where the exact chaotic dynamics may be obscured by measurement noise. Our results reveal that maintaining sufficient trait variation provides protection from boundary crises, with their often ecologically and economically undesirable consequences.

These conclusions rely on the presence of alternative stable states in our model. This is a prominent property in tritrophic systems, present in even a simple tritrophic chain with Holling-type-II functional responses and logistic growth of the basal species(Abrams and Roth, 1994). However, there always exist parameter regions where there is only one non-trivial stable state. We find that also in such cases, production at the top level and temporal stability both increase with Δ, as the attractor changes from resembling the low-production to resembling the high-production state in a gradual way (Fig. A.6, Appendix A).

Influence of a sigmoidal functional response

The use of sigmoidal functional responses such as the (generalized) Holling type-III ($h = \eta > 1$) has been an active area of discussion for quite some time. Sigmoidal functional responses are praised for their favorable effects on food web dynamics such as an increased dynamical stability (Williams and Martinez, 2004; Kalinkat et al., 2011). Such an increase is justified by the apparent discrepancy between the observed stability of natural ecosystems, and the highly unstable nature of ecosystem models describing them (McCann, 2000). While experimental evidence has traditionally mainly supported hyperbolic functional response shapes, such as Holling type-II ($h = \eta = 1$) (DeMott, 1982; A. W. W. Murdoch et al., 1998), sigmoidal functional responses such as Holling-type-III provide models with additional stability which may overcome this discrepancy. Recent experiments studies have found evidence for sigmoidal functional response shapes (Sarnelle and Wilson, 2008; Morozov, 2010; Kalinkat et al., 2013), or otherwise have shown the difficulty in distinguishing Holling type-II from type-III functional response shapes (Seifert et al., 2014). Furthermore, sigmoidal shapes account for natural processes not captured by the model such as spatial heterogeneity, refuges, formation of resting shapes, etc. Hence, Hill exponents close to—but higher than—one are likely to be relevant, and thus, the requirement of at least some grazing suppression at low densities for all species to coexist adds to the realism of the model. Even in the highly-controlled environment of the chemostat, some of the proposed mechanisms giving rise to the predation dampening at low prey densities, such as prey clumping (Oaten and W. W. Murdoch, 1975) or other induced defenses (Lurling and Beekman, 2006), may well be of importance. In addition, while a Hill exponent larger than 1 does facilitate

coexistence, it is not a guaranteed. For example, Fig. 2.6c shows that one of the top predators is not able to survive for $0 \lessapprox \Delta \lessapprox 0.1$.

Nonetheless, Fig. 2.5 also shows a significant, decreasing dependence on low prey density grazing suppression in order to reach the high-production state. For most of the range of Δ, the sharp border between the bistable region and the region where only the high-production state exists occurs at a lower value of the Hill-exponent as Δ is increased. Hence, while the grazing suppression at low prey densities is necessary to reach the high-production state, it becomes a less important factor as Δ is increased.

Concluding remarks

Despite the higher dynamical complexity of the resulting food web, the introduction of trait variation at all trophic levels to a linear food chain increased the overall reliability of ecosystem functions, such as resource use efficiency and high biomass production. Our results highlight that functional diversity on different trophic levels can reduce the overall temporal variability at the community level through compensatory dynamics among functionally different species within a trophic level. Investigating the phase relationships between the different species of adjacent trophic levels enabled us to identify the regulation of trophic interactions, such as changes in top-down or bottom-up control, in oscillatory dynamical regimes. Accordingly, we observed that strong deviations from the expected ¼ -lag between predator and prey are possible in a tritrophic system, even without any trait variation. Hence, observation of such deviations do not necessarily indicate the presence of eco-evolutionary dynamics as is often assumed. Furthermore, independent of the presence or absence of trait variation, our tritrophic model shows two alternative states with the top predator exhibiting either a relatively low or high biomass. However, while the high-production state is attainable in a tritrophic food chain, its basin of attraction is very small. It becomes more resilient when trait variation is added, underlining the role of functional diversity as an insurance against sudden pulse perturbations. In addition, as trait variation decreases, this state may suddenly disappear through a boundary crisis. Hence, high functional diversity also protects the high-production state under press perturbations. We thus highlight the importance of functional diversity regarding resilience against external perturbations, low community temporal variability, resource use efficiency, and maintenance of biomass in higher trophic levels.

Acknowledgments

References

Abrams, P. A. and Roth, J. D. (1994). "The effects of enrichment of three-species food chains with nonlinear functional responses". In: *Ecology* 75.4, pp. 1118–1130. DOI: 10.2307/1939435.

Abrams, P. A. and Matsuda, H. (1996). "Fitness minimization and dynamic instability as a consequence of predator-prey coevolution". In: *Evolutionary Ecology* 10.2, pp. 167–186. DOI: 10.1007/BF01241783.

Bauer, B., Vos, M., Klauschies, T., and Gaedke, U. (2014). "Diversity, Functional Similarity, and Top-Down Control Drive Synchronization and the Reliability of Ecosystem Function". In: *The American Naturalist* 183.3, pp. 394–409. DOI: 10.1086/674906.

Becks, L., Ellner, S. P., Jones, L. E., and Hairston Nelson G., J. G. (2010). "Reduction of adaptive genetic diversity radically alters eco-evolutionary community dynamics". In: *Ecology Letters* 13.8, pp. 989–997. DOI: 10.1111/j.1461-0248.2010.01490.x.

Beisner, B. E., Haydon, D. T., and Cuddington, K. (2003). "Alternative stable states in ecology". In: *Frontiers in Ecology and the Environment* 1.7, pp. 376–382. DOI: 10.1890/100071.

Bender, E. A., Case, T. J., and Gilpin, M. E. (1984). "Perturbation experiments in community ecology: theory and practice." In: *Ecology* 65.1, pp. 1–13. DOI: 10.2307/1939452.

Boettiger, C. and Hastings, A. (2012). "Early warning signals and the prosecutor's fallacy". In: *Proceedings of the Royal Society B: Biological Sciences* 279.1748, pp. 4734–4739. DOI: 10.1098/rspb.2012.2085.

Boit, A., Martinez, N. D., Williams, R. J., and Gaedke, U. (2012). "Mechanistic theory and modelling of complex food-web dynamics in Lake Constance". In: *Ecology Letters* 15.6, pp. 594–602. DOI: 10.1111/j.1461-0248.2012.01777.x.

Bracewell, R. N. (1999). *The Fourier Transform and its Applications*. 3rd. Electrical engineering series. McGraw Hill International Editions, pp. 351–356.

Brose, U., Williams, R. J., and Martinez, N. D. (2006). "Allometric scaling enhances stability in complex food webs". In: *Ecology Letters* 9.11, pp. 1228–1236. DOI: 10.1111/j.1461-0248.2006.00978.x.

Brown, J. H., Gillooly, J. F., Allen, A. P., Savage, V. M., and West, G. B. (2004). "Toward a metabolic theory of ecology". In: *Ecology* 85.7, pp. 1771–1789. DOI: 10.1890/03-9000.

Carpenter, S. R. et al. (2011). "Early warnings of regime shifts: A whole-ecosystem experiment". In: *Science* 332.6033, pp. 1079–1082. DOI: 10.1126/science.1203672.

Carpenter, S. R., Kitchell, J. F., and Hodgson, J. R. (1985). "Cascading Trophic Interactions and Lake Productivity". In: *BioScience* 35.10, pp. 634–639. DOI: 10.2307/1309989.

Coutinho, R. M., Klauschies, T., and Gaedke, U. (2016). "Bimodal trait distributions with large variances question the reliability of trait-based aggregate models". In: *Theoretical Ecology* 9.4, pp. 389–408. DOI: 10.1007/s12080-016-0297-9.

De Castro, F. and Gaedke, U. (2008). "The metabolism of lake plankton does not support the metabolic theory of ecology". In: *Oikos* 117.8, pp. 1218–1226. DOI: 10.1111/j.0030-1299.2008.16547.x.

DeMott, W. R. (1982). "Feeding selectivities and relative ingestion rates of Daphnia and Bosmina". In: *Limnology and Oceanography* 27.3, pp. 518–527. DOI: 10.4319/lo.1982.27.3.0518.

Digel, C., Curtsdotter, A., Riede, J., Klarner, B., and Brose, U. (2014). "Unravelling the complex structure of forest soil food webs: Higher omnivory and more trophic levels". In: *Oikos* 123.10, pp. 1157–1172. DOI: 10.1111/oik.00865.

Dublin, H. T., Sinclair, A., and McGlade, J. (1990). "Elephants and Fire as Causes of Multiple Stable States in the Serengeti-Mara Woodlands". In: *The Journal of Animal Ecology* 59.3, pp. 1147–1164. DOI: 10.2307/5037.

Duffy, J. E. (2002). "Biodiversity and ecosystem function: The consumer connection". In: *Oikos* 99.2, pp. 201–219. DOI: 10.1034/j.1600-0706.2002.990201.x.

Elena, S. F. and Lenski, R. E. (2003). "Evolution experiments with microorganisms: The dynamics and genetic bases of adaptation". In: *Nature Reviews Genetics* 4.6, pp. 457–469. DOI: 10.1038/nrg1088.

Ellner, S. P. and Becks, L. (2011). "Rapid prey evolution and the dynamics of two-predator food webs". In: *Theoretical Ecology* 4.2, pp. 133–152. DOI: 10.1007/s12080-010-0096-7.

Erbach, A., Lutscher, F., and Seo, G. (2013). "Bistability and limit cycles in generalist predator-prey dynamics". In: *Ecological Complexity* 14, pp. 48–55. DOI: 10.1016/j.ecocom.2013.02.005.

Filip, J., Bauer, B., Hillebrand, H., Beniermann, A., Gaedke, U., and Moorthi, S. D. (2014). "Multitrophic diversity effects depend on consumer specialization and species-specific growth and grazing rates". In: *Oikos* 123.8, pp. 912–922. DOI: 10.1111/oik.01219.

Fussmann, G. F., Ellner, S. P., Hairston, N. G., Jones, L. E., Shertzer, K. W., and Yoshida, T. (2005). "Ecological and Evolutionary Dynamics of Experimental Plankton Communities". In: *Advances in Ecological Research* 37.04, pp. 221–243. DOI: 10.1016/S0065-2504(04)37007-8.

Gamfeldt, L., Lefcheck, J. S., Byrnes, J. E., Cardinale, B. J., Duffy, J. E., and Griffin, J. N. (2015). "Marine biodiversity and ecosystem functioning: What's known and what's next?" In: *Oikos* 124.3, pp. 252–265. DOI: 10.1111/oik.01549.

Golubski, A. J., Westlund, E. E., Vandermeer, J., and Pascual, M. (2016). "Ecological Networks over the Edge: Hypergraph Trait-Mediated Indirect Interaction (TMII) Structure". In: *Trends in Ecology and Evolution* 31.5, pp. 344–354. DOI: 10.1016/j.tree.2016.02.006.

Gonzalez, A. and Loreau, M. (2009). "The Causes and Consequences of Compensatory Dynamics in Ecological Communities". In: *Annual Review of Ecology, Evolution, and Systematics* 40.1, pp. 393–414. DOI: 10.1146/annurev.ecolsys.39.110707.173349.

Grebogi, C., Ott, E., and Yorke, J. A. (1982). "Chaotic attractors in crisis". In: *Physical Review Letters* 48.22, pp. 1507–1510. DOI: 10.1103/PhysRevLett.48.1507.

Guill, C. (2009). "Alternative dynamical states in stage-structured consumer populations". In: *Theoretical Population Biology* 76.3, pp. 168–178. DOI: 10.1016/j.tpb.2009.06.002.

Hastings, A., Hom, C. L., Ellner, S., Turchin, P., and Godfray, H. C. (1993). "Chaos in ecology: Is mother nature a strange attractor?" In: *Annual Review of Ecology and Systematics* 24, pp. 1–33. DOI: 10.1146/annurev.es.24.110193.000245.

Hastings, A. and Wysham, D. B. (2010). "Regime shifts in ecological systems can occur with no warning". In: *Ecology Letters* 13.4, pp. 464–472. DOI: 10.1111/j.1461-0248.2010.01439.x.

Hillebrand, H. and Matthiessen, B. (2009). "Biodiversity in a complex world: Consolidation and progress in functional biodiversity research". In: *Ecology Letters* 12.12, pp. 1405–1419. DOI: 10.1111/j.1461-0248.2009.01388.x.

Hiltunen, T., Hairston, N. G., Hooker, G., Jones, L. E., and Ellner, S. P. (2014). "A newly discovered role of evolution in previously published consumer-resource dynamics". In: *Ecology Letters* 17.8, pp. 915–923. DOI: 10.1111/ele.12291.

Hindmarsh, A. C., Brown, P. N., Grant, K. E., Lee, S. L., Serban, R., Shumaker, D. E., and Woodward, C. S. (2005). "Sundials". In: *ACM Transactions on Mathematical Software* 31.3, pp. 363–396. DOI: 10.1145/1089014.1089020.

Hooper, D. U. et al. (2005). "Effects of biodiversity on ecosystem functioning: A consensus of current knowledge". In: *Ecological Monographs* 75.1, pp. 3–35. DOI: 10.1890/04-0922.

Hunter, J. D. (2007). "Matplotlib: A 2D graphics environment". In: *Computing in Science and Engineering* 9.3, pp. 99–104. DOI: 10.1109/MCSE.2007.55.

Kalinkat, G., Rall, B. C., Vucic-Pestic, O., and Brose, U. (2011). "The allometry of prey preferences". In: *PLoS ONE* 6.10, e25937. DOI: 10.1371/journal.pone.0025937.

Kalinkat, G., Schneider, F. D., Digel, C., Guill, C., Rall, B. C., and Brose, U. (2013). "Body masses, functional responses and predator-prey stability". In: *Ecology Letters* 16.9, pp. 1126–1134. DOI: 10.1111/ele.12147.

Kéfi, S., Guttal, V., Brock, W. A., Carpenter, S. R., Ellison, A. M., Livina, V. N., Seekell, D. A., Scheffer, M., Van Nes, E. H., and Dakos, V. (2014). "Early warning signals of ecological transitions: Methods for spatial patterns". In: *PLoS ONE* 9.3, e92097. DOI: 10.1371/journal.pone.0092097.

Keitt, T. H. and Fischer, J. (2006). "Detection of scale-specific community dynamics using wavelets". In: *Ecology* 87.11, pp. 2895–2904. DOI: 10.1890/0012-9658(2006)87[2895:DOSCDU]2.0.CO;2.

Kendall, B. E. (1998). "Estimating the magnitude of environmental stochasticity in survivorship data". In: *Ecological Applications* 8.1, pp. 184–193. DOI: 10.1890/1051-0761(1998)008[0184:ETMOES]2.0.CO;2.

Klug, J. L., Fischer, J. M., Ives, A. R., and Dennis, B. (2000). "Compensatory dynamics in planktonic community responses to pH perturbations". In: *Ecology* 81.2, pp. 387–398. DOI: 10.1890/0012-9658(2000)081[0387:CDIPCR]2.0.CO;2.

Kovach-Orr, C. and Fussmann, G. F. (2013). "Evolutionary and plastic rescue in multitrophic model communities". In: *Philosophical Transactions of the Royal Society B: Biological Sciences* 368.1610, p. 20120084. DOI: 10.1098/rstb.2012.0084.

Krause, S., Le Roux, X., Niklaus, P. A., Bodegom, P. M. van, Lennon T., J. T., Bertilsson, S., Grossart, H. P., Philippot, L., and Bodelier, P. L. (2014). "Trait-based approaches for understanding microbial biodiversity and ecosystem functioning". In: *Frontiers in Microbiology* 5, p. 251. DOI: 10.3389/fmicb.2014.00251.

Letellier, C. and Aziz-Alaoui, M. A. (2002). "Analysis of the dynamics of a realistic ecological model". In: *Chaos*, *Solitons and Fractals* 13.1, pp. 95–107. DOI: 10.1016/S0960-0779(00)00239-3.

Levine, J. M., Bascompte, J., Adler, P. B., and Allesina, S. (2017). "Beyond pairwise mechanisms of species coexistence in complex communities". In: *Nature* 546.7656, pp. 56–64. DOI: 10.1038/nature22898.

Litchman, E. and Klausmeier, C. A. (2008). "Trait-Based Community Ecology of Phytoplankton". In: *Annual Review of Ecology, Evolution, and Systematics* 39.1, pp. 615–639. DOI: 10.1146/annurev.ecolsys.39.110707.173549.

Litchman, E., Klausmeier, C. A., Schofield, O. M., and Falkowski, P. G. (2007). "The role of functional traits and trade-offs in structuring phytoplankton communities: Scaling from cellular to ecosystem level". In: *Ecology Letters* 10.12, pp. 1170–1181. DOI: 10.1111/j.1461-0248.2007.01117.x.

Loreau, M. et al. (2001). "Biodiversity and ecosystem functioning: Current knowledge and future challenges". In: *Science* 294.5543, pp. 804–808. DOI: 10.1126/science.1064088.

Lurling, M. and Beekman, W. (2006). "Palmelloids formation in Chlamydomonas reinhardtii : defence against rotifer predators?" In: *Annales de Limnologie - International Journal of Limnology* 42.2, pp. 65–72. DOI: 10.1051/limn/2006010.

May, R. M. (1972). "Limit cycles in predator-prey communities". In: *Science* 177.4052, pp. 900–902. DOI: 10.1126/science.177.4052.900.

McCann, K. S. (2000). "The diversity–stability debate". In: *Nature* 405.6783, pp. 228–233. DOI: 10.1038/35012234.

Micheli, F., Cottingham, K. L., Bascompte, J., Bjornstad, O. N., Eckert, G. L., Fischer, J. M., Keitt, T. H., Kendall, B. E., Klug, J. L., and Rusak, J. A. (1999). "The Dual Nature of Community Variability". In: *Oikos* 85.1, pp. 161–169. DOI: 10.2307/3546802.

Moloney, C. L. and Field, J. G. (1989). "General allometric equations for rates of nutrient uptake, ingestion, and respiration in plankton organisms". In: *Limnology and Oceanography* 34.7, pp. 1290–1299. DOI: 10.4319/lo.1989.34.7.1290.

Monod, J. (1950). "La technique de culture continue, theorie et applications". In: *Ann d'Institute Pasteur* 79.19, pp. 390–410. DOI: 10.1016/B978-0-12-460482-7.50023-3.

Morozov, A. Y. (2010). "Emergence of Holling type III zooplankton functional response: Bringing together field evidence and mathematical modelling". In: *Journal of Theoretical Biology* 265.1, pp. 45–54. DOI: 10.1016/j.jtbi.2010.04.016.

Murdoch, A. W. W., Nisbet, R. M., Mccauley, E., M, A., and Gurney, W. S. C. (1998). "Plankton Abundance and Dynamics across Nutrient Levels : Tests of Hypotheses". In: *Ecology* 79.4, pp. 1339–1356.

Naeem, S., Duffy, J. E., and Zavaleta, E. (2012). "The functions of biological diversity in an age of extinction". In: *Science* 336.6087, pp. 1401–1406. DOI: 10.1126/science.1215855.

Nakazawa, T. (2011). "Ontogenetic niche shift, food-web coupling, and alternative stable states". In: *Theoretical Ecology* 4.4, pp. 479–494. DOI: 10.1007/s12080-010-0090-0.

Oaten, A. and Murdoch, W. W. (1975). "Functional response and stability in predator-prey systems". In: *The American Naturalist* 109.967, pp. 289–298. DOI: 10.1086/282998.

Pace, M. L., Cole, J. J., Carpenter, S. R., and Kitchell, J. F. (1999). "Trophic cascades revealed in diverse ecosystems". In: *Trends in Ecology and Evolution* 14.12, pp. 483–488. DOI: 10.1016/S0169-5347(99)01723-1.

Peet, A. B., Deutsch, P. A., and Peacock-López, E. (2005). "Complex dynamics in a three-level trophic system with intraspecies interaction". In: *Journal of Theoretical Biology* 232.4, pp. 491–503. DOI: 10.1016/j.jtbi.2004.08.028.

Rasher, D. B., Hoey, A. S., and Hay, M. E. (2013). "Consumer diversity interacts with prey defenses to drive ecosystem function". In: *Ecology* 94.6, pp. 1347–1358. DOI: 10.1890/12-0389.1.

Sarnelle, O. and Wilson, A. E. (2008). "Type III functional response in Daphnia". In: *Ecology* 89.6, pp. 1723–1732. DOI: 10.1890/07-0935.1.

Scheffer, M., Hosper, S. H., Meijer, M. L., Moss, B., and Jeppesen, E. (1993). "Alternative equilibria in shallow lakes". In: *Trends in Ecology and Evolution* 8.8, pp. 275–279. DOI: 10.1016/0169-5347(93)90254-M.

Scheffer, M., Bascompte, J., Brock, W. A., Brovkin, V., Carpenter, S. R., Dakos, V., Held, H., Van Nes, E. H., Rietkerk, M., and Sugihara, G. (2009). "Early-warning signals for critical transitions". In: *Nature* 461.7260, pp. 53–59. DOI: 10.1038/nature08227.

Scheffer, M. and Carpenter, S. R. (2003). "Catastrophic regime shifts in ecosystems: Linking theory to observation". In: *Trends in Ecology and Evolution* 18.12, pp. 648–656. DOI: 10.1016/j.tree.2003.09.002.

Schneider, F. D., Brose, U., Rall, B. C., and Guill, C. (Dec. 2016). "Animal diversity and ecosystem functioning in dynamic food webs". In: *Nature Communications* 7, p. 12718. DOI: 10.1038/ncomms12718.

Seifert, L. I., De Castro, F., Marquart, A., Gaedke, U., Weithoff, G., and Vos, M. (2014). "Heated relations: Temperature-mediated shifts in consumption across trophic levels". In: *PLoS ONE* 9.5, e95046. DOI: 10.1371/journal.pone.0095046.

Steiner, C. F., Darcy-Hall, T. L., Dorn, N. J., Garcia, E. A., Mittelbach, G. G., and Wojdak, J. M. (2005). "The influence of consumer diversity and indirect facilitation on trophic level biomass and stability". In: *Oikos* 110.3, pp. 556–566. DOI: 10.1111/j.0030-1299.2005.13665.x.

Tilman, D., Kilham, S. S., and Kilham, P. (1982). "Phytoplankton Community Ecology: The Role of Limiting Nutrients". In: *Annual Review of Ecology and Systematics* 13.1, pp. 349–372. DOI: 10.1146/annurev.es.13.110182.002025.

Tilman, D., Isbell, F., and Cowles, J. M. (2014). "Biodiversity and Ecosystem Functioning". In: *Annual Review of Ecology, Evolution, and Systematics* 45.1, pp. 471–493. DOI: 10.1146/annurev-ecolsys-120213-091917.

Tilman, D., Knops, J., Wedin, D., Reich, P., Ritchie, M., and Siemann, E. (1997). "The influence of functional diversity and composition on ecosystem processes". In: *Science* 277.5330, pp. 1300–1302. DOI: 10.1126/science.277.5330.1300.

Tilman, D., Reich, P. B., and Knops, J. M. H. (2006). "Biodiversity and ecosystem stability in a decade-long grassland experiment". In: *Nature* 441.7093, pp. 629–632. DOI: 10.1038/nature04742.

Tirok, K. and Gaedke, U. (2010). "Internally driven alternation of functional traits in a multispecies predator- prey system". In: *Ecology* 91.6, pp. 1748–1762. DOI: 10.1890/09-1052.1.

Van Der Walt, S., Colbert, S. C., and Varoquaux, G. (2011). "The NumPy array: A structure for efficient numerical computation". In: *Computing in Science and Engineering* 13.2, pp. 22–30. DOI: 10.1109/MCSE.2011.37.

Van Velzen, E. and Gaedke, U. (2017). "Disentangling eco-evolutionary dynamics of predator-prey co-evolution: The case of antiphase cycles". In: *Scientific Reports* 7.1, p. 17125. DOI: 10.1038/s41598-017-17019-4.

Van Voorn, G. A. K., Kooi, B. W., and Boer, M. P. (2010). "Ecological consequences of global bifurcations in some food chain models". In: *Mathematical Biosciences* 226.2, pp. 120–133. DOI: 10.1016/j.mbs.2010.04.005.

Vasseur, D. A. and Gaedke, U. (2007). "Spectral analysis unmasks synchronous and compensatory dynamics in plankton communities". In: *Ecology* 88.8, pp. 2058–2071. DOI: 10.1890/06-1899.1.

Violle, C., Navas, M.-L., Vile, D., Kazakou, E., Fortunel, C., Hummel, I., and Garnier, E. (2007). "Let the concept of trait be functional!" In: *Oikos* 116.5, pp. 882–892. DOI: 10.1111/j.2007.0030-1299.15559.x.

Wang, S. and Brose, U. (2018). "Biodiversity and ecosystem functioning in food webs: the vertical diversity hypothesis". In: *Ecology Letters* 21.1, pp. 9–20. DOI: 10.1111/ele.12865.

Weithoff, G. (2003). "The concepts of 'plant functional types' and 'functional diversity' in lake phytoplankton – a new understanding of phytoplankton ecology?" In: *Freshwater Biology* 48.9, pp. 1669–1675.

Williams, R. J. and Martinez, N. D. (2004). "Stabilization of chaotic and non-permanent food-web dynamics". In: *European Physical Journal B* 38.2, pp. 297–303. DOI: 10.1140/epjb/e2004-00122-1.

Wissel, C. (1984). "A universal law of the characteristic return time near thresholds". In: *Oecologia* 65.1, pp. 101–107. DOI: 10.1007/BF00384470.

Wollrab, S., Diehl, S., and De Roos, A. M. (2012). "Simple rules describe bottom-up and top-down control in food webs with alternative energy pathways". In: *Ecology Letters* 15.9, pp. 935–946. DOI: 10.1111/j.1461-0248.2012.01823.x.

Worm, B. et al. (2006). "Impacts of Biodiversity Loss on Ocean Ecosystem Services". In: *Science* 314.5800, pp. 787–790. DOI: 10.1126/science.1132294.

Yachi, S. and Loreau, M. (1999). "Biodiversity and ecosystem productivity in a fluctuating environment: The insurance hypothesis". In: *Proceedings of the National Academy of Sciences* 96.4, pp. 1463–1468. DOI: 10.1073/pnas.96.4.1463.

Yamamichi, M., Yoshida, T., and Sasaki, A. (2011). "Comparing the Effects of Rapid Evolution and Phenotypic Plasticity on Predator-Prey Dynamics". In: *The American Naturalist* 178.3, pp. 287–304. DOI: 10.1086/661241.

Yoshida, T., Jones, L. E., Ellner, S. P., Fussmann, G. F., and Hairston, N. G. (2003). "Rapid evolution drives ecological dynamics in a predator-prey system". In: *Nature* 424.6946, pp. 303–306. DOI: 10.1038/nature01767.

Chapter 3

Top predators govern multitrophic diversity effects in tritrophic food webs

Ruben Ceulemans, Christian Guill, & Ursula Gaedke
Under review at Ecology, after *"major revision"*.

The data presented in this manuscript, the code required to produce it, and the code required to train the random forests on this data are available as an electronic supplement to our bioRxiv submission (Ceulemans, Guill, and Gaedke, 2020).

Abstract

It is well known that functional diversity strongly affects ecosystem functioning. However, even in rather simple model communities consisting of only two or, at best, three trophic levels, the relationship between multitrophic functional diversity and ecosystem functioning appears difficult to generalize, due to its high contextuality. In this study, we considered several differently structured tritrophic food webs, in which the amount of functional diversity was varied independently on each trophic level. To achieve generalizable results, largely independent of parametrization, we examined the outcomes of $128,000$ parameter combinations sampled from ecologically plausible intervals, with each tested for 200 randomly sampled initial conditions. Analysis of our data was done by training a Random Forest model. This method enables the identification of complex patterns in the data through partial dependence graphs, and the comparison of the relative influence of model parameters, including the degree of diversity, on food web properties. We found that bottom-up and top-down effects cascade simultaneously throughout the food web, intimately linking the effects of functional diversity of any trophic level to the amount of diversity of other trophic levels, which may explain the difficulty in unifying results from previous studies. Strikingly, only with high diversity throughout the whole food web, different interactions synergize to ensure efficient exploitation

of the available nutrients and efficient biomass transfer, ultimately leading to a high biomass and production on the top level. The temporal variation of biomass showed a more complex pattern with increasing multitrophic diversity: while the system initially became less variable, eventually the temporal variation rose again due to the increasingly complex dynamical patterns. Importantly, top predator diversity and food web parameters affecting the top trophic level were of highest importance to determine the biomass and temporal variability of any trophic level. Overall, our study reveals that the mechanisms by which diversity influences ecosystem functioning are affected by every part of the food web, hampering the extrapolation of insights from simple monotrophic or bitrophic systems to complex natural food webs.

3.1 Introduction

In the face of rapid global biodiversity loss (Pimm et al., 2014), investigating the influence of biodiversity on ecosystem functioning is a highly important area of research. It has become clear that biodiversity is a predominant factor in determining relevant functions of ecosystems such as biomass production, resource use efficiency, and stability (Hooper et al., 2005; Tilman, Reich, and Knops, 2006; Worm et al., 2006). A major factor affecting the link between biodiversity and these ecosystem functions is functional diversity, i.e., the range of differences between the functions of species contained within the ecosystem (Petchey and Gaston, 2006).

Mechanistically motivated studies into the role of functional diversity have mainly been performed in the context of simple communities consisting only of one or, at best, two trophic levels. Many of these studies restricted their focus to primary producer diversity, and were able to show its correlation with relevant ecosystem functions (reviewed by Cardinale et al., 2011). However, during the last two decades, more sophisticated theoretical and experimental studies linking both plant and consumer diversity to these ecosystem functions were conducted (see Thébault and Loreau, 2003; Tirok and Gaedke, 2010; Borer, Seabloom, and Tilman, 2012; Filip et al., 2014; Klauschies, Vasseur, and Gaedke, 2016; Schneider et al., 2016; Seabloom et al., 2017; Flöder, Bromann, and Moorthi, 2018, and reviews by Duffy et al., 2007; Griffin, Byrnes, and Cardinale, 2013; Barnes et al., 2018). In a recent experimental study, Wohlgemuth et al., 2017 demonstrated that producer diversity effects on the biomass distribution and production at higher trophic levels crucially depends on particular traits of the consumer level, such as specialization and selectivity. Such studies highlight how the links between multitrophic functional diversity and ecosystem functioning are difficult to generalize, due to their high contextuality. The specific food webs that are studied, and the theoretical models used to study them, are often too different to enable a meaningful attempt at synthesis of their findings (Thébault and Loreau, 2003; Barnes et al., 2018).

For this reason there is a clear need to understand the effects of diversity on ecosystem functions in a setting that is as general and context-free as possible. In addition, the high degree of interplay already observed between diversity of the primary producer and herbivore consumer level underlines the importance of including diversity of even higher trophic levels. In this study, we want to advance our understanding of how functional diversity affects ecosystem functioning in model communities by including a diverse third trophic level. While it has often been highlighted how important the effects of the third trophic level on ecosystem functions are (Bruno and O'Connor, 2005; Duffy et al., 2007; Daam et al., 2019; Abdala-Roberts et al., 2019; Ehrlich and Gaedke, 2020), relatively few studies have attempted to explicitly take these effects into account. Ceulemans et al., 2019 showed that functional diversity increases the biomass production, temporal stability, and biomass transfer efficiency to higher trophic levels of a tritrophic food web, when diversity is increased simultaneously at all three trophic levels. This model analyzed one particular food web structure in detail, which raises the question whether the observed trends are to be expected in general, or whether they are context-dependent as well.

Our study tackles this issue by investigating several different tritrophic food web configurations with respect to the same ecosystem functions. Such a method has been applied successfully in the past (Gilman et al., 2010; Kovach-Orr and Fussmann, 2013; Poisot, Mouquet, and Gravel, 2013), but this study is the first where the diversity can be independently controlled on three trophic levels. We investigated eight different food web configurations (Fig. 3.1), which differ in the trophic location at which functional diversity may be present. We measured functional diversity of a trophic level by the difference between the functional traits of the two species residing there: when the trait difference between the species is large, so is the functional diversity, and vice-versa. In this way, we were able to change the functional diversity of a trophic level without changing the number of species. Adopting such a trait-based rather than species-specific approach by analyzing functional diversity through trait differences, instead of using non-functional metrics of biodiversity such as species number, allows us to produce results of high generality (McGill et al., 2006; Hillebrand and Matthiessen, 2009; Krause et al., 2014). Furthermore, the relatively simple and general structure of our food webs (see Fig. 3.1) makes our results accessible for verification by experimental studies, as they are often limited in how much complexity can be included.

Our model rests on few very general assumptions. The first is allometry, which states that larger organisms tend to grow slower than smaller ones (Kalinkat et al., 2013). Combined with the assumption that consumers tend to be larger than their prey we obtain the general property that the mean growth rate should decrease as the trophic level increases. This strictly holds for pelagic systems (Gaedke and Kamjunke, 2006), but also for other ones, except for the plant-herbivore interface (Brose, Williams, and Martinez, 2006). The third basic assumption is the

frequently established trade-off between growth rate and defense (Herms and Mattson, 1992; Hillebrand, Worm, and Lotze, 2000; Kneitel and Chase, 2004; Ehrlich, Becks, and Gaedke, 2017; Ehrlich, Kath, and Gaedke, 2020). It implies that slow growing species are generally less affected by grazing than faster growing species, which invest less in defense mechanisms due to energetic limitations. In addition, the non-grazing mortality terms (see Eq. (3.8)) are of general nature and may be due to several different processes, such as basal respiration, the influence of parasites and viruses, or outflow in an experimental microcosm.

Importantly, food web dynamics do not only depend on the topology of the food web, but also on the specific parametrization used, regarding both external environmental parameters as well as internal parameters such as growth rates, attacks rates, and handling times. To sufficiently capture the potentially high variation in biomass dynamics, we randomly selected a total of 128,000 parameter combinations from ecologically plausible intervals for the eight different food webs, as well as tested 200 initial conditions per parameter combination. These parameter values were drawn from intervals geometrically centered around values which are particularly relevant for planktonic systems (Ceulemans et al., 2019), but are sufficiently wide to capture the behavior of many different types of food webs (see Table 3.1). This procedure allows us to obtain results of high generality, as they apply to the average behavior of tritrophic systems, independent of its parametrization.

3.2 Methods

The numerical data used in our study was obtained by storing the mean biomasses and coefficients of variation (CVs) of the following ordinary differential equation model:

$$\begin{cases} \dot{N} & = \delta\,(N_0 - N) - \dfrac{c_N}{c_C} \sum_i r_i B_i \\[2mm] \dot{B}_i & = r_i B_i - \sum_j g_{ji} I_j - d_{B_i} B_i \\[2mm] \dot{I}_i & = e \sum_j g_{ij} I_i - \sum_i \gamma_{ji} T_j - d_{I_i} I_i \\[2mm] \dot{T}_i & = e \sum_j \gamma_{ij} T_i - d_{T_i} T_i, \end{cases} \tag{3.1}$$

where the indices $i, j \in \{1, 2\}$. N describes the free inorganic nutrients in the system, with the inflow concentration N_0, inflow rate δ, and nutrient-to-carbon ratio $\frac{c_N}{c_C}$. The loss rates d_{B_i}, d_{I_i}, and d_{T_i} represent losses proportional to the biomass present, such as basal respiration, sedimentation, or wash-out. The basal species' B_i uptake rate r_i is described by their maximal growth rate r_i' and nutrient uptake half-saturation

constant h_N:

$$r_i = r_i' \frac{N}{N + h_N}.$$ (3.2)

The interaction between the intermediate species I_i and the basal species B_j is described by a Holling-Type-III functional response which is determined by the attack rate a_{ij}, handling time h_{ij} and the Hill exponent n:

$$g_{ij} = a_{ij} \frac{B_j^n}{\sum_{j'} a_{ij'} h_{ij'} B_{j'}^n + 1}.$$ (3.3)

In the same way, the interaction between top species T_i and intermediate species I_j is given by:

$$\gamma_{ij} = \alpha_{ij} \frac{I_j^\nu}{\sum_k \alpha_{ik} \eta_{ik} I_k^\nu + 1},$$ (3.4)

with attack rate α_{ij}, handling time η_{ij}, and Hill exponent ν. Finally, the biomass conversion efficiency for the intermediate and top species is described by e.

Influence of trait differences on trait parameters

The parameters $r_i', h_{ij}, a_{ij}, \eta_{ij}, \alpha_{ij}$, and all death rates are determined by the trait differences Δ_B, Δ_I, and Δ_T, which each can vary from 0 (the two species at each trophic level are equal) to 1 (maximal trait differences). As trait differences increase, the species B_1, I_1, and T_1 will be metabolically more active, whereas B_2, I_2, and T_2 will be less active through modifying their maximal feeding rates (which equal the inverse of the handling times h_{ij} and η_{ij} for the intermediate and top species).

In our model, trait differences affect the relevant species' parameters symmetrically, such that an increase for species 1 leads to a decrease for species 2 by the same factor. Explicitly:

$$
\begin{aligned}
&r_1' = r_0' \cdot B_{\text{inc}} &\quad h_{1i} &\sim \frac{h_0}{I_{\text{inc}}} &\quad \eta_{1i} &\sim \frac{\eta_0}{T_{\text{inc}}} \\
&r_2' = \frac{r_0'}{B_{\text{inc}}} &\quad h_{2i} &\sim h_0 \cdot I_{\text{inc}} &\quad \eta_{2i} &\sim \eta_0 \cdot T_{\text{inc}},
\end{aligned}
$$ (3.5)

with

$$B_{\text{inc}} = 1 + \Delta_B \cdot \tau_{\text{inc}} \qquad I_{\text{inc}} = 1 + \Delta_I \cdot \tau_{\text{inc}} \qquad T_{\text{inc}} = 1 + \Delta_T \cdot \tau_{\text{inc}},$$ (3.6)

so that they are unity for $\Delta_i = 0$, leaving the species' parameters unaffected, and maximal for $\Delta_i = 1$, where τ_{inc} determines their maximal increase. Note that the handling times h_{ij} and η_{ij} depend on the trait differences of both the predator and the prey level, hence the proportional relationship ($\sim$) instead of equality (more information is provided below, cf. Equations (3.7) & (3.9)).

The universality of trade-offs in natural systems (Kneitel and Chase, 2004; Ehrlich, Becks, and Gaedke, 2017) implies that for any increase or decrease in growth rates,

the species' loss rates must change correspondingly. Time and/or energy that is invested towards a certain defense strategy cannot be used for resource uptake, and thus, comes at the cost of a lower growth rate (and thus a higher handling time). Conversely, investing in a higher growth rate (lower handling time) tends to make a species more vulnerable to predation as it leaves less time and/or energy for employing defense strategies. For simplicity, the loss rates are affected in the same way as the growth rates. Thus, B_{inc} affects the handling times h_{ij} as well as the death rates d_{B_i}, I_{inc} affects η_{ij} and d_{I_i}, and T_{inc} affects d_{T_i}, in the following way:

$$
\begin{aligned}
h_{i1} &\sim \frac{h_0}{B_{\text{inc}}} & \eta_{i1} &\sim \frac{\eta_0}{I_{\text{inc}}} \\
h_{i2} &\sim h_0 \cdot B_{\text{inc}} & \eta_{i2} &\sim \eta_0 \cdot I_{\text{inc}},
\end{aligned}
\tag{3.7}
$$

and,

$$
\begin{aligned}
d_{B_1} &= \delta \cdot B_{\text{inc}} & d_{I_1} &= \delta \cdot I_{\text{inc}} & d_{T_1} &= \delta \cdot T_{\text{inc}} \\
d_{B_2} &= \frac{\delta}{B_{\text{inc}}} & d_{I_2} &= \frac{\delta}{I_{\text{inc}}} & d_{T_2} &= \frac{\delta}{T_{\text{inc}}}
\end{aligned}
\tag{3.8}
$$

The handling times h_{ij} and η_{ij} are thus dependent on both B_{inc} & I_{inc}, or I_{inc} & T_{inc}, respectively. While the linear relationship that describes this dependence is almost certainly a simplification of biological reality, specifying a more complex relationship might make our model unnecessarily more complicated. As described in the next section, multiple parameter combinations will be investigated, which means that our approach is not limited to one single distinct trade-off curve.

Summarizing:

$$
h = h_0 \begin{pmatrix} \frac{1}{B_{\text{inc}} I_{\text{inc}}} & \frac{B_{\text{inc}}}{I_{\text{inc}}} \\ \frac{I_{\text{inc}}}{B_{\text{inc}}} & B_{\text{inc}} I_{\text{inc}} \end{pmatrix}, \qquad \eta = \eta_0 \begin{pmatrix} \frac{1}{I_{\text{inc}} T_{\text{inc}}} & \frac{I_{\text{inc}}}{T_{\text{inc}}} \\ \frac{T_{\text{inc}}}{I_{\text{inc}}} & I_{\text{inc}} T_{\text{inc}} \end{pmatrix}.
\tag{3.9}
$$

The interaction between predator-prey pairs is not only determined by the handling times h_{ij} and η_{ij}, but also by the attack rates a_{ij} and α_{ij}. In our model, these are responsible for determining the relative strength of the "cross" links between two adjacent trophic levels (e.g. $B_1 \rightarrow I_2$, etc.). As the functional diversity on adjacent trophic levels increases, these "cross" links will decrease in strength relative to the "parallel" links (e.g. $B_1 \rightarrow I_1$, etc.). The rate at which their strength decreases is determined by the attack rate scaling parameter a_{scale}. For details see Section B.1, Appendix B. In this way, it is possible to describe a tightly linked food web for $a_{\text{scale}} \approx 1$, two largely separated tritrophic chains for $a_{\text{scale}} \gg 1$, or an intermediate situation.

Parameter selection

In order to capture a high diversity of dynamical outcomes, within a plausible eco-
logical setting, the parameters of the food web were sampled uniformly from certain
intervals determined by a standard value from which the boundaries are calculated
(Table 3.1). These standard values are based on Ceulemans et al., 2019, and describe
an ecologically realistic planktonic system with three trophic levels. In particular,
the maximal growth rates ($r'_0, e/h_0, \& e/\eta_0$) were set to correspond to an allometri-
cally scaled food chain with the body mass ratios between adjacent trophic levels of
10^3, with an allometric scaling exponent of -0.15. However, due to the spread of the
intervals the actual ratio between body masses (assuming the same scaling exponent
λ) can vary between approximately 1 and 10,000,000 (for details, see Section B.2,
Appendix B). In this way, a good balance is made between capturing a high amount
of dynamical variation, while still being ecologically realistic.

The trait difference parameters can take the following values:

$$\Delta_B \in \{0, 0.25, 0.5, 0.75, 1\},$$
$$\Delta_I \in \{0, 0.25, 0.5, 0.75, 1\}, \tag{3.10}$$
$$\Delta_T \in \{0, 0.25, 0.5, 0.75, 1\},$$

so that there are 125 combinations possible. These determine both the specific food
web topology and the amount of functional diversity present. For example, $\Delta_B = 1, \Delta_I = 0.25$, and $\Delta_T = 0$ implies that we are investigating the BI food web (Fig. 3.1),
where the basal level is highly diverse, but the species on the intermediate level are
still relatively similar.

In order to sample a large part of all the possible dynamical outcomes that can be
exhibited by our model, we randomly sampled 1024 different parameter combina-
tions, for each selection of Δ_B, Δ_I, and Δ_T (Eq. 3.10). Moreover, for every parameter
combination, 200 different initial conditions were tested to capture potential alter-
native stable states. These initial values were randomly sampled such that the total
amount of biomass in the initial state did not exceed $2 \cdot N_0$. The system was allowed
to relax to its attractor before the mean biomasses and the CV of each species, and of
each trophic level, were recorded for a sufficiently long time period. More detailed
information on this procedure can be found in Section B.3, Appendix B. Numerical
integration of the ordinary differential equations in Eq. (3.1) was done in C with the
SUNDIALS CVODE solver version 2.7.0 (Hindmarsh et al., 2005). Subsequent anal-
ysis of the food web data was performed in Python 3.6 using NumPy (Van Der Walt,
Colbert, and Varoquaux, 2011), pandas (McKinney, 2010), and Matplotlib (Hunter,
2007). Further details on our computational procedure, as well as the code itself and
the data required to produce Figs. 3.3-3.6 and various Appendix Figs. can be found
as an electronic supplement.

Random Forest Model

In order to simplify the presentation of our results, and to easily extract additional relevant information, we trained a Random Forest model on our dataset. A detailed description of how this works can be found in Section B.3, Appendix B. Essentially, Random Forests are a class of machine learning models which are popularly used due to their relatively simple structure and high versatility (Breiman, 2001; Cutler et al., 2007; Thomas et al., 2018).

For each quantity of interest (see Results), an Extremely Random Forest consisting of 2000 trees was trained using the Scikit-learn (Pedregosa et al., 2011) package in Python. Using only those parameter combinations that lead to coexistence of all species in the food web, the training dataset consisted of the 14 different parameters (see Table 3.1 and Eqs. 3.10) as input values, and the mean biomass and CVs of each trophic level as output values. During training, the random forest algorithm performed cross-validation by calculating the Out-Of-Bag (OOB) score, to estimate its accuracy. After training the random forest model, we used it to investigate how the basal, intermediate, and top diversity (Δ_B, Δ_I, and Δ_T) affect the quantities of interest, independently of all other parameters, by examining the partial dependency graphs. Finally, the random forest also provided us with a measure of the importance of each of the input parameters in determining the desired outcome (relative importance).

3.3 Results

In order to understand in which ways diversity of different trophic levels affects tritrophic systems, we analyzed the solutions of the ordinary differential equation model presented in the Methods (Equation (3.1)) for $128,000$ different parameter combinations. For each parameter combination, we saved the mean nutrient concentration and biomass density (in short biomass) and coefficient of variation (CV) of each individual population and trophic level over a long period of time (see also Section B.3, Appendix B). In the main text, we will focus in particular on diversity effects on:

- the nutrient concentration N and biomass per trophic level B_B, B_I, B_T (see Fig. 3.3); and

- the CV of the nutrient concentration and biomass per trophic level CV_N, CV_B, CV_I, CV_T (see Fig. 3.4).

Based on the mean biomasses, we also calculated several quantities related to the flow of energy through the food web. The following ones are shown in the main text (see Fig. 3.5, and Equation (3.1) and Section B.5, Appendix B for more information):

- the biomass production on the top level $P_T = \sum_i d_{T_i} T_i$;

- the amount of basal biomass flowing upward to the intermediate level B_{up};

- the production to biomass ratio of the basal level $(P/B)_B = (B_{up}+\sum_i d_{B_i} B_i)/(\sum_i B_i)$; and

- the food web efficiency, defined as the ratio between the biomass production at the top and the basal level: P_T/P_B.

Figs. 3.3-3.5 are partial dependence graphs revealing how trait differences on the basal (Δ_B), intermediate (Δ_I), and top (Δ_T) level affect the quantity of interest. Such partial dependence graphs are calculated from the Random Forest model trained on the food web data, and show the average value of the quantity of interest, independent of all other model parameters (see Methods). This presentation allows us to concisely capture the full behavior of all food webs, as they each occupy a certain location in the partial dependency graphs (Fig. 3.2). A concise summary of our main findings is presented in Table 3.2.

In most cases the OOB scores, which measure the accuracy of the Random Forest models, were above 0.60, with some exceptions (Table 3.3). Such scores indicate a sufficient model accuracy as we focus on the average trends in the predicted quantity as a function of the functional diversity of different trophic levels, rather than on predictions for specific parameter values.

The quantities of interest were only examined for those initial conditions and parameter combinations that actually led to coexistence of all species originally present (see Fig. 3.1). Interestingly, there were only very few parameter combinations that led to coexistence for the T (1 combination) and BT (8 combinations) food webs (see Section B.4, Appendix B). One of the two top species almost always outcompeted the other in these webs. As we cannot reliably investigate the behavior of these food webs in general, we did not include these parameter combinations in our dataset. This implies that our dataset contains no data points with $\Delta_T > 0, \Delta_I = 0$, and therefore the region below $\Delta_I = 0.25$ for $\Delta_T > 0$ in Figs. 3.3-3.5 remains empty.

3.3.1 Nutrient concentration and biomasses

The partial dependency graphs of the free nutrient concentration and the biomasses on each trophic level on the trait differences Δ_B, Δ_I, and Δ_T (Fig. 3.3) reveal strong differences between the simple chain without any diversity ($\Delta_B = \Delta_I = \Delta_T = 0$), and the food web with high trait differences at every trophic level ($\Delta_B = \Delta_I = 1$, and $\Delta_T = $ high). Comparing these two points shows that the linear chain has a higher average free nutrient concentration and a lower intermediate and top biomass than the diverse food web.

In between these two extremes, the tritrophic structure of our model gives rise to several interesting patterns. Comparing the chain and the B, I and BI food webs (i.e. $\Delta_T = 0$, Fig. 3.3, left panels) shows that when Δ_I is 0 or low, increasing Δ_B leads to a decrease in basal biomass, whereas if Δ_I is high, this pattern reverses as the basal biomass increases with Δ_B. In other words, if functional diversity is only present on the basal level, basal biomass tends to decrease with Δ_B. However, taking consumer

diversity into consideration in the BI food web shows that this pattern is not general and strongly depends on the actual level of consumer diversity (Δ_I).

Investigating the effect of Δ_I and Δ_T on the intermediate and top level biomasses shows exactly the same pattern. When Δ_T is 0, intermediate biomass tends to decrease as Δ_I increases, whereas when Δ_T is high, it increases with Δ_I (independently of Δ_B). Additionally, it is clear that top biomass increases with Δ_T in a gradual fashion.

The location and strength of trophic cascading in the food web is also affected by the amount of functional diversity present on the different trophic levels. For example, when Δ_T is zero, an inverse relationship between the biomass on the intermediate and basal level can be observed, whereas the top level biomass seems hardly affected by Δ_B and Δ_I (Fig. 3.3). When Δ_T is low, biomasses at the top and intermediate level are strongly negatively correlated, indicating that a diverse top level is able to exert a stronger influence on the whole food web as compared to a non-diverse top level. This negative relationship does not cascade downwards to the basal level, potentially due to the buffering properties of a diverse intermediate level. However, for Δ_T = high, the strong inverse relationship between top and intermediate biomass is replaced by a rather positive one, due to the sharp increase in intermediate biomass as Δ_I is increased.

3.3.2 Temporal variation

We also examined how the functional diversity at each trophic level (Δ_B, Δ_I, and Δ_T) influences the temporal variation of the nutrients and biomasses per trophic level, by calculating the coefficient of variation (CV) (Fig. 3.4). One clear overarching pattern is the covariation of the CVs along the different trophic levels. Temporal fluctuations at any trophic level propagate through the whole food web, affecting all other levels.

The left column shows how Δ_B and Δ_I affect the CVs of the food webs without top diversity ($\Delta_T = 0$). In this case, the CV of any trophic level depends almost solely on Δ_I. Only the CV of the nutrient concentration depends strongly on Δ_B.

These results are strongly affected by the top diversity. By increasing Δ_T from 0 to *low*, all CVs are considerably dampened. However, this trend reverses as Δ_T is increased further, as all CVs tend to increase again (Δ_T = high). Hence, while comparing the simple chain ($\Delta_B = \Delta_I = \Delta_T = 0$) to the food web with high trait differences ($\Delta_B = \Delta_I = 1$, and Δ_T = high) does not immediately show any notable differences, it is clear that temporal variability is strongly affected in an intricate way by the amount of functional diversity at the different trophic levels.

Additionally, there is a strong correlation between the CV of the basal trophic level, and the free nutrient concentration (Fig. 3.3, bottom row). A low temporal variability on the basal level leads to a strong increase in nutrient exploitation efficiency, and therefore low nutrient concentrations.

Biomass production and food web energetics

We also analyzed metrics related to biomass production and food web energetics: biomass production on the top level P_T, basal biomass flowing to the intermediate level B_{up}, basal biomass to production ratio $(P/B)_B$, and the food web efficiency P_T/P_B (Fig. 3.5, and Section B.5, Appendix B for more information on these quantities). Examining these (and related, see Section B.5, Appendix B) quantities helped us to understand why the biomass at the top level is highest when functional diversity everywhere is high (top right corner in Fig. 3.3 for $\Delta_T = high$). Importantly, we can infer the quantities P_I (total biomass production of the intermediate level) and I_{up} (biomass flowing from the intermediate to the top level) from B_{up} and P_T: $P_I = e \cdot B_{up}$, and $I_{up} = P_T/e$ (see also Section B.5, Appendix B).

The biomass production by the basal level P_B varies only little, as this quantity is completely determined by the interaction with the free nutrients (see Section B.6, Appendix B). This property lies at the basis for explaining the increase in top biomass and food web efficiency as functional diversity increases everywhere.

When $\Delta_T = 0$, the absence of a diverse top trophic level creates a slight relative advantage for the fast growing species I_1 (see Fig. B.12, Appendix B). Its effects on the basal level strongly depend on Δ_I. For high Δ_I, the fast growing B_1 is heavily suppressed and the basal biomass is concentrated in B_2, which is less edible for the prominent I_1. For low Δ_I (i.e., I_1 and I_2 are functionally similar and less specialized), the dominant I_1 can also graze significantly on the slow growing B_2, which strongly promotes the fast-growing B_1. The higher growth rate of B_1 causes strong fluctuations of the basal biomass (Fig.3.4), which, in turn, leads to less efficient nutrient exploitation (Fig. 3.3). Thus, for both low and high intermediate diversity, the basal level is unevenly exploited, which leads to a relatively high proportion of basal biomass being lost from the system, instead of being transferred up the food web (see also Section B.5, Appendix B). The rather low basal biomass that is transferred to the intermediate level supports only a modest amount of intermediate biomass, and hence, a low biomass and biomass production on the top level, and a low food web efficiency.

In contrast, when the top level is highly diverse ($\Delta_T = high$), the intermediate level is more evenly exploited, leading to a balanced presence of both intermediate species. In turn, this leads to an efficient exploitation of the basal level, especially when Δ_I is also high, which is reflected by high values of $(P/B)_B$ (Fig. 3.5). Even though P_B remains roughly the same (Appendix Section B.8, and Section B.6, Appendix B), B_{up} is increased (Fig. 3.5) which leads to a significantly higher intermediate biomass and biomass production (Fig. 3.3 and B.8, Appendix B), and, ultimately an increase in biomass on the top level. This increase subsequently explains the increase in food web efficiency through an increased top biomass production (Fig. 3.5).

Relative importance of parameters

The Random Forest model provides an estimate for the importance of each of the food web parameters in predicting the outcome (see Methods). Fig. 3.6 shows them for the different biomasses and CVs for each of the 14 model parameters (for the relative importance of the different production metrics, see Fig. B.10, Appendix B).

The parameters in each graph are grouped by their mean importance in descending order. For example, the Hill-exponent of the functional response describing the intermediate-top interaction (v) has the highest mean relative importance for predicting the biomasses on each trophic level (Fig. 3.6, top). In particular, it is very important for predicting the biomass on the top and intermediate level. On the other hand, the nutrient-uptake half saturation constant h_N is the least important.

One important observation in all three panels is that while the three possible trait differences Δ_B, Δ_I, and Δ_T have a strong influence on all the different quantities we have investigated (see Figs. 3.3-3.5), they are never amongst the most important parameters. However, this is not very surprising given the nature of the other parameters in our model: for example, it is very natural that increasing the nutrient inflow concentration N_0 has a very strong influence on species' biomasses.

Our results also show a balance between the relative importance of parameters affecting the external environment (such as the nutrient inflow concentration N_0 and the inflow rate δ), and internal parameters affecting the ecological dynamics within the food web (such as the handling times h_0, η_0, and Hill-exponents n, v). Remarkably, parameters affecting the intermediate-top interaction (v, η_0, α_0) are of higher importance than their intermediate-basal analogues (n, h_0, a_0). In particular, the importance of the different diversity measures $\Delta_T, \Delta_I, \Delta_B$ is ranked by trophic level. In this way, it is clear that food web parameters affecting the top level of are of highest importance.

3.4 Discussion

The food web model analyzed in this manuscript was built with the aim of being as general as possible, while still being ecologically realistic. Given the expansive range of different environmental and ecological situations that are effectively covered by the model, we did not intend to answer research questions about specific environmental or ecological conditions. Rather, we focused on how the *average* behavior of tritrophic systems depends on the diversity of each trophic level separately. In particular, we studied how functional diversity in tritrophic food webs affects the biomass distribution, temporal variability, and production, on average. The partial dependence graphs provided by training a Random Forest model on our data served as an ideal tool to answer these questions. Given the large amount of parameters that were randomly sampled, it is to be expected that the output data contains a large amount of variation. For example, parameters like the inflow nutrient concentration N_0, or the inflow rate δ naturally have a very strong influence on the

trophic level biomasses and temporal variation. Partial dependence graphs revealed how the predicted outcome changes as a function of one particular parameter, *on average*, i.e., independently of all other model parameters.

Absence of coexistence in some webs

In two of the food webs we investigated, T and BT (see Fig. 3.1), coexistence of all species was extremely rare (see Section B.4, Appendix B). In almost every case, one of the two top species outcompeted the other one, as expected when applying the competitive exclusion principle (Hardin, 1960; Armstrong and McGehee, 1980; Klauschies and Gaedke, 2019). For less than 0.1% of the parameter combinations, both top species still co-occurred at the end of the simulation time. The structure of these two food webs entails that the two top species are competing with each other for only one resource, I, with no other density dependent interaction.

In contrast, coexistence of all species is very likely in the I and IT food webs, even though the two intermediate species also share a single resource, B. This is due to an additional density dependent interaction acting on the intermediate species, by the presence of the top level (which may or may not be diverse). Therefore, more than one species can exist at the intermediate level without the necessity of fine-tuning their interaction parameters (Huntly, 1991; Brose, 2008; Velzen, 2020).

Viewed in this way, it is clear that the amount of functional diversity of one trophic level can drastically influence that of other trophic levels: a loss of functional diversity at the intermediate level in the IT or BIT food webs leads to a loss of functional diversity at the top level as well. It is therefore crucial to safeguard functional diversity of lower trophic levels to enable a diverse top predator community.

Relative parameter importance

The random forest model trained on the output data of our simulations (see Methods) provides information on which of the input parameters (see Table 3.1) are most important for estimating the predicted biomasses, CVs, and production metrics. In short, a parameter is of high importance when it tends to appear high up in many different trees in the forest. Conversely, when a parameter only appears near the end of the trees, it is of low importance in estimating the desired outcome. These relative importances are ranked from highest to lowest in Fig. 3.6.

Remarkably, parameters directly affecting the top trophic level tend to be of high importance, whereas parameters influencing the nutrient uptake by the basal species are all situated near the bottom end. The different diversity indices Δ_B, Δ_I, and Δ_T are also ranked by trophic level. This hierarchy shows how important the higher trophic levels are in determining the biomass distributions, temporal variation of biomass dynamics, and energetics of whole food webs. Our model is thus able to mechanistically support the general observation that changing the diversity of the top trophic level often has far-reaching consequences (Ripple et al., 2014).

In addition to most of the parameters governing the trophic interactions of the top trophic level, the nutrient inflow rate δ and concentration N_0 are also of high importance. As δ determines the death rates of all the species in the model (see Eq. 3.8), and in particular those of the top level, it has a strong influence on the quantities we have investigated (Kath et al., 2018). The nutrient inflow concentration is unsurprisingly also of high importance in estimating these quantities. Its level, representing the total biomass carrying capacity of our system, affects the basal trophic level most strongly (Fig. 3.6), which is in line with field observations (Gaedke, 1998).

This analysis shows that the relative importance measures provided by the random forest model provide useful information to uncover the underlying mechanisms that govern the dynamics of more complex models. Our results clearly show how external and internal food web parameters do not overpower each other. Information on both types is required for accurately predicting biomasses, biomass variability and food web energetics.

The complex relationships between diversity and ecosystem functioning

Our results show that functional diversity robustly increases biomass and production efficiency (Fig. 3.5) at high trophic levels (Fig. 3.3), and generally decreases temporal variation (Fig. 3.4), as summarized by Table 3.2. In addition, we reveal intricate and complicated interactions between the degree of diversity at different trophic levels and these ecosystem functions. These interactions complicate comparison of the numerous studies on the links between diversity and functioning to each other (Filip et al., 2014; Wohlgemuth et al., 2017; Flöder, Bromann, and Moorthi, 2018; Daam et al., 2019).

For instance, our model shows that the effect of increasing producer diversity on the biomasses of each trophic level highly depends on the amount of functional diversity of the other trophic levels (Fig. 3.3). When the top level is not functionally diverse ($\Delta_T = 0$), the direction of the effect of Δ_B on the basal biomass is determined by the amount of functional diversity of the intermediate level (Δ_I). When Δ_I is low (low functional diversity), basal and intermediate biomass tend to decrease with increasing Δ_B, whereas this trend reverses as Δ_I becomes higher. A recent experimental study revealed that the effects of producer diversity on food web functioning also depend on the trait values on the consumer level in a bitrophic system (Wohlgemuth et al., 2017). Our results indicate that this interdependency is of a very general nature, and moreover, is expected to hold for higher trophic levels as well, which are less manageable in experimental settings. Indeed, our model shows a similar pattern when investigating the effect of Δ_I and Δ_T on the intermediate and top biomasses. Starting from $\Delta_T = 0$, increasing Δ_I leads to a reduction in intermediate biomass, compared to an increase in intermediate biomass when Δ_T is high. Our tritrophic food web comparison also shows that, when functional diversity is increased everywhere, the biomass of the intermediate and top species increases significantly, whereas the basal biomass stays roughly constant. The same pattern was found in a

modeling study comparing food webs of up to 100 animal species (Schneider et al., 2016). This correspondency gives credibility to considering the effects of biodiversity on food web functioning through changing the functional diversity in simpler food webs, instead of changing the species number which significantly increases food web complexity.

The effect of functional diversity on the temporal variability (CV) of the biomasses at the different trophic levels also exhibited a complex dependency on the functional diversity of every single trophic level (Fig. 3.4). One particularly robust result, however, is the non-monotonous relationship between top diversity (Δ_T) and the CV of any trophic level. When Δ_T is increased from 0 to *low*, the CVs tended to strongly decrease. Such a reduction in the CV of a community as diversity increases has often been observed (Tilman and Downing, 1996), and can often be attributed to the presence of compensatory dynamical patterns (Gonzalez and Loreau, 2009; Bauer et al., 2014). However, as Δ_T is increased further from *low* to *high*, the CV of each trophic level increased again. Hence, additional mechanisms governing the dynamics must also have a strong influence of the trophic level CVs. In Ceulemans et al., 2019, we observed a similar pattern in the trophic level CVs, which could be explained by the increased relevance of an additional dynamical timescale at high Δ_T: the biomasses not only varied rapidly within predator-prey cycles, but also due to slower trait changes. As this slower timescale became more dominant, the CV increased again. Due to the similar model structure, this mechanism may be responsible for the increase in CV here as well. This result suggests that mechanisms for dampening community temporal variability established for simple but functionally diverse systems, such as compensatory dynamics arising from competition for a joint resource, may be counteracted by destabilizing effects in more complex—and thus more realistic—systems.

Examining how the functional composition at each trophic level and ecosystem functions are linked allows us to mechanistically understand why the biomass and biomass production on higher trophic levels is maximal when every trophic level is diverse, and why the diversity of the top level plays such a crucial role. This becomes particularly obvious when comparing the trends of the different metrics related to biomass production within the food web (see Results, Fig. 3.5, and Fig.B.10, Appendix B).

A functionally diverse consumer community leads to an efficient exploitation of the production at the prey level due to their functional complementarity (Gamfeldt, Hillebrand, and Jonsson, 2005). In our model, this mechanism is present between both the top and intermediate, as well as between the intermediate and basal level: a diverse top community efficiently exploits the intermediate production, which in turn results in the basal production being efficiently exploited. In contrast, when the top community is not functionally diverse, potentially functionally diverse intermediate and basal communities adjust in species composition so that they escape efficient predation (Filip et al., 2014; Seiler et al., 2017). As a consequence, a higher

proportion of the production is lost from the system by non-grazing mortality rather than transferred up to the level above. In this way, the effects of functional diversity of different trophic levels synergize to make the food web with diversity everywhere the most efficient configuration in transferring biomass from the basal to the top level (Fig. 3.5, P_T/P_B). Importantly, even though the trade-off structure in our model is comparatively simple, analysis of the individual populations' biomasses (Fig. B.12, Appendix B) confirms that they function as intended and prevent any one species from dominating others on average, thus providing additional evidence that the patterns we observe are caused by changes in trait differences between the species on each trophic level.

The importance of considering multitrophic diversity has been emphasized before (Gamfeldt, Hillebrand, and Jonsson, 2005; Filip et al., 2014; Soliveres et al., 2016; Lefcheck et al., 2015; Barnes et al., 2018; Ceulemans et al., 2019). With these complex interactions between functional diversity of different trophic levels clearly exhibited by our model, it is not surprising that studies focusing on a single food web structure or a single parametrization sometimes find incommensurable results. For example, increased primary producer diversity had often been linked to an increased producer biomass and production (Tilman, Lehman, and Thomson, 1997; Cardinale et al., 2011). Our results show that this relationship not only depends on the trait values of the consumer level (Seabloom et al., 2017; Wohlgemuth et al., 2017), but crucially also on the top level. Hence, we reveal considerable variation in the behavior of differently structured food webs with respect to the relationship between diversity and ecosystem functioning. Nevertheless, we are able to identify clear trends and uncover mechanisms governing the behavior of tritrophic systems, even when considering a large range of different parameter combinations.

Concluding remarks

Understanding the link between functional diversity and the functioning of complex food webs is crucial to accurately predict how losses in functional diversity will affect the functions of natural food webs everywhere around us. Considerable detailed knowledge about this link has been gained in communities comprising of one or two trophic levels. Partly, the knowledge gained from bitrophic systems helps to understand tritrophic ones, such as the enhanced exploitation of resources by a more diverse consumer community. However, accounting for the third trophic level clearly shows that a restriction to two trophic levels may yield misleading results for complex natural food webs. The present comparison of several different food webs consisting of three trophic levels (see Fig. 3.1) reveals simultaneously operating bottom-up and top-down cascading effects over three trophic levels. At high functional diversity throughout the whole food web, functional shifts within the individual trophic levels result in a high food web efficiency and biomass on higher trophic levels, and a high degree of nutrient exploitation. Additionally, we show that the functional diversity on the top level is a strongly regulating factor for

the biomass, temporal variability, and biomass production efficiency of any trophic level. Therefore, to prevent drastic reduction of important functions, as well as potentially irreversible transitions, it is of crucial importance to increase our efforts in conserving diversity of higher trophic levels, despite the often large operational problems involved.

Acknowledgements

Parameter	Meaning	Range
N_0	nutrient inflow concentration	$[1/2, 2] \cdot 1120 \, \mu g \, \text{N}/l$
h_N	nutrient uptake half-saturation const.	$[1/2, 2] \cdot 10 \, \mu g \, \text{N}/l$
r_0'	basal growth rate	$[1/2, 2] \cdot 1/\text{day}$
a_0	B-I attack rate	$[1/2, 2] \cdot 1.04 \cdot 10^{-3}/(\text{day} \cdot \mu g \, C/l)$
h_0	B-I handling time	$[1/2, 2] \cdot 1.15 \cdot \text{day}$
α_0	I-T attack rate	$[1/2, 2] \cdot 4.48 \cdot 10^{-4}/(\text{day} \cdot \mu g \, C/l)$
η_0	I-T handling time	$[1/2, 2] \cdot 2.62 \cdot \text{day}$
δ	inflow rate	$[0.03, 0.06] \cdot 1/\text{day}$
a_{scale}	cross link scaling factor	$[1, 500]$
n	B-I Hill exponent	$[1, 2]$
ν	I-T Hill exponent	$[1, 2]$
Parameter	Meaning	Value
e	biomass conversion efficiency	0.33 (not varied)
c_N/c_C	basal nitrogen-to-carbon ratio	0.175 (not varied)
τ_{inc}	maximal trait increase	1/2 (not varied)

TABLE 3.1: Name and meaning of the parameters that were used in the study, along with the range from which they were sampled. For example, the nutrient inflow concentration N_0 was randomly sampled from the interval $[1/2, 2] \cdot 1120 \approx [560, 2240] \, \mu g \, \text{N}/l$. In this table, B-I refers to the functional response between the Basal (B) and the Intermediate (I) trophic level, and I-T to the Intermediate and Top (T) level. The bottom three parameters were kept at fixed values.

Established knowledge	In our diverse tritrophic system	
Top predators are often keystone species.	Confirmed, Δ_T and trophic interactions between I & T are most decisive for the biomasses, CVs, and energetics at all trophic levels.	Fig. 3.6
More diverse consumers exploit resources more efficiently.	Diversity must be high throughout the whole food web for efficient exploitation.	Fig. 3.5
For a single trophic level in isolation: $\Delta_B \uparrow$ implies: $B_B \uparrow, P_B \uparrow$	Effects of changing Δ_i depend on each other.	
For bitrophic systems: $\Delta_B \& \Delta_I \uparrow$: context-dependent effects on biomasses & production	However, when all $\Delta_i \uparrow$: $B_B \downarrow, B_I \uparrow, B_T \uparrow$ $P_B \approx, P_I \nearrow, P_T \uparrow$	Fig. 3.3 Fig. 3.5
For a single trophic level in isolation: $\Delta \uparrow$ implies: $CV \downarrow$	Effects of changing Δ_i depend on each other, however all CVs first decrease, and then increase, with increasing Δ_T.	Fig. 3.4

TABLE 3.2: Comparison of established knowledge of the link between the functional diversity and certain ecosystem functions of communities consisting of one or two trophic levels (see text for references), to our model where diversity can be changed at three trophic levels (see Fig. 3.1). Δ_i, B_i, and P_i refer to the diversity, biomass, and biomass production at trophic level $i \in \{B, I, T\}$, respectively (see Fig. 3.1 and Results), and the arrows indicate the direction in which these quantities are changing ($\uparrow$: increase, $\nearrow$: moderate increase, $\approx$: approximately constant, $\downarrow$: decrease). Our model enables us to understand the mechanisms responsible for these top-down and bottom-up effects, which simultaneously cascade through the food web.

Outcome variable	OOB score
Nutrient density	0.44
Basal biomass	0.65
Intermediate biomass	0.92
Top biomass	0.77
Nutrient CV	0.26
Basal CV	0.73
Intermediate CV	0.68
Top CV	0.70
$P_{\mathrm{T}}/P_{\mathrm{B}}$	0.83
B_{up}	0.86
$(P/B)_{\mathrm{B}}$	0.34
P_T	0.78

TABLE 3.3: OOB scores estimating the accuracy of the random forest model, for all outcome quantities. An OOB score of 1 represents a perfect model prediction, whereas an OOB score of 0 means that the model is as accurate as simply predicting the mean outcome value every time.
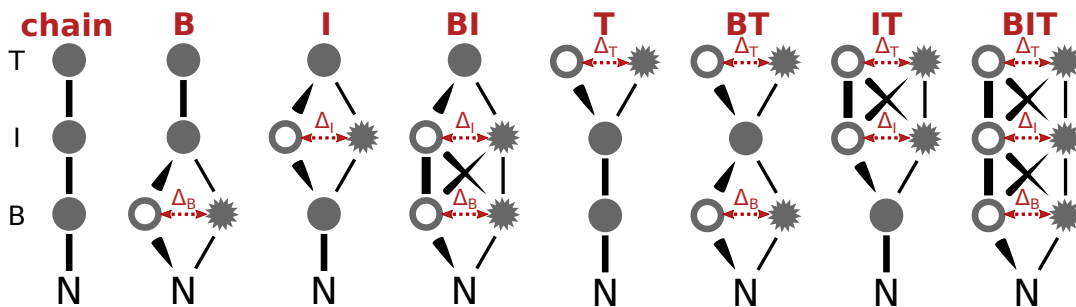
FIGURE 3.1: Schematic overview of the 8 different food webs compared in this study, which differ by the trophic levels (*B* for basal, *I* for intermediate, and *T* for top) on which diversity is possible (indicated above). In this way, chain refers to the linear chain which contains no diversity, B to the food web on which only the basal level is diverse, etc., and finally BIT denotes the food web which contains diversity on all trophic levels. The thickness of the connections between the nodes illustrates the comparative intensity of the trophic interaction, which is determined by the amount of diversity, or the trait difference, between the species on each trophic level (Δ_B, Δ_I, and Δ_T). Each of these food webs are analyzed as general as possible, with independently varying amounts of trait differences and parameters drawn randomly from biologically plausible intervals.
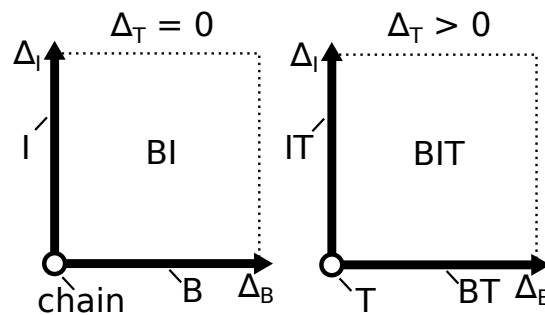
FIGURE 3.2: Pictorial representation of the location of the different food webs (Fig. 3.1) in the partial dependence graphs in Fig. 3.3-3.5. On the left-side graph ($\Delta_T = 0$, i.e., no diversity at the top level), the chain is on the point $(0, 0)$ ($\Delta_B = \Delta_I = 0$), the B food web is located on the line $\Delta_I = 0$, the I food web is located on the line $\Delta_B = 0$, and the BI web is located 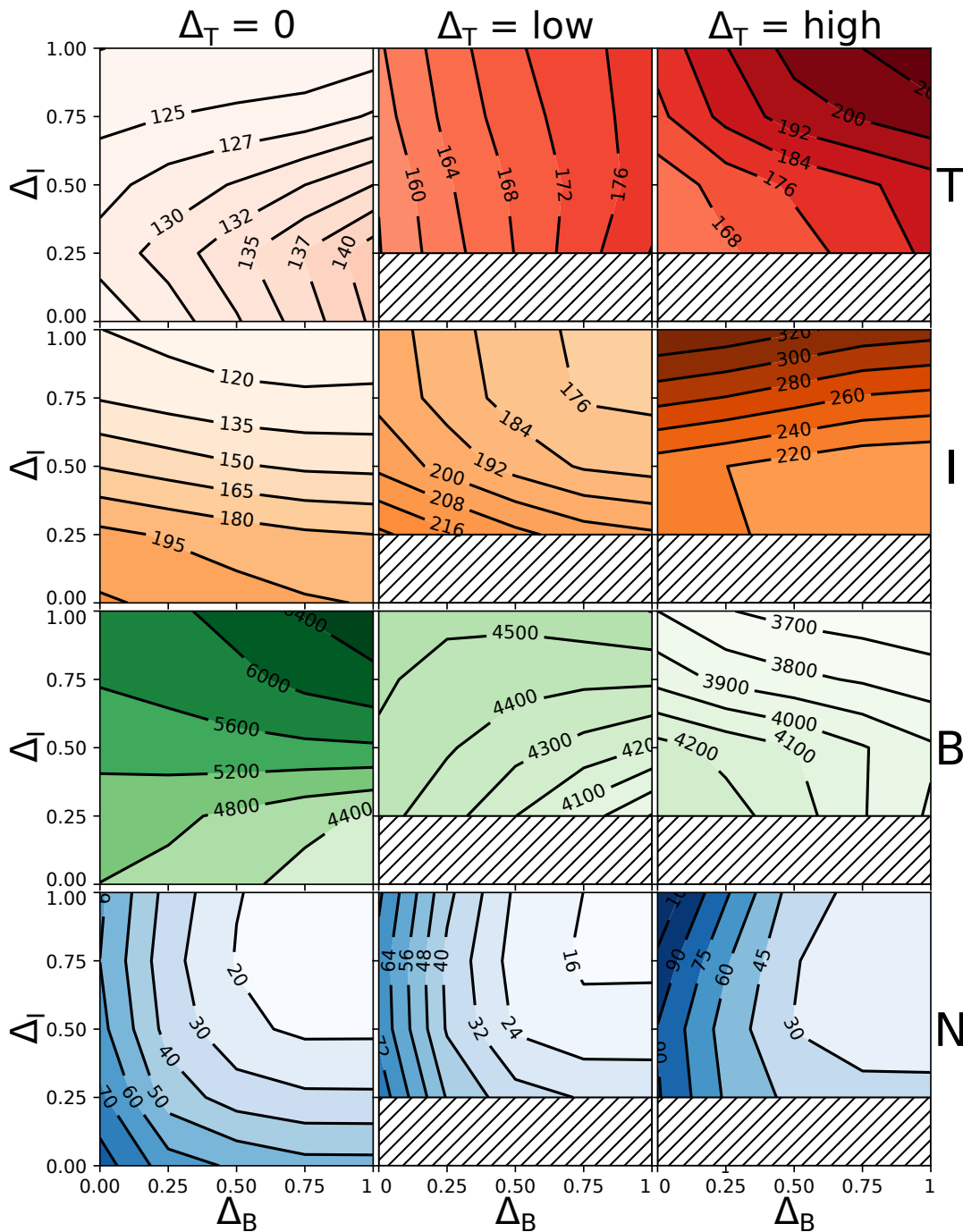in the plane where both Δ_B and Δ_I are non-zero. Similarly, on the right-side graph where $\Delta_T > 0$ (either *low* or *high* in Figs. 3.3-3.5), the T web is located on the point $(0, 0)$ ($\Delta_B = \Delta_I = 0$), the BT food web is located on the line $\Delta_I = 0$, the IT food web is located on the line $\Delta_B = 0$, and finally the BIT web is located in the plane where Δ_B, Δ_I, and Δ_T are non-zero.
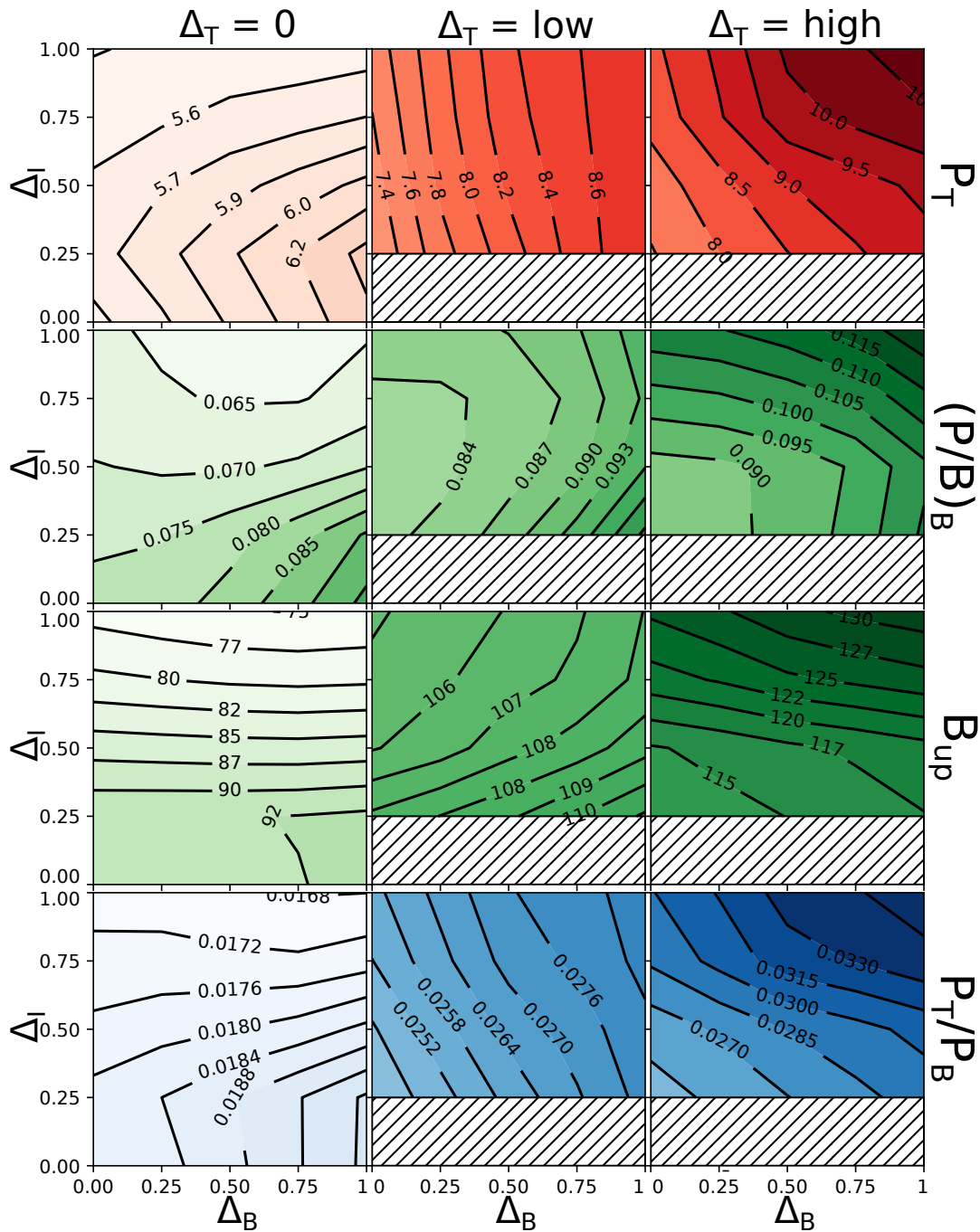
FIGURE 3.3: Effect of trait differences at the basal (Δ_B), intermediate (Δ_I), and top (Δ_T) trophic level on the free nutrient concentration (N, blue), and the biomasses on the basal (B, green), intermediate (I, orange), and top (T, red) trophic level, displayed as partial dependence graphs. To simplify the presentation, the effects of Δ_B and Δ_I are shown separately for three levels of Δ_T: $\Delta_T = 0$ (left), low Δ_T (0.25 and 0.5, middle), and high Δ_T (0.75 and 1, right). Fig. 3.2 shows a detailed explanation on how to read this figure. These graphs show the expected trends of N, B, I, & T as the amount of diversity on any trophic level is varied (for more information see Methods and Section B.5, Appendix B). For example, in the chain (lower left corner of each subplot for $\Delta_T = 0$), T is expected to be much lower than in the highly diverse BIT web (upper right corner for $\Delta_T = high$). When Δ_T is nonzero, the region below $\Delta_I = 0.25$ (T and BT webs) cannot be shown as no coexisting parameter combination exists here due to the two distinct top species sharing only one resource.
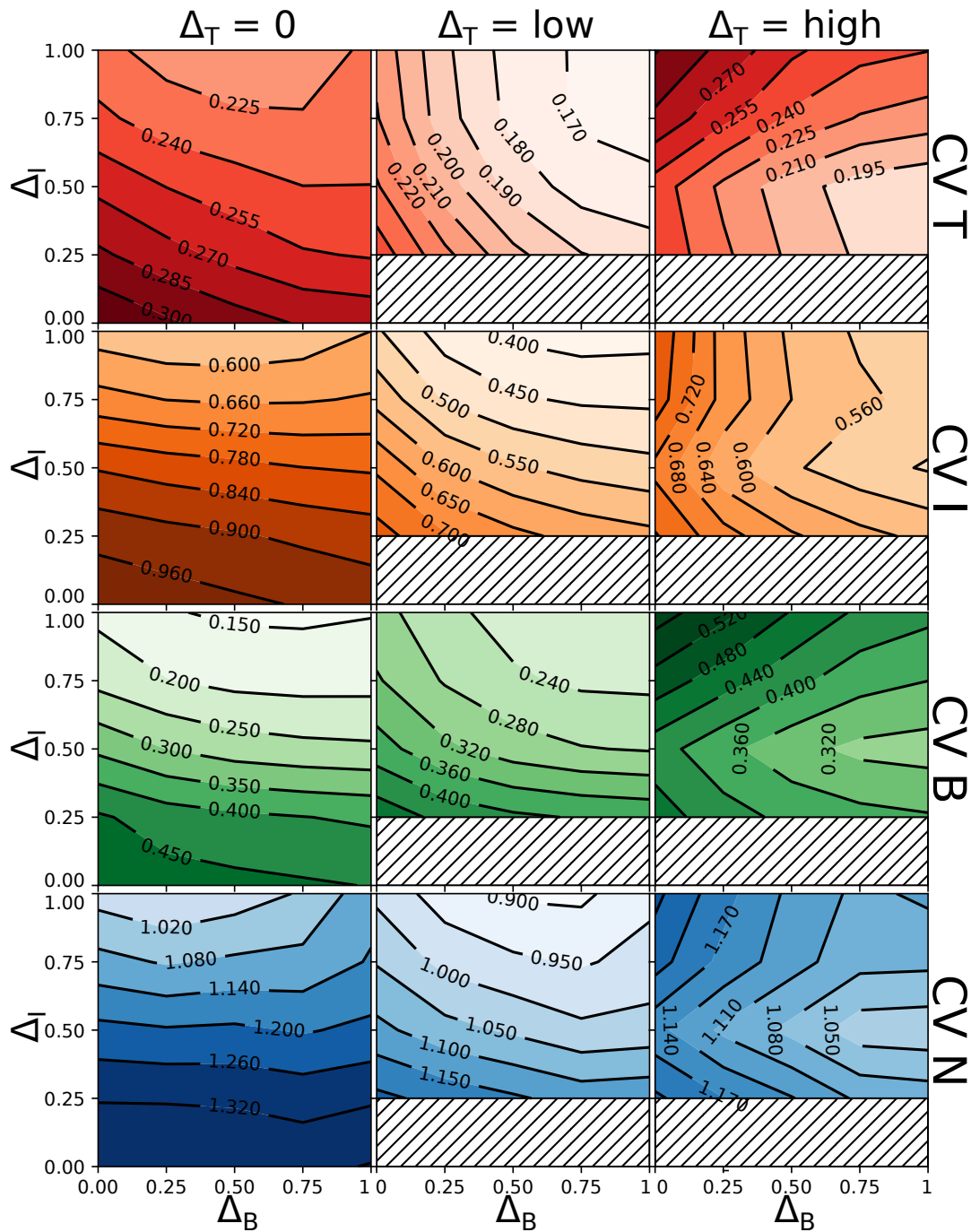
FIGURE 3.4: Effect of trait differences at the basal (Δ_B), intermediate (Δ_I), and top (Δ_T) trophic level on the coefficient of variation (CV) of the free nutrient concentration (N, blue), the total biomass at the basal (B, green), intermediate (I, orange), and top (T, red) trophic levels, displayed as partial dependence graphs. Consult Figs. 3.2 and 3.3 for a detailed description on how to read this Figure. Strikingly, we can see that Δ_T has a non-monotonous effect on the temporal variability of the whole food web: a moderate amount of top predator diversity tends to decrease the temporal variation, but adding yet more diversity to the food web causes it to increase again.

FIGURE 3.5: Effect of trait differences at the basal (Δ_B), intermediate (Δ_I), and top (Δ_T) trophic level on several different metrics related to the flow of biomass and energy through the food web, displayed as partial dependence graphs. From top to bottom: top biomass production P_T, basal production to biomass ratio (($P/B)_B$), basal biomass flowing to I (B_{up}), and the food web efficiency P_T/P_B. Consult the Results and Section B.5, Appendix B for more information on these quantities, and Figs. 3.2 and 3.3 for a detailed description on how to read this Figure. In the chain (lower left corner for $\Delta_T = 0$), we observe for example a much lower P_T/P_B than in the highly diverse BIT web (upper right corner for $\Delta_T = high$), which means biomass produced by the basal trophic level is transferred much more efficiently to the top level.
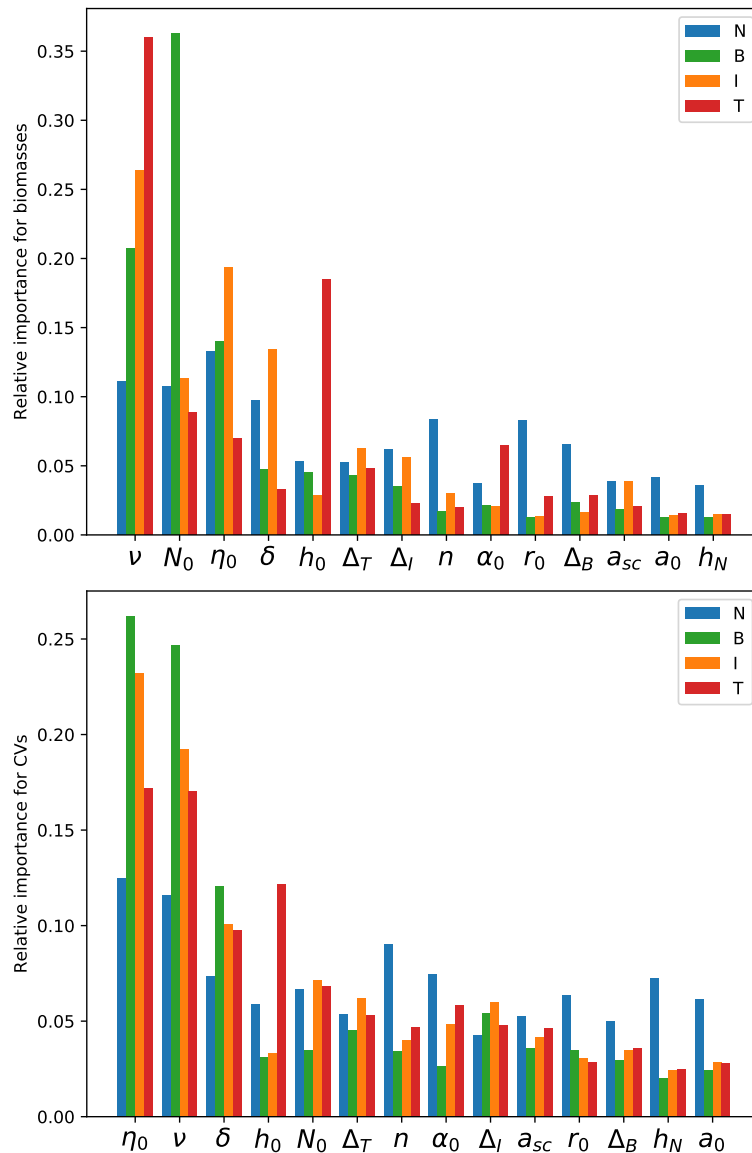
FIGURE 3.6: Relative importance of the different model parameters (see Table 3.1 on determining the biomasses and CVs of the different trophic levels. The relative importance quantifies how important the value of a certain parameter is to accurately predict the desired quantity, and they sum up to 1. The higher the relative importance of a parameter, the more relevant it is to make a prediction. In these graphs, the model parameters are ordered by their mean importance for each group of quantities (biomasses and CVs); for each parameter, the individual bars are ordered by trophic level.

References

Abdala-Roberts, L. et al. (2019). "Tri-trophic interactions: bridging species, communities and ecosystems". In: *Ecology Letters*. DOI: 10.1111/ele.13392.

Armstrong, R. A. and McGehee, R. (1980). "Competitive Exclusion". In: *American Naturalist* 115.2, pp. 151–170.

Barnes, A. D., Jochum, M., Lefcheck, J. S., Eisenhauer, N., Scherber, C., O'Connor, M. I., Ruiter, P. de, and Brose, U. (2018). "Energy Flux: The Link between Multitrophic Biodiversity and Ecosystem Functioning". In: *Trends in Ecology and Evolution* 33.3, pp. 186–197. DOI: 10.1016/j.tree.2017.12.007.

Bauer, B., Vos, M., Klauschies, T., and Gaedke, U. (2014). "Diversity, Functional Similarity, and Top-Down Control Drive Synchronization and the Reliability of Ecosystem Function". In: *The American Naturalist* 183.3, pp. 394–409. DOI: 10.1086/674906.

Borer, E. T., Seabloom, E. W., and Tilman, D. (2012). "Plant diversity controls arthropod biomass and temporal stability". In: *Ecology Letters* 15.12, pp. 1457–1464. DOI: 10.1111/ele.12006.

Breiman, L. (2001). "Random Forests". In: *Machine Learning* 45.1, pp. 5–32. DOI: 10.1017/CB09781107415324.004.

Brose, U. (2008). "Complex food webs prevent competitive exclusion among producer species". In: *Proceedings of the Royal Society B: Biological Sciences* 275.1650, pp. 2507–2514. DOI: 10.1098/rspb.2008.0718.

Brose, U., Williams, R. J., and Martinez, N. D. (2006). "Allometric scaling enhances stability in complex food webs". In: *Ecology Letters* 9.11, pp. 1228–1236. DOI: 10.1111/j.1461-0248.2006.00978.x.

Bruno, J. F. and O'Connor, M. I. (2005). "Cascading effects of predator diversity and omnivory in a marine food web". In: *Ecology Letters* 8.10, pp. 1048–1056. DOI: 10.1111/j.1461-0248.2005.00808.x.

Cardinale, B. J., Matulich, K. L., Hooper, D. U., Byrnes, J. E., Duffy, E., Gamfeldt, L., Balvanera, P., O'Connor, M. I., and Gonzalez, A. (2011). "The functional role of producer diversity in ecosystems". In: *American Journal of Botany* 98.3, pp. 572–592. DOI: 10.3732/ajb.1000364.

Ceulemans, R., Gaedke, U., Klauschies, T., and Guill, C. (2019). "The effects of functional diversity on biomass production, variability, and resilience of ecosystem functions in a tritrophic system". In: *Scientific Reports* 9.1. DOI: 10.1038/s41598-019-43974-1.

Ceulemans, R., Guill, C., and Gaedke, U. (2020). "Top predators govern multitrophic diversity effects in tritrophic food webs". In: *bioRxiv*, p. 2020.07.31.230375. DOI: 10.1101/2020.07.31.230375.

Cutler, D. R. et al. (2007). "Random Forests for Classification in Ecology". In: *Ecology* 88.11, pp. 2783–2792.

Daam, M. A., Teixeira, H., Lillebø, A. I., and Nogueira, A. J. (2019). "Establishing causal links between aquatic biodiversity and ecosystem functioning: Status and research needs". In: *Science of the Total Environment* 656, pp. 1145–1156. DOI: 10.1016/j.scitotenv.2018.11.413.

Duffy, J. E., Cardinale, B. J., France, K. E., McIntyre, P. B., Thébault, E., and Loreau, M. (2007). "The functional role of biodiversity in ecosystems: Incorporating trophic complexity". In: *Ecology Letters* 10.6, pp. 522–538. DOI: 10.1111/j.1461-0248.2007.01037.x.

Ehrlich, E., Becks, L., and Gaedke, U. (2017). "Trait-fitness relationships determine how trade-off shapes affect species coexistence". In: *Ecology* 98.12, pp. 3188–3198. DOI: 10.1002/ecy.2047.

Ehrlich, E. and Gaedke, U. (2020). "Coupled changes in traits and biomasses cascading through a tritrophic plankton food web". In: *Limnology and Oceanography*, lno.11466. DOI: 10.1002/lno.11466.

Ehrlich, E., Kath, N. J., and Gaedke, U. (2020). "The shape of a defense-growth trade-off governs seasonal trait dynamics in natural phytoplankton". In: *ISME Journal*, pp. 1451–1462. DOI: 10.1038/s41396-020-0619-1.

Filip, J., Bauer, B., Hillebrand, H., Beniermann, A., Gaedke, U., and Moorthi, S. D. (2014). "Multitrophic diversity effects depend on consumer specialization and species-specific growth and grazing rates". In: *Oikos* 123.8, pp. 912–922. DOI: 10.1111/oik.01219.

Flöder, S., Bromann, L., and Moorthi, S. (2018). "Inter- and intraspecific consumer trait variations determine consumer diversity effects in multispecies predator-prey systems". In: *Aquatic Microbial Ecology* 81.3, pp. 243–256. DOI: 10.3354/ame01866.

Gaedke, U. (1998). "The response of the pelagic community of a large and deep lake (L. Constance) to reoligotrophication: evidence for scale-dependent hierarchical patterns". In: *Arch. Hydrobiol. Spec. Issues: Advances in Limnology* 53, pp. 317–333.

Gaedke, U. and Kamjunke, N. (2006). "Structural and functional properties of low- and high-diversity planktonic food webs". In: *Journal of Plankton Research* 28.7, pp. 707–718. DOI: 10.1093/plankt/fbl003.

Gamfeldt, L., Hillebrand, H., and Jonsson, P. R. (2005). "Species richness changes across two trophic levels simultaneously affect prey and consumer biomass". In: *Ecology Letters* 8.7, pp. 696–703. DOI: 10.1111/j.1461-0248.2005.00765.x.

Gilman, S. E., Urban, M. C., Tewksbury, J., Gilchrist, G. W., and Holt, R. D. (2010). "A framework for community interactions under climate change". In: *Trends in Ecology and Evolution* 25.6, pp. 325–331. DOI: 10.1016/j.tree.2010.03.002.

Gonzalez, A. and Loreau, M. (2009). "The Causes and Consequences of Compensatory Dynamics in Ecological Communities". In: *Annual Review of Ecology, Evolution, and Systematics* 40.1, pp. 393–414. DOI: 10.1146/annurev.ecolsys.39.110707.173349.

Griffin, J. N., Byrnes, J. E. K., and Cardinale, B. J. (2013). "Effects of predator richness on prey suppression: A meta-analysis". In: *Ecology* 94.10, pp. 2180–2187. DOI: 10.1890/13-0179.1.

Hardin, G. (1960). "The Competitive Exclusion Principle". In: *Science* 131.3409, pp. 1292–1297. DOI: 10.1126/science.132.3419.95-a.

Herms, D. A. and Mattson, W. J. (1992). "The Dilemma of Plants : To Grow or Defend". In: *The Quarterly Review of Biology* 67.3, pp. 283–335. DOI: 10.1007/s11466-009-0028-z.

Hillebrand, H. and Matthiessen, B. (2009). "Biodiversity in a complex world: Consolidation and progress in functional biodiversity research". In: *Ecology Letters* 12.12, pp. 1405–1419. DOI: 10.1111/j.1461-0248.2009.01388.x.

Hillebrand, H., Worm, B., and Lotze, H. K. (2000). "Marine microbenthic community structure regulated by nitrogen loading and grazing pressure". In: *Marine Ecology Progress Series* 204, pp. 27–38.

Hindmarsh, A. C., Brown, P. N., Grant, K. E., Lee, S. L., Serban, R., Shumaker, D. E., and Woodward, C. S. (2005). "Sundials". In: *ACM Transactions on Mathematical Software* 31.3, pp. 363–396. DOI: 10.1145/1089014.1089020.

Hooper, D. U. et al. (2005). "Effects of biodiversity on ecosystem functioning: A consensus of current knowledge". In: *Ecological Monographs* 75.1, pp. 3–35. DOI: 10.1890/04-0922.

Hunter, J. D. (2007). "Matplotlib: A 2D graphics environment". In: *Computing in Science and Engineering* 9.3, pp. 99–104. DOI: 10.1109/MCSE.2007.55.

Huntly, N. (1991). "Herbivores and the dynamics of communities and ecosystems". In: *Annual Review of Ecology and Systematics* 22.1, pp. 477–503. DOI: 10.1146/annurev.es.22.110191.002401.

Kalinkat, G., Schneider, F. D., Digel, C., Guill, C., Rall, B. C., and Brose, U. (2013). "Body masses, functional responses and predator-prey stability". In: *Ecology Letters* 16.9, pp. 1126–1134. DOI: 10.1111/ele.12147.

Kath, N. J., Boit, A., Guill, C., and Gaedke, U. (2018). "Accounting for activity respiration results in realistic trophic transfer efficiencies in allometric trophic network (ATN) models". In: *Theoretical Ecology* 11.4, pp. 453–463. DOI: 10.1007/s12080-018-0378-z.

Klauschies, T. and Gaedke, U. (2019). "Nutrient retention by predators undermines predator coexistence on one prey". In: *Theoretical Ecology*. DOI: 10.1007/s12080-019-00440-y.

Klauschies, T., Vasseur, D. A., and Gaedke, U. (2016). "Trait adaptation promotes species coexistence in diverse predator and prey communities". In: *Ecology and Evolution* 6.12, pp. 4141–4159. DOI: 10.1002/ece3.2172.

Kneitel, J. M. and Chase, J. M. (2004). "Trade-offs in community ecology: Linking spatial scales and species coexistence". In: *Ecology Letters* 7.1, pp. 69–80. DOI: 10.1046/j.1461-0248.2003.00551.x.

Kovach-Orr, C. and Fussmann, G. F. (2013). "Evolutionary and plastic rescue in multitrophic model communities". In: *Philosophical Transactions of the Royal Society B: Biological Sciences* 368.1610, p. 20120084. DOI: 10.1098/rstb.2012.0084.

Krause, S., Le Roux, X., Niklaus, P. A., Bodegom, P. M. van, Lennon T., J. T., Bertilsson, S., Grossart, H. P., Philippot, L., and Bodelier, P. L. (2014). "Trait-based approaches for understanding microbial biodiversity and ecosystem functioning". In: *Frontiers in Microbiology* 5, p. 251. DOI: 10.3389/fmicb.2014.00251.

Lefcheck, J. S., Byrnes, J. E., Isbell, F., Gamfeldt, L., Griffin, J. N., Eisenhauer, N., Hensel, M. J., Hector, A., Cardinale, B. J., and Duffy, J. E. (2015). "Biodiversity enhances ecosystem multifunctionality across trophic levels and habitats". In: *Nature Communications* 6. DOI: 10.1038/ncomms7936.

McGill, B. J., Enquist, B. J., Weiher, E., and Westoby, M. (2006). "Rebuilding community ecology from functional traits". In: *Trends in Ecology and Evolution* 21.4, pp. 178–185. DOI: 10.1016/j.tree.2006.02.002.

McKinney, W. (2010). "Data Structures for Statistical Computing in Python". In: *Proceedings of the 9th Python in Science Conference* 1697900.Scipy, pp. 51–56.

Pedregosa, F. et al. (2011). "Scikit-learn: Machine learning in Python". In: *Journal of Machine Learning Research* 12, pp. 2825–2830.

Petchey, O. L. and Gaston, K. J. (2006). "Functional diversity: Back to basics and looking forward". In: *Ecology Letters* 9.6, pp. 741–758. DOI: 10.1111/j.1461-0248.2006.00924.x.

Pimm, S. L., Jenkins, C. N., Abell, R., Brooks, T. M., Gittleman, J. L., Joppa, L. N., Raven, P. H., Roberts, C. M., and Sexton, J. O. (2014). "The biodiversity of species and their rates of extinction, distribution, and protection". In: *Science* 344.6187. DOI: 10.1126/science.1246752.

Poisot, T., Mouquet, N., and Gravel, D. (July 2013). "Trophic complementarity drives the biodiversity-ecosystem functioning relationship in food webs". In: *Ecology Letters* 16.7. Ed. by F. Adler, pp. 853–861. DOI: 10.1111/ele.12118.

Ripple, W. J. et al. (2014). "Status and ecological effects of the world's largest carnivores". In: *Science* 343.6167. DOI: 10.1126/science.1241484.

Schneider, F. D., Brose, U., Rall, B. C., and Guill, C. (Dec. 2016). "Animal diversity and ecosystem functioning in dynamic food webs". In: *Nature Communications* 7, p. 12718. DOI: 10.1038/ncomms12718.

Seabloom, E. W., Kinkel, L., Borer, E. T., Hautier, Y., Montgomery, R. A., and Tilman, D. (2017). "Food webs obscure the strength of plant diversity effects on primary productivity". In: *Ecology Letters* 20.4, pp. 505–512. DOI: 10.1111/ele.12754.

Seiler, C., Velzen, E. van, Neu, T. R., Gaedke, U., Berendonk, T. U., and Weitere, M. (2017). "Grazing resistance of bacterial biofilms: A matter of predators' feeding trait". In: *FEMS Microbiology Ecology* 93.9, pp. 1–9. DOI: 10.1093/femsec/fix112.

Soliveres, S. et al. (2016). "Biodiversity at multiple trophic levels is needed for ecosystem multifunctionality". In: *Nature* 536.7617, pp. 456–459. DOI: 10.1038/nature19092.

Thébault, E. and Loreau, M. (2003). "Food-web constraints on biodiversity-ecosystem relationships". In: *Proceedings of the National Academy of Sciences* 100.25, pp. 14949–14954.

Thomas, M. K., Fontana, S., Reyes, M., Kehoe, M., and Pomati, F. (2018). "The predictability of a lake phytoplankton community, over time-scales of hours to years". In: *Ecology Letters* 21.5, pp. 619–628. DOI: 10.1111/ele.12927.

Tilman, D. and Downing, J. A. (1996). "Biodiversity and Stability in Grasslands". In: *Ecosystem Management: Selected Readings*. New York, NY: Springer New York, pp. 3–7. DOI: 10.1007/978-1-4612-4018-1_1.

Tilman, D., Lehman, C. L., and Thomson, K. T. (1997). "Plant diversity and ecosystem productivity: Theoretical considerations". In: *Proceedings of the National Academy of Sciences of the United States of America* 94.5, pp. 1857–1861. DOI: 10.1073/pnas.94.5.1857.

Tilman, D., Reich, P. B., and Knops, J. M. H. (2006). "Biodiversity and ecosystem stability in a decade-long grassland experiment". In: *Nature* 441.7093, pp. 629–632. DOI: 10.1038/nature04742.

Tirok, K. and Gaedke, U. (2010). "Internally driven alternation of functional traits in a multispecies predator- prey system". In: *Ecology* 91.6, pp. 1748–1762. DOI: 10.1890/09-1052.1.

Van Der Walt, S., Colbert, S. C., and Varoquaux, G. (2011). "The NumPy array: A structure for efficient numerical computation". In: *Computing in Science and Engineering* 13.2, pp. 22–30. DOI: 10.1109/MCSE.2011.37.

Velzen, E. van (2020). "Predator coexistence through emergent fitness equalization". In: *Ecology* 0.0, pp. 1–10. DOI: 10.1002/ecy.2995.

Wohlgemuth, D., Filip, J., Hillebrand, H., and Moorthi, S. D. (2017). "Prey diversity effects on ecosystem functioning depend on consumer identity and prey composition". In: *Oecologia* 184.3, pp. 653–661. DOI: 10.1007/s00442-017-3892-6.

Worm, B. et al. (2006). "Impacts of Biodiversity Loss on Ocean Ecosystem Services". In: *Science* 314.5800, pp. 787–790. DOI: 10.1126/science.1132294.

Chapter 4

Functional diversity alters the effects of a nutrient pulse on food web resistance, resilience, and elasticity

Ruben Ceulemans*, Laurie Anne Wojcik*, & Ursula Gaedke
*: Equally contributing authors
To be submitted.

Abstract

The global biodiversity decline threatens ecosystems through a dangerous feedback loop. Biodiversity loss causes functional diversity loss, which may hamper the ecosystem's ability to buffer against environmental changes, leading to further reductions of biodiversity. Previous trait-based studies have investigated how functional diversity influences the response of food webs to disturbances caused by extreme events. However, they mainly considered bitrophic systems with at most two functionally diverse trophic levels. In this study, we investigate the effects of a nutrient pulse on the resistance, resilience and elasticity of a tritrophic—and thus more realistic—food web, depending on its functional diversity at every trophic level. We compare a simple linear food chain with low diversity to a highly diverse food web with three adaptive trophic levels, where prey are either defended or undefended against predation by selective or non-selective predators. The species fitness differences are balanced through trade-offs between defense/growth rate and selectivity/half-saturation constant. We show that the resistance, resilience and elasticity of tritrophic food webs depend on the perturbation size and on the moment of perturbation, but crucially also on the shape and type of the dynamical attractors and top-down processes regulated by the top trophic level. The latter properties highly depend on the functional diversity of the food web. We show that a more diverse food web is more resistant, resilient, and elastic to a nutrient pulse perturbation, and find that the influence of functional diversity becomes complex under

certain conditions. Overall, using a food web model of realistic complexity, this study confirms the destructive potential of the positive feedback loop between biodiversity loss and robustness to disturbances, by uncovering mechanisms leading to a decrease in resistance, resilience and elasticity as diversity declines.

Introduction

Human activities undeniably disrupt ecosystems structure and functioning (Hooper et al., 2005; Worm et al., 2006; Cardinale et al., 2012; Hautier et al., 2015). Direct effects such as habitat loss due to pollution (Dudgeon et al., 2006; Butchart et al., 2010; Hölker et al., 2010) and increased land requirements for agricultural or industrial use (Brooks et al., 2002; Ryser et al., 2019; Horváth et al., 2019) are major causes of the observed losses in biodiversity worldwide. Moreover, climate change effects have a decisive influence (Bestion et al., 2020): in addition to the global temperature rise (Hansen et al., 2006), the frequency of disruptive extreme weather events has increased steadily (Easterling et al., 2000). For instance, recurrent storms or heavy rainfalls amplify excessive nutrient loading in rivers, lakes, and coastal areas, causing species losses (Øygarden et al., 2014). The combined effect of these processes on biodiversity creates a potentially dangerous feedback loop. When biodiversity is lost, the respective decrease in functional diversity may alter the ecosystem's ability to buffer perturbations (Cardinale et al., 2012; García-Palacios et al., 2018; Ceulemans et al., 2019). This leads to additional biodiversity losses, and consequently to more vulnerable ecosystems.

To accurately quantify the effects of biodiversity loss on ecosystem functioning, it has proven useful to consider biodiversity from a functional perspective (Violle et al., 2007; Tirok and Gaedke, 2010). This entails sorting out the members a the food web into groups with similar functional trait values. In this way, e.g. morphological, physiological or behavioral individual characteristics are linked to a certain function, such as growth rate or nutrient uptake (Garnier, Navas, and Grigulis, 2016), and depend on each other by trade-offs to determine the overall fitness (McGill et al., 2006; Violle et al., 2007). This approach makes explicit how trait changes can feed back to population and food web dynamics, and partly regulate the response of food webs to environmental changes (Yamamichi and Miner, 2015; Theodosiou, Hiltunen, and Becks, 2019; Raatz, Velzen, and Gaedke, 2019).

Most studies investigating the responses of food webs to perturbations are restricted to systems with two adaptive trophic levels (Persson et al., 2001; Křivan and Diehl, 2005; Visser, Mariani, and Pigolotti, 2012; Kovach-Orr and Fussmann, 2013), or on bitrophic systems (Jones, 2008; Fussmann and Gonzalez, 2013; Yamamichi, Yoshida, and Sasaki, 2011; Bell et al., 2019; Govaert et al., 2019; Raatz, Velzen, and Gaedke, 2019). However, tritrophic systems are more realistic, since strictly bitrophic interactions are rare in nature (Pimm et al., 2014; Matsuno and Nobuaki, 1996; Abdala-Roberts et al., 2019), and top predators can have a large influence on

ecosystem functioning and dynamics (Estes et al., 2011; Brose et al., 2019; Ceulemans, Guill, and Gaedke, 2020).

To properly understand how tritrophic food webs respond to environmental changes, insights are needed into the mechanisms driving their response. External disturbances come in a variety of forms, and each can affect the food web and its functions in different ways. Broadly, external disturbances can be separated into two types, called press and pulse perturbations (Tilman and Downing, 1996; Raatz, Velzen, and Gaedke, 2019). Press perturbations are long term or permanent changes to a system component, such as increased harvesting or warming. In contrast, pulse perturbations are short-term and quasi-instantaneous changes to state variables, such as species biomasses or nutrient concentration, e.g. due to a forest fire or massive rainfall causing heavy run-off (Bender, Case, and Gilpin, 1984; Harris et al., 2018).

In this study, we investigate the effects of a nutrient pulse on the dynamics of tritrophic food webs with different amounts of biodiversity. Nutrient pulses correspond to a temporary increase in the carrying capacity, which can destabilize the dynamics of food webs and put species at increased risk of extinction (Rosenzweig, 1971). In aquatic systems, these events can drastically reduce water quality by contributing to eutrophication (Kaushal et al., 2014; Couture et al., 2018; Díaz et al., 2019) and to the apparition of anoxic dead zones (Diaz and Rosenberg, 2008). Such events are happening with increased frequency and magnitude (Galloway et al., 2008; Kaushal et al., 2014).

Accurate discussion of how a nutrient pulse may affect the dynamics of a tritrophic food web requires clear definitions of the different aspects characterizing its response. Analogous to Grimm and Wissel, 1997 and Raatz, Velzen, and Gaedke, 2019, the following terms are used:

- **Resilience** refers to whether or not the system returns to its original state after a pulse perturbation.

- **Resistance** refers to the maximum temporary change in dynamics after a pulse perturbation.

- **Elasticity** refers to how quickly the system returns to its original state.

These three quantities are all relevant in the context of pulse perturbations, and are evaluated by several properties of the food web dynamics. The resilience is simply determined by examining the dynamics after a long time period following the perturbation. If the system returns to its original state, it is resilient. Conversely, resistance is evaluated shortly after the perturbation. When the dynamics are strongly affected before the system returns to its original state, the resistance is nonetheless low. Finally, the elasticity is estimated through the return time, which is the time it takes for the system to return to the original state. A lower return time corresponds to a higher elasticity.

We investigated the response of tritrophic food webs with low and high functional diversity to nutrient enrichment by comparing a simple tritrophic linear food chain to a tritrophic food web which is adaptive at each trophic level. In this model, trophic levels are adaptive in the sense of species sorting, as described in Ceulemans et al. (2019). Prey species are either defended or undefended, and predator species are either selective or non-selective feeders (Fig. 4.1), and their relative importance changes according to ambient conditions, leading to continual trait changes at each trophic level. Our hypotheses are that the food web response depends on (i) the perturbation size, (ii) the time at which the perturbation is applied, and (iii) on the functional diversity present, i.e., an adaptive food web is less affected than a simple linear food chain. To enlarge generality and accurately capture the complex behavior that such system can exhibit, we study this response in different parameter regions with multiple attractors.

Methods

As a basis for our study, we used the chemostat tritrophic model described in Chapter 2, consisting of free inorganic nutrients (nitrogen, N) and three trophic levels: basal (B), intermediate (I) and top (T) (see Section 2.2 and Fig. 4.1). In this model, the amount of diversity in the food web can be varied by changing the trait differences between the species on all trophic levels (Δ). When $\Delta = 0$, the species' trait values within trophic levels are equal and the food web simplifies to a linear chain (cf. Section A.2, Appendix A). Alternatively, when $\Delta = 1$ the trait differences are maximal and a fully trait-separated food web is described (Fig. 4.1). For a detailed model description, please see section 2.2, Chapter 2.

Importantly, our previous study showed that the Hill exponents of the functional responses of the $B - I$ and $I - T$ interaction (h, η, cf. Equations (2.5) and (2.6)) play an important role in determining the nature of the dynamical attractor to which the system relaxes. In particular, two attractors exist for both the food chain and the food web. The "low production state" (LP) has a low top biomass production and high variability, whereas the "high production state" (HP) has a high top biomass production and low variability. To fully capture these different dynamical outcomes, including cases where either the chain or the web are bistable (see Table 4.1), we have selected three values of Hill exponents ($h = \eta = 1.05$, $h = \eta = 1.10$, and $h = \eta = 1.15$) for which we will investigate the system's response.

To evaluate the system's response to a nutrient pulse, we always took care to ensure that the system is at an attractor (Fig. 4.2), and not still in a transient state. Importantly, the attractor may have a more complex structure than a simple fixed point: it can be a limit cycle, or a chaotic attractor. In the latter cases, the individual populations do not settle down to a fixed value but remain oscillating perpetually. When the system has relaxed to the attractor, the perturbation is applied at time t_P by setting the free nutrient concentration N, to $N + N_P$. This instantaneous change
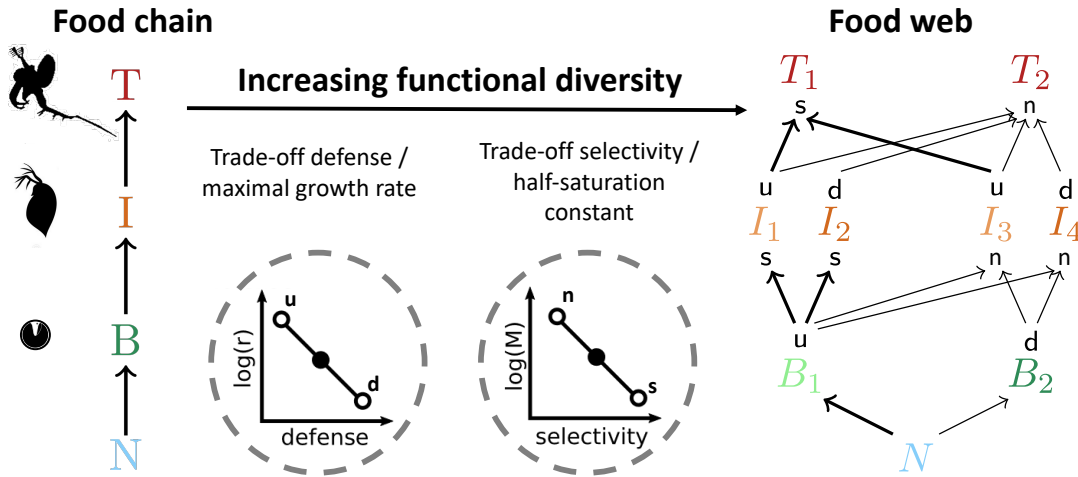
FIGURE 4.1: Comparison of two food webs with different functional diversity. The lowly diverse system (left side) is a simple linear food chain, where nutrients (N) are taken up by a basal species (B), which is consumed by an intermediate species (I), which is preyed on by a top species (T). In the highly diverse system (right side), prey species are either undefended (u), or defended (d), and predators are either selective (s) or non-selective (n) feeders. The basal and the top species each have one trait, whereas the intermediate species, being both consumers and prey, have two traits, resulting in four functionally unique species. Two trade-offs are used to balance the fitness of the species: a higher defense comes at the cost of a lower growth rate (r), and being less selective implies a larger prey spectrum, but also an increased prey uptake half-saturation constant (M). In this way, a defended species grows slower than an undefended one and a selective feeder can more efficiently exploit low prey concentrations. The resulting differences in trophic interaction strengths are shown by the arrow thickness between the species.

of the state variable N moves the system from its former location on the attractor to a point farther away from the attractor (Fig. 4.2).

Additionally, when the attractor is more complex than a fixed point (i.e., a limit cycle or chaotic attractor), we investigated how the effect of the perturbation on the dynamics depends on where on the attractor it is applied. In particular, to accurately estimate the return time, it is required to sample the different attractors in a high spatial resolution. This was achieved in multiple steps. First, starting from an initial condition known to be in the basin of attraction of the relevant attractor, the system was allowed to relax for 10^5 time units using a large timestep $\Delta_t = 10^{-1}$ such that a point sufficiently close to the attractor could be obtained. If the attractor was a limit cycle, the system was further integrated for approximately one period using a high temporal resolution ($\Delta_t = 10^{-3}$). This creates a set of points $\mathcal{S}_t$ on the attractor. Finally, to sample the attractor in a way such that the distances between the sampled points on the attractor do not become very large when the dynamics are moving very fast, the attractor was interpolated and resampled such that the arc length between consecutive sampled points is equal to 1 (in units of biomass). For this set of spatially sampled points $\mathcal{S}_x$, the distance between a point on the attractor and the closest point to it in $\mathcal{S}_x$ is guaranteed to be smaller than 1. However, when the attractor is chaotic, even when performing this procedure over multiple periods, the return time could not accurately be calculated using this method,

Hill exponent	Attractor and structure	
	chain	web
1.05	*LP*: limit cycle	*LP*: chaotic HP: limit cycle
1.10	*LP*: limit cycle *HP*: limit cycle	*HP*: limit cycle
1.15	*HP*: limit cycle	*HP*: fixed point

TABLE 4.1: Summary of the effect of the three values of Hill exponent on the attractors found in the food chain and food web. The system either relaxes to the low-production state (*LP*), the high production state (*HP*), or is bistable. A visual representation of the dynamics on each attractor is given in Fig. C.1, Appendix C. In this text, we distinguish between attractor *type*, denoting whether the attractor is a fixed point, limit cycle, or chaotic, and attractor *shape*, distinguishing between the *HP* or *LP* state.

After the perturbation, we continued with numerical integration of the system and recorded the minimum biomass reached by each population, as well as by each trophic level as a whole. Additionally, we estimated the time it takes for the trajectory to return to its original attractor (return time t_R). Both of these quantities are explained schematically in Fig. 4.2.

There are three possible outcomes for the perturbed system to evolve towards. The first option is that the pulse perturbation temporarily disturbs the system by altering its dynamics during the transient phase in which the system relaxes back to the attractor. In this case, the time it took for the system to return to the attractor (return time t_R), as well as the biomass minima and maxima of the populations and trophic levels during this phase were recorded (see also Fig. 4.2). A second outcome may occur when the biomass of at least one population reaches such a low value that it crosses an extinction threshold, which we have set to 10^{-9} biomass units. In this case, this population is set to 0 and is said to have gone extinct. Such a threshold is necessary to prevent numerical problems that can occur when state variables reach values that are extremely close to 0. When it is crossed, the system can never return to the initial attractor. Finally, a third outcome is possible when the system is bistable. In that case, it may happen that the trajectory is pushed inside the other attractor's basin of attraction. In this case, the system also never returns to the initial system, but all populations are still present in the food web.

Results

We investigated the response of a non-diverse and diverse tritrophic food web to a nutrient pulse, by quantifying its resistance, resilience, and elasticity (see Fig. 4.3 for a schematic overview how these responses differ, and Fig. 4.2 for an explanation of the properties of the timeseries required to estimate these quantities). Alongside
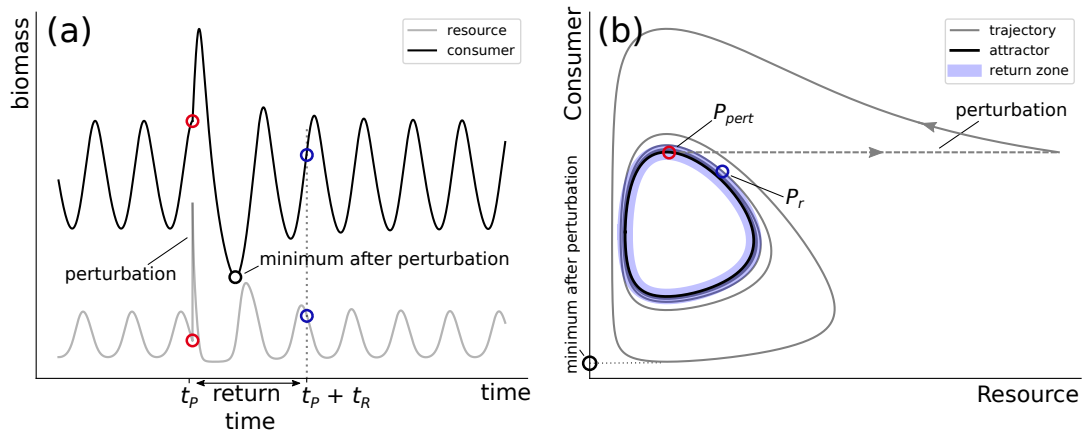
FIGURE 4.2: Schematic graphical examples of the different quantities calculated for our results. To quantify and compare the response of an ecological system to a perturbation, we recorded the minimal biomasses reached by the populations after the perturbation, as well as the time it took for the trajectory to return to the vicinity of the attractor. Panel (a) shows the timeseries of a simple consumer-resource model. The system is oscillating on its stable limit cycle until a nutrient pulse perturbation is applied at time t_P (red circle), after which the consumer increases and then declines to very low values. Panel (b) shows the same timeseries data but plotted in phase space. The limit cycle on which the system is oscillating originally is shown by the black curve. The nutrient pulse perturbation is applied at the red point P_{pert} (also shown in panel (a)), after which the system relaxes back to the attractor. The return time t_R is measured by the time it takes for the trajectory to remain inside the close neighborhood of the attractor (return zone, indicated by the colored region). This happens at the blue point P_r (also indicated in panel (a)).

this analysis, we investigated the actual timeseries in detail in order to uncover the mechanisms responsible for the observed responses.

As a general pattern, the biomass minima reached after a perturbation tend to decrease as the perturbation size increases (Fig. 4.4). This implies that, as the amount of added nutrients increases, the biomass amplitudes immediately after the perturbation increase correspondingly, in a highly nonlinear way (see also Appendix Fig. C.2 showing an increase in the maxima as well). We observe that, in all cases, the basal level is most strongly affected by the nutrient pulse, whereas the top level is least affected. The minimum reduction in the timeseries spans a larger range for the basal level, as compared to higher trophic levels. Following this strong reduction, in all cases, the basal level crosses the numerical extinction threshold of 10^{-9} first, leading to additional extinctions on the I and T level.

By trying multiple different time points at which the perturbation is applied per perturbation size, we capture how the system response to a perturbation depends on the specific time at which the perturbation is applied. If the equilibrium state of a system is a fixed point (as is the case for the food web at $h = 1.15$), the response does not depend on the time at which the perturbation is applied. All 1000 different initial conditions lead exactly to the same post-perturbation minimum and therefore the median, upper, and lower quartiles are all equal. On the other hand, when the equilibrium state of the system is not a fixed point but a limit cycle (or a chaotic attractor), the minimum reached by the time series may strongly vary depending on
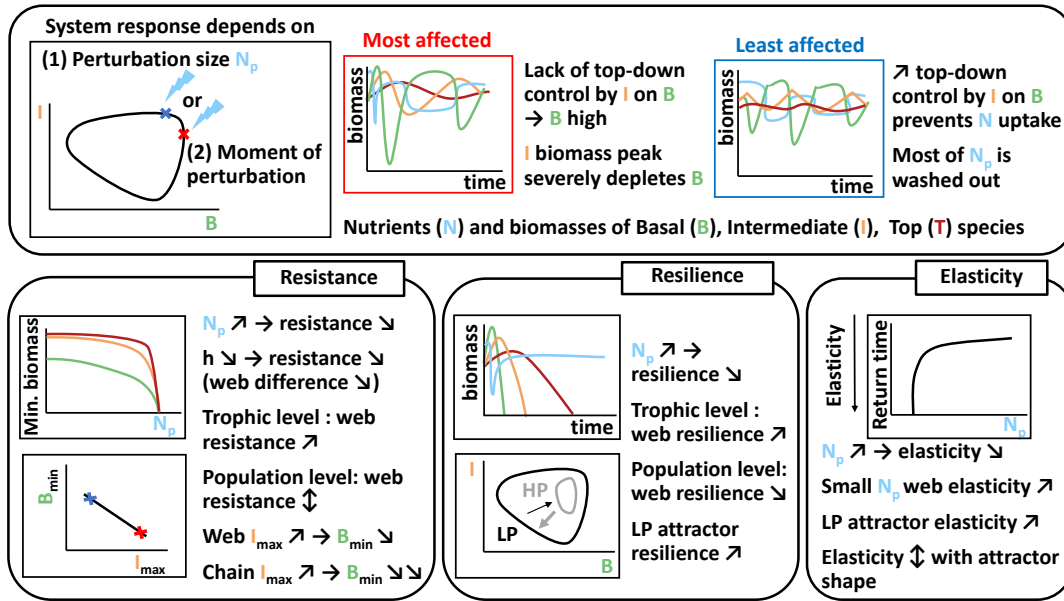
FIGURE 4.3: Sketch of the response of a tritrophic food web to a nutrient pulse. This response depends on the amount of extra nutrients added (the perturbation size N_p), and on the moment at which the perturbation is applied (i.e., the position on the attractor). Two extreme areas on the attractor could be distinguished: the most (red) and the least (blue) affected locations. The three studied characteristics—resistance, resilience and elasticity—show different aspects of how a food web responds to a nutrient pulse perturbation, depending on the Hill exponent, the nature of the attractor (cf. Table 4.1) and its functional diversity.

where on the limit cycle the perturbation is applied. How much this response varies is reflected by the difference between the upper and lower quantiles.

When applying only a very small perturbation to the food web, the spread of the biomass minima is correspondingly small (Fig. 4.4). However, this spread appears very large for the food web when $h = 1.05$ (Fig. 4.4, middle panel). This apparent discrepancy can be explained by the presence of the two attractors (cf. Table 4.1), each with a basin of attraction of approximately equal size. Because the actual timeseries minima differ between the attractors, so do the minima after a small perturbation. Thus, what appears as a very large range between which the minima are distributed, is actually a strongly bimodal distribution centered around the respective minima of each attractor. While the food chain for $h = 1.1$ also exhibits bistability (with both the high and low production attractor), the basin of attraction of the high production attractor is so small that this effect does not significantly impact our results (only one initial condition out of 1000 ended up on the high production attractor).

Our results also show a clear dependence on the Hill exponent of the functional responses. In both the chain and the web, the minima of all trophic levels decrease when reducing the Hill exponent. That is, the closer the Hill exponent comes to unity, the more the populations are at risk of stochastic extinction. Besides, the whole range of possible minima tends to increase as the Hill exponent decreases, making the system response to the pulse perturbation harder to predict. Ultimately,
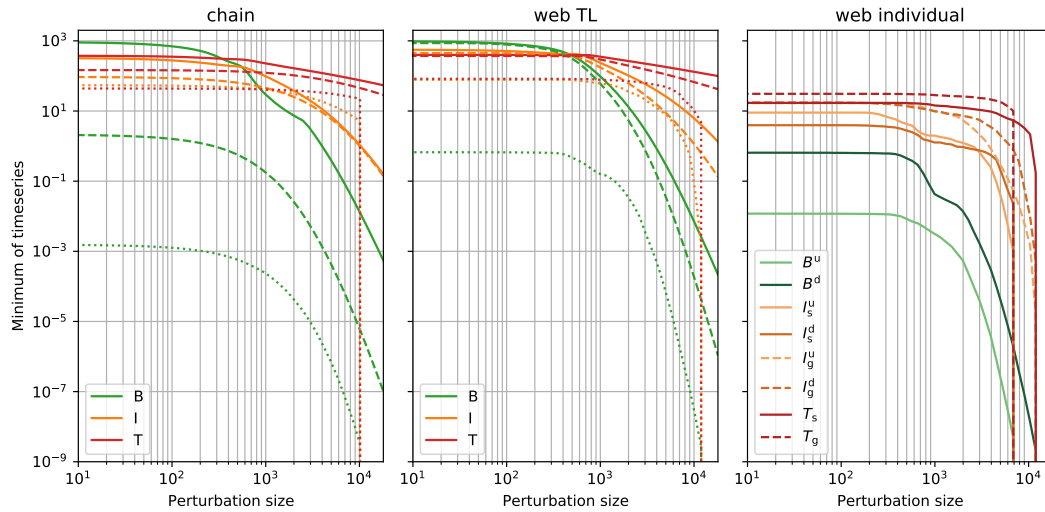
FIGURE 4.4: Minima reached by the timeseries after the perturbation, for the chain (left), the total biomass per trophic level in the diverse food web (middle), and the individual populations in the food web (right), as a function of the perturbation size. Each line corresponds to the median of 1000 different randomly sampled initial conditions that lead to coexistence of all species, with the shaded area showing the upper and lower quantiles. These initial conditions were first allowed to relax to the attractor for $3 \cdot 10^4$ time units before the perturbation was applied. For the chain and trophic level biomass in the food web, the solid lines show the minima for Hill exponents $h = 1.15$, dashed for $h = 1.10$, and dotted for $h = 1.05$. The individual populations' minima for the food web are only shown in the case of $h = 1.05$.

the dependence on the Hill exponent is less strong for the food web than for the food chain. That is, the timeseries minima differ less when comparing the different Hill exponents for the food web than for the food chain, revealing that the moment of the perturbation becomes less relevant.

In addition, for $h = 1.05$, the basal trophic level goes extinct for perturbation sizes of approximately $3 \cdot 10^3$ or higher in the food chain, whereas it takes a perturbation size of approximately $7 \cdot 10^3$ to cause the whole basal trophic level to go extinct in the food web (Fig. 4.4). Importantly, extinctions of individual populations may happen already for smaller perturbation sizes in the food web, and these lead to extinctions on higher trophic levels as well. However, the remaining population on the basal level can still support at least a part of the food web. In contrast, the extinction of the basal population in the food chain invariably leads to the complete disappearance of all the upper trophic levels as well. When $h = 1.1$ or 1.15, a significant proportion of extinctions only happens for unrealistically large perturbation sizes outside of the range we considered.

The pronounced differences between the minimal biomass reached by the basal trophic level B_{min}, can be understood by explicitly examining how this quantity varies depending on where on the attractor the perturbation (Fig. 4.5, for $h = 1.10$) is applied, as well as the post-perturbation timeseries (Fig. 4.6), in more detail. In these figures, we show the location in phase space of 6 selected points, and the response to a large perturbation of size 10^4 applied at each of these points. While P_1
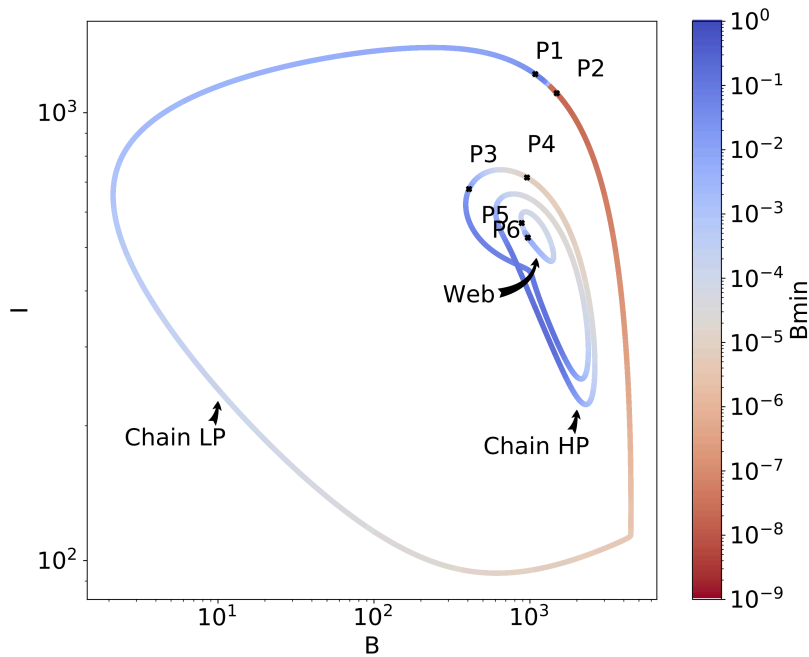
FIGURE 4.5: Minima reached by the basal trophic level after the perturbation, depending on where on the attractor a nutrient pulse of size 10^4 is applied, projected on the $B - I$ plane. The two attractors of the food chain (LP, HP), and the food web, when $h = 1.1$, are all shown. The points P_1 to P_6 are picked to highlight the large differences in response that are possible by perturbing the system on points that may be very close together. See Fig. C.3, Appendix C for all Hill exponents and for different perturbation sizes.

and P_2 are very close together on the attractor, the effect of the perturbation on the resulting dynamics is very different between these two points (Fig. 4.5, 4.6a-c). In both these cases, the basal species are in decline at the moment of the perturbation. At P_1 (Fig. 4.6b), they are under sufficient top-down control by the intermediate level, such that the free nutrient concentration remains very high for a long period of time. In this case, most of the extra nutrients due to the perturbation are simply washed out of the system. In the case of P_2 (Fig. 4.6c), however, the basal species are able to exploit almost all of the newly available nutrients immediately. This leads to an extremely high peak biomass on the basal level, which is in turn exploited by the intermediate level. Because of the delayed reaction time in the top level, the intermediate species are able to stay at a high biomass for an extended period of time and thus graze the basal level down to a very low biomass density.

This pattern describes what is observed generally in both the food chain and the food web after a nutrient pulse perturbation. A portion of the supplementary nutrients are quickly taken up by the basal trophic level, which subsequently causes a biomass peak in the intermediate trophic level. The higher this peak is, the more affected the basal level will be by the surplus grazing of the intermediate level. Points P_3 and P_4 (Fig. 4.6d-f) illustrate how, when a perturbation is applied in the HP state, the system's dynamics also follow this pattern after the perturbation, and consequently, return to the LP state instead of the HP state.
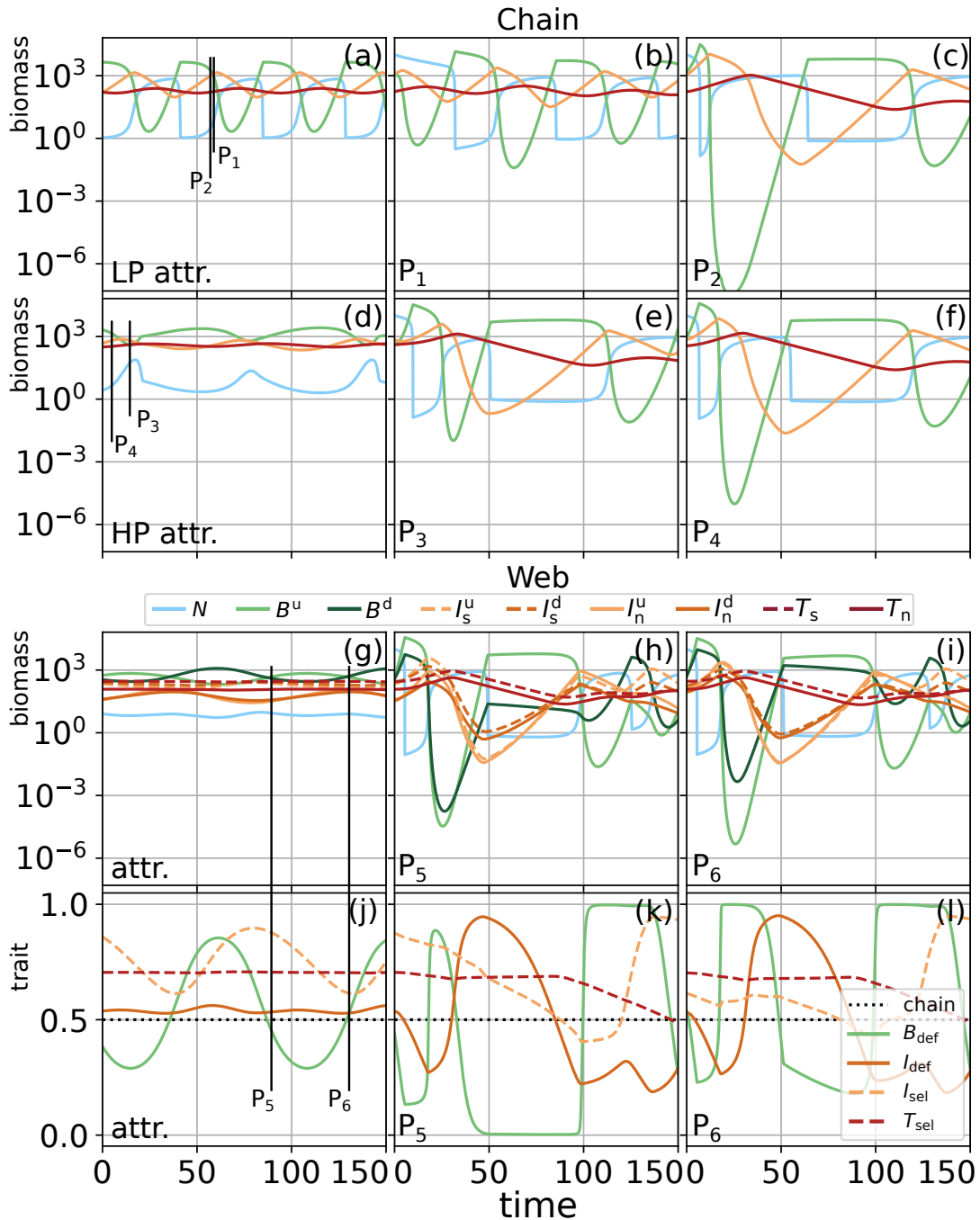
FIGURE 4.6: Timeseries of the dynamics of the chain and food web for $h = 1.10$, showing first the dynamics on the attractor, i.e., prior to the perturbation (chain LP: panel (a), HP: panel (d), web: panel (g)), and in the middle and right columns the system's behavior after a perturbation of size 10^4 on points P_1-P_6 (cf. Fig. 4.5). The locations of these points in time on the attractor are indicated by the vertical black lines in the leftmost column. The bottom row (j-l) shows the temporal development of the trait value for the biomass dynamics shown in the panel above (basal and intermediate defense B_{def} & I_{def}, and intermediate and top selectivity I_{sel} & T_{sel}, cf. Fig. 4.1). Notably, while P_3 and P_4 are on the HP attractor before the perturbation, the extremely high inflow of nutrients pushes the system into the LP state, where it remains. Because the *LP* state is not attractive when $h = 1.1$ in the food web, the trajectories of P_5 and P_6 must eventually return to the *HP* state (cf. Fig. C.4, Appendix C).

Investigating not only the biomass but also the trait dynamics after the perturbation in the food web highlights the way in which a diverse food web may be able to buffer the nutrient pulse (Fig. 4.6j-l). Here, the temporal evolution of the mean trait values is shown, where e.g. the basal defense level B_{def} is the proportion of the defended basal species B^{d} (cf. Fig. 4.1) of the total amount of basal biomass. The other traits are calculated equivalently. Right after the perturbation, the abundance of available nutrients causes the basal biomass to increase, but the undefended species will increase faster due to its higher growth rate. If the selective intermediate species are sufficiently high in biomass, they are able to graze down the undefended basal species to very low densities, potentially causing the defended basal species to outweigh the undefended species by several orders of magnitude. Importantly, the defended species are not grazed down to such low levels, preventing the potentially very strong reduction in total biomass on the basal level observed in the food chain. Additionally, a clear hierarchy in when the trophic levels are significantly affected is observed (Fig. 4.6j-l). In particular, the trait composition of the top trophic level is only substantially altered a considerably long time after the perturbation.

In the short-term after the perturbation, a general negative correlation emerges between the minimal basal biomass (B_{min}) and the maximal intermediate biomass (I_{max}). The higher the intermediate species grow after the pulse, the more severely they deplete the basal species (Fig. 4.7). Hence, the most (and respectively, least) affected area on the attractor has the lowest B_{min} with the highest I_{max} (and respectively highest B_{min} with the lowest I_{max}). The negative relationship between B_{min} and I_{max} is strengthened as the Hill exponent decreases (Fig. 4.7a). Lowering the Hill exponent increases the oscillation amplitude of the dynamics, such that food webs with a Hill exponent $h = 1.05$ at the LP state obtain the lowest B_{min} values (below 10^{-2}). We also observe that the HP state has lower I_{max}, and higher B_{min} values, as compared to the LP state (Fig. 4.7a). Because the HP state is characterized by a higher top species biomass and smaller amplitudes (Fig. 4.6a and d), reaching the extreme values of the LP state is not possible (Fig. 4.6c and f). Moreover, the top species keep the intermediate species under stronger top-down control, which limits the effects of nutrient enrichment.

Importantly, our results show that B_{min} tends to be higher in the food web than in the food chain (Fig. 4.7a). A given I_{max} leads to a higher B_{min} in the food web (insofar as they can be compared). This suggests that a diverse food web is more resistant to a pulse perturbation than a food chain with little or no diversity.

To untangle the actual effect of diversity on the $B_{\mathrm{min}} - I_{\mathrm{max}}$ relationship from the effect of comparing basal and intermediate species with different growth rates and interaction parameters, we also compare the food web to differently parametrized food chains (Fig. 4.7b). The basal growth rate in the food chain ($r_{\mathrm{chain}} \approx 0.81$) lies in-between the defended basal growth rate ($r_{\mathrm{d}} = 0.66$) and the undefended basal growth rate ($r_{\mathrm{u}} = 1$) of the diverse food web. Additionally, the basal-intermediate half-saturation constant in the food chain ($M_{\mathrm{chain}} \approx 424$) also lies in-between the
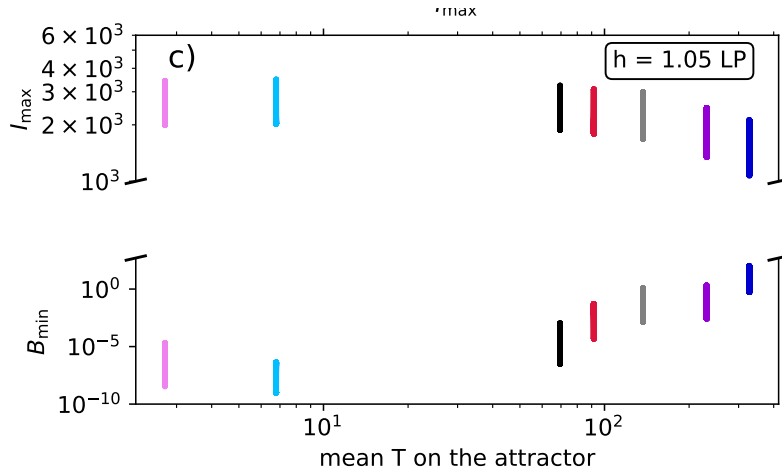
FIGURE 4.7: Relationship between the minimal biomass reached by the basal level (B_{min}), and the maximal biomass reached by the intermediate level (I_{max}), after a nutrient pulse perturbation $N_p = 1000$, depending on where on the attractor the perturbation is applied. The collections of points in the graph are grouped per attractor (LP: low-production state, HP: high-production state, cf. Table 4.1). A general negative correlation between B_{min} and I_{max} can be observed: the higher the intermediate level is able to grow after the perturbation, the lower it will graze down the basal level. This relationship becomes more pronounced for lower Hill exponents, as the amplitude of the dynamics increases (panel a). Importantly, when comparing the food web to the food chain while keeping the Hill exponent constant, the same I_{max} leads to a higher B_{min} in the food web. This ratio is influenced by the growth rate of the basal species and the half-saturation constant of the basal-intermediate interaction (panel b) as well as the biomass of the top trophic level on the attractor before the perturbation (panel c). Here, the growth rate of the basal species only is set to r_B (standard $r_B \approx 0.81$), and/or the $B - I$ half-saturation constant is set by M (standard $M \approx 424$).

values of the basal-selective ($M_s = 300$) and basal-non-selective ($M_n = 600$) interactions of the food web. Evidently, changing these parameters in the food chain also modifies the resulting $B_{min} - I_{max}$ relationship, either through direct (such as grazing suppression at low prey densities when M is high), or indirect effects (such as a different amount of top biomass when the basal growth rate r_B is changed, Fig. 4.7c).

Importantly, in the food web, the growth rates of the undefended and defended *I* species differ from the growth rate of the I species in the food chain. However, in both a chain where all growth rates are scaled to reflect the value of the defended species, as well as of the undefended species, it not possible for the top trophic level to survive. We therefore compare the food web to a chain where only the basal growth rate is affected. We find that for the food chain with r_B set to the high value of the undefended species, B_{min} increases to approximately one order of magnitude below the food web, whereas decreasing r_B to the value for the defended species decreases B_{min} (Fig. 4.7b). These changes are due to strong differences in the mean biomass on the top level in the alternative food chains: when r_B is high, the increased basal productivity translated to an increased biomass in the top level, and vice-versa (cf. Figs. 4.7c and C.5, Appendix C. When the top biomass is higher, stronger grazing pressure on the intermediate level prevents excessive grazing of B. On the other hand, for low top biomass the intermediate level can remain at high biomass

for an extended period of time, until they find no more food.

Similarly, increasing the $B - I$ half saturation constant to the value of the non-selective consumers ($M = 600$) increases B_{min}; and decreasing M to the value of the selective consumers (300) correspondingly decreases B_{min}. These changes are caused by the grazing suppression at low B densities, when M is increased. However, the changed mean top biomass caused by the altered basal productivity boosts the changes in B_{min} when varying M (cf. Figs. 4.7c and C.5, Appendix C).

In the food web, B^u is generally grazed to lower densities than B^d (Fig. 4.6h, i). This means that the $B^d - I_n$ interaction (low r_B, high M), is principally responsible for the value of B_{min} (Fig. 4.1). In a chain parametrized to have this interaction, B_{min} is still approximately one order of magnitude below that of the food web.

Comparing the resilience of the HP and LP state to a perturbation shows that the HP state is more vulnerable in both the food chain and the food web (Fig. 4.8). In the chain, with $h = 1.1$, perturbation sizes of maximally ≈ 1000, but even as small as ≈ 100 on the HP state can move the system outside its basin of attraction, such that it relaxes to the LP state. In contrast, the LP state is much more resilient: even after perturbations of size $10,000$ anywhere on the attractor, the system still returns to it.
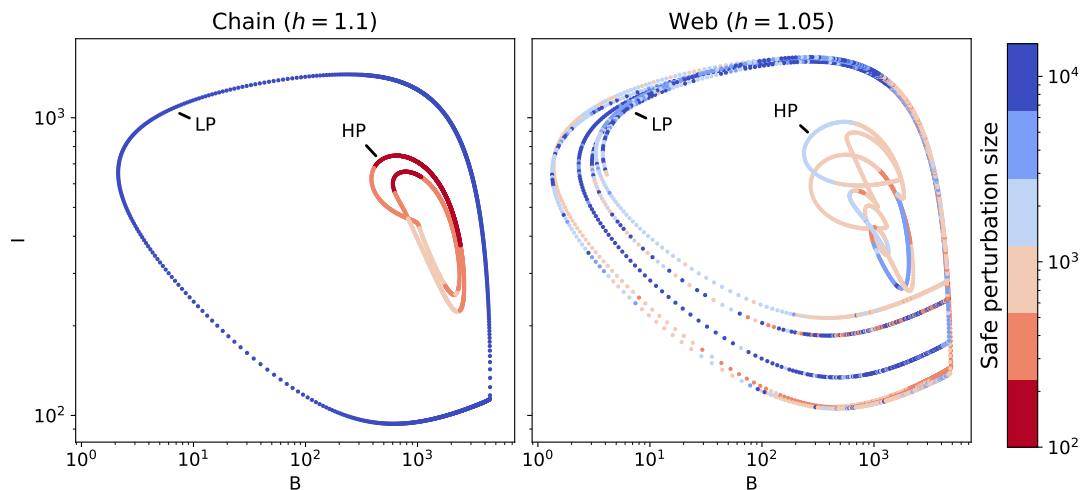

FIGURE 4.8: Total basal (B) and intermediate (I) biomass on the low production (LP) and high production (HP) attractors, for both the chain (left) and web (right) when they exhibit bistability. This happens when the Hill exponent $h = 1.1$ in the chain, and $h = 1.05$ in the web. The color indicates the maximum perturbation size for which the system, when perturbed at this point in the attractor, still returns to its original state. When the perturbation is larger than this "safe" perturbation size, the system either relaxes to the other attractor, or to another non-coexistence attractor. On the chain (left), the LP state is very resilient to perturbations, because even for perturbations of size 10^4, the system returns to this state, independently of where on the attractor it is applied. Conversely, the HP state is very vulnerable: a perturbation size of ≈ 200 frequently moves the system outside the HP's basin of attraction, and the maximum safe perturbation is ≈ 1000. For the food web, the same pattern is observed: the HP state is less resilient than the LP state. However, the HP state for the food web is much more resilient than it is in the food chain, despite its lower Hill exponent of $h = 1.05$.

For the food web, with $h = 1.05$, the situation is qualitatively similar, but there are some important differences. The LP state still shows resilience to perturbations

of $\approx 10,000$, but not anymore over its full length. Recall that, when $h = 1.05$, the likelihood of extinctions becomes non-negligible for perturbation sizes of approximately 3000 or higher (cf. Fig. 4.4). Furthermore, because there are some regions where perturbations of ≈ 200 are unsafe, by causing a transition from the LP to the HP state. The HP attractor is resilient to perturbation sizes of ≈ 5000 for some areas, in contrast to the chain.

To quantify the elasticity in our system, we estimated the median return time as a function of the perturbation size (Fig. 4.9). This is defined as the time required for the system to stay in the attractor's near vicinity (maximal distance to a point on the attractor must be < 5 in units of total biomass) after a perturbation (cf. Fig. 4.2). Because this time may vary depending on where on the attractor the perturbation is applied, the median return time, as well as the lower and upper quantiles of 100 evenly spaced points on the attractor are displayed. The perturbation size is only increased up to 10^2 to prevent the influence of trajectories not returning to their original attractor when the perturbation size gets very large.
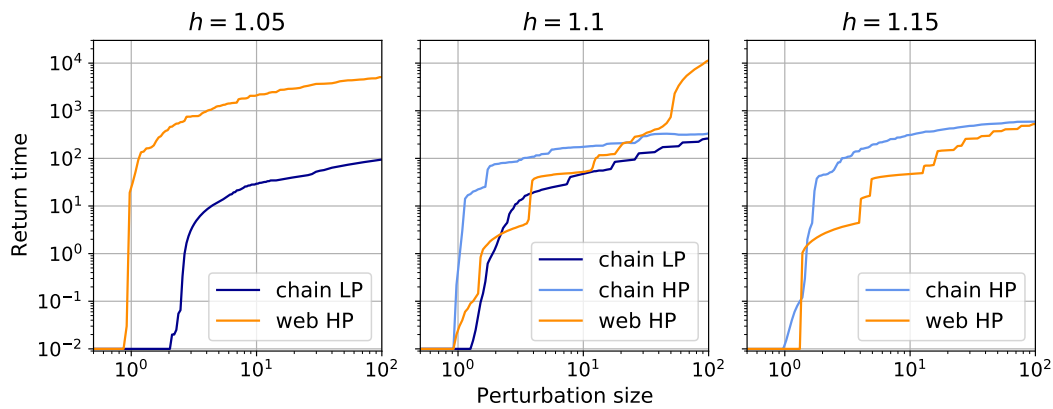
FIGURE 4.9: Return time as a function of the perturbation size for the different attractors in our system, for the three different Hill exponents (h) we investigated. Due to its complex structure, the return time for the LP state in the food web when $h = 1.05$ (cf. Table 4.1) could not be accurately calculated. In all other cases, the median and lower and upper quantiles of the return times for 100 evenly spaced points on the attractor are shown for each perturbation size where applicable (when $h = 1.15$, the food web relaxes to a fixed point, cf. Table 4.1). The minimum return time (10^{-2}) is determined by the time step at which the timeseries were sampled. A lower return time means that the system is faster to return to its original attractor, implying a higher elasticity. While a straightforward comparison of the elasticity of a food chain versus a food web proves difficult, our results show that the *LP* state in the food chain tends to have a higher elasticity to nutrient pulse perturbations than the *HP* state. The elasticity of the food web is higher for small perturbations than that of the equivalent state in the food chain, when both exist.

Due to the significant structural differences between a food chain and a food web (Fig. 4.1), a straightforward comparison between the elasticity of these two systems is very difficult. An additional complicating factor is the different number and/or type of attractors for the food chain and food web for a given Hill exponent. Despite these complicating factors, our results show that the elasticity of the *LP* attractor tends to be higher than that of the *HP* attractor.

With this effect of the attractor shape in mind, our results show that the return time of the food web tends to be lower than that of the food chain, insofar as they can be fairly compared. For $h = 1.05$, the chain is on the *LP* state, while only for the *HP* state could the return time be accurately calculated. When $h = 1.10$, the food web is on the *HP* state, and its return time is approximately an order of magnitude lower than the food chain on the *HP* state when the perturbation is low. For higher perturbation sizes, the increased complexity of the food web causes the return time to increase faster than it does for the chain. Lastly, for $h = 1.15$, both web and chain are on the *HP* state, and there is roughly an order of magnitude difference between the return time of the two again, in favor of the food web. In line with expectations, the elasticity increases with h for the food web, whereas this this effect is less pronounced for the chain.

Discussion

We investigated the consequences of a nutrient pulse on the dynamics of a non-diverse and a diverse tritrophic food web. The non-diverse food web is a simple linear food chain, whereas the diverse food web has three adaptive trophic levels. Prey species can be defended or undefended against predation, and the consumer species can be selective or non-selective feeders. Their fitness is balanced through two trade-offs: defended species grow slower, and non-selective feeders exploit low resource densities less efficiently.

As expected by the paradox of enrichment (Rosenzweig, 1971; Abrams and Roth, 1994), increasing the available nutrients does usually not benefit all species. The higher the pulse perturbation is—and so the richer the environment becomes—the stronger the effects of the pulse perturbation on the food web dynamics are (Figs. 4.3, 4.4 and 4.9). Additionally, the food web response varies significantly depending on the moment of perturbation (i.e., the point on the attractor). In particular, we can distinguish two neighboring zones on the attractor which are either the most or the least affected (Figs. 4.3 and 4.6). This difference arises from the intermediate species' ability to keep the basal level under sufficient top-down control. Under weak top-down control, the basal species are immediately able to grow to very high densities after the nutrient pulse. This basal biomass peak is followed by a peak in intermediate species biomass, which in turn leads to a depleted basal biomass level. On the other hand, if the top-down control is strong, the basal species are unable to efficiently exploit the extra nutrients, such that most of the nutrient pulse simply washes out of the system. This corresponds to previous findings in a bitrophic food web (Rall, Guill, and Brose, 2008). Similarly to previous studies, we found that the effect of the top level may be key to determining the response of the food web as a whole, because of their decisive influence on the biomasses of the lower trophic levels (Wollrab, Diehl, and De Roos, 2012; Ceulemans, Guill, and Gaedke, 2020).

By examining different values of the Hill-exponent in the basal-intermediate and intermediate-top interactions, for a non-diverse and highly diverse system, we uncover how the type and shape of the attractor affects the response of a food web (Fig. 4.3 and see Table 4.1). Previously, (Rall, Guill, and Brose, 2008) showed that after nutrient enrichment in a simple consumer-resource system, a higher Hill exponent stabilized the population dynamics. We found that this pattern generally holds for tritrophic systems as well, but show additional effects of the shape and type of attractor present in the complete state space (Fig. 4.3).

Nutrient pulse pushes system to low-production state

In our model, both the food chain and the food web exhibit bistability for a large part of the parameter space (Table 4.1). In these cases, the system can relax to either the low-production (LP) or high-production (HP) state, depending on the initial conditions. This implies that a sufficiently large perturbation can result in the system relaxing to the other state. Such behavior, commonly called a regime shift, is a widely observed phenomenon that can occur in many different types of ecosystems (Scheffer and Carpenter, 2003; Folke et al., 2004). Regime shifts are often the cause of major concern, because the two states may vary considerably in their ecological properties. Some examples are changes in vegetation patterns (Dublin, Sinclair, and McGlade, 1990), in particular under desertification (Bestelmeyer et al., 2015); or transitions between a clear and a turbid state in lakes (Scheffer et al., 1993; Scheffer and Jeppesen, 2007).

We previously showed that diversity loss likely causes our system to transition from the ecologically desirable HP state to the LP state, where top level biomass is much lower, and the biomass dynamics more variable (Ceulemans et al., 2019). Here, we showed how that transition probabilities between the LP and the HP state are unequal when the system is exposed to a sudden nutrient pulse (Fig. 4.8): it is more likely for the system to transition to the LP than to the HP attractor. This asymmetry can be explained by a closer analysis of the post-perturbation timeseries shown in Fig. 4.6. After a nutrient pulse, both basal species increase due to the high amount of readily available nutrients. As a response all intermediate species increase, which causes a concurrent decrease of all basal species, and increase of all top species. In other words, immediately after a perturbation, species on the same trophic level tend to move synchronously, largely independently of their trait values. This is exactly the dynamical pattern that governs the behavior of the LP state. In contrast, on the HP state, the species tend to exhibit compensatory dynamical patterns (Fig. 4.6g, and (Ceulemans et al., 2019)). Therefore, a nutrient pulse causes the system to behave like the LP state, and only a relatively small ($\sim N_0$, the normal inflow nutrient concentration, or less) disturbance forces the system to stay permanently in this state. In summary, a nutrient pulse can cause a regime shift between the HP and LP states, preferably in the $HP \rightarrow LP$ direction, and this transition is more likely at low rather than high functional diversity.

Resistance varies with the functional diversity

The system's resistance varies with the organization level studied, i.e., the population or trophic level (Fig. 4.3). On the trophic level scale, the diverse food web is generally more resistant since the biomasses do not reach as low values as in the non-diverse system (Figs. 4.4 and 4.5). However, at the population level, the undefended basal species (B_u) may be more affected in the diverse system than the only basal species in the non-diverse system for instance (Figs. 4.4 and 4.6f, i). Under the extremely nutrient-rich conditions immediately following the perturbation, B_u is at a competitive advantage due to its higher growth rate. At the basal biomass peak following the perturbation, B_u completely dominates the basal trophic level, by having taken up the majority of the added nutrients. As a consequence the main consumers of B_u strongly increase, which in turn leads to B_u being grazed down to very low biomasses. On the other hand, because of the initial dominance of B_u over the basal defended species (B_d), B_d only experiences limited additional growth, and thus only contributes little to the growth of the non-selective intermediate species. In turn, B_d is grazed down less, despite its lower growth rate and stabilizes the trophic level biomass (Fig. 4.6i, l). In this way, our model shows the mechanism behind how a species' functional trait determines its behavior in a food web, leading to explicit manifestations of the insurance hypothesis (Naeem and Li, 1997).

The above analysis rests on the general relationship between B_{min} and I_{max} after a nutrient pulse perturbation (Figs. 4.3 and 4.7). We show that, after a perturbation, a higher I_{max} leads to a lower B_{min} due to the increased grazing of the basal level. The food web structure has an important influence on this relationship since a diverse food web can maintain a considerably higher B_{min} at a given I_{max}, compared to a food chain (Fig. 4.7a). Naturally, this relationship depends on the parametrization of the food chain (Fig. 4.7b). A chain with a high $B - I$ half-saturation constant ($M = 600$) has a higher resistance due to grazing suppression at low B densities. The intermediate species thus reaches lower I_{max} values and the basal species higher B_{min} values.

However, even in a single three-species food chain, additional mechanisms are at play. When $M = 600$, the dynamics of the chain are completely different than with the standard parametrization ($M \approx 424$, see Appendix C.5, Appendix C). In particular, the biomass of the top trophic level has increased substantially (4.7c) . This high top-down control limits the increase of the intermediate species after a perturbation, and thus, protects the basal species to be grazed down to very low densities. This also holds for the food chain with a higher r_{basal}: the increased basal productivity is translated into higher biomass on the top trophic level. On the other hand, for the parameterizations leading to food chains with low top biomasses, the intermediate level is able to deplete the basal level to very low B_{min} values after the perturbation.

These results show how knowledge about the whole food web is necessary to predict its response to a disturbance. The effect of a nutrient pulse, which only

directly affects the basal trophic level, depends on its interaction with the intermediate trophic level and ultimately also on the top trophic level. Combined with our knowledge of the resilience of the different attractors—a regime shift from the HP to the LP state is less likely in a diverse food web—this result highlights the key role played by functional diversity in governing the response of the food web. When functional diversity is high, the persistence of the high-production state on which the top biomass level is high is safeguarded, such that adequate control on the intermediate level is ensured. A reduction in functional diversity can therefore abruptly affect food web resistance as the system is then easily kicked to the low-production attractor where top level biomass is much lower.

Elasticity depends on attractor structure, shape, and diversity

Another way to quantify a system response after a perturbation is by measuring its elasticity, that is, the time it takes to return to the pre-perturbation state (return time, cf. Fig. 4.2). In an economical context, elasticity is an important quantity, because low elasticity means that the desired functioning of an ecosystem may be interrupted for a substantial period of time before possibly returning back to normal (Oliver et al., 2015).

Our results show that the return time increases with the size of the nutrient pulse, and, moreover, this increase can happen in discrete jumps: suddenly, the dynamics require almost a whole additional revolution in state space before being close enough to the attractor (Fig. 4.9). We also observed that the return time depends on the food web structure and the shape of the attractor to which the perturbed system is returning. In particular, we find that the return time on the HP state tends to be higher than on the LP state. This observation can be made plausible by comparing the shape of the two attractors. On the LP attractor, individual species' amplitudes are significantly higher than on the HP attractor, in particular, both the nutrients and the basal trophic level routinely reach densities that are close to their carrying capacity. Moreover, our results have shown that perturbing the HP state can lead to the dynamics temporarily (cf. Figs. 4.6 and C.4, Appendix C) or permanently (cf. Fig. 4.8) behaving like the LP attractor. Importantly, this behavior is also observed in cases where the LP state is not a dynamical attractor. The time spent by the transient on this ghost attractor increases with the distance to the bifurcation (Hastings et al., 2018; Morozov et al., 2020), ultimately strongly affecting the return time of the HP state as the Hill exponent decreases.

A meaningful comparison between food webs of low and high diversity, thus requires precise knowledge about the system. The food web elasticity may strongly depend on the shape and type of the attractor, and of other nearby attractors in both the phase and parameter space. Notwithstanding these complexities, our results suggest that the return time is lower in the food web than in the food chain for low perturbation sizes (Fig. 4.9).

Concluding remarks

Our results show that the resistance, resilience and elasticity of a tritrophic food web to a pulse perturbation depends on its ecological structure in a complex manner (cf. Fig. 4.3). By showing that the food web response strongly depends on the state of every population in the food web at the moment of perturbation, as well as on the shape and type of the attractor. In particular, even though a nutrient pulse only directly affects the basal trophic level, we show how top-down regulatory processes driven by the top trophic level play an important role. These processes depend themselves on the functional diversity of the food web. In this way the potentially destructive positive feedback loop is mechanistically understood: the loss in functional diversity resulting from any extinctions caused by a disturbance affects food web functioning in such a way that its resilience, resistance and elasticity are even lower making it more vulnerable to further perturbations.

Acknowledgements

References

Abdala-Roberts, L. et al. (2019). "Tri-trophic interactions: bridging species, communities and ecosystems". In: *Ecology Letters*. DOI: 10.1111/ele.13392.

Abrams, P. A. and Roth, J. D. (1994). "The effects of enrichment of three-species food chains with nonlinear functional responses". In: *Ecology* 75.4, pp. 1118–1130. DOI: 10.2307/1939435.

Bell, G., Fugère, V., Barrett, R., Beisner, B., Cristescu, M., Fussmann, G., Shapiro, J., and Gonzalez, A. (2019). "Trophic structure modulates community rescue following acidification". In: *Proceedings of the Royal Society B: Biological Sciences* 286.1904. DOI: 10.1098/rspb.2019.0856.

Bender, E. A., Case, T. J., and Gilpin, M. E. (1984). "Perturbation experiments in community ecology: theory and practice." In: *Ecology* 65.1, pp. 1–13. DOI: 10.2307/1939452.

Bestelmeyer, B. T., Okin, G. S., Duniway, M. C., Archer, S. R., Sayre, N. F., Williamson, J. C., and Herrick, J. E. (2015). "Desertification, land use, and the transformation of global drylands". In: *Frontiers in Ecology and the Environment* 13.1, pp. 28–36. DOI: 10.1890/140162.

Bestion, E., Barton, S., García, F. C., Warfield, R., and Yvon-Durocher, G. (2020). "Abrupt declines in marine phytoplankton production driven by warming and biodiversity loss in a microcosm experiment". In: *Ecology Letters* 23.3, pp. 457–466. DOI: 10.1111/ele.13444.

Brooks, T. M. et al. (2002). "Habitat loss and extinction in the hotspots of biodiversity". In: *Conservation Biology* 16.4, pp. 909–923. DOI: 10.1046/j.1523-1739.2002.00530.x.

Brose, U. et al. (2019). "Predator traits determine food-web architecture across ecosystems". In: *Nature Ecology and Evolution* 3.6, pp. 919–927. DOI: 10.1038/s41559-019-0899-x.

Butchart, S. H. et al. (2010). "Global biodiversity: Indicators of recent declines". In: *Science* 328.5982, pp. 1164–1168. DOI: 10.1126/science.1187512.

Cardinale, B. J. et al. (2012). "Biodiversity loss and its impact on humanity". In: *Nature* 486.7401, pp. 59–67. DOI: 10.1038/nature11148.

Ceulemans, R., Gaedke, U., Klauschies, T., and Guill, C. (2019). "The effects of functional diversity on biomass production, variability, and resilience of ecosystem functions in a tritrophic system". In: *Scientific Reports* 9.1. DOI: 10.1038/s41598-019-43974-1.

Ceulemans, R., Guill, C., and Gaedke, U. (2020). "Top predators govern multitrophic diversity effects in tritrophic food webs". In: *bioRxiv*, p. 2020.07.31.230375. DOI: 10.1101/2020.07.31.230375.

Couture, R. M., Moe, S. J., Lin, Y., Kaste, Ø., Haande, S., and Lyche Solheim, A. (2018). "Simulating water quality and ecological status of Lake Vansjø, Norway, under land-use and climate change by linking process-oriented models with a Bayesian network". In: *Science of the Total Environment* 621, pp. 713–724. DOI: 10.1016/j.scitotenv.2017.11.303.

Diaz, R. J. and Rosenberg, R. (2008). "Spreading dead zones and consequences for marine ecosystems". In: *Science* 321.5891, pp. 926–929. DOI: 10.1126/science.1156401.

Díaz, S. et al. (2019). "Summary for policymakers of the global assessment report on biodiversity and ecosystem services of the Intergovernmental Science-Policy Platform on Biodiversity and Ecosystem Services". In: *Population and Development Review* 45.3, pp. 680–681. DOI: 10.1111/padr.12283.

Dublin, H. T., Sinclair, A., and McGlade, J. (1990). "Elephants and Fire as Causes of Multiple Stable States in the Serengeti-Mara Woodlands". In: *The Journal of Animal Ecology* 59.3, pp. 1147–1164. DOI: 10.2307/5037.

Dudgeon, D. et al. (2006). "Freshwater biodiversity: Importance, threats, status and conservation challenges". In: *Biological Reviews of the Cambridge Philosophical Society* 81.2, pp. 163–182. DOI: 10.1017/S1464793105006950.

Easterling, D. R., Meehl, G. A., Parmesan, C., Changnon, S. A., Karl, T. R., and Mearns, L. O. (2000). "Climate extremes: Observations, modeling, and impacts". In: *Science* 289.5487, pp. 2068–2074. DOI: 10.1126/science.289.5487.2068.

Estes, J. A. et al. (2011). "Trophic downgrading of planet earth". In: *Science* 333.6040, pp. 301–306. DOI: 10.1126/science.1205106.

Folke, C., Carpenter, S., Walker, B., Scheffer, M., Elmqvist, T., Gunderson, L., and Holling, C. S. (2004). "Regime shifts, resilience, and biodiversity in ecosystem management". In: *Annual Review of Ecology, Evolution, and Systematics* 35, pp. 557–581. DOI: 10.1146/annurev.ecolsys.35.021103.105711.

Fussmann, G. F. and Gonzalez, A. (2013). "Evolutionary rescue can maintain an oscillating community undergoing environmental change". In: *Interface Focus* 3.6. DOI: 10.1098/rsfs.2013.0036.

Galloway, J. N., Townsend, A. R., Erisman, J. W., Bekunda, M., Cai, Z., Freney, J. R., Martinelli, L. A., Seitzinger, S. P., and Sutton, M. A. (2008). "Transformation of the nitrogen cycle: Recent trends, questions, and potential solutions". In: *Science* 320.5878, pp. 889–892. DOI: 10.1126/science.1136674.

García-Palacios, P., Gross, N., Gaitán, J., and Maestre, F. T. (2018). "Climate mediates the biodiversity–ecosystem stability relationship globally". In: *Proceedings of the National Academy of Sciences of the United States of America* 115.33, pp. 8400–8405. DOI: 10.1073/pnas.1800425115.

Garnier, E., Navas, M.-L., and Grigulis, K. (2016). *Plant Functional Diversity. Organism traits, community structure, and ecosystem properties.*

Govaert, L. et al. (2019). "Eco-evolutionary feedbacks—Theoretical models and perspectives". In: *Functional Ecology* 33.1, pp. 13–30. DOI: 10.1111/1365-2435.13241.

Grimm, V. and Wissel, C. (1997). "Babel, or the ecological stability discussions: An inventory and analysis of terminology and a guide for avoiding confusion". In: *Oecologia* 109.3, pp. 323–334. DOI: 10.1007/s004420050090.

Hansen, J., Sato, M., Ruedy, R., Lo, K., Lea, D. W., and Medina-Elizade, M. (2006). "Global temperature change". In: *Proceedings of the National Academy of Sciences of the United States of America* 103.39, pp. 14288–14293. DOI: 10.1073/pnas.0606291103.

Harris, R. M. et al. (2018). "Biological responses to the press and pulse of climate trends and extreme events". In: *Nature Climate Change* 8.7, pp. 579–587. DOI: 10.1038/s41558-018-0187-9.

Hastings, A., Abbott, K. C., Cuddington, K., Francis, T., Gellner, G., Lai, Y. C., Morozov, A., Petrovskii, S., Scranton, K., and Zeeman, M. L. (2018). "Transient phenomena in ecology". In: *Science* 361.6406. DOI: 10.1126/science.aat6412.

Hautier, Y., Tilman, D., Isbell, F., Seabloom, E. W., Borer, E. T., and Reich, P. B. (2015). "Anthropogenic environmental changes affect ecosystem stability via biodiversity". In: *Science* 348.6232, pp. 336–340. DOI: 10.1126/science.aaa1788.

Hölker, F., Wolter, C., Perkin, E. K., and Tockner, K. (2010). "Light pollution as a biodiversity threat". In: *Trends in Ecology and Evolution* 25.12, pp. 681–682. DOI: 10.1016/j.tree.2010.09.007.

Hooper, D. U. et al. (2005). "Effects of biodiversity on ecosystem functioning: A consensus of current knowledge". In: *Ecological Monographs* 75.1, pp. 3–35. DOI: 10.1890/04-0922.

Horváth, Z., Ptacnik, R., Vad, C. F., and Chase, J. M. (2019). "Habitat loss over six decades accelerates regional and local biodiversity loss via changing landscape connectance". In: *Ecology Letters* 22.6, pp. 1019–1027. DOI: 10.1111/ele.13260.

Jones, A. G. (2008). "A theoretical quantitative genetic study of negative ecological interactions and extinction times in changing environments". In: *BMC Evolutionary Biology* 8.1, pp. 1–10. DOI: 10.1186/1471-2148-8-119.

Kaushal, S. S., Mayer, P. M., Vidon, P. G., Smith, R. M., Pennino, M. J., Newcomer, T. A., Duan, S., Welty, C., and Belt, K. T. (2014). "Land use and climate variability amplify carbon, nutrient, and contaminant pulses: A review with management implications". In: *Journal of the American Water Resources Association* 50.3, pp. 585–614. DOI: 10.1111/jawr.12204.

Kovach-Orr, C. and Fussmann, G. F. (2013). "Evolutionary and plastic rescue in multitrophic model communities". In: *Philosophical Transactions of the Royal Society B: Biological Sciences* 368.1610, p. 20120084. DOI: 10.1098/rstb.2012.0084.

Křivan, V. and Diehl, S. (2005). "Adaptive omnivory and species coexistence in tri-trophic food webs". In: *Theoretical Population Biology* 67.2, pp. 85–99. DOI: 10.1016/j.tpb.2004.09.003.

Matsuno, K. and Nobuaki, O. (1996). "How many trophic levels are there?" In: *Journal of Theoretical Biology* 180.2, pp. 105–109. DOI: 10.1006/jtbi.1996.0085.

McGill, B. J., Enquist, B. J., Weiher, E., and Westoby, M. (2006). "Rebuilding community ecology from functional traits". In: *Trends in Ecology and Evolution* 21.4, pp. 178–185. DOI: 10.1016/j.tree.2006.02.002.

Morozov, A., Abbott, K., Cuddington, K., Francis, T., Gellner, G., Hastings, A., Lai, Y. C., Petrovskii, S., Scranton, K., and Zeeman, M. L. (2020). "Long transients in ecology: Theory and applications". In: *Physics of Life Reviews* 32, pp. 1–40. DOI: 10.1016/j.plrev.2019.09.004.

Naeem, S. and Li, S. (1997). "Biodiversity enhances reliability". In: *Nature* 390.December, pp. 507–509.

Oliver, T. H. et al. (2015). "Biodiversity and Resilience of Ecosystem Functions". In: *Trends in Ecology and Evolution* 30.11, pp. 673–684. DOI: 10.1016/j.tree.2015.08.009.

Øygarden, L., Deelstra, J., Lagzdins, A., Bechmann, M., Greipsland, I., Kyllmar, K., Povilaitis, A., and Iital, A. (2014). "Climate change and the potential effects on runoff and nitrogen losses in the Nordic-Baltic region". In: *Agriculture, Ecosystems and Environment* 198, pp. 114–126. DOI: 10.1016/j.agee.2014.06.025.

Persson, A., Hansson, L. A., Brönmark, C., Lundberg, P., Pettersson, L. B., Greenberg, L., Nilsson, P. A., Nyström, P., Romare, P., and Tranvik, L. (2001). "Effects of enrichment on simple aquatic food webs". In: *American Naturalist* 157.6, pp. 654–669. DOI: 10.1086/320620.

Pimm, S. L., Jenkins, C. N., Abell, R., Brooks, T. M., Gittleman, J. L., Joppa, L. N., Raven, P. H., Roberts, C. M., and Sexton, J. O. (2014). "The biodiversity of species and their rates of extinction, distribution, and protection". In: *Science* 344.6187. DOI: 10.1126/science.1246752.

Raatz, M., Velzen, E. van, and Gaedke, U. (2019). "Co-adaptation impacts the robustness of predator–prey dynamics against perturbations". In: *Ecology and Evolution* 9.7, pp. 3823–3836. DOI: 10.1002/ece3.5006.

Rall, B. C., Guill, C., and Brose, U. (2008). "Food-web connectance and predator interference dampen the paradox of enrichment". In: *Oikos* 117.2, pp. 202–213. DOI: 10.1111/j.2007.0030-1299.15491.x.

Rosenzweig, M. L. (Jan. 1971). "Paradox of Enrichment: Destabilization of Exploitation Ecosystems in Ecological Time". In: *Science* 171.3969, pp. 385–387. DOI: 10.1126/science.171.3969.385.

Ryser, R., Häussler, J., Stark, M., Brose, U., Rall, B. C., and Guill, C. (2019). "The biggest losers: Habitat isolation deconstructs complex food webs from top to bottom". In: *Proceedings of the Royal Society B: Biological Sciences* 286.1908. DOI: 10.1098/rspb.2019.1177.

Scheffer, M., Hosper, S. H., Meijer, M. L., Moss, B., and Jeppesen, E. (1993). "Alternative equilibria in shallow lakes". In: *Trends in Ecology and Evolution* 8.8, pp. 275–279. DOI: 10.1016/0169-5347(93)90254-M.

Scheffer, M. and Carpenter, S. R. (2003). "Catastrophic regime shifts in ecosystems: Linking theory to observation". In: *Trends in Ecology and Evolution* 18.12, pp. 648–656. DOI: 10.1016/j.tree.2003.09.002.

Scheffer, M. and Jeppesen, E. (2007). "Regime shifts in shallow lakes". In: *Ecosystems* 10.1, pp. 1–3. DOI: 10.1007/s10021-006-9002-y.

Theodosiou, L., Hiltunen, T., and Becks, L. (2019). "The role of stressors in altering eco-evolutionary dynamics". In: *Functional Ecology* 33.1, pp. 73–83. DOI: 10.1111/1365-2435.13263.

Tilman, D. and Downing, J. A. (1996). "Biodiversity and Stability in Grasslands". In: *Ecosystem Management: Selected Readings*. New York, NY: Springer New York, pp. 3–7. DOI: 10.1007/978-1-4612-4018-1_1.

Tirok, K. and Gaedke, U. (2010). "Internally driven alternation of functional traits in a multispecies predator- prey system". In: *Ecology* 91.6, pp. 1748–1762. DOI: 10.1890/09-1052.1.

Violle, C., Navas, M.-L., Vile, D., Kazakou, E., Fortunel, C., Hummel, I., and Garnier, E. (2007). "Let the concept of trait be functional!" In: *Oikos* 116.5, pp. 882–892. DOI: 10.1111/j.2007.0030-1299.15559.x.

Visser, A. W., Mariani, P., and Pigolotti, S. (2012). "Adaptive behaviour, tri-trophic food-web stability and damping of chaos". In: *Journal of the Royal Society Interface* 9.71, pp. 1373–1380. DOI: 10.1098/rsif.2011.0686.

Wollrab, S., Diehl, S., and De Roos, A. M. (2012). "Simple rules describe bottom-up and top-down control in food webs with alternative energy pathways". In: *Ecology Letters* 15.9, pp. 935–946. DOI: 10.1111/j.1461-0248.2012.01823.x.

Worm, B. et al. (2006). "Impacts of Biodiversity Loss on Ocean Ecosystem Services". In: *Science* 314.5800, pp. 787–790. DOI: 10.1126/science.1132294.

Yamamichi, M. and Miner, B. E. (2015). "Indirect evolutionary rescue: Prey adapts, predator avoids extinction". In: *Evolutionary Applications* 8.8, pp. 787–795. DOI: 10.1111/eva.12295.

Yamamichi, M., Yoshida, T., and Sasaki, A. (2011). "Comparing the Effects of Rapid Evolution and Phenotypic Plasticity on Predator-Prey Dynamics". In: *The American Naturalist* 178.3, pp. 287–304. DOI: 10.1086/661241.

Chapter 5

Phase relationships in consumer-resource systems

Ruben Ceulemans*, Christian Guill*, Michael Raatz, & Ellen van Velzen
*: Equally contributing authors

To be submitted.

The text for this chapter is written by me, and constitutes my contribution to a yet-to-be-finalized project in cooperation with Dr. Christian Guill, Dr. Michael Raatz, and Dr. Ellen van Velzen (cf. Section 1.5, Chapter 1 for a detailed overview of the author contributions). In the final project, the observed phenomena and their intuitive mechanistic explanations will be combined with additional insights obtained from analyzing the phase relationships between populations in a food chain relative to an artificial external driver.

Abstract

The quarter-cycle phase difference between a predator-prey pair is considered a fundamental property of predator-prey cycles (the quarter-cycle lag rule). On this basis, observed deviations from this behavior, such as anti-phase cycling, are commonly attributed to the presence of evolutionary mechanisms influencing processes on the ecological timescale. However, research into the origin of the quarter-cycle lag rule shows that it stems from analytical calculations in a system where the predator-prey oscillations are assumed to be sinusoidal. In this text, we show that even in the standard Rosenzweig-MacArthur consumer-resource model, cycle deformation leads to phase differences substantially different from a quarter of a cycle. Moreover, in an extended tritrophic Rosenzweig-MacArthur predator-consumer-resource model, such deviating phase differences become increasingly likely, and even anti-phase cycling behavior between the consumer and the resource are possible. We emphasize that these deviations from the quarter-cycle lag rule are observed in simple systems with purely ecological dynamics. Caution must thus be taken when purely relying on phase differences to infer the presence of eco-evolutionary dynamics in a consumer-resource system, and especially in natural food webs containing more than two trophic levels.

5.1 Introduction

The cyclic behavior that can be exhibited by populations in a wide variety of communities is one of the most fundamental concepts in community ecology. Already in 1555, the archbishop of Uppsala, Olaus Magnus, determined that the observed fluctuations in lemming populations occurred in a regular pattern (Magnus, 1555; Lundberg et al., 1994). In more recent history, many of the ecological mechanisms responsible for creating population cycles and governing their shape have been studied using mathematical models of varying complexity.

An important feature of an oscillating ecological system is the difference between the phases of the individual population biomasses. One particularly prominent example is the general observation that the phase difference between a predator population and its prey is close to one quarter of a cycle. This property can be found in a wide array of experimental and field observations, such as the famous Lynx-Snowshoe Hare cycle, as well as in simple mathematical models such as the Lotka-Volterra model (Maclulich, 1937; Bulmer, 1976; Nedorezov, 2016). Observing such a quarter-cycle phase difference between a predator and its prey is so common, that this property is considered inherent to predator-prey cycles (Cortez and Ellner, 2010; Cortez, 2011; Ellner and Becks, 2011; Koch et al., 2014; Krysiak-Baltyn et al., 2016; Van Velzen and Gaedke, 2017). In these publications, it is claimed that any deviation from a quarter-cycle phase-difference indicates the presence of additional mechanisms, such as evolutionary processes, influencing the dynamics. In other words, a predator-prey pair in isolation is supposed to behave following the quarter-cycle lag "rule", and observation of larger phase differences (in particular anti-phase cycles where the phase difference is one half of a cycle) is considered to be a "smoking gun" for eco-evolutionary processes.

Scientific validation of the quarter-cycle lag rule is often given by referring to Bulmer (1975). This publication shows that the predator-prey phase lag must be less than a quarter of a cycle, when no additional interactions are present. While this statement follows from analytical calculations, they are based on a model in which the predator-prey oscillations are assumed to be sinusoidal, similar to the Lotka-Volterra model. This is a very strong assumption, that often does not hold for many simple predator-prey systems, such as the ubiquitous Rosenzweig-MacArthur predator-prey model (Rosenzweig and MacArthur, 1963).

In this text, we will show that even for the simple Rosenzweig-MacArthur consumer-resource model, substantial deviations from the quarter-cycle "rule" are possible. We specifically show that phase-differences substantially larger than a quarter-cycle are not uncommon. Moreover, under the influence of a top predator preying on the consumer, anti-phase cycles between the resource and consumer are possible. These anti-phase cycles are purely caused by ecological processes, without the need for additional evolutionary mechanisms.

5.2 Methods

In this study, we have analyzed the phase relationships within consumer-resource pairs in several different contexts. Firstly, we have studied an isolated pair, based on the (non-dimensionalized) Rosenzweig-MacArthur model (Rosenzweig and MacArthur, 1963):

$$\begin{cases} \dfrac{dR}{dt} & = R(1-R) - \dfrac{aR}{1+ahR}C \\ \dfrac{dC}{dt} & = \dfrac{aR}{1+ahR}C - dC \end{cases} \tag{5.1}$$

where the resource R is undergoing logistic growth, and is interacting with the consumer C through a Holling-type-II functional response with attack rate a and handling time h. The consumer loss rate is determined by d (cf. Section D.1, Appendix D for details on the non-dimensionalization transformations).

Secondly, we have expanded the Rosenzweig-MacArthur model by adding a third trophic level, the predator P on top:

$$\begin{cases} \dfrac{dR}{dt} & = R(1-R) - \dfrac{aR}{1+ahR}C \\ \dfrac{dC}{dt} & = \dfrac{aR}{1+ahR}C - \dfrac{\alpha C}{1+\alpha\eta C}P - dC \\ \dfrac{dP}{dt} & = \dfrac{\alpha C}{1+\alpha\eta C}P - \delta P \end{cases} \tag{5.2}$$

where, analogously to the $C - R$ interaction, the $P - C$ interaction is described by a Holling-type-II functional response with attack rate α and handling time η, and the predator loss rate is determined by δ.

The phase relationships between the pairs of species in the food chains were calculated by analyzing the Discrete Fourier Transforms (DFT) of the solutions obtained by numerical integration of Eqs. (5.1) and (5.2). The DFT was calculated using the NumPy package in Python (Van Der Walt, Colbert, and Varoquaux, 2011), where it is defined as:

$$A_k = \sum_{m=0}^{n-1} a_m \exp\left(-2\pi i \frac{mk}{n}\right) \qquad k = 0, \cdots, n-1. \tag{5.3}$$

In words, from the discrete sequence $a = \{a_0, \cdots, a_{n-1}\}$ of length n, the DFT algorithm calculates another sequence $A = \{A_0, \cdots, A_{n-1}\}$ (with $A_i \in \mathbb{C}$) using Equation (5.3). The sequence A is thus called the DFT of sequence a. While a describes the timeseries in the temporal domain, A describes it in the frequency domain.

If the timeseries contains a periodic pattern with frequency f, the magnitude of the element of A corresponding to f will be a local maximum. Thus, by finding the elements of A of which the magnitude a local maximum, we can find the frequencies

of the processes that govern the temporal dynamics of the timeseries. Importantly, since the A_i are complex numbers, the DFT also calculates the phase corresponding to this frequency, given by $\arg(A_i)$. By identifying the dominant frequency in the timeseries of each of the populations, we can thus estimate the phase difference $\Delta\phi_{CR}$ between the consumer and the resource, and $\Delta\phi_{PC}$ between the predator and the consumer, as follows:

$$\Delta\phi_{CR} = \phi_R - \phi_C$$
$$\Delta\phi_{PC} = \phi_C - \phi_P \tag{5.4}$$

where ϕ_R, ϕ_C, and ϕ_P are the phases of the dominant frequency of the resource, consumer, and predator, respectively. In our results, these will be expressed as fractions of 2π, such that a phase difference of one quarter of a cycle corresponds to $\frac{1}{4}$. To extract the dominant frequency of the timeseries from the DFT, we selected the peak for the lowest frequency in the DFT, with a peak prominence larger than 100 using the find_peaks algorithm in SciPy (Virtanen et al., 2020).

Numerical integration of the ordinary differential equations was done in *C* with the SUNDIALS CVODE solver version 2.7.0 (Hindmarsh et al., 2005). Calculation of the phase relationships using the DFT and further analysis and plotting of the data was performed using Python and Matplotlib (Hunter, 2007).

5.3 Results

The $C - R$ system defined in Eq. (5.1) contains only three parameters in its non-dimensionalized form: the $R - C$ attack rate a and handling time h, and the C death rate d. To get a complete overview of all possible values of the phase relationship between R and C can have, we varied a and h for several different values of d (Fig. 5.1).

These graphs contain several regions. In the green region, the combination of attack rate a, handling time h, and death rate d is such that the consumer cannot subsist on the resource, and thus the resource can grow to its carrying capacity. This happens when $a < \frac{d}{1-hd}$ (cf. Section D.2, Appendix D). In the dark blue region, both R and C coexist at a stable equilibrium. The phase difference is therefore defined as 0. When $a > \frac{1+dh}{h-dh^2}$ (solid black line, cf. Section D.2, Appendix D) the system has undergone a Hopf bifurcation and exhibits oscillatory dynamics. In this region, the phase difference $\Delta\phi_{CR}$ between the resource and the consumer is non-zero, and deviations from a quarter-cycle phase difference (white) increase with the intensity of the color. Our results show that the direction of deviation mainly depends on the value of h, in relation to d. Specifically, when $dh < 0.5$, $\Delta\phi_{CR}$ tends to be smaller than $\frac{1}{4}$, and the opposite when $dh > 0.5$. In the intermediate region, where $dh \approx 0.5$, $\Delta\phi_{CR} \approx \frac{1}{4}$. The size of deviations further depends on d, when $d = 0.05$, we find that $\Delta\phi_{CR}$ can sometimes be higher than 5/16, whereas when $d = 0.20$, phase differences above 3/8 are possible, and also below 3/16.
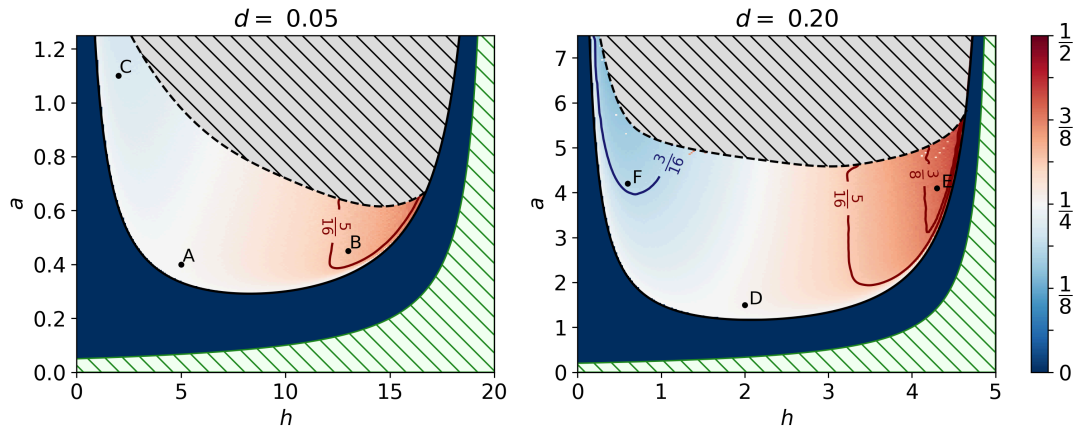
FIGURE 5.1: Phase difference $\Delta\phi_{CR}$ in the $C-R$ system (cf. Eq. (5.1)) as a function of the handling time h and the attack rate a, for different values of the consumer mortality d, expressed as a fraction of 2π. Red colors denote phase lags larger than a quarter cycle period, while blue colors denote phase lags smaller than a quarter cycle period. The solid black line denotes the Hopf bifurcation below which the system settles at a stable equilibrium. The solid green line denotes the coexistence boundary, below which only the resource is present in the system (green area). The grey area indicates the part of the parameter space where the system exhibits predator-prey cycles that were so extreme that the extinction threshold, set to 10^{-9}, was crossed and hence no phase difference could be calculated. Deviations from quarter-cycle period phase difference are highlighted by contour curves at selected threshold values. When the death rate of the consumer is low ($d = 0.05$) it exerts a relatively strong grazing pressure on the resource, and most of the calculated phase differences are close to a quarter-cycle period. However, when the consumer death rate is high, grazing pressure is lower and stronger deviations from quarter-cycle period phase differences are found ($d = 0.20$). Example timeseries for the points $A-F$ are shown in Fig. 5.2.

Finally, the dashed black line approximately indicates where the biomass minima reach 10^{-9}. If the attack rate a is above this line, the amplitude is such that biomass minima fall below this threshold. The extreme amplitude of the biomass oscillations (over ≈ 9 orders of magnitude) causes the algorithm for estimating the phase differences to occasionally output unreliable results. While pronounced deviations of $\Delta\phi_{CR}$ from quarter-cycle phase difference are common in this region, the amplitude of the biomass dynamics is unrealistically high from an ecological perspective.

Some selected exemplary timeseries for combinations of the parameters a, h and d, indicated by points $A-F$ in Fig. 5.1 are shown in Fig. 5.2. These examples also make the effect of these parameters on the dynamics and the phase relationships of the $C-R$ system clear. It can be seen that increasing the consumer loss rate d tends to directly decrease its density, which, in turn, may affect the density of the resource in a positive way. The effect of changing the handling time h is also clear: because $h \equiv 1/g$, where g is the maximum consumer growth rate, increasing h clearly shows the consumer requires a longer time to respond to changes in resource density (note the different ranges of the axes in Fig. 5.2), and vice-versa. However, the decay rate of C is given by d and is thus the same for points $A-C$ and $D-F$, respectively. Because of the linear scale on the biomass axes, the effect of the attack rate a is
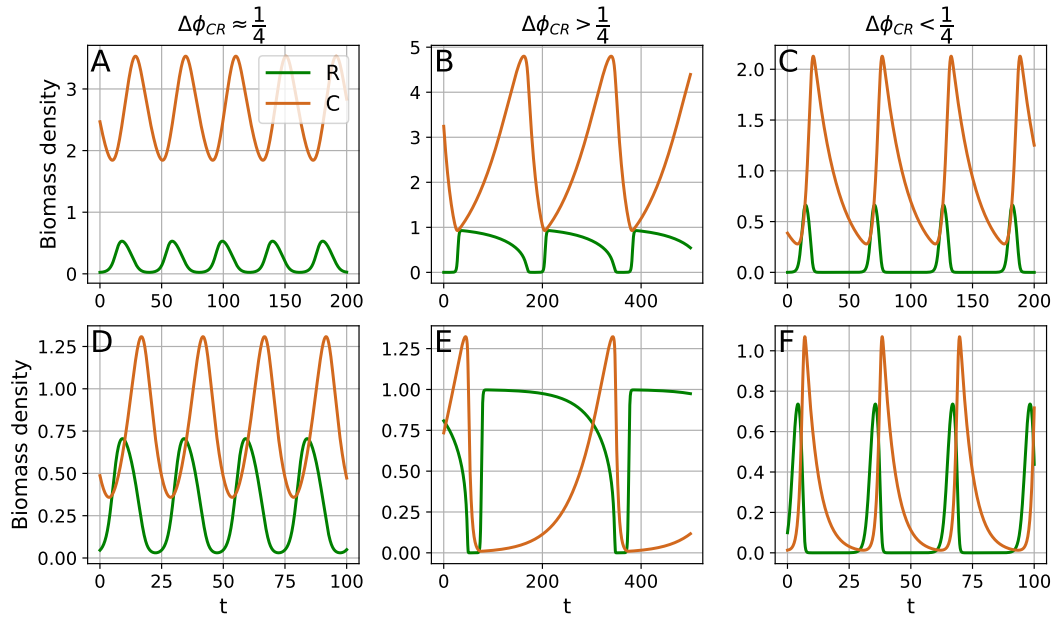
FIGURE 5.2: Example timeseries of the dynamics on the limit cycle for different combinations of attack rate a and handling time h, as indicated in Fig. 5.1, for the $C - R$ system defined in Eq. (5.1). The resource R is shown in green, and the consumer C in orange. The exact (h, a) values are $A : (5, 0.4)$, $B : (13, 0.45)$, $C : (2, 1.1)$ with $d = 0.05$ (top row), and $D : (2, 1.5)$, $E : (4.3, 4.1)$, $F : (0.6, 4.2)$ with $d = 0.20$ (bottom row). Note the different ranges on the axes caused by different values of h (affecting the consumer growth rate) and/or d (affecting its decay rate). When the consumer-resource phase difference $\Delta\phi_{CR} \approx 1/4$ (A, D), the timeseries appear quasi-sinusoidal. In contrast, when $\Delta\phi_{CR} < 1/4$ (B, E), or $\Delta\phi_{CR} > 1/4$ (C, F) the dynamics on the limit cycle appear strongly deformed. In the case of B and E, h is relatively large, leading to a longer time required for the consumer to reach a high density again. For C and F, the situation is opposite: h is sufficiently small such that the consumer can immediately catch up with the resource and graze it down to low densities.

less clear, but it can be observed that in general, increasing a tends to increase the amplitude of the dynamics. In particular, the biomass minima tend to go much closer to zero when a is high.

Unlike for the $C - R$ system defined in Eq. (5.1), we must restrict our analysis of the $P - C - R$ system (Eq. (5.2)) to a subset of the whole available parameter space. As we are mainly interested in the behavior of the $C - R$ part, we varied h and a for several values of the predator loss rate δ, while fixing d, η and α (Fig. 5.3, cf. Fig. D.1, Appendix D for two other combinations these three parameters). This approach allows for easy observation of how the $C - R$ interaction is affected by the presence of P, by direct comparison to Fig. 5.1. When the predator's loss rate is high, it is only able to survive in a small region of the $h - a$ parameter space (compare Fig. 5.3, top left, to 5.1, right). In a substantial part of this region, the addition of P causes anti-phase cycles ($\Delta\phi_{CR} \approx 1/2$) to appear between C and R. Because $\Delta\phi_{PC} \approx 1/4$ (Fig. 5.3, bottom left), the anti-phase cycles may be explained by R simply tracking the changes in C caused by the $P - C$ predator-prey cycles. As C goes up, R goes down and vice-versa (Fig. 5.4, point G).

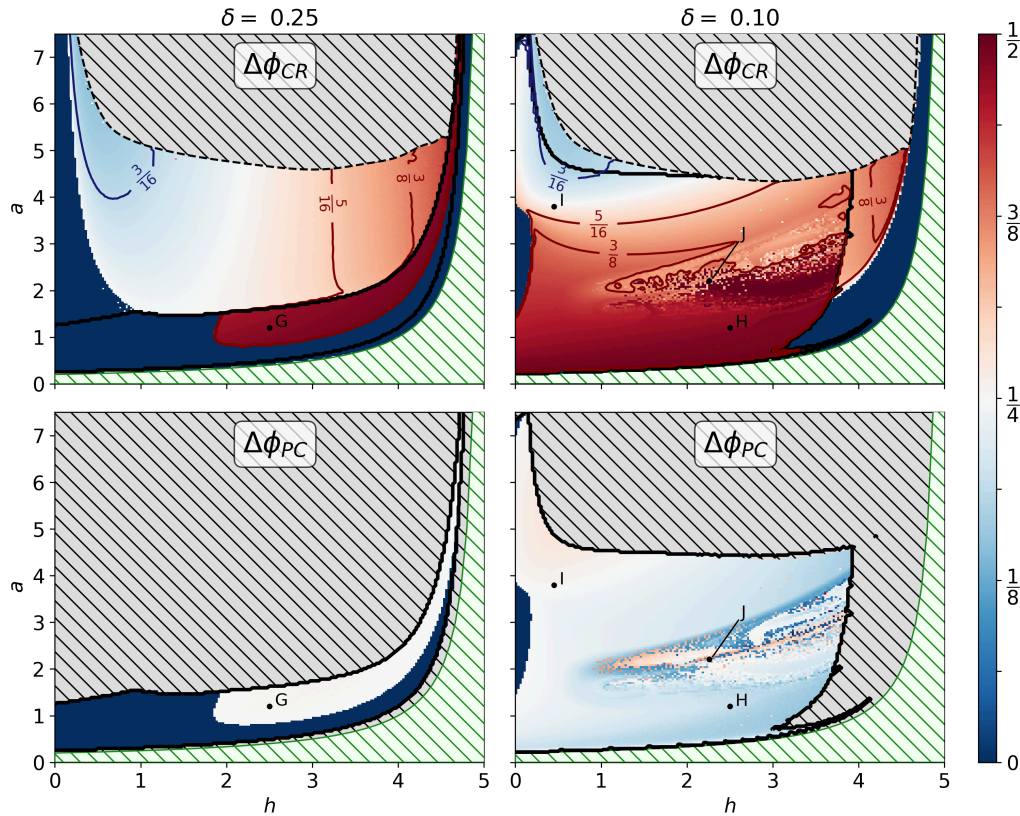By decreasing the predator's loss rate, its influence on the dynamics of the $C - R$

FIGURE 5.3: Phase differences $\Delta\phi_{CR}$ and $\Delta\phi_{PC}$ in the $P-R-C$ system (cf. Eq. (5.2)) as a function of the $C-R$ handling time h and attack rate a, for different values of the predator mortality δ, with $\eta = 2.5, \alpha = 1$ and $d = 0.20$. Red colors denote phase lags larger than a quarter cycle period, while blue colors denote phase lags smaller than a quarter cycle period. The region encompassed by the fat solid black line is the region in which the predator is present in the system. Outside of this region, $\Delta\phi_{CR}$ is necessarily exactly the same as in the right panel of Fig. 5.1). In the top two panels, the grey area indicates where the system exhibits predator-prey cycles that are too extreme, like in Fig. 5.1. Even when the death rate of the predator is high ($\delta = 0.25$, left panels), $\Delta\phi_{CR} \approx 1/2$ (anti-phase cycles) for a substantial region in $h - a$ parameter space. For a lower predator death rate ($\delta = 0.10$, right panels) the dynamics of the $C-R$ system are strongly affected: phase differences substantially larger than a quarter-cycle, and even anti-phase cycles, are common. Example timeseries for the points $G - J$ are shown in Fig. 5.4.

interaction can be increased (Fig. 5.3, right panels). For point H, the predator top-down control is now so high that they quickly graze down C causing long periods of low C and P biomass (Fig. 5.4). Promoting C by decreasing h and increasing a shows that coupled $C-R$ and $P-C$ predator-prey oscillations are possible (Figs. 5.3 and 5.4, point I). In-between, there exists a region where complex chaotic oscillatory patterns are possible (Fig. 5.4, point J, notice the varying height of the predator peaks in particular).
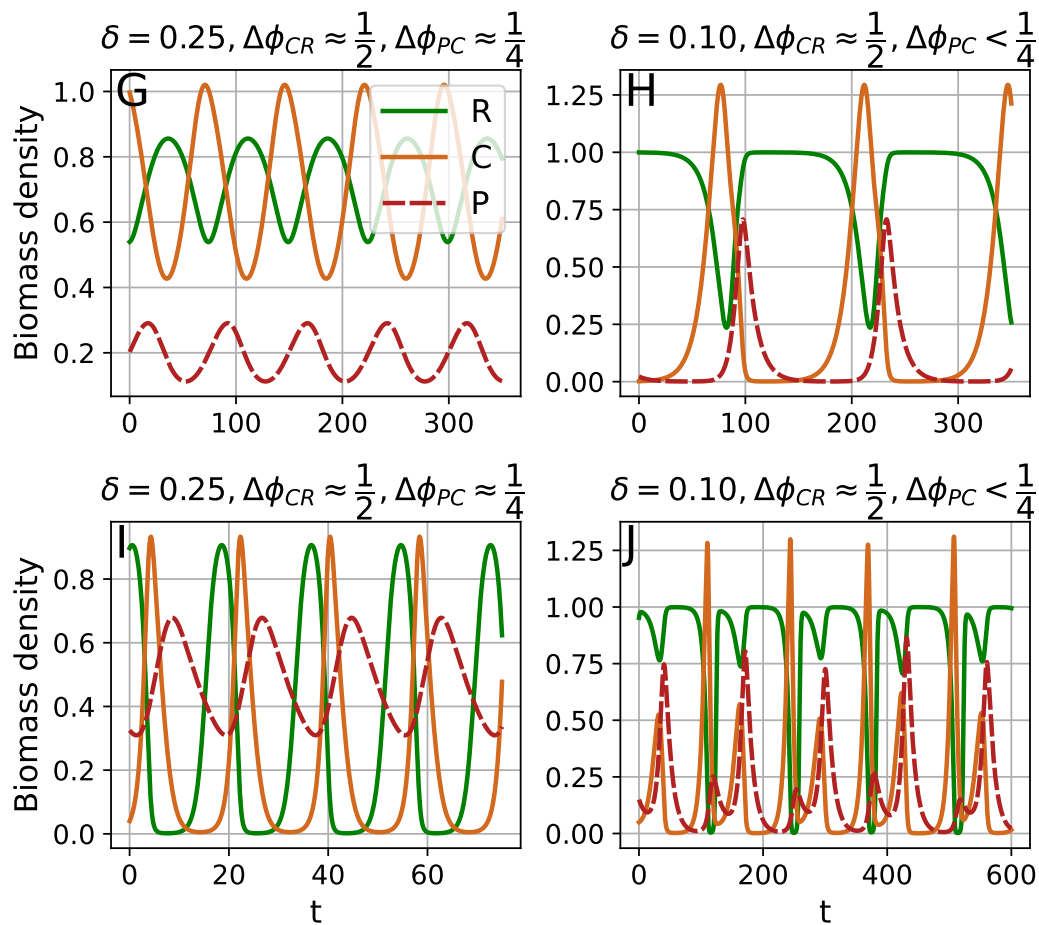
FIGURE 5.4: Example timeseries of the dynamics on the limit cycle for different combinations of $C - R$ attack rate a and handling time h, as indicated in Fig. 5.3, for the $P - C - R$ system defined in Eq. (5.2), with the other parameters set to $d = 0.20$, $\eta = 2.5$, $\alpha = 1$. The resource R is shown in green, the consumer C in orange, and the predator P in red (dashed). The exact (h, a) values are $G : (2.5, 1.2)$ with $\delta = 0.25$, and $H : (2.5, 1.2)$, $I : (0.45, 3.8)$, and $J : (2.26, 2.21)$ with $\delta = 0.10$. Note the different ranges on the axes. For the $P - C - R$ system, $\Delta\phi_{CR}$ may be substantially different from 1/4, even when the timeseries appear quasi-sinusoidal (G, I). The presence of the predator may also lead to more complex dynamical patterns causing a complex dependency of the phase differences on the model parameters $(J$, see Fig. 5.3).

5.4 Discussion

Our results show that phase differences between a consumer and its resource ($\Delta\phi_{CR}$) substantially different from a quarter of a cycle are possible in the simple Rosenzweig-MacArthur consumer-resource ($C - R$) system (Eq. (5.1), Fig. 5.1), and increasingly likely in the modified tritrophic Rosenzweig-MacArthur $P - C - R$ system (Eq. (5.2), Fig. 5.3). In particular, anti-phase cycles between C and R are a common occurrence in the $P - C - R$ model.

In the $C - R$ system, the only interaction is the consumption of R by C, modeled using a Holling-type-II functional response. Ecological intuition would then suggest that the $C - R$ phase difference $\Delta\phi_{CR}$ should be close to $\frac{1}{4}$. However, we find that this relation only holds for a limited region of the parameter space (Fig. 5.1, white

region). If the handling time h is high, the growth rate of C is so low that R is close to its carrying capacity for a long time before being grazed down by C (Fig. 5.2 B, E). On the other hand, if h is low, the growth rate of C is so high that R is almost immediately depleted and requires a long time to recover (Fig. 5.2 C, F). In both cases, the mismatch between h and d creates cycles of asymmetrical shape: the decay time (set by d) is either too short or too long relative to the ascent time, which is determined by h. In the intermediate situation where the ascent and decay times are approximately equal, h and d are well-balanced and the cycles acquire a sinusoidal shape.

It is in this regime that $\Delta\phi_{RC} \approx \frac{1}{4}$, as also argued by Bulmer (1975). Nevertheless, cycle deformation purely caused by mechanisms inherent to the predator-prey interaction leads to phase differences substantially different from a quarter-cycle. While it is impossible for a dynamical system with two state variables to exhibit exact anti-phase cycling as it requires the trajectory to cross itself in state space (Ellner and Becks, 2011), the phase difference can, in principle, become arbitrarily close to $\frac{1}{2}$ in extreme cases where top-down control is very weak (Fig. 5.2E). However, the shape of this cycle differs from what is usually predicted by eco-evolutionary models, such as in Becks et al. (2010) and Cortez and Ellner (2010). In those cases, the cycle deformation is not caused by a mismatch of the consumer maximal growth rate and its death rate, but rather by the extended period of time in which the consumer is simply not able to consume its prey due to a genetic shift in the prey population. When the consumer is eventually able to grow again, it can do so quickly, causing the shape of the consumer cycles to be more symmetric, rather than appearing left-tailed (such as in Fig. 5.2E).

In the $P-C-R$ system, the trajectory would no longer need to cross itself for anti-phase cycling behavior between C and R. Our exploration of the higher dimensional parameter space of this system shows that such behavior does indeed happen. In the situation where the $C-R$ system would relax to a fixed point without P, any biomass changes in C induced by P will simply be tracked by R (Fig. 5.4G and H). In some cases, such as for point G, these anti-phase cycles may be almost perfectly sinusoidal.

Our results imply particular care must be taken when attempting to infer the presence of evolutionary processes from ecological data using only information on the phase relationships between consumers (Cortez and Ellner, 2010; Ellner and Becks, 2011; Hiltunen et al., 2014). Both systems we investigated do not contain any kind of diversity within a trophic level, which means that no evolutionary or any other not strictly ecological interactions are possible. Recent research into how the dynamics of predator-prey interactions is affected by eco-evolutionary effects, have quantitatively shown that anti-phase cycling occurs when the consumer is unable to control the prey population (Van Velzen and Gaedke, 2017). However, as our results demonstrate, they are not the only processes that can do so: anti-phase cycles and in particular deviations from quarter-cycle phase differences can occur just as well in simple purely ecological systems, by the same mechanism.

Acknowledgements

References

Becks, L., Ellner, S. P., Jones, L. E., and Hairston Nelson G., J. G. (2010). "Reduction of adaptive genetic diversity radically alters eco-evolutionary community dynamics". In: *Ecology Letters* 13.8, pp. 989–997. DOI: 10.1111/j.1461-0248.2010.01490.x.

Bulmer, M. G. (1975). "Phase Relations in the Ten-Year Cycle". In: *The Journal of Animal Ecology* 44.2, p. 609. DOI: 10.2307/3614.

Bulmer, M. G. (1976). "The theory of prey-predator oscillations". In: *Theoretical Population Biology* 9.2, pp. 137–150. DOI: 10.1016/0040-5809(76)90041-1.

Cortez, M. H. (2011). "Comparing the qualitatively different effects rapidly evolving and rapidly induced defences have on predator-prey interactions". In: *Ecology Letters* 14.2, pp. 202–209. DOI: 10.1111/j.1461-0248.2010.01572.x.

Cortez, M. H. and Ellner, S. P. (2010). "Understanding rapid evolution in predator-prey interactions using the theory of fast-slow dynamical systems". In: *American Naturalist* 176.5. DOI: 10.1086/656485.

Ellner, S. P. and Becks, L. (2011). "Rapid prey evolution and the dynamics of two-predator food webs". In: *Theoretical Ecology* 4.2, pp. 133–152. DOI: 10.1007/s12080-010-0096-7.

Hiltunen, T., Hairston, N. G., Hooker, G., Jones, L. E., and Ellner, S. P. (2014). "A newly discovered role of evolution in previously published consumer-resource dynamics". In: *Ecology Letters* 17.8, pp. 915–923. DOI: 10.1111/ele.12291.

Hindmarsh, A. C., Brown, P. N., Grant, K. E., Lee, S. L., Serban, R., Shumaker, D. E., and Woodward, C. S. (2005). "Sundials". In: *ACM Transactions on Mathematical Software* 31.3, pp. 363–396. DOI: 10.1145/1089014.1089020.

Hunter, J. D. (2007). "Matplotlib: A 2D graphics environment". In: *Computing in Science and Engineering* 9.3, pp. 99–104. DOI: 10.1109/MCSE.2007.55.

Koch, H., Frickel, J., Valiadi, M., and Becks, L. (2014). "Why rapid, adaptive evolution matters for community dynamics". In: *Frontiers in Ecology and Evolution* 2.MAY, pp. 1–10. DOI: 10.3389/fevo.2014.00017.

Krysiak-Baltyn, K., Martin, G. J., Stickland, A. D., Scales, P. J., and Gras, S. L. (2016). "Computational models of populations of bacteria and lytic phage". In: *Critical Reviews in Microbiology* 42.6, pp. 942–968. DOI: 10.3109/1040841X.2015.1114466.

Lundberg, S., Järemo, J., Nilsson, P., and Jaremo, J. (1994). "Herbivory, Inducible Defence and Population Oscillations: A Preliminary Theoretical Analysis". In: *Oikos* 71.3, p. 537. DOI: 10.2307/3545843.

Maclulich, D. A. (1937). *Fluctuations in the Numbers of the Varying Hare (Lepus Americanus)*. University of Toronto Press.

Magnus, O. (1555). *Historia de Gentibus Septentrionalibus*. Rome.

Nedorezov, L. V. (2016). "The dynamics of the lynx–hare system: an application of the Lotka–Volterra model". In: *Biophysics (Russian Federation)* 61.1, pp. 149–154. DOI: 10.1134/S000635091601019X.

Rosenzweig, M. L. and MacArthur, R. H. (1963). "Graphical Representation and Stability Conditions of Predator-Prey Interactions". In: *The American Naturalist* 97.895, pp. 209–223. DOI: 10.1086/282272.

Van Der Walt, S., Colbert, S. C., and Varoquaux, G. (2011). "The NumPy array: A structure for efficient numerical computation". In: *Computing in Science and Engineering* 13.2, pp. 22–30. DOI: 10.1109/MCSE.2011.37.

Van Velzen, E. and Gaedke, U. (2017). "Disentangling eco-evolutionary dynamics of predator-prey co-evolution: The case of antiphase cycles". In: *Scientific Reports* 7.1, p. 17125. DOI: 10.1038/s41598-017-17019-4.

Virtanen, P. et al. (2020). "SciPy 1.0: fundamental algorithms for scientific computing in Python". In: *Nature Methods* 17.3, pp. 261–272. DOI: 10.1038/s41592-019-0686-2.

Chapter 6

Discussion

The previous four chapters each presented a research project on examining the mechanisms behind the functioning of tritrophic food webs from a different angle, and with the exception of Chapter 5, exposed how these mechanisms are affected by functional diversity. The projects presented in Chapters 3, 4, and 5 each attempt to build further from the knowledge obtained in Chapter 2 in a different direction. In this chapter, their findings will be compared to build a more complete picture of the link between diversity and functioning in a tritrophic context.

6.1 Overcoming context-dependency in complex models

In Chapter 2, we built a tritrophic food web in which coexistence was ensured by the introduction of two trade-offs, each governing two functional traits. As outlined in Section 1.3, the food web contains two species per applicable trade-off on each trophic level. Prey species can be either defended or undefended against predation, where defense comes at the cost of a lower maximal growth rate; and consumer species can be either selective or non-selective, such that selective species have a narrower prey spectrum, but can exploit low prey densities more efficiently (such that the food web contains eight species, cf. Fig. 2.1, Chapter 2). The trait difference Δ between each pair of trait values can be controlled as an input parameter to the model. Our results show that when Δ is high, biomass is transferred efficiently throughout the food web, leading to a high biomass on the top trophic level (Figure 2.2). We also show how the CV decreases, and later increases again with Δ, which we were able to attribute to the increased relevance of additional trait-related dynamics creating highly complex oscillations (Figs. 2.6e and f, Chapter 2).

An important property of the model used in Chapter 2 is that all trait differences are controlled simultaneously by Δ: when $\Delta = 1$, the functional diversity is high on every trophic level. To further understand the effects of the interplay between diversity on different trophic levels, the model was adapted such that the diversity on each trophic level can be set independently of that in the rest of the food web (cf. 3.1, Chapter 3). Theoretical and experimental work on the combined interaction of consumer and prey diversity on food web functioning have uncovered the key role

played by consumer diversity on food web functioning (Filip et al., 2014; Wohlge-muth et al., 2017). Extending this approach to include a third adaptive trophic level is a reasonable step towards understanding the functioning of complex natural food webs. However, each of the aforementioned studies have stressed the complex nature and context-dependency of the combined effects of diversity on two trophic levels, and the difficulty in meaningful comparison and synthesis of the results of distinct studies.

We therefore set out to test the model in Chapter 3 as context-free as possible. To achieve this, we calculated aggregate quantities, such as the population and trophic level biomasses and CVs, for a large amount of randomly selected parameter combinations (cf. 3.1, Chapter 3). This large collection of data was analyzed using a Random Forest machine learning model. We were able to identify the same overarching patterns that followed from detailed analysis of the dynamics of the model in Chapter 2. When diversity is high on every trophic level, biomass gets transferred to the top trophic level most efficiently (cf. Table 3.2 and Figs. 3.3 and 3.5). Likewise, the temporal variability of the trophic level biomass exhibits a similar dependency on functional diversity: as the functional diversity increases, the availability of temporal niches for functionally different species causes the CV to decrease through compensatory dynamical behavior. However, for highly diverse systems, an increase in CV is observed, which may be attributed to the increased relevance of additional trait-related dynamics creating highly complex oscillations (compare Figs. 2.6e and f, Chapter 2, to Fig. 3.4, Chapter 3).

Comparison of the results of Chapters 2 and 3 highlights the complementarity of the two distinct approaches. On the one hand, conclusions drawn from detailed inspection of the dynamical possibilities of the food web in Chapter 2 may be anecdotal. In order to confidently generalize these conclusions, it has to be shown that they also hold in food webs with a different parametrization. On the other hand, the large number of parameters that have to be varied creates practical difficulties in efficiently visualizing and analyzing the huge amount of data produced in Chapter 3. Some kind of representative aggregate quantity has to be selected from which conclusions can be drawn out of the data set. Such quantities can only be meaningfully understood using the detailed knowledge gained from the analysis in Chapter 2.

6.2 The different aspects of stability in complex tritrophic systems

Due to its complex structure, solutions to the model developed in Chapter 2 exhibit some very interesting properties. Notably, we find the existence of two different stable states. The easiest way to distinguish them is by comparing biomass of the top trophic level and the free nutrient concentration (Figs. 2.3 and 2.4, Chapter 2): on the low-production (HP) state, the nutrients are unexploited for extended periods of time and the top biomass is low, whereas on the high-production (HP) state, the

nutrients are efficiently exploited and the top biomass is much higher. These two states retain these properties over a large range of parameter space, and may coexist together as alternative stable states (Fig. 2.5, Chapter 2, see also Appendix A.1, Appendix A).

A key result from Chapter 2 is that the resilience of the *HP* state increases with functional diversity. This result was obtained by calculating the relative frequency of a random initial condition reaching this state (Fig. 2.5, Chapter 2). This measure was used as an estimate of the basin of attraction of the *HP* state: if the frequency was very small, only for a very small region of state space do trajectories end up on this state, and vice-versa. In Chapter 4, we set out to reveal the mechanism behind this result by detailed examination of the response of the food web in Chapter 2 to a nutrient pulse perturbation.

To fully grasp the impact of a perturbation on food web dynamics and functioning, it is essential to look at more than one aspect of food web stability (Kéfi et al., 2019). Following Raatz, Velzen, and Gaedke (2019), we investigated the food web's response by measuring the resistance, resilience and elasticity, as defined by (Grimm and Wissel, 1997). These three quantities provide complementary information on the short (resistance, elasticity) and long term (resilience) response, and may be influenced by both local (e.g. attractor shape) and global (presence of alternative stable states) properties of the food web. For example, our results show that perturbing the food web when it is on the *HP* likely induces a transition to the *LP* state, because of the synchronous dynamics that occur in the post-perturbation transient, which are characteristic of the *LP* state (cf. Figs. 4.6h and i, Chapter 4, and C.1 and C.4, Appendix C). This explains the asymmetry between the maximum perturbation sizes for which the system returns to the pre-perturbation state for the *LP* and *HP* state (Fig. 4.8).

Remarkably, the post-perturbation transient from a point on the *HP* state may behave like the *LP* state for an extended period of time, even for regions in the parameter space for which the *LP* state is not stable. It appears that the transient relaxes to the "ghost" of the *LP* attractor, but eventually it must return to the stable *HP* state. We observed similar behavior near the *HP* attractor crisis in Chapter 2 (see Fig. A.12, Appendix A), however, in this case, the dynamics mimicked the behavior of the *HP* attractor for a long time period before relaxing to the *LP* state. Fully understanding the ecological meaning and implications of the presence of ghost attractors is a relatively new but highly fascinating field of research (Hastings et al., 2018; Morozov et al., 2020; Drake et al., 2020). The increased frequency of observation of these phenomena is cause for concern, because accurately distinguishing a ghost transient from actual stable oscillatory behavior may require an observation time which is significantly longer than ecological or practically feasible timescales. They thus create an interesting challenge for our current understanding of predicting tipping points and catastrophic regime shifts using early warning signals (Scheffer and Carpenter, 2003; Scheffer et al., 2009; Dakos et al., 2019). Especially if the dynamics

are chaotic, it may not only be impossible to predict whether a transition is near, but the presence of a ghost attractor after the transition may even make detecting that the transition has happened hopeless.

These results in Chapters 2 and 4 highlight the importance of explicitly considering the complete phase space of a system to fully understand its dynamics. In Chapter 3, we also accommodated for the potential impact of alternative stable states when investigating the parameter-independent behavior of tritrophic food webs. For each of the $128,000$ parameter conditions, we actually calculated the average biomasses and CVs for 200 randomly sampled parameter conditions, so as to make our estimation of these quantities for a certain parameter combination also independent on the initial conditions.

6.3   Anti-phase cycles caused by lack of top-down control

Chapters 2 and 5 show how detailed analysis of the phase relationships of all consumer-resource pairs in a food web provides a comprehensive picture of its trophic interactions (cf. Fig. 2.2-2.4, Chapter 2 and Fig. 5.1, 5.3, Chapter 5). The starting point from which this analysis is performed is the property that the phase difference between the biomass dynamics of a predator and its prey is one quarter of a cycle. As discussed in detail in Chapter 5, this property has been observed in a wide variety of predator-prey pairs, and theoretical legitimation is often attributed to Bulmer, who proves that this property holds when the cycles are sinusoidal in shape (Bulmer, 1975).

In Chapter 2, estimation of the phase relationships between all predator-prey pairs in a complex functionally diverse tritrophic community suggests that this "rule" is not as general as is presumed: deviations from quarter-cycle phase differences are observed, even in a simple tritrophic food chain. Specifically, our results uncover how phase differences significantly larger than a quarter of a cycle, up to half a cycle (anti-phase cycles) can occur in tritrophic systems: when the top-down control of the top trophic level is sufficiently high, the intermediate trophic level is unable to exert sufficient grazing pressure on the basal trophic level to create predator-prey-like cycles. By systematic exploration of the parameter space of a simple tritrophic extension of the Rosenzweig-MacArthur consumer-resource model (Rosenzweig and MacArthur, 1963), this suggested mechanism behind the observation of anti-phase cycles in Chapter 2 is confirmed. Moreover, even in the standard bitrophic Rosenzweig-MacArthur consumer-resource system, we show that significant deviations from quarter-cycle phase relationships can occur. This happens when the cycles becomes deformed due to a mismatch between the predator's growth and loss rates. In particular, when the loss rate is too high, the prey species are able to escape control by their predator and the phase difference becomes substantially larger than a quarter of a cycle. Thus, also in this most simple system, lack of sufficient top-down control causes anti-phase-like cycling behavior.

It is important to emphasize that our observation of predator-prey phase cycles showing clear deviations from a quarter-cycle phase difference in a simple consumer-resource system is not directly in contradiction with recent literature on the attribution of such deviations to the influence of evolutionary processes on ecological dynamics. For example, Becks et al. (2010) observe that in the presence of multiple prey genotypes which differ in their defense against predation, predator-prey dynamics often exhibit anti-phase cycles. When predator density is high, defended genotypes will be selected for, causing the predator density to remain low for an extended period of time. Eventually, the undefended genotypes will become dominant again and the predator population can recover. Observation of this type of eco-evolutionary feedback has become so common that deviations from quarter-cycle predator-prey phase relationships are considered a strong indicator hereof (Hiltunen et al., 2014). Clearly, it is again the lack of top-down control on the prey community that lies at the basis of the observed anti-phase cycling pattern (Van Velzen and Gaedke, 2017), which, as demonstrated by the models uses in Chapter 2 and 5, can also happen in the absence of diversity within trophic levels. It is thus possible that the presence of evolutionary processes is falsely inferred, when simply relying on the observation of (quasi-)anti-phase cycling, especially in complex natural food webs with more than two trophic levels. When it is sure that a community contains only two trophic levels, such as in controlled microcosm experiments, our results suggest that the shape of the cycles (in particular, whether they are symmetric or not) may be conclusive to infer functional diversity in the prey community (cf. Chapter 5, Discussion).

6.4 Regulating effects of the top trophic level

One common theme that links all four chapters together is the decisive role played by the top trophic level on the dynamics and functioning of food webs.

In Chapter 2, we show how functional trait differences in the predator community cascade downwards throughout the functionally diverse food web, creating trait-separated compensatory dynamical patterns on every trophic level. This causes a more efficient exploitation of nutrients by the basal community. The same pattern is shown to hold in general for a broad range of differently parametrized tritrophic food webs in Chapter 3. Moreover, by independently varying the functional diversity on every trophic level, we show that the functional diversity on the top trophic level is of high importance for determining the biomass, biomass variability, and biomass production efficiency of every trophic level. In Chapter 4, we show that the top trophic level plays an important role in preventing extinctions on the basal trophic level after a nutrient pulse perturbation: when the top level biomass is high, high predation pressure on the intermediate level renders the intermediate species unable to fully exploit the basal growth peak following the nutrient pulse. Finally, in Chapter 5, the presence of a top predator, even with low biomass, affects the

consumer-resource phase relationships in a considerable region of the parameter space.

The central motif behind each of these observations is that the top trophic level is able to exert considerable influence on the whole food web, through direct and indirect effects. This is in line with a large body of experimental and theoretical evidence of the key role that top predators often have in ecosystems (Bruno and O'Connor, 2005; Estes et al., 2011; Schneider et al., 2016; Donohue et al., 2017; Brose et al., 2019; Ehrlich and Gaedke, 2020). Simultaneous consideration of all four chapters in this dissertation reveals the explicit mechanisms through which changes to the biomass and functional diversity of the top trophic level affect the food web as a whole, in a two step process. Firstly, we show the general relevance of the traditional top-down trophic cascade. Increased top-down control on the intermediate level, facilitated by a high top level biomass, decreases the intermediate level's ability to control the basal level, in turn leading to increased nutrient exploitation efficiency. Secondly, we find that the increased productivity of the basal level may then feed back to increase the biomass of the top trophic level further. However, this process only works well if the functional diversity on every trophic level is high. High basal diversity causes efficient exploitation of the nutrients by compensatory dynamical patterns; high intermediate diversity ensures the basal level cannot escape efficient consumption by adjusting its trait composition; and similarly, high top diversity ensures that the intermediate biomass production is transferred upwards efficiently.

Importantly, when functional diversity is altered, these changes to the biomasses of each trophic level may not depend on the functional diversity in a continuous, gradual way. When diversity is high, the high-top-biomass state is dominant. A reduction in functional diversity can then induce a sudden and irreversible change to ecosystem functioning when the system transitions to the low-top-biomass state.

6.5 Future perspectives

Experimental demonstration

The food web models described in Chapters 2-4 have been created to fit the structure of planktonic food webs. This means that the mechanisms revealed by the model may potentially be tested using microcosm experiments. This approach has proven fruitful to demonstrate the validity of model predictions and discover novel effects in planktonic systems with one or two adaptive trophic levels (e.g., Boraas, 1983; Becks et al., 2005; Blasius et al., 2020; Flöder, Bromann, and Moorthi, 2018), thanks to their many practical advantages such as a short generation time, simple life structure, and potentially highly complex food web structure. However, the increased trophic complexity of our tritrophic models may present problems to find suitable candidates that fit the model structure and can be tested in microcosms. Very recently, Rakowski et al. (2020) have been able to study the effects of top predator

diversity on a food web with three adaptive trophic levels, by combining microcosm and mesocosm experiments, and report effects that are in line with the mathematical predictions presented here.

Multiple perturbation types

In Chapter 4, we present a mechanistic analysis of the response of an adaptive tritrophic food to a nutrient pulse perturbation. This type of perturbation constitutes an instantaneous change to one of the state variables (such as the free nutrient concentration N), after which different aspects of the transient dynamics back to the original attractor (or to another attractor if there are alternative stable states) are studied, quantifying the systems resistance, resilience, and elasticity. However, to get a complete picture of the different mechanisms that may be responsible for governing the response of complex food webs to perturbations, more than one type of perturbation should be applied to the same system (Kéfi et al., 2019). For example, by performing press perturbations on our models, the effect of warming due to climate change on adaptive tritrophic food webs could be investigated. In contrast to pulse perturbations, press perturbations permanently affect model parameters (for example, the Hill exponent of the functional response). The system is then forced to relax an attractor in a different location, corresponding to the new value of the perturbed parameters.

Model extensions

Care was taken to make the models used in Chapters 2-4 as realistic as possible. Compared to bitrophic systems, the incorporation of an adaptive third trophic level makes the observed phenomena and their underlying mechanisms arguably more relevant for natural food webs (Matsuno and Nobuaki, 1996; Abdala-Roberts et al., 2019). Nonetheless, our models still represent a highly simplified picture of the complexity of nature. Communities with four—sometimes five—trophic levels exist in nature (Fry, 1988; Williams and Martinez, 2004), and the number of trophic levels, and how they interact with each other, may have a decisive influence on trophic cascades (Wollrab, Diehl, and De Roos, 2012). Therefore, adding a fourth adaptive trophic level in our models would be a relevant possible extension, which could lead to further generalisation of our results, but would make empirical verification even more difficult.

One common interaction thus far ignored in our models is omnivory or intraguild predation. Such interactions are also common in natural food webs (Polis, Myers, and Holt, 1989), and known to alter many important ecological properties, such as biomass distributions (Wang and Brose, 2018), trophic cascades (Thompson et al., 2007), and species persistence (Křivan and Diehl, 2005). Investigation of the influence of these interactions on the phenomena discussed in this text (such as trophic

level biomasses and phase relationships between predator-prey pairs) would therefore be a highly relevant extension.

References

Abdala-Roberts, L. et al. (2019). "Tri-trophic interactions: bridging species, communities and ecosystems". In: *Ecology Letters*. DOI: 10.1111/ele.13392.

Becks, L., Ellner, S. P., Jones, L. E., and Hairston Nelson G., J. G. (2010). "Reduction of adaptive genetic diversity radically alters eco-evolutionary community dynamics". In: *Ecology Letters* 13.8, pp. 989–997. DOI: 10.1111/j.1461-0248.2010.01490.x.

Becks, L., Hilker, F. M., Malchow, H., Jürgens, K., and Arndt, H. (2005). "Experimental demonstration of chaos in a microbial food web". In: *Nature* 435.7046, pp. 1226–1229. DOI: 10.1038/nature03627.

Blasius, B., Rudolf, L., Weithoff, G., Gaedke, U., and Fussmann, G. F. (2020). "Long-term cyclic persistence in an experimental predator–prey system". In: *Nature* 577.7789, pp. 226–230. DOI: 10.1038/s41586-019-1857-0.

Boraas, M. E. (1983). "Population dynamics of food-limited rotifers in two-stage chemostat culture". In: *Limnology and Oceanography* 28.3, pp. 546–563. DOI: 10.4319/lo.1983.28.3.0546.

Brose, U. et al. (2019). "Predator traits determine food-web architecture across ecosystems". In: *Nature Ecology and Evolution* 3.6, pp. 919–927. DOI: 10.1038/s41559-019-0899-x.

Bruno, J. F. and O'Connor, M. I. (2005). "Cascading effects of predator diversity and omnivory in a marine food web". In: *Ecology Letters* 8.10, pp. 1048–1056. DOI: 10.1111/j.1461-0248.2005.00808.x.

Bulmer, M. G. (1975). "Phase Relations in the Ten-Year Cycle". In: *The Journal of Animal Ecology* 44.2, p. 609. DOI: 10.2307/3614.

Dakos, V., Matthews, B., Hendry, A. P., Levine, J., Loeuille, N., Norberg, J., Nosil, P., Scheffer, M., and De Meester, L. (2019). "Ecosystem tipping points in an evolving world". In: *Nature Ecology and Evolution* 3.3, pp. 355–362. DOI: 10.1038/s41559-019-0797-2.

Donohue, I., Petchey, O. L., Kéfi, S., Génin, A., Jackson, A. L., Yang, Q., and O'Connor, N. E. (2017). "Loss of predator species, not intermediate consumers, triggers rapid and dramatic extinction cascades". In: *Global Change Biology* 23.8, pp. 2962–2972. DOI: 10.1111/gcb.13703.

Drake, J. M., O'Regan, S. M., Dakos, V., Kéfi, S., and Rohani, P. (2020). "Alternative stable states, tipping points, and early warning signals of ecological transitions". In: *Theoretical Ecology: Concepts and Applications*. Ed. by K. S. McCann and G. Gellner. Oxford University Press. DOI: 10.1093/oso/9780198824282.003.0015.

Ehrlich, E. and Gaedke, U. (2020). "Coupled changes in traits and biomasses cascading through a tritrophic plankton food web". In: *Limnology and Oceanography*, lno.11466. DOI: 10.1002/lno.11466.

Estes, J. A. et al. (2011). "Trophic downgrading of planet earth". In: *Science* 333.6040, pp. 301–306. DOI: 10.1126/science.1205106.

Filip, J., Bauer, B., Hillebrand, H., Beniermann, A., Gaedke, U., and Moorthi, S. D. (2014). "Multitrophic diversity effects depend on consumer specialization and species-specific growth and grazing rates". In: *Oikos* 123.8, pp. 912–922. DOI: 10.1111/oik.01219.

Flöder, S., Bromann, L., and Moorthi, S. (2018). "Inter- and intraspecific consumer trait variations determine consumer diversity effects in multispecies predator-prey systems". In: *Aquatic Microbial Ecology* 81.3, pp. 243–256. DOI: 10.3354/ame01866.

Fry, B. (1988). "Food web structure on Georges Bank from stable C, N, and S isotopic compositions". In: *Limnology and Oceanography* 33.5, pp. 1182–1190. DOI: 10.4319/lo.1988.33.5.1182.

Grimm, V. and Wissel, C. (1997). "Babel, or the ecological stability discussions: An inventory and analysis of terminology and a guide for avoiding confusion". In: *Oecologia* 109.3, pp. 323–334. DOI: 10.1007/s004420050090.

Hastings, A., Abbott, K. C., Cuddington, K., Francis, T., Gellner, G., Lai, Y. C., Morozov, A., Petrovskii, S., Scranton, K., and Zeeman, M. L. (2018). "Transient phenomena in ecology". In: *Science* 361.6406. DOI: 10.1126/science.aat6412.

Hiltunen, T., Hairston, N. G., Hooker, G., Jones, L. E., and Ellner, S. P. (2014). "A newly discovered role of evolution in previously published consumer-resource dynamics". In: *Ecology Letters* 17.8, pp. 915–923. DOI: 10.1111/ele.12291.

Kéfi, S., Domínguez-García, V., Donohue, I., Fontaine, C., Thébault, E., and Dakos, V. (2019). "Advancing our understanding of ecological stability". In: *Ecology Letters* 22.9, pp. 1349–1356. DOI: 10.1111/ele.13340.

Křivan, V. and Diehl, S. (2005). "Adaptive omnivory and species coexistence in tri-trophic food webs". In: *Theoretical Population Biology* 67.2, pp. 85–99. DOI: 10.1016/j.tpb.2004.09.003.

Matsuno, K. and Nobuaki, O. (1996). "How many trophic levels are there?" In: *Journal of Theoretical Biology* 180.2, pp. 105–109. DOI: 10.1006/jtbi.1996.0085.

Morozov, A., Abbott, K., Cuddington, K., Francis, T., Gellner, G., Hastings, A., Lai, Y. C., Petrovskii, S., Scranton, K., and Zeeman, M. L. (2020). "Long transients in ecology: Theory and applications". In: *Physics of Life Reviews* 32, pp. 1–40. DOI: 10.1016/j.plrev.2019.09.004.

Polis, G. A., Myers, C. A., and Holt, R. D. (1989). "The ecology and evolution of intraguild predation: potential competitors that eat each other". In: *Annual review of ecology and systematics. Vol. 20* 20, pp. 297–330. DOI: 10.1146/annurev.es.20.110189.001501.

Raatz, M., Velzen, E. van, and Gaedke, U. (2019). "Co-adaptation impacts the robustness of predator–prey dynamics against perturbations". In: *Ecology and Evolution* 9.7, pp. 3823–3836. DOI: 10.1002/ece3.5006.

Rakowski, C. J., Farrior, C. E., Manning, S. R., and Leibold, M. A. (2020). "Predator complementarity dampens variability of phytoplankton biomass in a diversity-stability trophic cascade". In: *bioRxiv*, p. 851642. DOI: 10.1101/851642.

Rosenzweig, M. L. and MacArthur, R. H. (1963). "Graphical Representation and Stability Conditions of Predator-Prey Interactions". In: *The American Naturalist* 97.895, pp. 209–223. DOI: 10.1086/282272.

Scheffer, M., Bascompte, J., Brock, W. A., Brovkin, V., Carpenter, S. R., Dakos, V., Held, H., Van Nes, E. H., Rietkerk, M., and Sugihara, G. (2009). "Early-warning signals for critical transitions". In: *Nature* 461.7260, pp. 53–59. DOI: 10.1038/nature08227.

Scheffer, M. and Carpenter, S. R. (2003). "Catastrophic regime shifts in ecosystems: Linking theory to observation". In: *Trends in Ecology and Evolution* 18.12, pp. 648–656. DOI: 10.1016/j.tree.2003.09.002.

Schneider, F. D., Brose, U., Rall, B. C., and Guill, C. (Dec. 2016). "Animal diversity and ecosystem functioning in dynamic food webs". In: *Nature Communications* 7, p. 12718. DOI: 10.1038/ncomms12718.

Thompson, R. M., Hemberg, M., Starzomski, B. M., and Shurin, J. B. (2007). "Trophic levels and trophic tangles: The prevalence of omnivory in real food webs". In: *Ecology* 88.3, pp. 612–617. DOI: 10.1890/05-1454.

Van Velzen, E. and Gaedke, U. (2017). "Disentangling eco-evolutionary dynamics of predator-prey coevolution: The case of antiphase cycles". In: *Scientific Reports* 7.1, p. 17125. DOI: 10.1038/s41598-017-17019-4.

Wang, S. and Brose, U. (2018). "Biodiversity and ecosystem functioning in food webs: the vertical diversity hypothesis". In: *Ecology Letters* 21.1, pp. 9–20. DOI: 10.1111/ele.12865.

Williams, R. J. and Martinez, N. D. (2004). "Limits to trophic levels and omnivory in complex food webs: Theory and data". In: *American Naturalist* 163.3, pp. 458–468. DOI: 10.1086/381964.

Wohlgemuth, D., Filip, J., Hillebrand, H., and Moorthi, S. D. (2017). "Prey diversity effects on ecosystem functioning depend on consumer identity and prey composition". In: *Oecologia* 184.3, pp. 653–661. DOI: 10.1007/s00442-017-3892-6.

Wollrab, S., Diehl, S., and De Roos, A. M. (2012). "Simple rules describe bottom-up and top-down control in food webs with alternative energy pathways". In: *Ecology Letters* 15.9, pp. 935–946. DOI: 10.1111/j.1461-0248.2012.01823.x.

Appendix A

Supplementary information to Chapter 2

A.1 Exploration of parameter space and food web structure

The model described in the main text contains many parameters of different types. The effect of parameters which control the environmental conditions, such as the inflow nutrient concentration N_0 and the dilution rate δ will be studied in section A.1.1.

Other parameters relating to the species properties also influence the structure of the food web. In particular, the mass ratio $\frac{m_I}{m_B} = \frac{m_T}{m_I}$ and the allometric scaling exponent λ influence the species' maximum growth rate and thus the intensity of trophic interactions. In the main text, the mass ratio between the species of adjacent trophic levels was set to 1000, with $\lambda = -0.15$ in order to represent aquatic communities. In this case, going up in trophic level rescales the maximal growth rate by a factor of $1000^{-0.15} \approx 0.35$. It should be noted that in terrestrial communities, where mass ratios of 100 and scaling exponents of $\lambda = -0.25$ might be more representative (Brose et al., 2006), the species' maximal growth rate is scaled with a factor that is almost equal to the one for aquatic systems: $100^{-0.25} \approx 0.32$. However, in order to verify our results for different food web structures, we have looked at variations of these mass ratios while keeping the scaling exponent fixed at $\lambda = -0.15$, such that the maximal grazing rates are altered significantly (section A.1.2). In addition, we have also investigated what happens when we also scale the dilution rate δ allometrically, transforming it to a more traditional death rate, such that higher trophic levels experience a lower death rate.
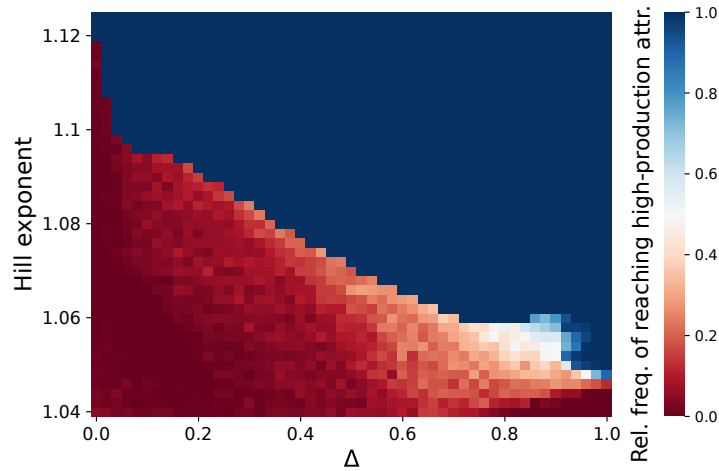
A.1.1 Varying environment parameters

FIGURE A.1: Equivalent of Fig. 2.5 (main text), when the interaction strength between the defended prey species and the selective consumer species is set to 10^{-6} instead of 10^{-4}. Comparison between these two figures shows no significant differences, emphasizing that the value of 10^{-4} as used in the main text is sufficiently low, and lowering it further does not alter our results.
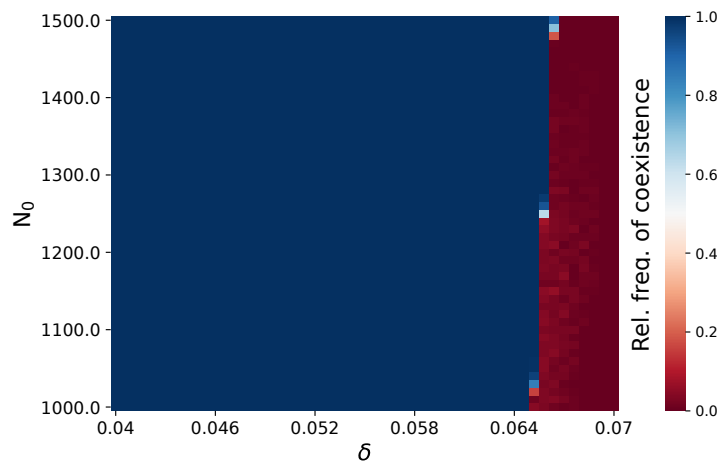

FIGURE A.2: Relative frequency of initial conditions leading to a state for which all species coexist for $\Delta = 1$ (maximal trait variation). For each combination of the inflow concentration N_0 and the dilution rate δ, 200 randomly sampled initial conditions were tested. As long as the dilution rate is small enough such that the slowest growing top species T_n can remain in the system, coexistence is very probable in our model, independent of these external environmental factors.
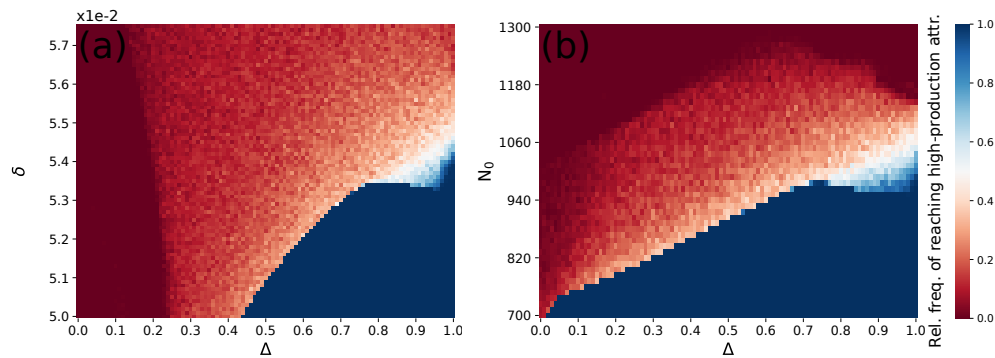
FIGURE A.3: (a) Relative frequencies of reaching the high-production attractor, as a function of the trait difference Δ and the dilution rate δ, for $h = 1.05$. Each of the points in the 101×76 grid shows the relative frequency of reaching the high-production attractor, sampling 200 random initial conditions. The patterns described in the main text are also present as δ is varied. The basin of attraction generally increases in size as the trait difference increases, meaning the high-production state is more resilient against pulse perturbations. In addition, the high-production attractor's boundary crisis is present over the whole range of δ when trait differences are low, hence, higher trait differences also protect the high-production state against press perturbations. However, as δ increases the high-production attractor becomes less resilient, possibly due to the high sensitivity of the top species to the dilution rate, as they have the lowest growth rates. (b) Relative frequencies of reaching the high-production attractor as a function of the trait difference Δ and the nutrient inflow concentration N_0, for $h = 1.05$. Each of the points in the 101×51 grid shows the relative frequency of reaching the high-production attractor. The basin of attraction generally increases in size as the trait difference increases, meaning the high-production state is more resilient against pulse perturbations. However, for increasing nutrient inflow concentration, there is a clear trend towards the more variable low-production state, and eventually the high-production state disappears through a boundary crisis as N_0 is increased further. This result is in accordance with the paradox of enrichment, a commonly observed effect where a consumer-resource system is destabilized when food becomes more available.
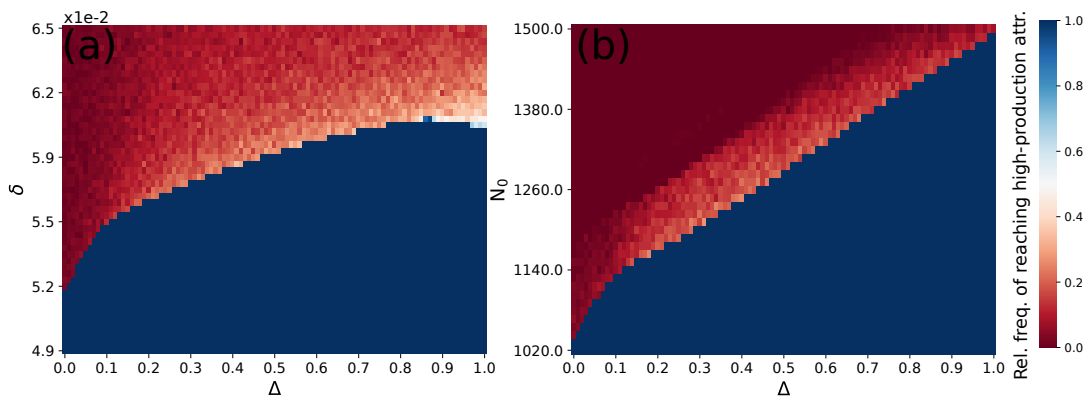

FIGURE A.4: (a), (b) Relative frequencies of reaching the high-production attractor, as a function of the trait difference Δ and the dilution rate δ and the nutrient inflow concentration N_0, respectively, for $h = 1.1$. Each of the points shows the relative frequency of reaching the high-production attractor, sampling 200 random initial conditions. The patterns described in the main text, as well as in Fig. A.3 are also present. Increasing δ further leads to extinction of one of the top species.

A.1.2 Varying the body mass ratio between trophic levels

Using the standard parameter values defined in Table 2.1 (main text), but with a mass ratio of 500 instead of 1000, also shows a similar trend as found in Fig. 2.5 (main text), underlining the robustness of our results (Fig. A.5).
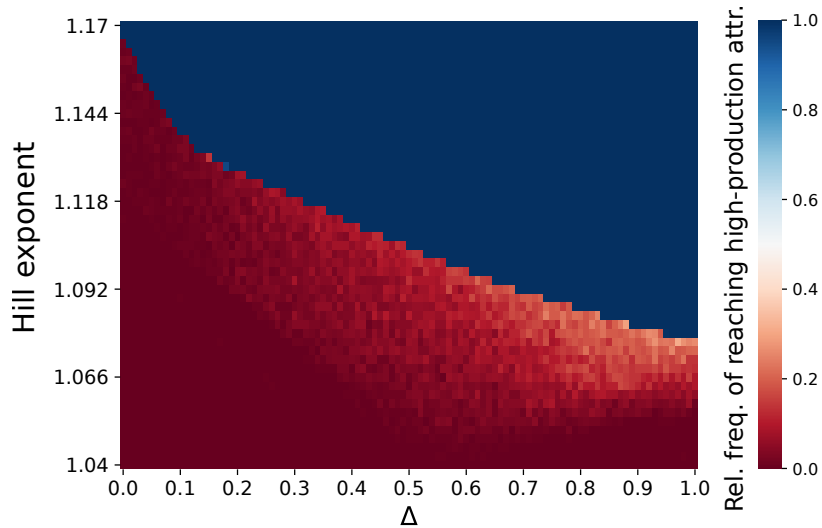

FIGURE A.5: Relative frequencies of reaching the high-production attractor, as a function of the trait difference Δ and the Hill exponents $h = \eta$, for a body mass ratio of 500 instead of 1000 between all trophic levels. Each of the points shows the relative frequency of reaching the high-production attractor, sampling 200 random initial conditions. The patterns described in the main text (Fig. 2.5) are again present. To compensate for the higher growth rate of the top species when the body mass ratio is lowered, the dilution rate δ has been slightly increased to 0.065 instead of 0.055. All other parameters are the standard ones given in Table 2.1.

However, lowering the body mass ratio between adjacent trophic levels further down to 100, we find that only one attractor exists over the whole range of Δ (Figs. A.6a & A.6b). Interestingly, this single attractor changes continuously from appearing like the low-production attractor when Δ is low (Fig. A.6a), to resembling the high-production attractor when Δ is high (Fig. A.6b). This means that, as trait variation increases, the mean free nutrient level decreases, the mean biomass at the top level increases, and the temporal variability decreases. Hence, in the case where there is only one attractor, the relevant conclusion are still supported.
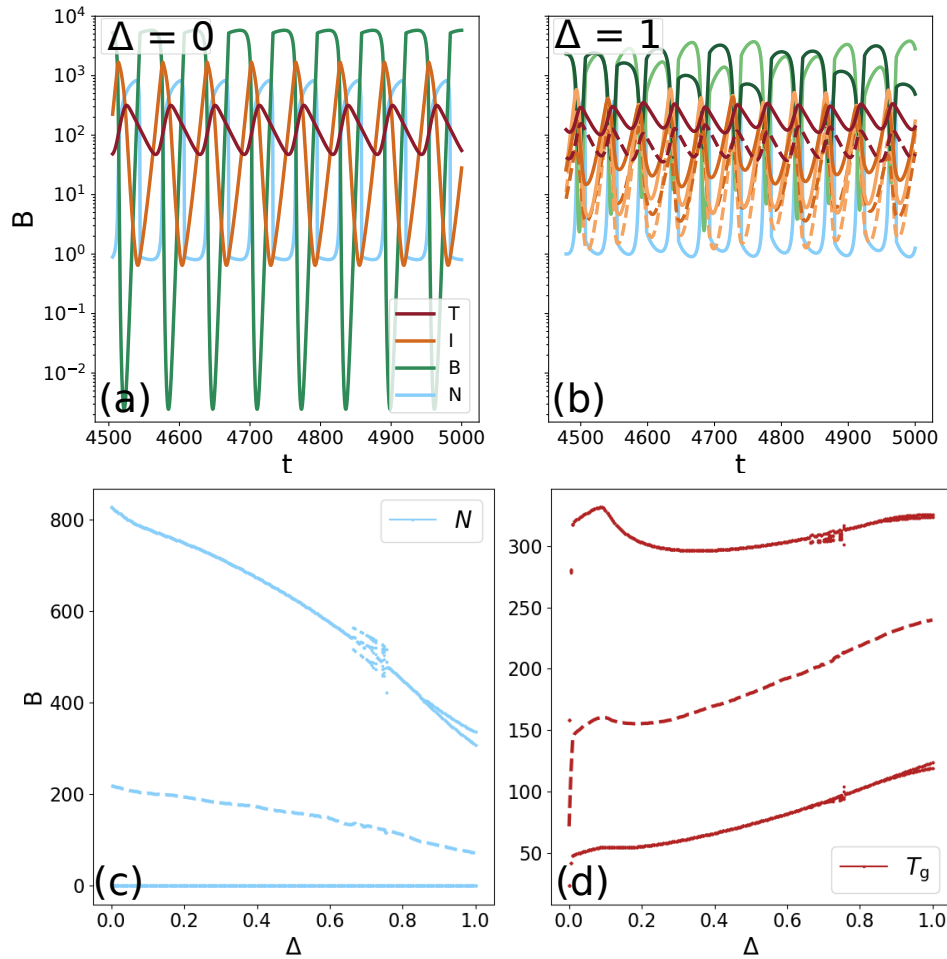
FIGURE A.6: (a), (b): Biomass dynamics for the linear chain ($\Delta = 0$) and fully separated web ($\Delta = 1$), respectively, when the body mass ratio is set to 100, for $h = 1.05$. (c), (d) Bifurcation diagram showing only one single attractor exists over the whole range of Δ, for N and T_n respectively (T_s shows a similar upward trend). The dashed line in the middle shows the mean level. As Δ is increased from 0 to 1 the mean free nutrient level drops from $\approx 220 \, \mu g \, N/l$ to $\approx 70 \, \mu g \, N/l$, while the mean total biomass at the top level increases from $\approx 140 \, \mu g \, C/l$ to $\approx 270 \, \mu g \, C/l$.

Lastly, in order to properly compensate for the increased grazing pressure when the mass ratios are lowered in a chemostat model, we investigated a different model structure where the death rate of each species is also linked to their body mass. In this way, an increase in the maximal grazing rate of a species is accompanied by an increased death rate (Fig. A.7).
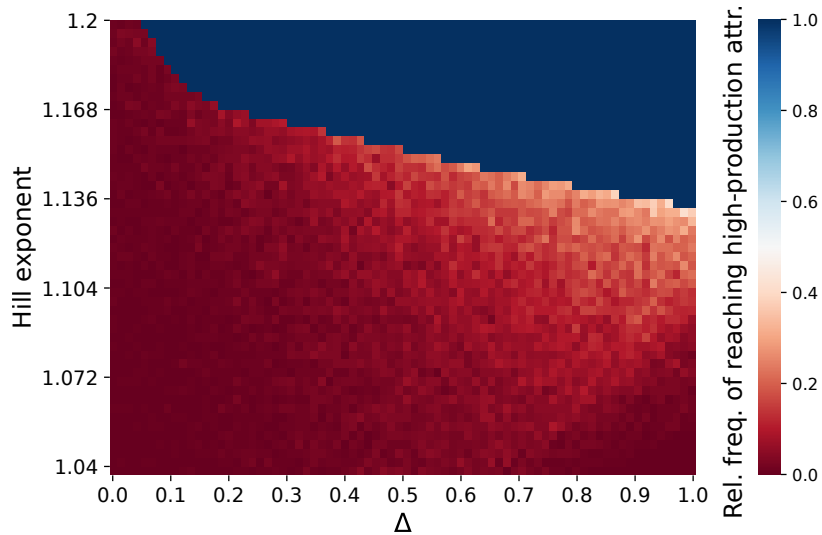
FIGURE A.7: Relative frequencies of reaching the high-production attractor, as a function of the trait difference Δ and the Hill exponents $h = \eta$, for a body mass ratio of 200, with the dilution rate δ scaled allometrically. In this case, the species on each trophic level get a distinct death rate which depends on their body mass and their growth rate. Specifically, the death rates d for the different species are defined as follows:

$$I_1 \text{ and } I_3 : \quad d = \delta r_1' (200/1000)^{-\lambda}$$
$$I_2 \text{ and } I_4 : \quad d = \delta r_2' (200/1000)^{-\lambda}$$
$$T_1 : \quad d = \delta r_1' (200/1000)^{-2\lambda}$$
$$T_2 : \quad d = \delta r_2' (200/1000)^{-2\lambda},$$

where 200 is the body mass ratio used for making the figure, and 1000 is the standard body mass ratio used in the study. In this way species that grow faster get a higher death rate. Each of the points shows the relative frequency of reaching the high-production attractor, sampling 200 random initial conditions. The patterns described in the main text (Fig. 2.5) are again present. All other parameters are the standard ones given in Table 2.1.

A.2 Food web when $\Delta = 0$

In this appendix, the details and meaning of the transition from a food chain with 3 elements (Fig. A.8) to a food web with 9 elements, where all the species on a trophic level are equal, will be presented. It is a priori not clear how these two systems are related, but it can be shown easily that the $\Delta = 0$ food web in Fig. A.8b does indeed describe a food chain, but with a different half-saturation constant in the predator-prey functional response.
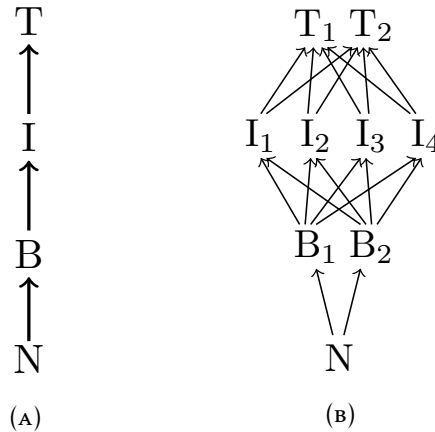

Figure A.8: (a) A simple linear tritrophic chain, described by 4 equations. (b) Food web where all species on a trophic level are exactly equal ($\Delta = 0$), described by 9 equations.

As the equations are somewhat cumbersome when two species are interacting with four species and vice-versa, let us calculate what happens for a simpler toy system of two resources (R) and one consumer C:

$$\begin{cases} \dot{R}_1 & = r\,R_1 - \dfrac{R_1^h}{R_1^h + R_2^h + M^h}\,C \\[2ex] \dot{R}_2 & = r\,R_2 - \dfrac{R_2^h}{R_1^h + R_2^h + M^h}\,C \\[2ex] \dot{C} & = e\,\dfrac{R_1^h + R_2^h}{R_1^h + R_2^h + M^h}\,C - d\,C \end{cases} \qquad (A.1)$$

where r is the resources' growth rate, h the Hill-exponent of the predator-prey interaction's functional response, M its half-saturation constant, and d the consumer's death rate. Assume now that the two resources are actually the same species, i.e., $R_1 + R_2 = R$[1], this gives:

---

[1] This leads to a somewhat inconsistent description, as the mechanism leading to the grazing suppression at low resource densities requires either the predator to be able to distinguish the different resource types, or the prey to have a particular means of more efficiently escaping predation at low resource densities. Both options are not possible when the two resources are the same species, since it implies they cannot be distinguished in any way, and would e.g. use similar hiding spaces to escape predation.

$$\begin{cases} \dot{R} & = \dot{R}_1 + \dot{R}_2 = r\,R - \dfrac{R_1^h + R_2^h}{R_1^h + R_2^h + M^h}\,C \\[3ex] \dot{C} & = e\,\dfrac{R_1^h + R_2^h}{R_1^h + R_2^h + M^h}\,C - d\,C. \end{cases} \tag{A.2}$$

Assuming in addition that $R_1 = R_2$ (which we are free to do so when setting the initial conditions):

$$\begin{cases} \dot{R} & = r\,R - \dfrac{\left(\frac{R}{2}\right)^h + \left(\frac{R}{2}\right)^h}{\left(\frac{R}{2}\right)^h + \left(\frac{R}{2}\right)^h + M^h}\,C \\[4ex] \dot{C} & = e\,\dfrac{\left(\frac{R}{2}\right)^h + \left(\frac{R}{2}\right)^h}{\left(\frac{R}{2}\right)^h + \left(\frac{R}{2}\right)^h + M^h}\,C - d\,C. \end{cases} \tag{A.3}$$

Rewriting $\left(\frac{R}{2}\right)^h + \left(\frac{R}{2}\right)^h = 2^{1-h}R^h$ gives:

$$\begin{cases} \dot{R} & = r\,R - \dfrac{R^h}{R^h + \left(2^{\frac{h-1}{h}}M\right)^h}\,C \\[4ex] \dot{C} & = e\,\dfrac{R^h}{R^h + \left(2^{\frac{h-1}{h}}M\right)^h}\,C - d\,C. \end{cases} \tag{A.4}$$

This shows that a system with 2 identical resources and one consumer with a generalized Holling-Type-III predator-prey functional response does in fact describe a food chain, but with a different half-saturation constant: $M \to 2^{(h-1)/h}M$.

The above reasoning is easily applied to the more complex case shown in Fig. A.8. The 'web' of nine equations:

$$\begin{cases} \dot{N} & = \delta\,(N - N_0) - \dfrac{c_N}{c_C}\,r\,\displaystyle\sum_i B_i \\[3ex] \dot{B}_i & = r\,B_i - g_i \displaystyle\sum_j I_j - \delta B_i \\[3ex] \dot{I}_j & = e\,\displaystyle\sum_i g_i I_j - \gamma_j \displaystyle\sum_i T_i - \delta I_j \\[3ex] \dot{T}_i & = \epsilon\,\displaystyle\sum_j \gamma_j T_i - \delta\,T_i \end{cases} \tag{A.5}$$

with $i \in \{1,2\}$, $j \in \{1,2,3,4\}$, and

$$r = r' \frac{N}{N + h_N} \tag{A.6}$$

$$g_i = g' \frac{B_i^h}{\sum_{i'} B_{i'}^h + M^h} \tag{A.7}$$

$$\gamma_j = \gamma' \frac{I_j^\eta}{\sum_{j'} I_{j'}^\eta + \mu^\eta} \tag{A.8}$$

can easily be calculated to correspond to a linear chain described by four equations:

$$\begin{cases} \dot{N} &= \delta (N_0 - N) - \dfrac{c_N}{c_C} \cdot r\, B \\[2mm] \dot{B} &= r B - g I - \delta B \\[2mm] \dot{I} &= e \cdot g I - \gamma T - \delta I \\[2mm] \dot{T} &= \epsilon \cdot \gamma T - \delta T, \end{cases} \tag{A.9}$$

with

$$r = r' \frac{N}{N + h_N} \tag{A.10}$$

$$g = g' \frac{B^h}{B^h + M^h} \tag{A.11}$$

$$\gamma = \gamma' \frac{I^\eta}{I^\eta + \mu^\eta}, \tag{A.12}$$

when

$$B_1 = B_2, \qquad I_1 = I_2 = I_3 = I_4, \qquad T_1 = T_2, \tag{A.13}$$

by setting

$$\sum_i B_i = B, \qquad \sum_j I_j = I, \qquad \sum_i T_i = T, \tag{A.14}$$

and

$$M \to 2^{(h-1)/h} M, \qquad \mu \to 4^{(h-1)/h} \mu. \tag{A.15}$$

Values of h used in our study are very close to one, hence, the difference is not very large. For example, $h = 1.1$ implies roughly $M \to 1.07\, M$ and $\mu \to 1.13\, \mu$.

A.3   Additional information

This appendix contains some extra figures and tables supporting the results discussed in the main text. The bifurcation diagrams of all other species as well as the nutrients (Figs. A.9 & A.10) confirm that the information extracted from the one shown in the main text are universal. The frequency spectra from which the relevant timescales were identified are shown in Fig. A.11. Fig. A.12 shows the long chaotic transient which is present right after the boundary crisis of the high-production attractor.
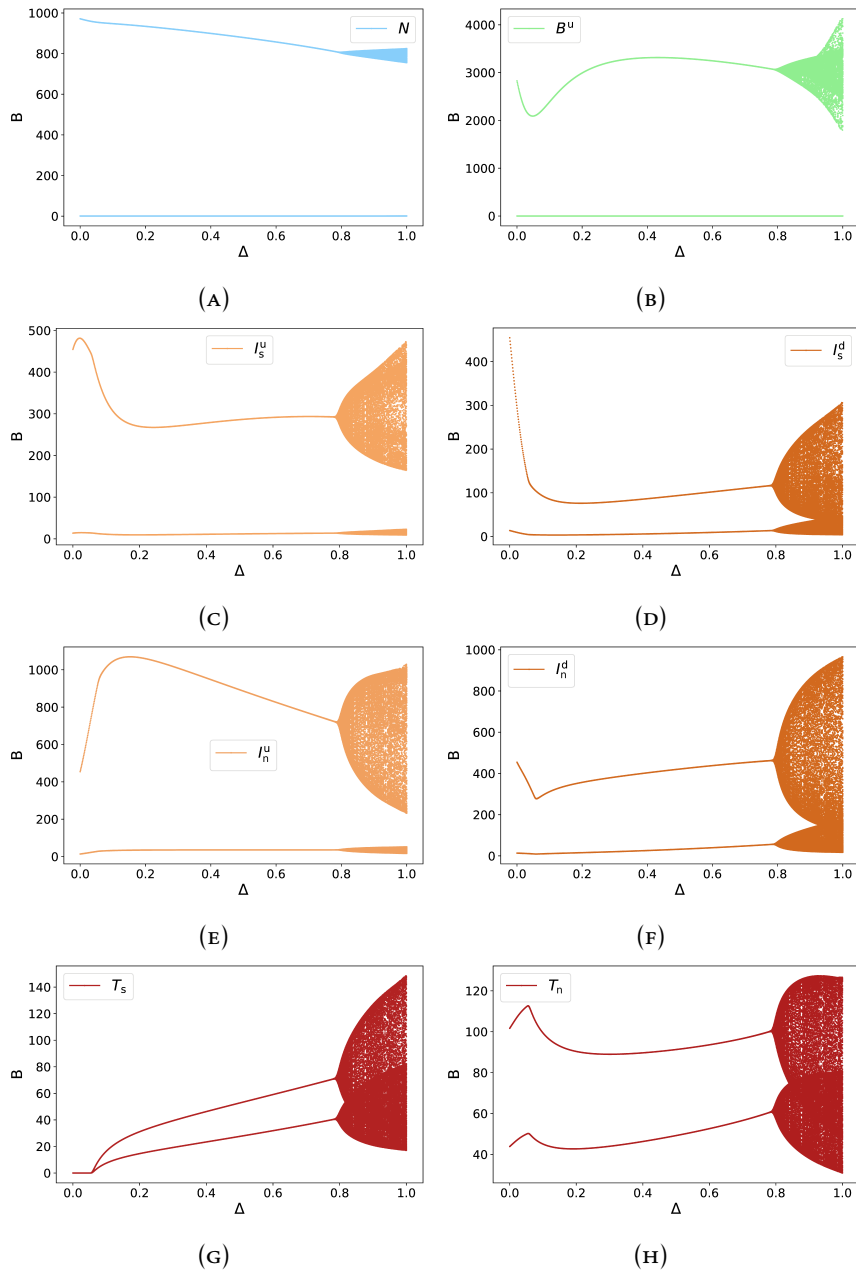
FIGURE A.9: Bifurcation diagrams of the low-production attractor for $h = \eta = 1.05$, as the trait difference parameter Δ is varied from 0 to 1. For small to intermediate sizes of the maximum trait difference, the oscillations are simple in the sense that the maxima and minima are always at the same height. At $\Delta \approx 0.8$ a transition occurs to a region where the oscillations become complex, as indicated by the varying locations of the maxima and minima.
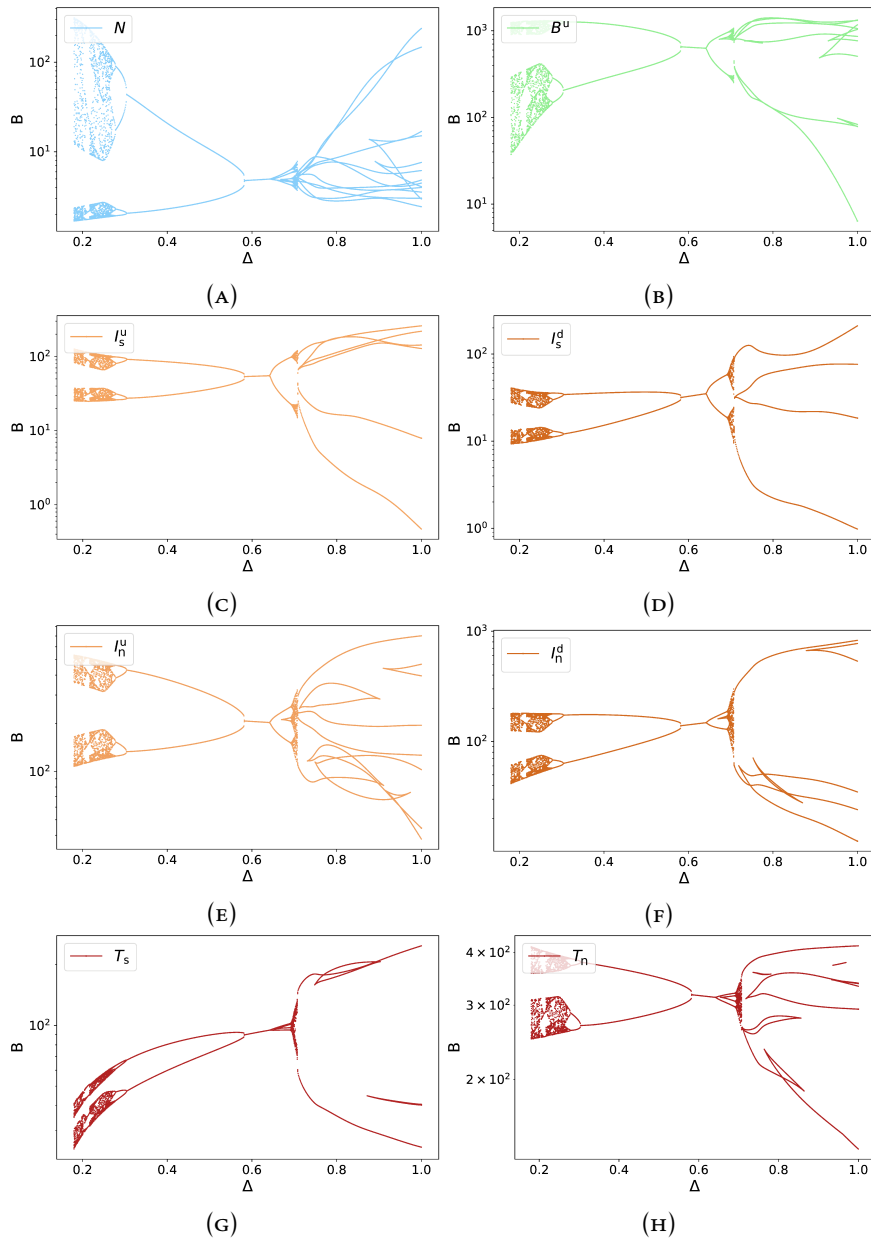
FIGURE A.10: Bifurcation diagrams of the high-production attractor for $h = \eta = 1.05$, as the trait difference parameter Δ is varied from 0 to 1. The attractor disappears for $\Delta \lessgtr 0.18$, and undergoes several bifurcations in the region $0.18 \lessgtr \Delta \leq 1$.
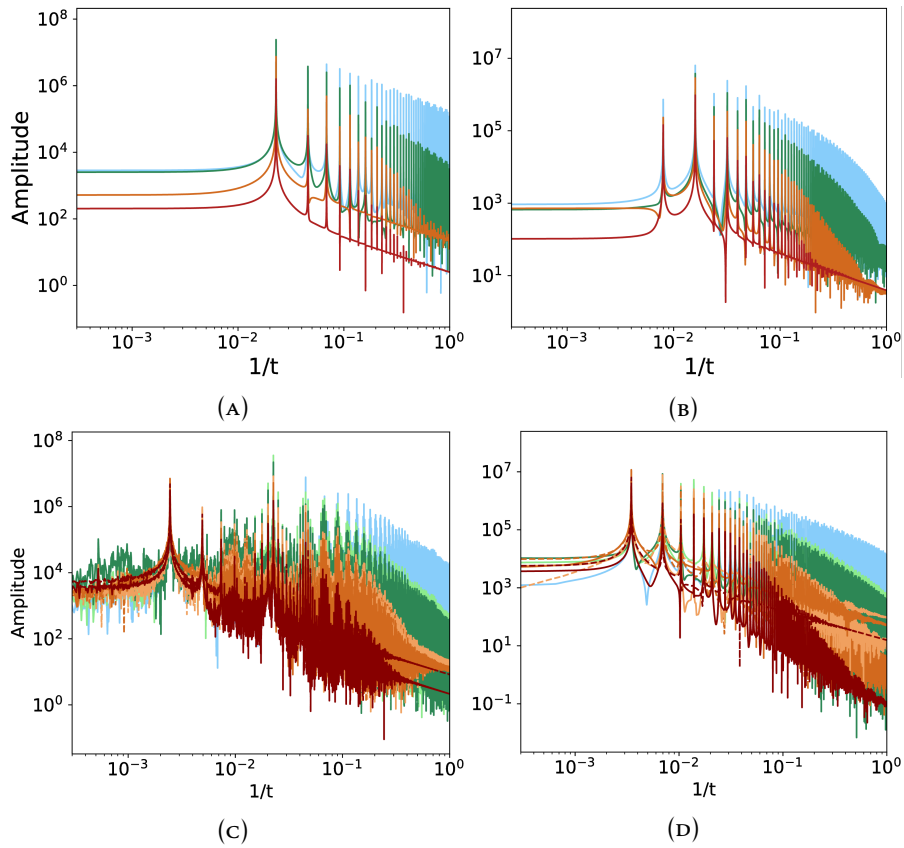
(A)

(B)

(C)

(D)

FIGURE A.11: Fourier spectra of the linear chain ($\Delta = 0$), for $h = \eta = 1.1$ (top), and for the separated food web ($\Delta = 1$), for $h = \eta = 1.05$ (bottom). The left-most figures show the low-production attractor, and the rightmost the high-production attractor. These spectra show that the trait dynamics impose a much longer timescale than the one already present in the linear chain.
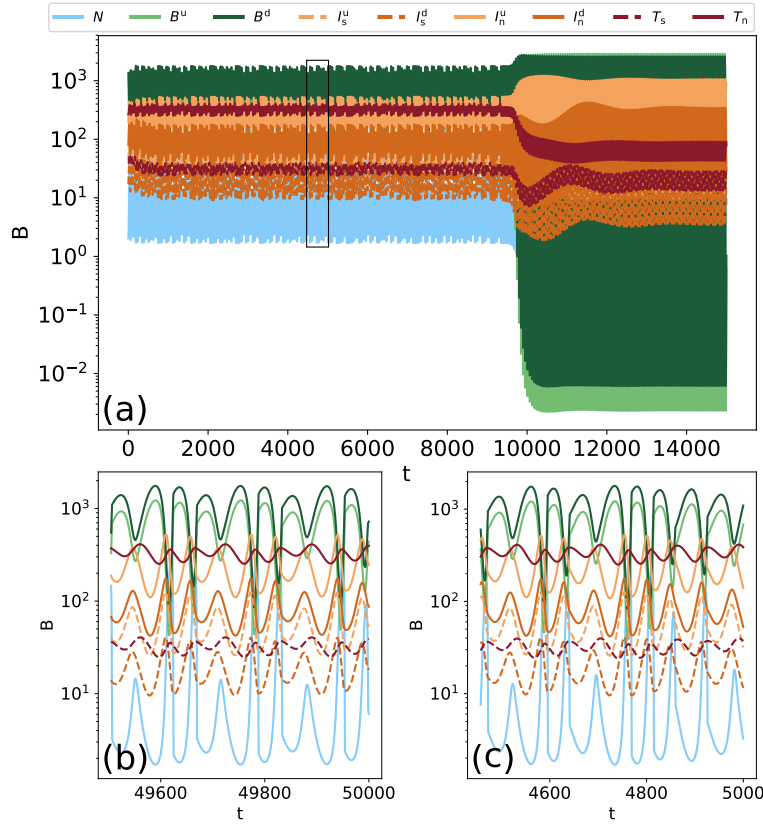
FIGURE A.12: (a): Biomass dynamics for $h = \eta = 1.05$ and $\Delta = 0.177$, slightly smaller than the value where the high-production attractor disappears. A long chaotic transient is observed before the system suddenly accelerates towards the only remaining attractor, the low-production attractor. Figure (b) shows the dynamics for $\Delta = 0.18$ where the attractor still exists, and demonstrates that they are virtually indistinguishable from those on the transient shown in Figure (c) (close-up of the box in Figure (a)).

	$\Delta = 0$		$\Delta = 1$	
	HP	LP	HP	LP
$(P/B)_{\text{Top}}$	5.5	5.5	5.6	5.5
$(P/B)_{\text{Basal}}$	21.8	16.8	30.3	20.2
$P_{\text{Top}}/P_{\text{Basal}}$	6.0	3.9	6.3	3.1

TABLE A.1: Production (P) to Biomass (B) ratios of the Top and Basal trophic levels, for the linear chain ($\Delta = 0$) and the maximally separated food web ($\Delta = 1$), for both the high-production (HP) and the low-production (LP) states. The bottom row shows that the top-production per unit of basal production also increases on the high-production state, resulting in a more efficient system.

References

Brose, U. et al. (2006). "Consumer-resource body-size relationships in natural food webs". In: *Ecology* 87.10, pp. 2411–2417. DOI: 10.1890/0012-9658(2006)87[2411:CBRINF]2.0.CO;2.

Appendix B

Supplementary information to Chapter 3

B.1 Meaning and effect of the cross link scaling parameter

When functional diversity is present on adjacent trophic levels, as is the case for the BI, IT, and BIT food webs, there exist cross links between the species on the different sides of the web. In our model, the relative strength of these cross links can be varied independently of the amount of functional diversity through changing the relevant attack rates by multiplying them with a_{scale}. For higher a_{scale}, the cross links get relatively weaker.

The interaction between two species via a Holling-Type-III functional response is determined by both handling time (h or η) and attack rate (a or α). In our model, trait differences affect the attack rates such that increasing trait differences on adjacent trophic levels may lead to increased specialization of the consumer species on their prey through reduction of the cross link strengths. Explicitly:

$$a = a_0 \begin{pmatrix} 1 & a_x \\ a_x & 1 \end{pmatrix}, \qquad \alpha = \alpha_0 \begin{pmatrix} 1 & \alpha_x \\ \alpha_x & 1 \end{pmatrix}, \tag{B.1}$$

with

$$a_x = a_{\text{scale}}^{-\min(\Delta_B, \Delta_I)}, \qquad \alpha_x = a_{\text{scale}}^{-\min(\Delta_I, \Delta_T)}, \tag{B.2}$$

such that this reduction depends on the minimal trait difference of the relevant trophic levels, and the feeding links are unaffected when one of the trait differences is equal to zero (Fig. B.1).

In a way, the cross link scaling parameter a_{scale} affects the structure of the different food webs we have compared (see also Fig. 3.1, main text). As the ratio between the parallel and the cross links in those food webs where diversity is present on adjacent trophic levels (i.e. BI, IT, and BIT) is varied, the food web structure changes from either a strongly linked ($a_{\text{scale}} \approx 1$), to two weakly connected chains ($a_{\text{scale}} \gg 1$).
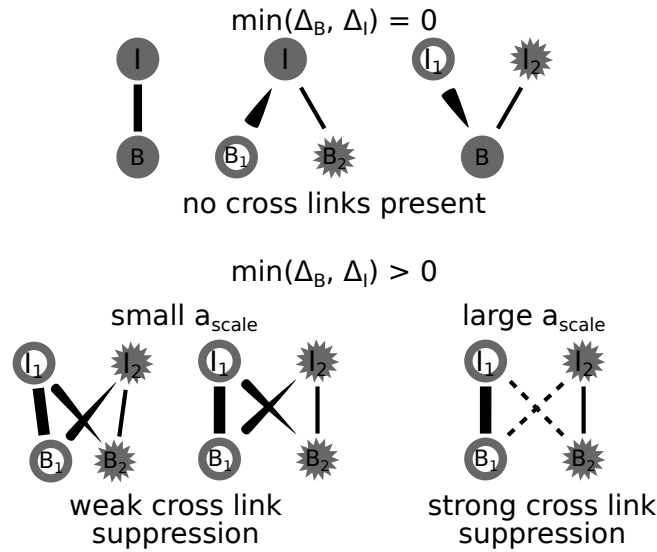
FIGURE B.1: Pictorial representation of the effect of a_{scale} on the food web structure. Only effects on the basal and intermediate level are shown for simplicity, but the interactions between the intermediate and top level is parametrized equivalently. When either $\Delta_B = 0$ or $\Delta_I = 0$ (top row), there are no cross links present and a_{scale} has no effect. It is only when both Δ_B and Δ_I are positive that cross links appear between the basal and intermediate level in the food web. In this case, when a_{scale} is small (close to 1), the cross links $B_1 - I_2$ and $B_2 - I_1$ are not significantly suppressed. Contrarily, for large a_{scale} the trophic links between B_1, I_2 and B_2, I_1 are strongly suppressed, as indicated by the dashed lines.

B.2 Details of the allometric properties

Allometric scaling entails that species' growth rates are linked to their body mass. In particular:

$$\frac{\text{maximal growth rate of trophic level } k+1}{\text{maximal growth rate of trophic level } k} = \left[\frac{m_{k+1}}{m_k}\right]^{\lambda} \tag{B.3}$$

where $k \in \{1, 2\}$, m_k is the body mass of the species on level k, and λ the allometric scaling exponent. As mentioned in the main text, the centers of the intervals for which the maximal growth and grazing rated are selected corresponds to a food chain with biomass ratios between adjacent trophic levels on the order of 10^3, and $\lambda = -0.15$. However, assuming the same scaling exponent λ, the body mass ratio can vary from approximately 1 to approximately $10,000,000$ at the extreme cases for either maximal prey and minimal predator growth rates, or minimal prey and maximal predator growth rates, respectively.

B.3 Detailed description of data production and analysis procedure

The goal of our study is to gain understanding in the general behaviour and ecological patterns that can be expected in tritrophic food webs, as a function of their

diversity. Any serious attempt at studying these general properties cannot be limited to a certain small subset of the parameter space. On the other hand, there is a practical limit in the extent to which the whole ecologically parameter space can be explored.

In addition, fully capturing the behaviour of complex dynamical systems, such as ours, requires going beyond linear stability analysis. Due to modeling the interactions between species as non-linear generalized Holling-type-III functional responses, the resulting population dynamics will often relax to complex limit cycles or chaotic attractors.

As described in the main text, we balanced these limitations by adopting a two-step process. First, we numerically integrated the ordinary differential equations (ODEs) describing our food webs (cf. Eq. (3.1), main text) for 128,000 parameter combinations, and saved aggregate properties of the resulting dynamics (the population and trophic level biomasses and Coefficients of Variation (CV)). This dataset was subsequently used for training a Random Forest model, in order to be able to predict these quantities for many more parameter combinations for which the ODEs were not solved.

In this Appendix, we will describe in detail what kind of data we have used for our results, and how it was produced. Our whole procedure can be split up into three main parts: producing the training dataset, training the Random Forest, and producing the Partial Dependence plots (Figs. 3.3, 3.4 and 3.5 in the main text, and others in the Supplementary Materials).

B.3.1 Producing the training dataset

As described above, the starting point for obtaining our results is the set of ODEs (cf. Eq. (3.1), main text). These equations can be used to describe any of the food webs shown in Fig. 3.1 (main text), through their explicit dependence on the different trait difference parameters Δ_B, Δ_I & Δ_T.

The only way to gain some insight in the behaviour of the solutions describing the population dynamics is to solve these equations. Other techniques such as calculating the fixed points and analyzing their stability through the eigenvalues of the Jacobian matrix are not suitable, because of the high degree of non-linearity in the terms that define the interactions between the different populations in the food web (the generalized Holling Type-III functional responses). Due to these non-linear interaction terms the population dynamics frequently do not relax to a simple stable point, but rather to more complex attractors, such as limit cycles or chaotic attractors.

Fig. B.2 provides a schematic overview of the different steps that were taken to produce the data on which the Random Forest model will later be trained.

1. **Select** $(\Delta_B, \Delta_I, \Delta_T)$: While Fig. 3.1 (main text) shows the different food webs ordered by the presence or absence of functional diversity on each trophic level,
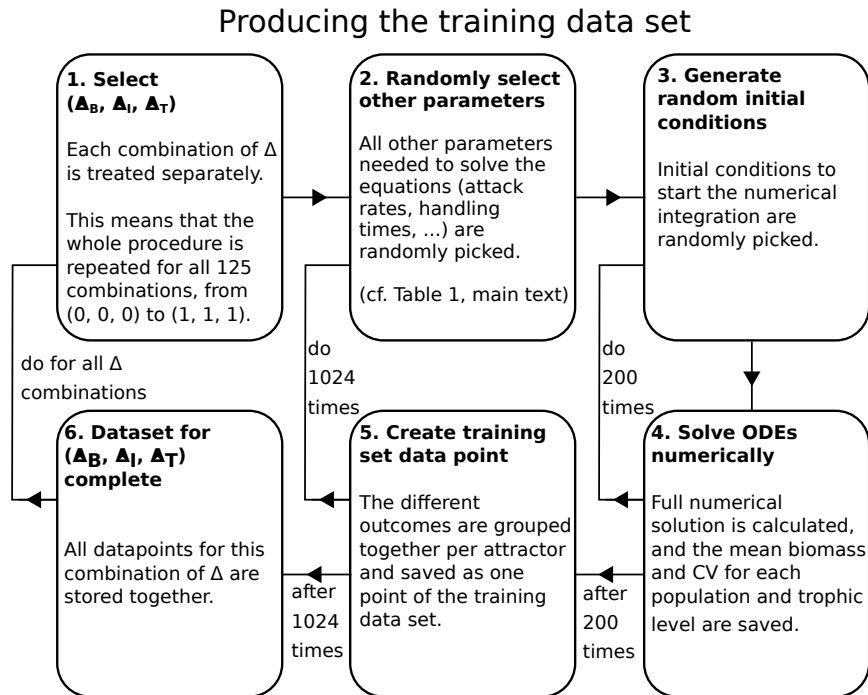
Producing the training data set

FIGURE B.2: Schematic overview of the steps required to produce the training data set. See the text for more details on each step.

it can also be helpful to think about a different partitioning of all possibilities. Particularly, one could imagine ordering the food webs simply by their values of Δ_B, Δ_I, and Δ_T. In that case there are not eight, but 125 different possibilities, since each $\Delta_i \in \{0, 0.25, 0.5, 0.75, 1\}$.

It is then for each of these 125 cases that the dynamics of 1024 randomly sampled parameter combinations will be investigated.

2. **Randomly select other parameters**: The other eleven parameters required to solve the ODE model are randomly sampled from well defined intervals (see Table 3.1, main text).

3. **Generate random initial conditions**: Because of the increased complexity of the food webs we describe, it is possible that there is a strong dependence of the outcome of the ODE model on the initial conditions. Several different scenarios are possible: any particular initial condition may not lead to coexistence of all species in the food web, or, there may be multiple attractors for which all species do coexist. It would thus be highly inaccurate to assume that one single initial condition is representative for all possible outcomes of this particular parametrization. Therefore, for each parameter combination, it is additionally necessary to record the outcomes of several different initial conditions. To obtain the datasets used to train the RF model in the main text, we recorded the outcomes of 200 randomly sampled initial conditions per parameter combination. As described in the main text, these initial conditions were sampled in a way that the total biomass of each trophic level does not exceed twice its

theoretical maximum, in order to remain ecologically reasonable and prevent very strong oscillations when the system is relaxing to its attractor.

4. **Solve ODEs numerically**: Now that all parameters have been assigned a value, and an initial value has been set, numerical integration of the ODE model is performed. To prevent any influence from the potential presence of very slow transient dynamical patterns, the system is allowed to relax to its equilibrium state for $100,000$ time units. After this time, the mean biomass of each population, as well as for each trophic level as a whole, is calculated over $30,000$ time units. Similarly, the standard deviation of the dynamics is calculated for each individual population and each trophic level, from which the coefficient of variation can be computed ($CV = \sigma/\mu$, where σ is the standard deviation and μ the mean). For schematic details of this procedure, see Fig. B.3. A real example timeseries from our model is shown in Fig. B.4.

5. **Create training set data point**: After the mean biomasses and CVs of 200 unique randomly sampled initial conditions have been calculated, all the numerical simulations for one parameter combination have been completed. However, typically, many initial conditions will relax to the same attractor. It is therefore very useful to group the different outcomes together per attractor: when *all* of the different species' means and CVs are sufficiently close to each other (absolute tolerance of 5 for the means, 0.01 for the CVs, and relative tolerance of 0.1), the initial conditions are assumed to relax to the same attractor.

The structure of a data point belonging to one parameter combination is the following:

```
dict; # Python dictionary containing all parameter values
num_attr; # number of different attractors
ext; # whether any species are extinct or not on each attractor
TL_B; # total biomass on each trophic level
odd_B; # biomass of B1, I1, T1
ind_CV; # CV of each population
TL_CV; # CV of each trophic level
attr_prop # proportion of initial conditions relaxing to each attractor
```

A typical data point:

```
{'B_diff': 0.75, 'I_diff': 0.75, 'T_diff': 0.25, 'N0': 666.210112394016,
'h_N': 18.91630737427768, 'r0': 1.8743678849645211,
'a0': 0.0015176450564662867, 'h0': 0.79237825772891,
'alpha0': 0.0003298639600209292, 'eta0': 3.209067776129767,
'delta': 0.05710530459267592, 'n': 1.907283906197544,
'nu': 1.3633537312107176, 'a_scale': 1.2903979398824104, 'id': 2824000};
2;
```

```
[0,1];
[[100.677904   ,168.3763992 ,198.2327592 ,233.3333859 ],
 [535.659272   , 19.29489409,268.8575037 ,  1.64734166]];
[[105.72043   ,170.586387 ,168.072246 ],
 [ 14.6636983, 59.3558927,  0.         ]];
[[0.61712753,1.32296074,0.47741629,0.04292298],
 [0.         ,0.         ,0.         ,0.         ]];
[[1.42259412,0.51964668,0.04594913],
  [0.         ,0.         ,0.         ]];
[[1.19062106,0.21908273,0.03512972],
  [0.         ,0.         ,0.         ]];
[0.83,0.17]
```

This data point has $\Delta_B = 0.75, \Delta_I = 0.75, \Delta_T = 0.25$, and thus belongs to the
BIT food web and there are two different attractors found. 83% of the initial
conditions relaxed to the first one listed, for which all species coexist, whereas
17% relaxed to the second one listed, which has only one species on the top
level (as the biomass of T_1 equals zero). Additionally, one can see that the
second attractor listed must be a stable fixed point (due to the CVs being zero),
whereas the first attractor cannot be a stable fixed point and must therefore be
a limit cycle or a more complex type of attractor. Investigation of the actual
timeseries confirms that the attractor is a limit cycle in this case (Fig. B.4).

6. **Dataset for** $(\Delta_B, \Delta_I, \Delta_T)$ **complete**: After 1024 randomly sampled parameter
   combinations have been investigated (each for 200 initial conditions), and thus
   1024 data points have been added to the training data set, all the *ODE* simu-
   lations for this combination of Δ_B, Δ_I, and Δ_T have been completed.

This whole process is now repeated for the next combination of trait differences
until there are 1024 data points for each combination. This means that the ODE
model described in Equation (3.1) (main text) will have been solved $125 \cdot 1024 \cdot 200 =$
$25,600,000$ times. If we assume that each individual integration takes just one sec-
ond, this requires just under 300 *days* of total integration time. Luckily, this whole
process is easily parallelizable, which can substantially reduce the required time,
depending on the amount of available computing cores.

B.3.2   Training the Random Forest

The next step required to produce our results is to train a Random Forest (RF) on the
training dataset, produced by solving the ODE model millions of times and record-
ing the mean biomasses and coefficients of variation (CVs), as described above.
There are two main benefits of using a RF to analyze and present our data. Firstly,
assuming that the RF model predictions are accurate, the ability to predict the out-
put value of parameter combinations that are not in the training dataset increases
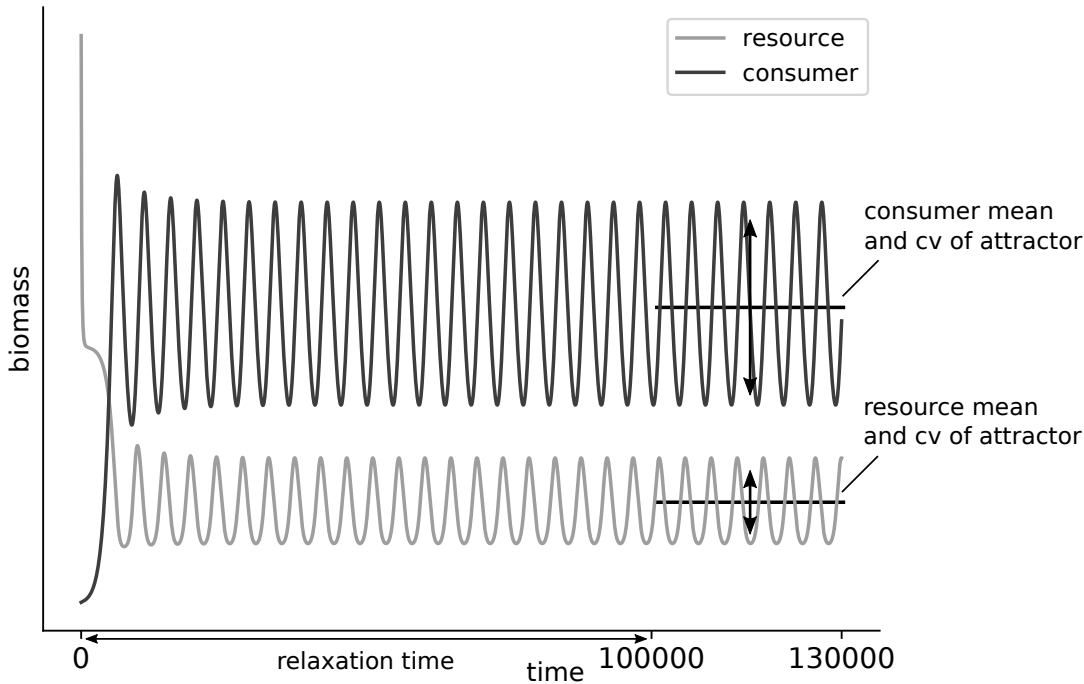
FIGURE B.3: Schematic example of a trajectory starting from a random initial condition, for a simple consumer-resource system. To estimate the mean biomasses and biomass CVs on the attractor, they are calculated over a period of $30,000$ time units, after the system has been allowed to relax to the attractor for $100,000$ time units.

the confidence level of any trends that can be identified (see Fig. B.6). Secondly, the RF model provides us with a measure of the importance of each of the input parameters (see Table 3.1, main text) in determining the output value (see Fig. 3.6, main text).

Short overview of how a Random Forest works

The goal of any model is to estimate each output value y_i ($i \in \{1, \dots, n\}$, where n is the number of data points) as well as possible by constructing a function f, for which

$$\hat{y}_i = f(\boldsymbol{x}_i) \tag{B.4}$$

where $\boldsymbol{x}_i = (x_{i,1}, x_{i,2}, \cdots, x_{i,p})$ are the input variables (or features), with p the amount of features, such that $\hat{y}_i$ is the model estimate of y_i.

Random Forest Models are a class of machine learning models, which are popularly used due to their relatively simple structure and high versatility. In a random forest, each $\hat{y}_i$ is calculated by averaging the predictions of many different regression trees. Each individual regression tree has a certain degree of randomness: only a random subset of the data ($\sim 63\%$) is used to calculate the tree, and at each node only a randomly selected subset of the data features is taken into account. By averaging the predictions of a large amount of such quasi-randomly generated regression trees, a random forest model can make more accurate predictions than a single optimized regression tree (Breiman, 2001).
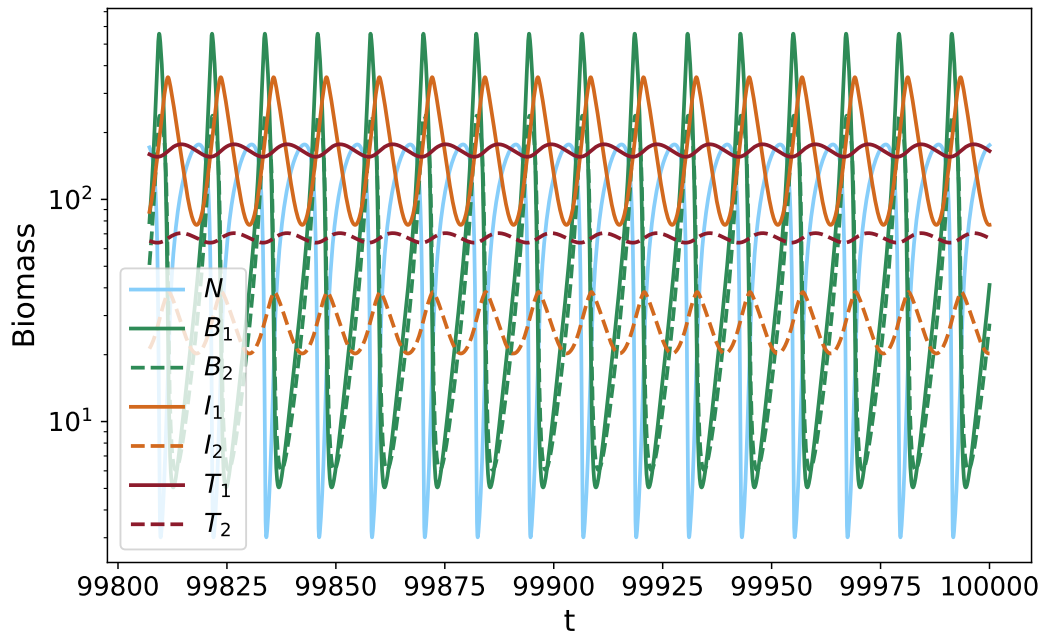
FIGURE B.4: Example timeseries of the dynamics possible in our model. This timeseries was created using the parameters given in the example datapoint above. It can clearly be seen that the attractor is a limit cycle, which means that the dynamics will oscillate in this way perpetually.

Because each individual tree in the forest has only been trained on a subset of the data, the remaining data points can be used to estimate the accuracy of that tree. This process is called Out-Of-Bag (OOB) error estimation, and gives a measure for the accuracy of the model:

$$OOB_{score} = 1 - \frac{MSE_{OOB}}{\hat{\sigma}_y^2}, \tag{B.5}$$

where $\hat{\sigma}_y^2$ is the variance estimator of the outcome variable y, and

$$MSE_{OOB} = \frac{1}{n} \sum_{i=1}^{n} \left(y_i - \bar{y}_i^{OOB} \right)^2, \tag{B.6}$$

with $\bar{y}_i^{OOB}$ being the mean OOB predicted value of y_i. In this way, an OOB score of 1 signifies that the model is able to predict the outcome perfectly. Using the OOB error estimation, it is also possible to evaluate the importance of each of the input parameters in predicting the output value. This is done by quantifying the change in the random forest's accuracy when the input parameter's values are permuted. A large change in accuracy indicates a high importance in predicting the correct value, and vice-versa.

For each quantity of interest (see Results, main text), an Extremely Random Forest consisting of 2000 trees was trained using the Scikit-learn (Pedregosa et al., 2011)

package in Python. Importantly, each forest was only trained on the subset of parameter combinations for which coexistence was found to be possible (see also Appendix S4). In case multiple attractors were found for which all species were in coexistence, the weighted average of the different outcomes was used.

How Random Forests were used to analyze our data

For extra clarity, let us apply the general equation (B.4) to a specific example: the biomass produced by the top trophic level (P_T). The procedure for using the RF model to predict any of the other quantities presented in the main text and appendices is similar.

As described above, the goal of the RF algorithm is to be able to accurately predict the output values y_i. In this example, let $y_i = P_{Ti}$, such that P_{Ti} denotes the biomass production on the top level for the ith data point. This quantity can easily be calculated using the biomasses on the top trophic level and the relevant input parameters (see Appendix S5 for a more elaborate explanation). The input information that the RF algorithm will use to make these predictions is the collection of parameters we have varied to produce the data. Explicitly, the RF algorithms will thus estimate the function F for which:

$$y = F(\boldsymbol{x}) \Longleftrightarrow \forall i : y_i = F(\boldsymbol{x}_i), \tag{B.7}$$

with

$$y_i = P_{Ti} \quad \text{and} \quad \boldsymbol{x}_i = \left[\Delta_{Bi}, \Delta_{Ii}, \Delta_{Ti}, N_{0i}, h_{Ni}, r'_{0i}, a_{0i}, h_{0i}, \alpha_{0i}, \eta_{0i}, \delta_i, a_{\text{scale},i}, n_i, \nu_i \right] \tag{B.8}$$

describing the predicted value and all the relevant parameters that belong to it. These two arrays contain all the information the RF algorithm needs to be able to estimate the function F, and calculate the *OOB* score and parameter importances.

B.3.3 Application of the Random Forest model to produce partial dependence plots

Now that the Random Forest (RF) has been trained on the training data, it can finally be used to gain an increased understanding of the system we set out to study. The parameter importances (see Fig. 3.6, main text) are calculated during the training phase of the RF model, and thus are readily available for further analysis. In contrast, to construct the partial dependence plots (Figs. 3.3, 3.4 and 3.5 in the main text, and others in the Supplementary Materials), additional calculations using the RF model are necessary.

As explained above, by training the RF we have constructed a function with which we can predict the desired outcome quantity, using the input parameters used to train the model (cf. Eq. B.4). Importantly, we can now use our model to make predictions for parameter combinations that are not in the training dataset, with

which we can calculate the partial dependence (PD) of the quantities predicted by the RF on the different input parameters. In other words, the partial dependence of the RF prediction $f(x)$ on the input parameter x_j ($j \in \{0,...,p\}$ with p the number of input parameters) is typically defined as $f_j(x_j)$ (Hastie, Tibshirani, and Friedman, 2009):

$$f_j(x_j) = \frac{1}{n} \sum_{i=1}^{n} f(x_{i,1},...,x_j,...,x_{i,p}),$$

(B.9)

where $x_{i,k}$ is the value of the kth input parameter in the ith data point.[1]

A graphical explanation of calculating the partial effects in this way is shown in Fig. B.5, for f_1. For each value of x_1, the RF makes n (number of data points) predictions, of which the median value is taken. These n predictions are the predicted output values of all data points, where the actual value of x_1 in the data point has been substituted by the currently evaluated one. The procedure is then repeated for the next value of x_1. Using this definition, the degree of extrapolation necessary to calculate the partial effects is kept minimal.
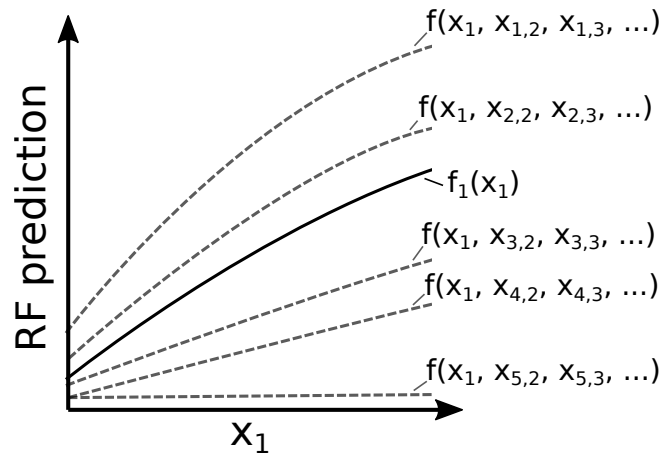

FIGURE B.5: Schematic example of the construction of the partial dependence (PD) of the RF prediction on the input parameter x_1: f_1. See the text for a detailed explanation.

Increased accuracy of estimate due to the Random Forest

The Partial Dependence Plots (PDPs) additionally allow for a clear visualization of the benefit of using the RF trained on our data, as compared to simply using the data itself (Fig. B.6). In this graph, the 99% confidence intervals on the mean are estimated by $3\sigma/\sqrt{n_s}$, where σ and n_s denote the standard deviation and size of the sample, respectively.

The most important reason for the difference in size between in the error bars lies in the potentially huge difference between n_s for the data itself as compared to what is predicted by the PDP. When using the data itself to estimate the mean top biomass for a given value of Δ_T, n_s is the number of data points in the training

---

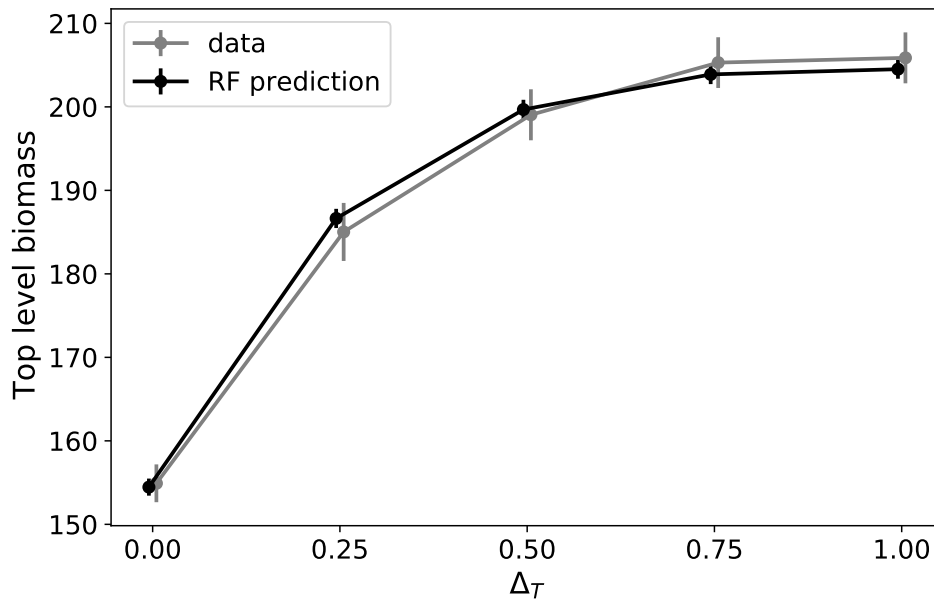[1] Note that, by this definition, f_j does *not* denote the j-th component of f.

FIGURE B.6: Partial Dependence Plot (PDP) of the total biomass on the top level on the trait difference on the top level Δ_T (black line), compared to what can be extracted from the data itself (gray line). The circles indicate the estimated mean biomass for each value of Δ_T, and the error bars an estimate for for the 99% confidence intervals. One can see that the mean biomass on the top level is more accurately estimated by using the PDP provided by the RF, rather than simply estimating this quantity from the training itself.

data set that actually have that value of Δ_T as an input. In general, this number will be only a fraction of the total dataset as there will be many other data points with different values of Δ_T. However, for the PDP estimate, n_s is always the total number of data points in the whole training data set. This is because, for a certain value of Δ_T, the PDP predicts the top level biomass by substituting that value of Δ_T into every single data point in the training set. The error on the estimate of the mean top level biomass will therefore generally be much smaller. In Fig. B.6, the error on the estimate of the data itself is also rather small, because there are still many data points for each value of Δ_T in this one-dimensional division of the data. However, one can easily imagine partitioning the data into a much higher number of categories such that the number of data points in each category is much lower compared to the total number of data points in the training set (such as in the pseudo-three-dimensional PDPs shown in Figs. 3.3-3.5 (main text) and similar ones in Appendices S5 and S7).

B.4 Proportion of coexistence of all species

All the results presented only apply to those parameter combinations that actually lead to coexistence of all species in the food web. In most cases, coexistence of all species was probable to very probable. However, for the T and IT food webs,

coexistence of all species was very rare (only in resp. 1 and 8 cases, out of resp. 4096 and 16384). See the corresponding paragraph in the Discussion (main text) for an explanation of these results.

Web	Coexistence proportion
chain	0.945
B	0.931
I	0.936
BI	0.938
T	< 0.001
BT	< 0.001
IT	0.637
BIT	0.647

B.5 On calculating the average biomass production

We calculated the mean biomass production and P/B ratios from the mean biomasses of the the individual species and of the trophic levels per parameter combination and initial condition (Fig. B.7). See also Section B.3 for a details description of how these quantities were obtained.

$$T_{\text{out}} = \sum d_{T_i} T_i$$

$$I_{\text{up}} \equiv \frac{T_{\text{out}}}{e} = \frac{\sum d_{T_i} T_i}{e}$$

$$I_{\text{out}} = \sum d_{I_i} I_i$$

$$B_{\text{up}} \equiv \frac{I_{\text{up}} + I_{\text{out}}}{e} = \frac{\sum d_{T_i} T_i}{e^2} + \frac{\sum d_{I_i} I_i}{e}$$

$$B_{\text{out}} = \sum d_{B_i} B_i$$

$$N_{\text{up}} \equiv B_{\text{up}} + B_{\text{out}} = \frac{\sum d_{T_i} T_i}{e^2} + \frac{\sum d_{I_i} I_i}{e} + \sum d_{B_i} B_i$$
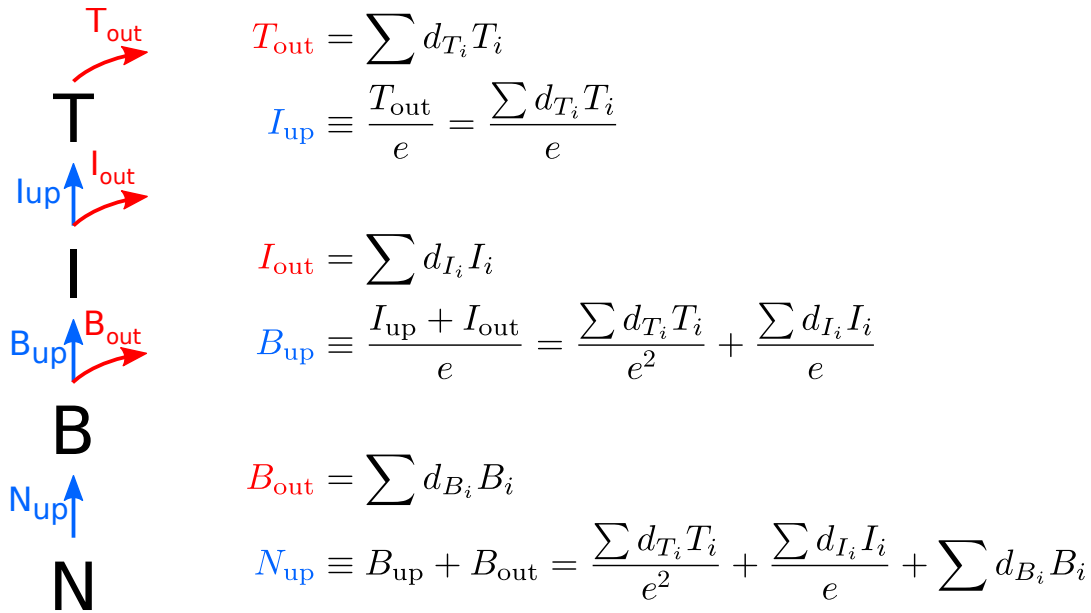
FIGURE B.7: Step by step illustration on how to calculate the biomass flows between trophic levels in our system. These equations hold for all of the different food webs we compared. When there are two species on a trophic level, the sums run over $i \in \{1, 2\}$; when there is only one, no summation is required. N_{up} denotes the nutrient uptake by the basal species, and B_{up} & I_{up} the total biomass flowing upwards from the basal and intermediate level respectively.

The time-averaged mean biomass production $\bar{P}$ of each trophic level is then given by:

$$\bar{P}_T = \bar{T}_{\text{out}} = \sum d_{T_i} \bar{T}_i$$

$$\bar{P}_I = \bar{I}_{\text{up}} + \bar{I}_{\text{out}} = \frac{\sum d_{T_i} \bar{T}_i}{e} + \sum d_{I_i} \bar{I}_i \tag{B.10}$$

$$\bar{P}_B = \bar{B}_{\text{up}} + \bar{B}_{\text{out}} = \frac{\sum d_{T_i} \bar{T}_i}{e^2} + \frac{\sum d_{I_i} \bar{I}_i}{e} + \sum d_{B_i} \bar{B}_i,$$

since all the loss rates d are density-independent (cf. Eqs. (3.1) and (3.8), main text). In these equations, the bar is simply present to emphasize that our data consists of long-term temporal averages. The quantities $\bar{B}_i, \bar{I}_i$, and $\bar{T}_i$ are exactly the mean biomasses per population calculated by solving the ODE system (Equation (3.8)) and stored in the dataset (see also Section B.3).

Shown below are the partial dependence graphs for some of these quantities, to support the mechanisms which yield increased biomass on the top level when diversity on all trophic levels is high. Importantly, these figures also support our claim that the random forests trained on our data are actually accurate: the equalities $P_T = e \cdot I_{\text{up}}$ and $P_I = e \cdot B_{\text{up}}$ hold throughout the whole range of Δ_B, Δ_T, and Δ_T.

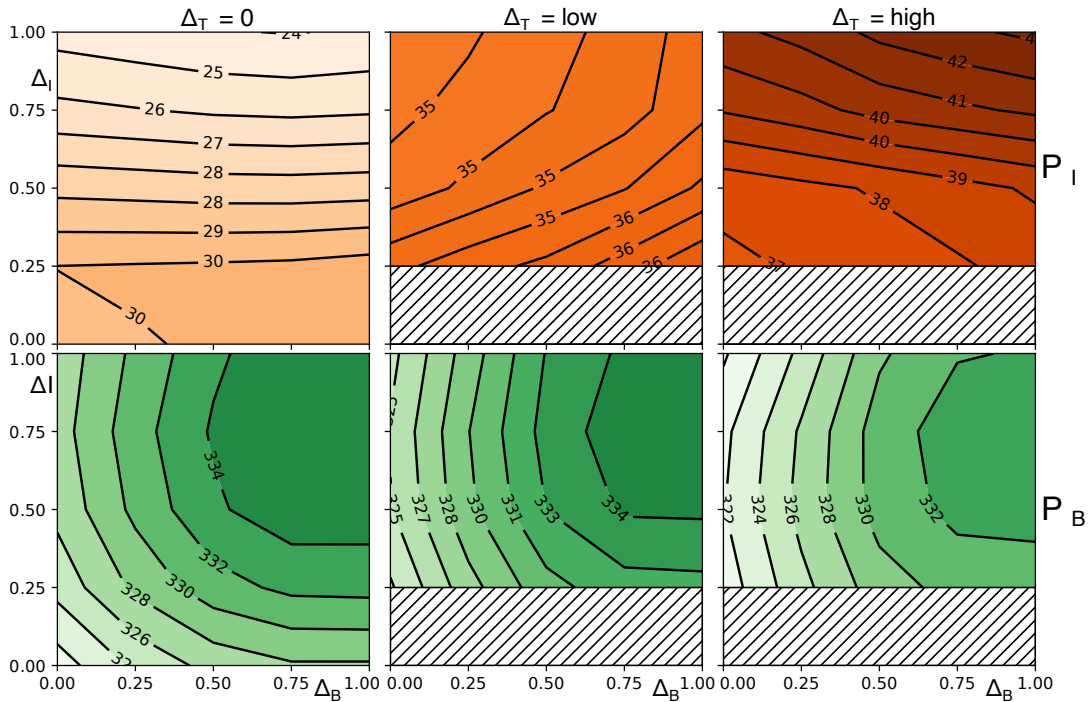The quantities P_T, B_{up}, $(P/B)_B$, and P_T/P_B are shown in Fig. 3.5 (main text).

FIGURE B.8: Partial dependence graphs of the total biomass production on the basal (P_B) and intermediate (P_I) level, in the same style as the figures in the main text. See the next section for an explanation for why P_B is approximately constant.
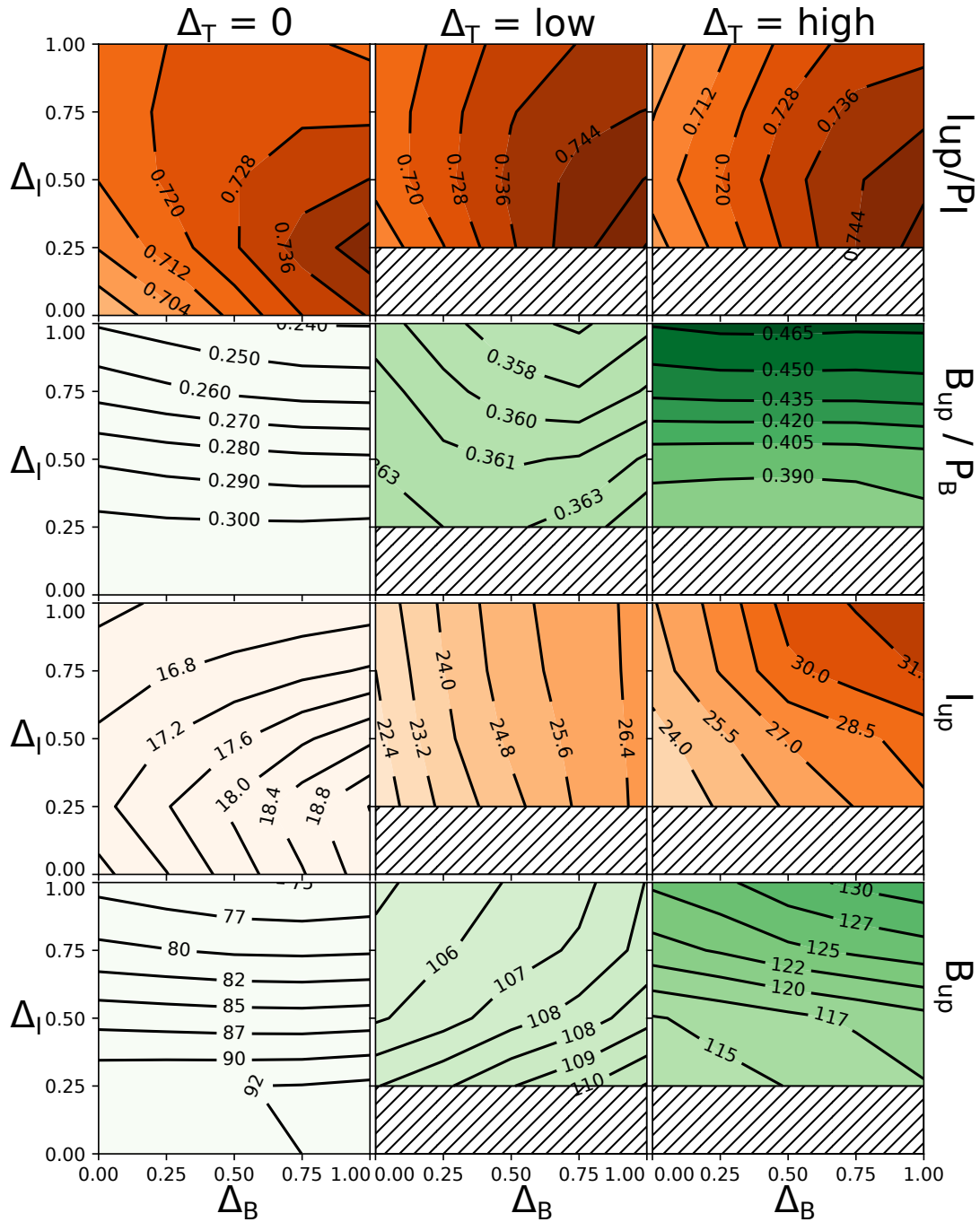
FIGURE B.9: Partial dependence graphs of the total biomass flowing to the top and intermediate level (I_{up} and B_{up}, respectively), and as a fraction of the total biomass production of the intermediate and top level (I_{up}/P_I and B_{up}/P_B).

B.6 Link between mean free nutrient level and biomass production on the basal level

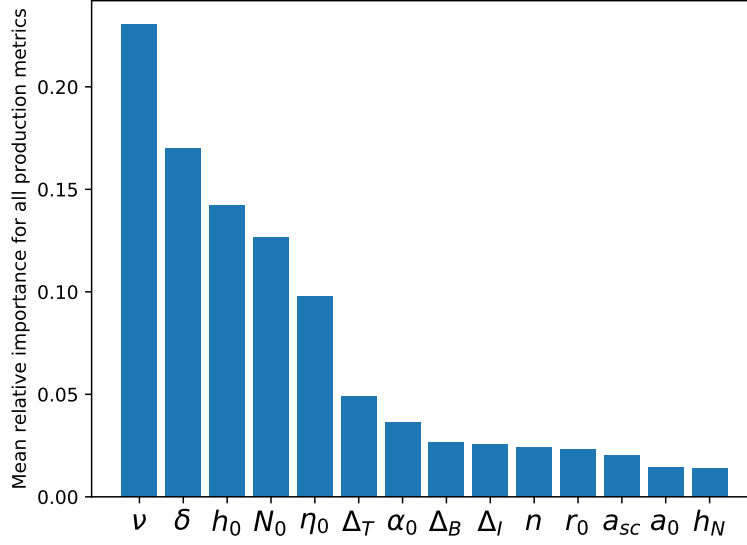Here, we motivate why the biomass production of the basal level (P_B) is approximately constant in our model. Equation (3.1) (main text) reads:

FIGURE B.10: Mean relative importance of the different input parameters over *all* production metrics shown in the main text and this appendix: P_B, P_I, P_T, B_{up}, I_{up}, B_{up}/P_B, I_{up}/P_I, $(P/B)_B$, $(P/B)_I$, $(P/B)_T$, P_T/P_B. Like for the biomasses and CVs (Fig. 3.6, main text), parameters regulating the interaction between the top and intermediate level tend to be of higher importance than those of the intermediate-basal interaction. In particular, the trait difference between the top species Δ_T is of higher importance than that of Δ_I and Δ_B.

$$\dot{N} = \delta(N_0 - N) - \frac{c_N}{c_C} \sum_i r_i B_i. \tag{B.11}$$

Since $\sum_i r_i B_i = P_B$ we get:

$$\dot{N} = \delta(N_0 - N) - \frac{c_N}{c_C} P_B. \tag{B.12}$$

When averaging over time, $\bar{\dot{N}} = 0$ must hold, hence:

$$\bar{P}_B = \frac{c_C}{c_N} \delta(N_0 - \bar{N}). \tag{B.13}$$

This means that the time-averaged basal production $\bar{P}_B$ is fully determined by δ, N_0, and $\bar{N}$. This relationship can clearly be observed when comparing the partial dependence plots of N (Fig. 3.3, main text) and P_B (Fig. B.8). Moreover, the fact that P_B barely varies is explained by the relatively low average values of N (between approx. 45 and 190), as compared to the average N_0 of approximately 1200 (cf. Table 3.1, main text).

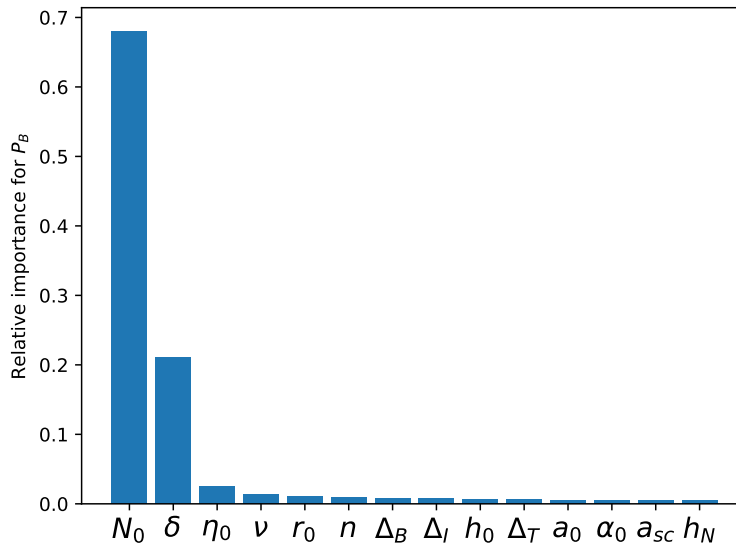This property is nicely captured by the random forest trained on the data for P_B (cf. Fig. B.11).

FIGURE B.11: Relative importance of the different parameters for predicting the total biomass production on the basal level, P_B. Even though the random forest has no knowledge of the dynamical equations of our food webs, it accurately predicts that only N_0 and δ are of high importance to determine P_B.

B.7 Relative biomasses per trophic level

Information on the contribution of individual species' biomasses to their respective trophic level helps with understanding the patterns of the biomass production efficiencies and food web efficiency (see Fig. 3.5, main text). For example, a higher proportion of the fast growing species B_1 leads to an increased basal biomass production of the trophic level as a whole. In Fig. B.12, the proportion of X_1 is defined as $\frac{X_1}{X_1+X_2}$, with $X \in \{B, I, T\}$. To fairly asses the relative biomass of the fast growing species, two species have to be present on that trophic level. For that reason, all regions where $\Delta_X < 0.25$ have been excluded when calculating the relative biomass of X_1.

While the OOB-scores (measure for the goodness-of-fit of the random forest model, see Section B.3.2) for I_1 and T_1 are good, they are negative for B_1 (cf. Table B.1). This means that the random forest's prediction is worse than a constant prediction of the mean relative biomass B_1 every time. However, splitting the dataset by the amount of top diversity in the same way as for the partial dependence plots shows that the OOB score in the case of $\Delta_T = 0$ is still relatively accurate.

Outcome variable	Overall OOB score	$\Delta_T = 0$	$\Delta_T = $ low	$\Delta_T = $ high
rel. T_1	0.54	n.a.	0.53	0.46
rel. I_1	0.88	0.74	0.84	0.88
rel. B_1	-0.05	0.52	-0.39	-0.19

TABLE B.1: OOB scores estimating the accuracy of the random forest model, for the relative biomasses of $B_1, I_1,$ and T_1. The second column shows the overall OOB score, i.e., of all the data, whereas the next three show the OOB scores separated by Δ_T, as in Fig. B.12. An OOB score of 1 represents a perfect model prediction, whereas an OOB score of 0 means that the model is as accurate as simply predicting the mean outcome value every time. Therefore, we do not rely on the predictions for B_1 when $\Delta_T > 0$.
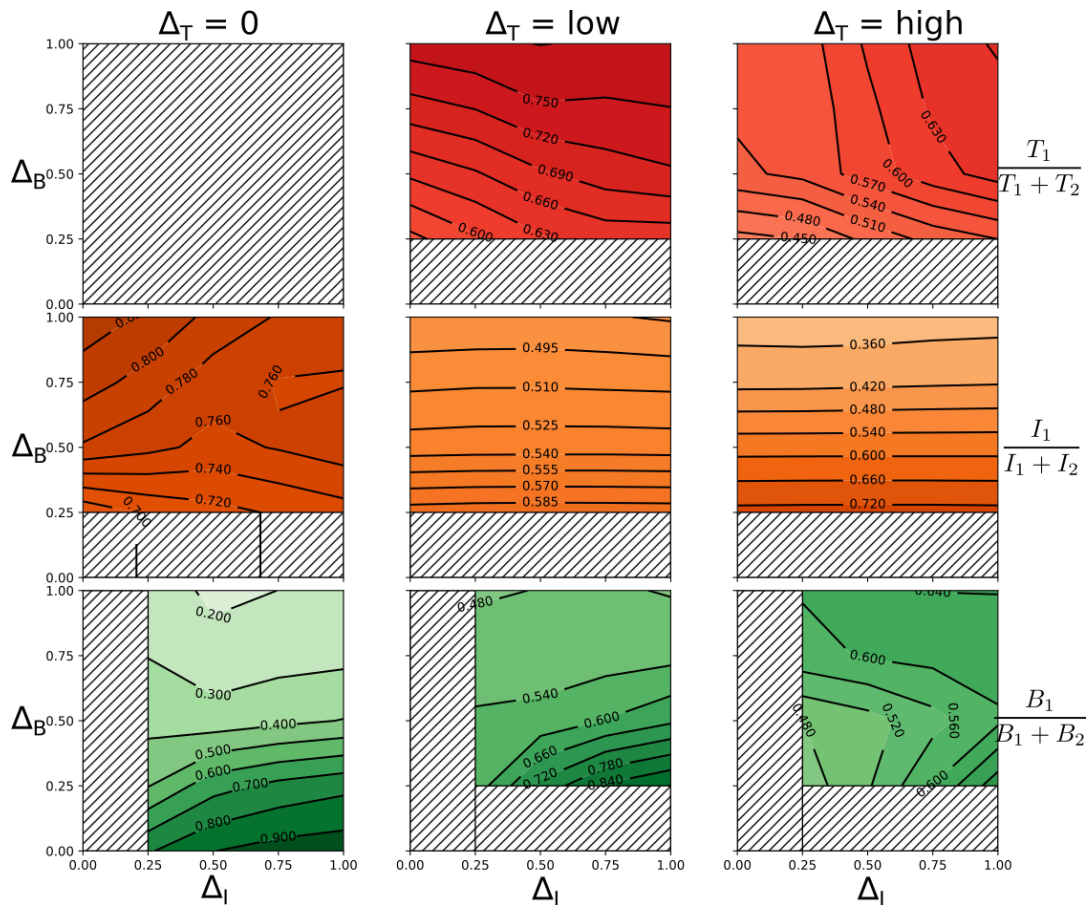

FIGURE B.12: Partial dependence graphs of the trait differences Δ_B and Δ_I, for $\Delta_T = 0$, low Δ_T, and high $\Delta_T = 1$ (for more information see Methods), on the relative biomass of the fast growing B_1 (green), I_1 (orange), and T_1 (red), in the same style as Figs. 3.3-3.5. See text for details on the additionally excluded areas.

References

Breiman, L. (2001). "Random Forests". In: *Machine Learning* 45.1, pp. 5–32. DOI: 10.1017/CBO9781107415324.004.

Hastie, T., Tibshirani, R., and Friedman, J. (2009). *The Elements of Statistical Learning: Data Mining, Inference, and Prediction*. Second Edition. DOI: 10.1111/j.1751-5823.2009.00095_18.x.

Pedregosa, F. et al. (2011). "Scikit-learn: Machine learning in Python". In: *Journal of Machine Learning Research* 12, pp. 2825–2830.

Appendix C

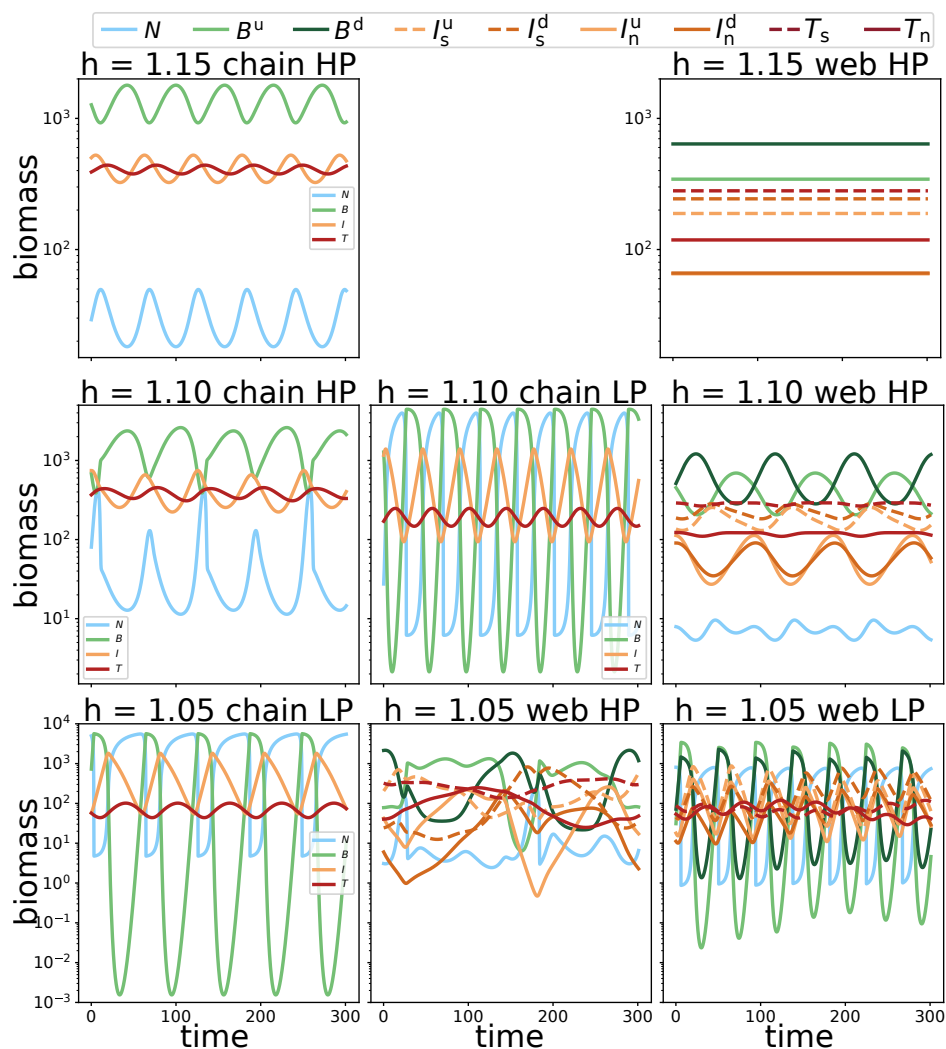# Supplementary information to Chapter 4

FIGURE C.1: Short overview of the dynamics on each of the different attractor (cf. Table 4.1, main text). Note the different biomass scales per row. The top legend only applies to panels in which the dynamics of the food web are shown. Notice how the high production (*HP*) state is characterized by a low mean free nutrient concentration, high top biomass, and generally low temporal variability, in contrast to the low-production (*LP*) state.
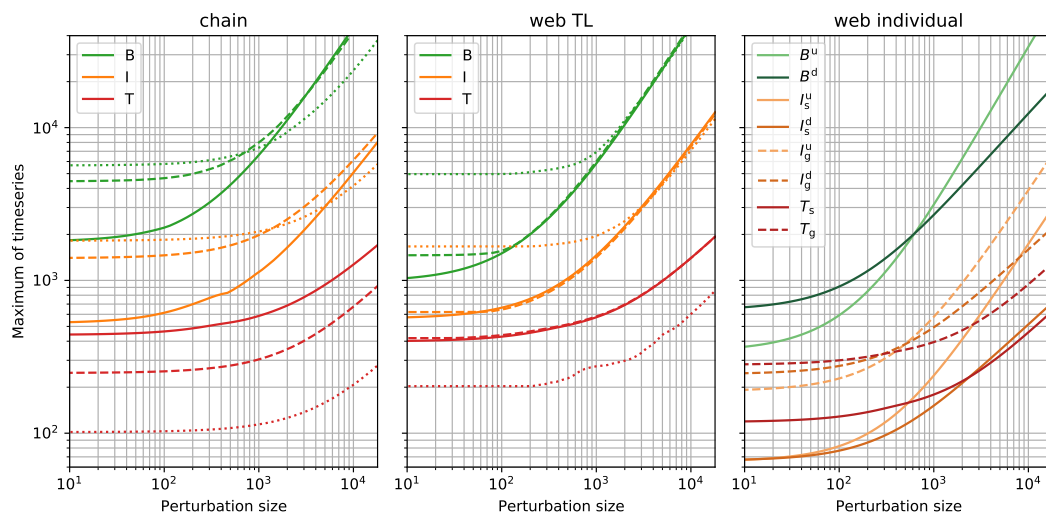
Figure C.2: Biomass maxima reached by the timeseries after the perturbation, for the chain (left), the total biomass per trophic level in the food web (middle), and the individual populations in the food web (right), as a function of the perturbation size. Each line corresponds to the median of 1000 different randomly sampled initial conditions that lead to coexistence of all species, with the shaded area showing the upper and lower quantiles. These initial conditions were first allowed to relax to the attractor for $3 \cdot 10^4$ time units before the perturbation was applied. For the chain and trophic level biomass in the food web, the solid lines show the maxima for Hill exponents $h = 1.15$, dashed for $h = 1.10$, and dotted for $h = 1.05$. The individual populations' maxima for the food web are only shown in the case of $h = 1.05$.
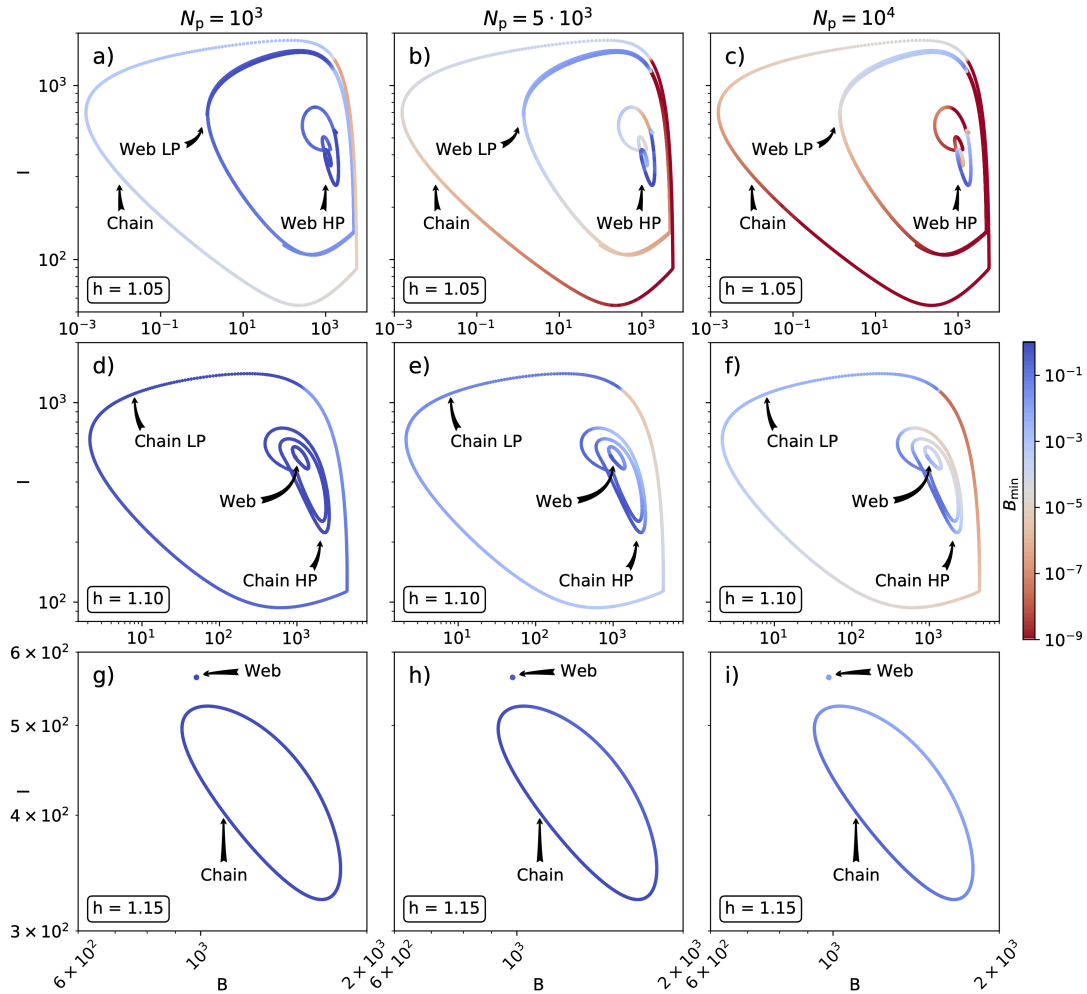
FIGURE C.3: Biomass minima reached by the basal species after a perturbation, $B_{\min}$ depending on its location on the attractor, for different perturbation sizes. The general pattern that the web and *LP* state resistance tend to be higher than the chain and *HP* state, respectively, holds for different perturbation sizes and different Hill exponents.
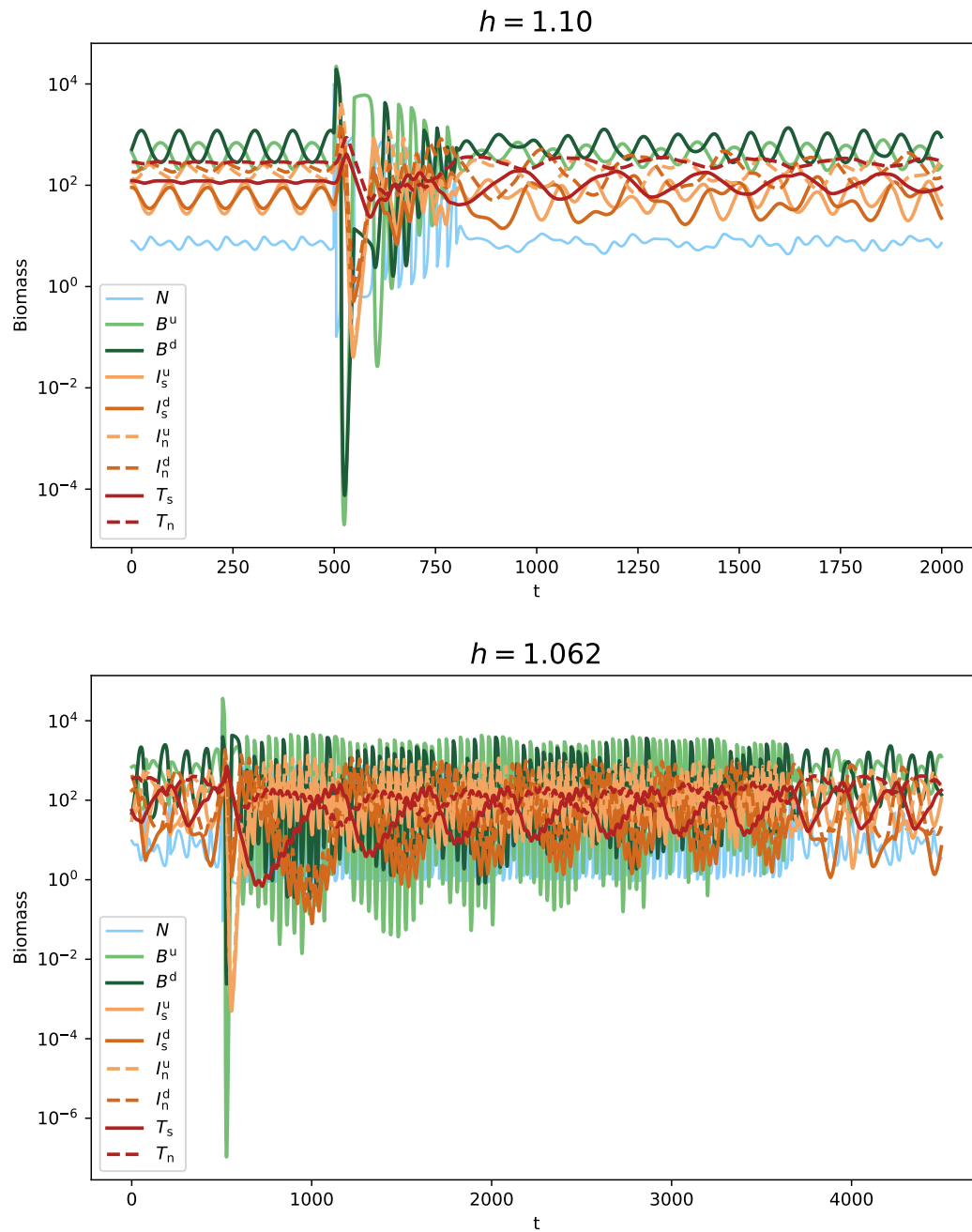
FIGURE C.4: The ghost attractor phenomenon in the post-perturbation transient. When $h = 1.10$, the only stable state in the food web is the HP state (cf. Fig. C.1, and Table 4.1, main text). However, when perturbed by a nutrient pulse (in this case $N_P = 10^4$ at $t = 500$), the dynamics temporarily behave like the LP state (see also Fig. 4.6, main text). After approx. 250 time units, the dynamics shift again to that of the HP state, but require a long time to settle down to regular oscillations. The LP state becomes unstable for approximately $h > 1.06$ (cf. Fig. 2.5, Chapter 2 for $\Delta = 1$). Close to this threshold, the dynamics may be on the ghost state for much longer after the same perturbation (note the different time scales in the plots).
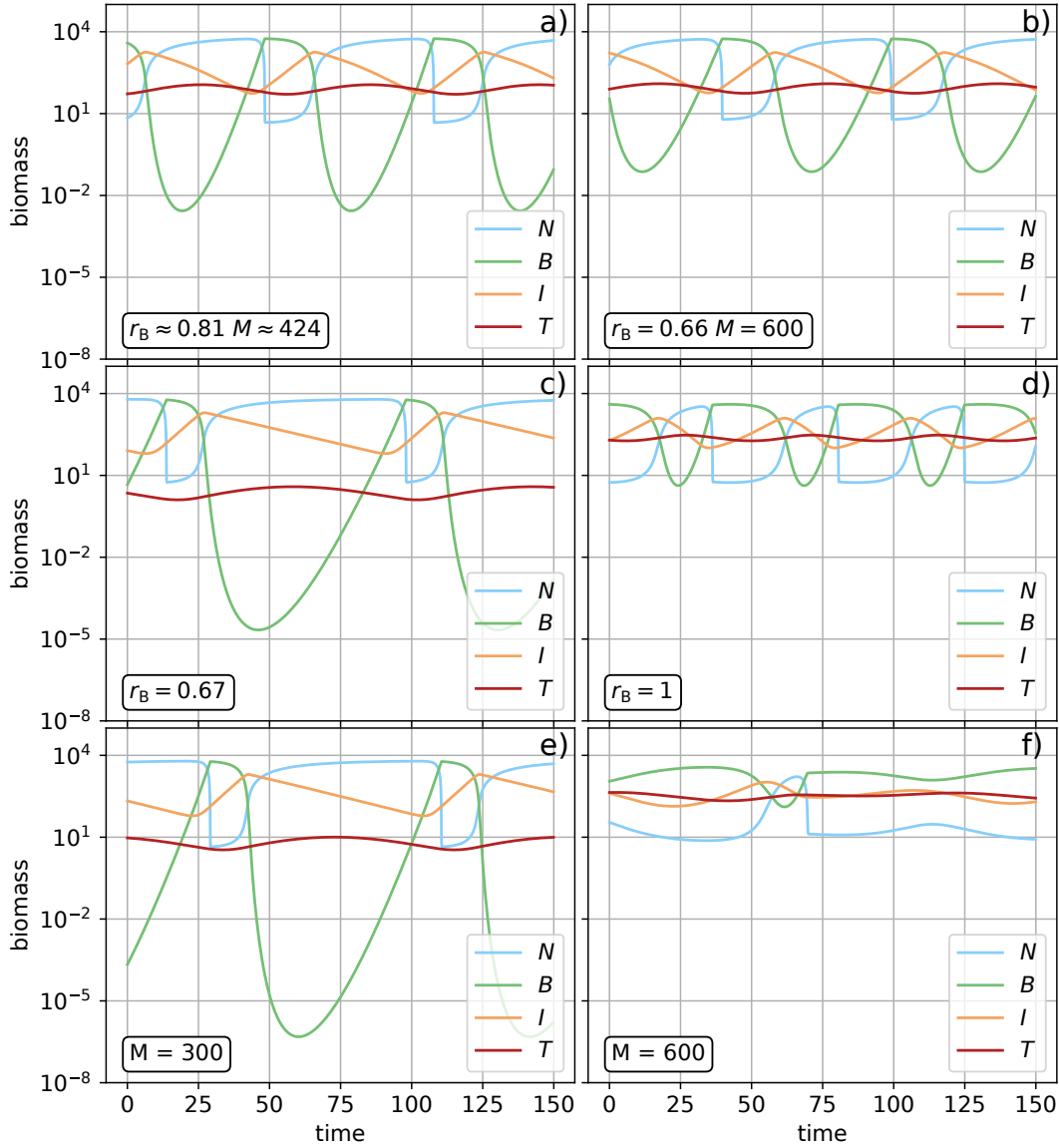
FIGURE C.5: Timeseries of the dynamics on the attractor for the differently parametrized food chains in Fig. 4.7. Panel a shows the standard parametrization of the chain where r_b and M are logarithmic in-between the defended and undefended growth rate, and selective and non-selective half-saturation constant, respectively. Panels c and d show how the dynamics are affected by setting r_B to that of the defended basal species (c), and undefended basal species (d). The change in basal biomass production directly translates to a change in biomass on the top level, which in turn changes top-down control on the intermediate level. Panels e and f show how changes to the basal-intermediate half-saturation constant M has a similar effect on the top level, and thus, indirectly also on the basal level.

Appendix D

Supplementary information to Chapter 5

D.1 Non-dimensionalization

In its dimension-full form, the $C - R$ system given in Eq. (5.1) (main text), would typically look like:

$$\begin{cases} \dfrac{d R'}{d t'} & = rR'\left(1 - \dfrac{R'}{K}\right) - \dfrac{a' R'}{1 + a' h' R'} C' \\[2ex] \dfrac{d C'}{d t'} & = e\dfrac{a' R'}{1 + a' h' R'} C' - d' C' \end{cases} \tag{D.1}$$

where r is the growth rate of the resource R', K its carrying capacity, a' and h' the attack rate and handling time of the $C' - R'$ interaction, e the biomass conversion efficiency and d' the death rate of the consumer C'. Using the following transformations: $t = rt'$, $R = \frac{R'}{K}$, $C = \frac{C'}{eK}$, $a = \frac{eKa'}{r}$, $h = \frac{rh'}{e}$, and $d = \frac{d'}{r}$, the non-dimensionalised form is obtained

$$\begin{cases} \dot{R} & = R(1 - R) - \dfrac{a R}{1 + a h R} C \\[2ex] \dot{C} & = \dfrac{a R}{1 + a h R} C - d C \end{cases} \tag{D.2}$$

where $\dot{R} = \frac{d R}{d t}$, $\dot{C} = \frac{d C}{d t}$.

Similarly, the dimension-full form of the predator equation would be described by:

$$\frac{d P'}{d t'} = \varepsilon \frac{\alpha' C'}{1 + \alpha' \eta' C'} P' - \delta' P' \tag{D.3}$$

where α', η' are the attack rate and handling time of the $P' - C'$ interaction, ε the biomass conversion efficiency and δ' the death rate of the predator P'. The additional transformations $P = \frac{P'}{\varepsilon eK}$, $\alpha = \frac{\varepsilon eK\alpha'}{r}$, $\eta = \frac{r\eta'}{\varepsilon}$, and $\delta = \frac{\delta'}{r}$ (as well as adding the $P' - C'$ interaction term, without ε, to the consumer equation as well) would then provide the non-dimensionalised form of the $P - C - R$ system given in Eq. (5.2) (main text).

D.2 Analytical calculation of boundaries in Fig. 5.1

The boundaries between the different regions that appear in Fig. 5.1 can be calculated analytically, because they follow from the two-dimensional Rosenzweig-MacArthur $C - R$ system (cf. Eq. (5.1), main text, or above).

D.2.1 Coexistence boundary

The boundary between the green and blue region describes the minimum attack rate a required for the resource and consumer to coexist, for a given handling time h: when a is below this boundary, the resource grows to its carrying capacity as the consumer goes extinct. This boundary can be found by calculating the fixed points of the system (D.2).

At a fixed point, $\dot{R} = \dot{C} = 0$, which gives

$$\begin{cases} R(1 - R) = \dfrac{aR}{1 + ahR} C \\ \dfrac{aR}{1 + ahR} C = dC. \end{cases} \tag{D.4}$$

There are several solutions to this system, but only the non-trivial cases where $R \neq 0$ and $C \neq 0$ are of interest:

$$\begin{cases} 1 - R = \dfrac{a}{1 + ahR} C \\ \dfrac{aR}{1 + ahR} = d \end{cases} \Leftrightarrow \begin{cases} R = \dfrac{d}{a - ahd} \\ C = \dfrac{R(1 - R)}{d}. \end{cases} \tag{D.5}$$

There is thus a unique non-trivial fixed point in this system. Because R, C, a, h, d must all be positive, it follows that $R < 1$, and thus $d < a - ahd$, which is equivalent to $a > a/(1 - hd)$. The boundary between the green and blue regions is therefore described by

$$a = \frac{d}{1 - hd}. \tag{D.6}$$

D.2.2 Hopf bifurcation

The transition between the blue region (where the attractor is a stable fixed point), and the oscillatory region (where the attractor is a limit cycle) is called a Hopf-bifurcation. The location of this boundary can be found by evaluating the Jacobian $\mathbf{J}_{ij} = \partial \dot{x}_i / \partial x_j$ of system (D.2), where $x_1 \equiv R$ and $x_2 \equiv C$, at the non-trivial fixed point and calculating where the real parts of its eigenvalues become positive.

The Jacobian, evaluated at the non-trivial fixed point (D.5), is given by:

$$\mathbf{J}\big|_{\text{non-triv.}} = \begin{pmatrix} hd - \dfrac{d(1 + hd)}{a(1 - hd)} & -d \\ 1 - hd - \dfrac{d}{a} & 0 \end{pmatrix}. \tag{D.7}$$

$J\big|_{\text{non-triv.}}$ is necessarily a real matrix, so its eigenvalues λ_1, λ_2 must be either real numbers, or complex conjugates. Because the Hopf-bifurcation occurs when the real part of both eigenvalues equals zero, it follows that the sum of the eigenvalues equals exactly zero. The location of the Hopf-bifurcation is thus given by:

$$\lambda_1 + \lambda_2 = \text{Tr}\, J\big|_{\text{non-triv.}} = h\,d - \frac{d\,(1 + h\,d)}{a\,(1 - h\,d)} = 0, \tag{D.8}$$

where Tr denotes the trace of the matrix. The boundary between the blue region of stable dynamics and the oscillatory region is therefore described by

$$a = \frac{1 + h\,d}{h(1 - h\,d)}, \tag{D.9}$$

with $hd < 1$ since a, h, d must all be positive.
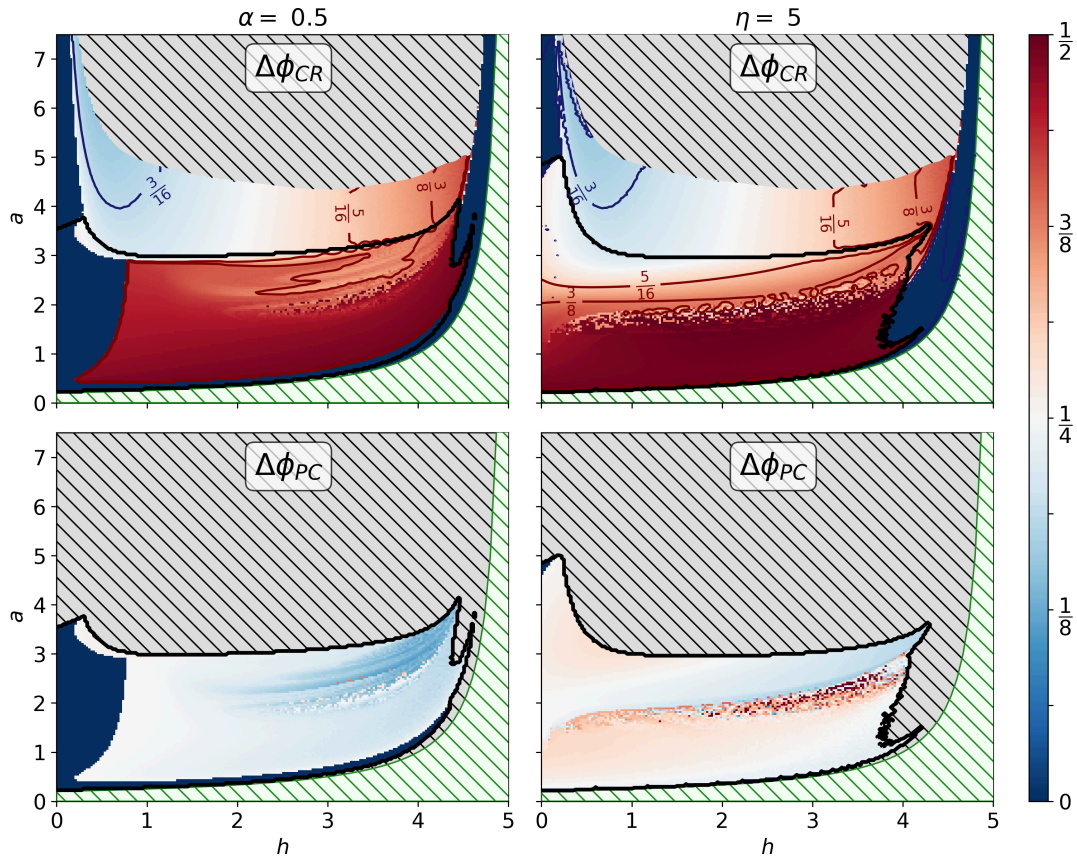
D.3 More $P - C - R$ phase relationships

FIGURE D.1: To show that the observed phase differences in Fig. 5.3 (main text) for different values of the P loss rate δ are not unique to the specific values of the $P-C$ interaction's attack rate α and handling time *eta*. Using $\delta = 0.10$ and $d = 0.10$ as in the main text, we show the phase relationships for $\alpha = 0.5$ (half), with $\eta = 2.5$ (left panels), and for $\eta = 5$ (double), with $\alpha = 1$ (right panels). Anti-phase cycles between C and R are still common for a large region of $h-a$ space. The lower attack rate in the left panels causes the phase relationships to behave more smoothly due to the less pronounced oscillations, and the region of coexistence indicated by the fat black curve has decreased. When the handling time is increased (right panels), the coexistence region also becomes smaller, and complex oscillations may occur due to the inability of P to keep up with C.

Appendix E

Curriculum vitae

Pages 162-165 contain private information and have thus been removed from this document.

Pages 162-165 contain private information and have thus been removed from this document.

Pages 162-165 contain private information and have thus been removed from this document.

Pages 162-165 contain private information and have thus been removed from this document.

Declaration of Authorship

I, Ruben Ceulemans, declare that this dissertation titled, "Diversity effects on ecosystem functions of tritrophic food webs" and the work presented in it are my own. I confirm that:

- This work was done wholly or mainly while in candidature for a research degree at this University.

- No part of this thesis has previously been submitted for a degree or any other qualification at this University or any other institution.

- Where I have consulted the published work of others, this is always clearly attributed.

- Where I have quoted from the work of others, the source is always given. With the exception of such quotations, this thesis is entirely my own work.

- I have acknowledged all main sources of help.

- Where the thesis is based on work done by myself jointly with others, I have made clear exactly what was done by others and what I have contributed myself.

Signed:

_____

Date:

_____